Report No.359

epaResearch
Climate - Water - Sustainability
Identifying pressures • Informing policy • Developing solutions

Modelling Irish Transitional and Coastal Systems to Determine Nutrient Reduction Measures to Achieve Good Status

Authors: Joseph V. McGovern, Stephen Nash and Michael Hartnett

www.epa.ie

Rialtas na hÉireann
Government of Ireland

ENVIRONMENTAL PROTECTION AGENCY

The Environmental Protection Agency (EPA) is responsible for protecting and improving the environment as a valuable asset for the people of Ireland. We are committed to protecting people and the environment from the harmful effects of radiation and pollution.

The work of the EPA can be divided into three main areas:

Regulation: *We implement effective regulation and environmental compliance systems to deliver good environmental outcomes and target those who don't comply.*

Knowledge: *We provide high quality, targeted and timely environmental data, information and assessment to inform decision making at all levels.*

Advocacy: *We work with others to advocate for a clean, productive and well protected environment and for sustainable environmental behaviour.*

Our Responsibilities

Licensing

We regulate the following activities so that they do not endanger human health or harm the environment:

- waste facilities *(e.g. landfills, incinerators, waste transfer stations)*;
- large scale industrial activities (*e.g. pharmaceutical, cement manufacturing, power plants)*;
- intensive agriculture *(e.g. pigs, poultry)*;
- the contained use and controlled release of Genetically Modified Organisms *(GMOs)*;
- sources of ionising radiation *(e.g. x-ray and radiotherapy equipment, industrial sources)*;
- large petrol storage facilities;
- waste water discharges;
- dumping at sea activities.

National Environmental Enforcement

- Conducting an annual programme of audits and inspections of EPA licensed facilities.
- Overseeing local authorities' environmental protection responsibilities.
- Supervising the supply of drinking water by public water suppliers.
- Working with local authorities and other agencies to tackle environmental crime by co-ordinating a national enforcement network, targeting offenders and overseeing remediation.
- Enforcing Regulations such as Waste Electrical and Electronic Equipment (WEEE), Restriction of Hazardous Substances (RoHS) and substances that deplete the ozone layer.
- Prosecuting those who flout environmental law and damage the environment.

Water Management

- Monitoring and reporting on the quality of rivers, lakes, transitional and coastal waters of Ireland and groundwaters; measuring water levels and river flows.
- National coordination and oversight of the Water Framework Directive.
- Monitoring and reporting on Bathing Water Quality.

Monitoring, Analysing and Reporting on the Environment

- Monitoring air quality and implementing the EU Clean Air for Europe (CAFÉ) Directive.
- Independent reporting to inform decision making by national and local government *(e.g. periodic reporting on the State of Ireland's Environment and Indicator Reports)*.

Regulating Ireland's Greenhouse Gas Emissions

- Preparing Ireland's greenhouse gas inventories and projections.
- Implementing the Emissions Trading Directive, for over 100 of the largest producers of carbon dioxide in Ireland.

Environmental Research and Development

- Funding environmental research to identify pressures, inform policy and provide solutions in the areas of climate, water and sustainability.

Strategic Environmental Assessment

- Assessing the impact of proposed plans and programmes on the Irish environment *(e.g. major development plans)*.

Radiological Protection

- Monitoring radiation levels, assessing exposure of people in Ireland to ionising radiation.
- Assisting in developing national plans for emergencies arising from nuclear accidents.
- Monitoring developments abroad relating to nuclear installations and radiological safety.
- Providing, or overseeing the provision of, specialist radiation protection services.

Guidance, Accessible Information and Education

- Providing advice and guidance to industry and the public on environmental and radiological protection topics.
- Providing timely and easily accessible environmental information to encourage public participation in environmental decision-making *(e.g. My Local Environment, Radon Maps)*.
- Advising Government on matters relating to radiological safety and emergency response.
- Developing a National Hazardous Waste Management Plan to prevent and manage hazardous waste.

Awareness Raising and Behavioural Change

- Generating greater environmental awareness and influencing positive behavioural change by supporting businesses, communities and householders to become more resource efficient.
- Promoting radon testing in homes and workplaces and encouraging remediation where necessary.

Management and structure of the EPA

The EPA is managed by a full time Board, consisting of a Director General and five Directors. The work is carried out across five Offices:

- Office of Environmental Sustainability
- Office of Environmental Enforcement
- Office of Evidence and Assessment
- Office of Radiation Protection and Environmental Monitoring
- Office of Communications and Corporate Services

The EPA is assisted by an Advisory Committee of twelve members who meet regularly to discuss issues of concern and provide advice to the Board.

EPA RESEARCH PROGRAMME 2014–2020

Modelling Irish Transitional and Coastal Systems to Determine Nutrient Reduction Measures to Achieve Good Status

(2015-W-FS-17)

EPA Research Report

Prepared for the Environmental Protection Agency

by

Civil Engineering Department, School of Engineering and Informatics, National University of Ireland Galway

Authors:

Joseph V. McGovern, Stephen Nash and Michael Hartnett

ENVIRONMENTAL PROTECTION AGENCY
An Ghníomhaireacht um Chaomhnú Comhshaoil
PO Box 3000, Johnstown Castle, Co. Wexford, Ireland

Telephone: +353 53 916 0600 Fax: +353 53 916 0699
Email: info@epa.ie Website: www.epa.ie

ACKNOWLEDGEMENTS

This report is published as part of the EPA Research Programme 2014–2020. The EPA Research Programme is a Government of Ireland initiative funded by the Department of the Environment, Climate and Communications. It is administered by the Environmental Protection Agency, which has the statutory function of co-ordinating and promoting environmental research.

The authors would like to thank Alice Wemaere (EPA) and Oonagh Monahan (Research Project Manager on behalf of the EPA). The authors would also like to thank the members of the project steering committee, namely Sorcha Ni Longphuirt (EPA), Tomasz Dabrowski and Joe Silke (Marine Institute) and Ronan Kane and Trudy Higgins (Irish Water), for their many helpful contributions. Sincere thanks are also extended to the SeaMat team (2015-W-MS-20) (Liam Morrison, Edna Curley and Ricardo Bermejo), Robert Wilkes (EPA) for macroalgae survey data, Eva Mockler (EPA) for nutrient loads from the souce load apportionment model, John Aldridge (Centre for Environment, Fisheries and Aquaculture Science), Paul Tett (Scottish Association for Marine Science) and Karen Edwards (UK Environment Agency) for making the DCPM code available under licence, the EPA Transitional and Coastal Waters team for all monitoring data provided, Per-Erik Mellander and Sara Vero (Teagasc Agricultural Catchments Programme) for providing data for the Timoleague River, and Eleanor Jennings (Dundalk Institute of Technology) for providing her PhD thesis and associated reports relating to macroalgae in the Tolka Estuary. Thanks also to David Hendrick (ESB International) for providing river flow measurement data.

Cover image: Image provided by Robert Wilkes (EPA).

EPA RESEARCH PROGRAMME 2014–2020
Published by the Environmental Protection Agency, Ireland

ISBN: 978-1-84095-964-2 November 2020

Price: Free Online version

Project Partners

Dr Joseph McGovern
Civil Engineering
School of Engineering and Informatics
Ryan Institute for Environmental, Marine and Energy Research
National University of Ireland Galway
Galway
Ireland
Email: joseph.mcgovern@nuigalway.ie

Currently:
Marine Institute
Rinville
Oranmore
Co. Galway
Ireland
Email: joe.mcgovern@marine.ie

Dr Stephen Nash
Civil Engineering
School of Engineering and Informatics
Ryan Institute for Environmental, Marine and Energy Research
National University of Ireland Galway
Galway
Ireland
Email: stephen.nash@nuigalway.ie

Professor Michael Hartnett
Civil Engineering
School of Engineering and Informatics
Ryan Institute for Environmental, Marine and Energy Research
National University of Ireland Galway
Galway
Ireland
Email: michael.hartnett@nuigalway.ie

Contents

List of Figures

List of Tables

Executive Summary

Restoration of good environmental status may entail changing the intensity, timings and magnitude of nutrient loading. Identification of the requisite changes to estuarine nutrient loading is a non-trivial process, not least because of the highly dynamic nature of estuaries. Tidal ebb and flood delivers nutrients in varying concentrations and ratios, which are a function of coastal upwelling and far-field processes. In addition, riverine non-point loading to estuaries reflects the range of anthropogenic pressures upstream. As the proportion of the population living in coastal cities increases, the associated nutrient point loading from wastewater and industrial sources is likely to increase.

The research summarised in this report was primarily directed at increasing the confidence with which combined phytoplankton and macroalgae models can be applied in an Irish context.

Firstly, the dynamic combined phytoplankton and macroalgae (DCPM) model, developed by the Centre for Environment, Fisheries and Aquaculture Science (CEFAS) in the United Kingdom and licensed by the UK Environment Agency, was applied to the Cork Harbour and environs, where eutrophication has historically taken the form of nuisance phytoplankton blooms, without any concurrent macroalgae blooms. Average concentrations of nutrients and phytoplankton in each water body simulated by the DCPM model were compared with the equivalent results simulated by the Multi-scale Nesting and Water Quality (MSN_WQ) model, an industry-standard, high-resolution, depth-integrated hydrodynamic, solute transport and water quality model that has been adapted to Cork Harbour. The MSN_WQ model provided a better approximation of the prevailing nutrient concentrations in Cork Harbour than the DCPM model.

To fully assess the performance of the DCPM model in a system affected by both phytoplankton and macroalgae blooms, the model was applied to the system comprising the Liffey and Tolka estuaries and Dublin Bay, as nuisance macroalgae blooms occur annually in the intertidal portion of the Tolka Estuary. The existing version of the MSN_WQ model did not describe macroalgae growth and decay and, therefore, did not facilitate comparison between the MSN_WQ and the DCPM models. In response to this shortcoming, a full review of the state of the art of macroalgae modelling was completed to inform the inclusion of macroalgae growth and decay in the MSN_WQ model. The resulting high-resolution model was applied to the Liffey–Tolka–Dublin Bay system. The model was compared at different stages of development with the DCPM model, to identify the most pertinent aspects of the model to retain, and the associated parameters. A detailed case study of Dublin Bay and its adjoining estuaries was also carried out to identify the magnitude of nutrient load reductions necessary to inhibit the occurrence of opportunistic macroalgae blooms in the Tolka Estuary.

Following the benchmarking of the DCPM model against the MSN_WQ model, two additional case studies were completed using the DCPM model, in the Argideen Estuary–Courtmacsherry Bay system and the Clonakilty Harbour–Bay system, both of which have been considered in recent environmental assessments as areas where opportunistic macroalgae blooms could develop. Calibration and validation of the DCPM models were carried out with a view to informing the future application of the model to other problematic Irish coastal systems. In each case, ambient conditions were matched as closely as possible, while the best available nutrient load estimates were adopted. Various load reduction scenarios were simulated post validation, to inform future actions within the integrated catchment management framework.

In the three case study systems, growth was variously limited by nitrogen, phosphorus and light. The following observations were made regarding the nature of load reductions necessary to eradicate opportunistic macroalgae blooms:

- Dublin Bay: addressing wastewater infrastructure or improving nutrient loading from the rivers would have the equivalent effect of restoring the intertidal zone of the Tolka Estuary to high status with respect to opportunistic macroalgae bloom occurrence.

- Courtmacsherry Bay: none of the measures considered would reduce macroalgae wet weight density to the extent that high status would be achieved.
- Clonakilty Bay: a 25% reduction in riverine phosphorus would restore high status as defined by the opportunistic macroalgae bloom tool.

1 Introduction

1.1 Irish Estuarine Water Quality Challenges in Context

Across the European Union, diffuse and point nutrient pressures account for 38% and 18%, respectively, of the significant pressures during the second Water Framework Directive (WFD) river basin management plan cycle (EEA, 2018), with agriculture accounting for the majority of the former and urban wastewater most of the latter. Eutrophication as a direct consequence of nutrient enrichment from agriculture and wastewater discharges remains the most prominent issue currently affecting water quality (DECLG, 2015), with both sources combined accounting for 93% of nitrogen load and 88% of phosphorus load. Diffuse discharge from agriculture generates the majority of both nutrients while urban discharges account for almost a third of phosphorus. According to the most recent indicator report on water quality in Ireland (Trodd and O'Boyle, 2018), in 2017, 43% of transitional and coastal water bodies were presenting symptoms of eutrophication while nitrogen load exceeded the median winter threshold in 24% of transitional and coastal water bodies. The winter median phosphorus threshold was exceeded in one water body. Thirty-one per cent of transitional waters and 79% of coastal waters achieved good or high WFD status in the period 2013–2015 (DHPLG, 2018).

In the period from 2000 to 2013, Irish efforts to reduce nutrient transfer from catchments to transitional and coastal waters in response to European environmental directives yielded greater reductions in phosphorus than in nitrogen (Ní Longphuirt *et al.*, 2016a). This may have the consequence of reducing the growth of primary producers in phosphorus-limited estuaries, leading to a lower uptake of nitrogen and a resultant transfer of unassimilated nitrogen to the coastal zone.

The most recent account of annual total nitrogen and phosphorus emissions to Irish surface waters from 1990 to 2013 yielded average figures of [1]122,718 t N y^{-1} and [2]3841 t P y^{-1} (O'Boyle *et al.*, 2016). Although nitrogen is nationally attributed to agriculture, phosphorus sources vary by land use, and the associated impacts are a function of the presence, or absence, of hydrogeological attenuation (Mockler *et al.*, 2017).

Food Harvest 2020 was launched in 2010 to provide a strategy for agri-food, forestry and fisheries to 2020. Full implementation of Food Harvest 2020 entailed an increase in the primary output of the main sectors of the agri-food industry (DAFF, 2010). In an environmental analysis, Farrelly *et al.* (2014) posited that Food Harvest 2020 may eventually lead to a 26% increase in dairy sector nitrogen and phosphorus from organic fertiliser under optimum circumstances. This could be offset by a reduction in organic fertiliser requirements for the beef sector. An increase in inorganic fertiliser application for both the dairy and beef industry was also forecast, consisting of over 2000 tonnes of dissolved available inorganic phosphorus (DAIP) and 47,000 tonnes of dissolved available inorganic nitrogen (DAIN). Intensification of dairy farming in response to removal of milk quotas may have a moderately deleterious effect on trophic status, with increases of up to 20% in trophic status parameters (O'Boyle *et al.*, 2017). Food Wise 2025, the successor to Food Harvest 2020, sets out to increase primary production by 65%, to €10 billion, although the environmental analysis of Food Wise 2025 (Philip Farrelly & Co., 2015) does not identify specific increases in inorganic or organic nitrogen and phosphorus inputs to the agri-food sector.

Hydrological and biogeochemical time lags may obscure the impact of measures implemented to improve water quality, with the delay between implementation and confident detection of change ranging from 4 to 20 years (Melland *et al.*, 2018), while interannual climate oscillations between wet and dry weather patterns may also offset or magnify improvements in water quality in response to better

1 Minimum annual load of 92,740 tonnes, maximum of 152,136 tonnes.

2 Minimum annual load of 1848 tonnes, maximum of 6564 tonnes.

catchment management practice (Dupas *et al.*, 2018). The time lag between implementation of specific catchment management measures to reduce excessive soil fertility and eventual achievement of a suitable soil index score may vary considerably in an Irish context. Schulte *et al.* (2010) identified a lag of between 7 and 15 years from the time of cessation of fertiliser spreading to high-phosphorus soils to the point of soil phosphorus reducing to a soil index of 3. Meanwhile, climate change may lead to a general increase in nutrient loading to water bodies throughout the year. It is apparent that measures taken at catchment level may have variable effects on transitional waters. Although not suggested in the current Nitrates Action Plan,[3] at some stage in the future, measures may need to be taken to improve soil phosphorus fertility, which may have a detrimental effect on transitional water quality.

The most recent evaluation of wastewater infrastructure performance in Ireland, in 2017, highlights a number of deficiencies that have directly affected water quality in Irish water bodies (EPA, 2018):

- Thirty-eight areas discharge untreated wastewater to surface waters. Six areas were removed from this list between 2016 and 2017, leaving 32 areas, as a result of the commissioning of treatment plants and the connection of effluent discharge to these plants.
- Twenty-eight urban areas do not comply with either or both:
  - the secondary treatment requirements of the Urban Waste Water Treatment Regulations (UWWTR) (DOEHLG, 2001, 2004, 2010a);
  - the stringent treatment requirements of the UWWTR.
- Tertiary treatment to reduce nutrient concentrations in the final effluent is needed at nine urban areas.

Irish Water aims to comply with the UWWTR for 90% of the population equivalent (PE)[4] by 2021, growing to 99% by 2027 and 100% by 2040 (Irish Water, 2015a). The second Irish River Basin Management Plan (DHPLG, 2018) sets out to improve water quality through improving agricultural sustainability, recruiting implementation teams to liaise with stakeholders, improving urban and domestic wastewater treatment efficiency and regulating forestry and peat extraction. Nationally, agriculture is the predominant pressure, having been identified as the main threat for 53% of surface water bodies identified as being at risk of not meeting their environmental objective.

Given the high percentage of nitrogen and phosphorus that can be directly attributed to agriculture and wastewater discharges, any efforts to limit eutrophication and oxygen depletion in transitional and coastal waters must involve nutrient load reduction modelling in order to determine the magnitude of reductions necessary to bring about good status under the WFD. Mathematical models of varying complexity, from empirical black box models underpinned by multiple linear regression through to detailed catchment modelling such as HSPF (Hydrological Simulation Program-FORTRAN) and the Soil & Water Assessment Tool (SWAT), have been previously identified as potential tools in the implementation of the WFD in Ireland (Irvine *et al.*, 2004). The identification of suitable nutrient reductions to limit phytoplankton and macroalgae growth has been made feasible through the application of modelling tools to realistic scenarios. Joint commitments under the Convention for the Marine Environment of the North-East Atlantic (OSPAR) recently required information on nutrient allocations for transitional and coastal water bodies that would restore non-problem area status with regard to eutrophication. Whereas other contracting countries considered larger expanses of coastal waters and seas to evaluate the contributions of transboundary nutrient transport (OSPAR Commission, 2013), eutrophic waters were limited to estuarine and adjacent near-shore coastal waters along the south and east of Ireland (O'Boyle *et al.*, 2011), thus allowing the application of the dynamic combined phytoplankton and macroalgae (DCPM) model developed by Aldridge *et al.* (2010). The DCPM

3 The Nitrates Action Plan is given legal effect in (1) S.I. No. 605/2017 – European Union (Good Agricultural Practice for Protection of Waters) Regulations 2017 and (2) S.I. No. 65/2018 – European Union (Good Agricultural Practice for Protection of Waters) (Amendment) Regulations 2018.

4 Population equivalent is a standard unit of effluent loading that amounts to the waste generated by one person.

model combines two previous models that individually modelled phytoplankton (Painting *et al.*, 2007) and macroalgae (Aldridge and Trimmer, 2009). Models such as the DCPM model give an overall perspective on nutrient reductions required within an entire water body and are compromised in their spatial resolution by the completely mixed reactor approach. In a study into the wider implications of macroalgal cultivation, both a 3-D coupled hydrodynamic–biogeochemistry model and a variation of the DCPM model were applied to waters on opposite sides of Scotland, and it was found that the dry mass of the macroalgae growth was better estimated by the compartment model whereas the spatial extent of growth was better predicted by the coupled 3-D hydrodynamic model (Aldridge *et al.*, 2012).

In an Irish context, the DIVAST (Depth-Integrated Velocity and Solute Transport) model, which combines depth-integrated hydrodynamics, solute transport and biogeochemistry, has been utilised to simulate phytoplankton dynamics in a complex harbour, with promising results (Hartnett and Nash, 2004; Hartnett *et al.*, 2011a; Nash *et al.*, 2011). A model that incorporated site-specific data on light attenuation and water column chlorophyll measurements better predicted phytoplankton growth (as determined by chlorophyll concentration) than using a fixed light attenuation coefficient value (Hartnett and Nash, 2004; Nash *et al.*, 2011). The same model was utilised to simulate nutrient, oxygenation and phytoplankton growth data before and after the commissioning of a wastewater treatment plant (WWTP) in Cork Harbour (Hartnett *et al.*, 2011a). Trophic status classifications using numerical model data corroborated the Environmental Protection Agency's (EPA) previous classification for the same water bodies.

1.2 Opportunism and Impact of Macroalgae

Opportunistic macroalgae blooms have become a common indicator of and response to nutrient enrichment, with effects including displacement of primary producers, increased frequency of eutrophication-induced hypoxia and uncoupling of interactions between sediment and the water column (Valiela *et al.*, 2003). Dominance of opportunistic macroalgae or phytoplankton in response to nutrient enrichment, and competition with seagrasses (Nelson and Lee, 2001; Burkholder *et al.*, 2007), which would reflect good ecological status, have been attributed to differing compensation irradiance and rates of nitrogen uptake, growth and grazing (Duarte, 1995). A single macroalgae bloom event increases the likelihood of recurrence of a bloom at a later time (Zhang *et al.*, 2010). Varying tolerances for salinity extrema and nitrogen availability differentiate green macroalgae species such as *Ectocarpus* and *Ulva* (Fong *et al.*, 1996). *Ulva* and *Ulvaria*, which occur in the intertidal and subtidal waters, respectively, each dominates its habitat because their tolerance of nitrogen and light availability and grazers differs (Nelson *et al.*, 2008). *Ulva* exhibits allelopathy, defined as the release of inhibitory or toxic compounds, which both prevents the development of other species of macroalgae (Van Alstyne *et al.*, 2015) and oyster larvae (Green-Gavrielidis *et al.*, 2018) and allows *Ulva* to outcompete *Gracilaria* (Gao *et al.*, 2014). *Ulva* spp. also have a higher photosynthetic efficiency than other macroalgae spp. such as *Gracilaria* and *Hypnea* because their sheet-like structure provides a higher ratio of surface area to volume (Whitehouse and Lapointe, 2015). *Ulva* spp. have a greater capability than other species to physiologically capitalise on the combination of higher temperatures, CO_2 enrichment and increased nitrogen loads that it is anticipated will result from climate change and ocean acidification (Parages *et al.*, 2014; Chen *et al.*, 2015). However, the higher growth rate of *Ulva* induces nitrogen limitation under exposure to higher CO_2 concentrations, which may lead to increasing competition from *Gracilaria* (Young and Gobler, 2017).

In a selection of Irish transitional waters, *Ulva rigida* was found to be the dominant species (Wan *et al.*, 2017). In the same work, Clonakilty Bay and Courtmacsherry Bay were both assessed as having poor ecological status classified using the WFD opportunistic macroalgal blooming tool (Wells *et al.*, 2009). These water bodies were assessed as having moderate and poor status, respectively, in the most recent national assessment of water quality (Fanning *et al.*, 2017). O'Boyle *et al.* (2015) observed that 90 transitional and coastal water bodies were grouped into four groups and one of these groups was characterised by short residence time. In all

water bodies in this group, growth of macroalgae was favoured over growth of phytoplankton.

1.3 Overarching Research Objectives

Given sufficient time and resources, high-resolution water quality modelling would be the ideal. In an Irish context, it is not practicable to complete full-scale calibration and validation of a fully coupled, high-resolution hydrodynamic, solute transport and water quality model for each surface water body identified as at risk in tier 1 risk assessments. Increasing confidence in the accuracy of the DCPM model was the ultimate aim of this research.

The main objectives of this project were:

- to carry out a detailed literature review to inform the overall scope of the research;
- to benchmark the DCPM model against a fully validated 2-D depth-integrated coupled hydrodynamic, solute transport and water quality model;
- to estimate nutrient loading curves for a selected catchment and associated transitional water body, and investigate the efficacy of changes in agricultural nutrient management practice;
- for each of three transitional/coastal systems, to apply the DCPM model to identify the limiting nutrient and the order of magnitude of nutrient reduction necessary to eradicate macroalgae blooms and restore good trophic status, and to consider the consequences of nutrient reductions from point and diffuse sources, where possible.

2 DCPM Benchmark I: Cork Harbour and Environs

2.1 Introduction

The DCPM model (Aldridge *et al.*, 2010) was established as a simple box model to establish baseline water quality in transitional and adjacent coastal waters under prevailing environmental conditions, and thus to predict the effect of anticipated or planned changes in point and non-point nutrient loadings.

The DCPM model describes the growth and decay of phytoplankton and macroalgae in response to available nitrogen, phosphorus and light. The model domain is represented by a number of contiguous water bodies that are subject to tidal exchange with the tidal boundary at the most downstream water body. Each water body is approximated by a box, which is defined in terms of the water body surface area (km^2) and depth distribution; further information on the DCPM model and an abridged description of the DCPM model set-up can be found in Appendix 2.

The DCPM model was benchmarked against the Multi-scale Nesting and Water Quality (MSN_WQ) model (Hartnett and Nash, 2004) in Cork Harbour and environs (Figure 2.1). The MSN_WQ model is a hydrodynamic, solute transport and water quality model that solves the depth-integrated continuity and Navier–Stokes equations. Further information on the model, including solution schemes and water quality formulations, is given in Appendix 1. The benchmarking process was also completed to establish a baseline for the MSN_WQ model performance in advance of detailed coding of the macroalgae life cycle in the MSN_WQ model and application of the expanded model to Dublin Bay and its neighbouring Tolka and Liffey estuaries.

The MSN_WQ model in Cork Harbour has been subject to iterative improvement and peer review (Hartnett *et al.*, 2011a; Nash *et al.*, 2011). The water quality module describes the interactions between NH_4, NO_3, organic nitrogen, PO_4, organic phosphorus, chlorophyll, biochemical oxygen demand (BOD) and dissolved oxygen. The model is forced by monthly values for:

- riverine and point source discharges from industrial and municipal wastewater facilities;
- tidal boundary nutrient concentrations;
- irradiance, photoperiod and water temperature.

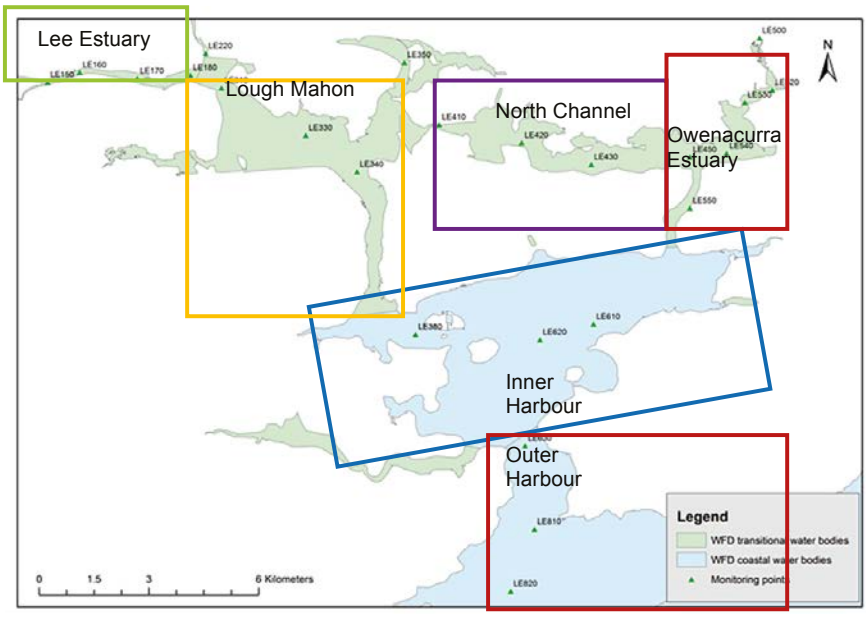

Figure 2.1. Cork Harbour and its constituent water bodies as defined in the DCPM model.

2.2 Model Set-up

To compare the performance of the models, the point and diffuse nutrient loading data and tidal boundary nutrient concentrations from the MSN_WQ model for Cork Harbour and environs were reduced to the equivalent input data for the DCPM model, such as annual average discharges from point sources ($m^3 s^{-1}$), annual DAIN and DAIP ($kg y^{-1}$), and the ratio of summer total to annual total loading (R_{SA}). All point and diffuse loading data, tidal boundary data and monitoring data pertain to the period prior to the commissioning of Carrigrennan WWTP.

2.2.1 MSN_WQ

The MSN_WQ model of Cork Harbour resolves the bathymetry of the domain into 30-m^2 grid cells. To shorten the model runtime, the MSN_WQ model in Cork Harbour was forced by velocity, water elevation and wet/dry indices, which were averaged in a separate hydrodynamic model at 30-minute intervals throughout the spring–neap cycle.

Table 2.1 shows the water quality parameters that were attributed to the rivers entering the Cork Harbour system; whereas nutrient concentrations are constant throughout the year, the discharge from each river, and therefore the nutrient mass loading, differs between months, as seen in Table 2.2.

Industrial and municipal wastewater discharge volumes and effluent water quality characteristics throughout the year, as defined in Table 2.3, are also constant.

Coastal water quality characteristics vary throughout the year, as seen in Table 2.4. Light attenuation, k_d (m^{-1}), is described by equation 2.1, relating k_d to chlorophyll concentration:

$$k_d = 0.79012 + 0.004296\,\mathrm{Chl} \qquad (2.1)$$

2.2.2 DCPM

Riverine flow to each water body was defined in terms of the annual average discharge ($m^3 s^{-1}$) and the ratio of summer to annual average discharge, R_{SA}. The nutrient loading to each water body was the summation of point and diffuse nutrient loadings, with the loading specified as the total mass of nitrogen and phosphorus in $kg y^{-1}$ and the annual variation of the total load ascribed using R_{SA}, as with freshwater discharge specification. Table 2.5 summarises loadings to the Cork Harbour system DCPM model, which were aggregated from nutrient loading data specified for the equivalent MSN_WQ model in Tables 2.1, 2.2 and 2.3. Table 2.6 reflects the relevant

Table 2.1. Water quality characteristics for all of the rivers entering the Cork Harbour system (Costello *et al.*, 2001) in the period prior to the commissioning of Carrigrennan WWTP

Salinity (psu)	BOD ($mg l^{-1}$)	Organic N (µM)	NH_4 (µM)	NO_3 (µM)	DAIN (µM)	Chl ($mg m^{-3}$)	Organic P (µM)	DAIP (µM)
0.000	2.213	101.786	6.286	221.857	228.143	6.890	0.871	1.548

Chl, chlorophyll; psu, practical salininty unit.

Table 2.2. Monthly discharge of each catchment flowing into the Cork Harbour system (Costello *et al.*, 2001)

	Flow rate ($m^3 s^{-1}$)											
Catchment	Jan	Feb	Mar	Apr	May	Jun	Jul	Aug	Sep	Oct	Nov	Dec
Lee North	63.1	57.3	37.4	26.1	13.9	9.01	6.81	5.16	9.11	19.6	39.4	43.5
Lee South	2.58	2.46	1.76	1.52	0.72	0.31	0.27	0.41	0.37	0.37	1.47	2.01
Glashaboy	9.78	9.32	6.68	5.75	2.72	1.17	1.01	1.55	1.40	1.90	5.59	7.61
Owenbuidhe	8.07	8.55	4.96	4.73	2.30	1.13	0.94	1.00	1.26	1.98	4.25	6.94
Owenacurra	6.66	6.28	4.59	3.81	1.91	0.95	0.75	0.96	0.82	1.62	3.97	4.97
Catchment 1	1.98	1.88	1.35	1.16	0.55	0.24	0.20	0.31	0.28	0.28	1.13	1.54
Catchment 2	0.67	0.64	0.46	0.39	0.19	0.08	0.07	0.11	0.10	0.10	0.38	0.52
Catchment 3	1.62	1.54	1.10	0.95	0.45	0.19	0.17	0.26	0.23	0.23	0.92	1.26

Table 2.3. Flow rate and characteristics of industrial and municipal wastewater entering the Cork Harbour system (Costello *et al.*, 2001) in the period prior to the commissioning of Carrigrennan WWTP

Discharge source	Flow rate ($m^3 s^{-1}$)	Organic N (µM)	NH_4 (µM)	NO_3 (µM)	DAIN (µM)	Organic P (µM)	DAIP (µM)	DO ($mg l^{-1}$)	Chl ($mg m^{-3}$)
Industry and sewers									
Cork City north sewer[a]	0.347	0	8857	1071	9929	0	774	0	0
Cork City south sewer[a]	0.347	0	8857	1071	9929	0	774	0	0
Glounthane[a]	0.011	857	214	71	286	32	0	0	0
Rams Head	0.066	0	3214	4143	7357	677	226	0	0
Lough Beg	0.012	3143	3071	143	3214	290	65	0	0
Passage West	0.035	0	9500	214	9714	742	0	0	0
Middleton	0.003	0	214	4429	4643	65	0	0	0
Lough Mahon West[a]	0.015	6000	6429	286	6714	1097	1484	0	0
Lough Mahon East[a]	0.002	571	429	71	500	65	32	0	0
Irish Fertiliser Industries	0.034	2357	4714	714	5429	97	226	0	0
WWTPs									
Ballincollig	0.041	5929	0	0	0	548	0	0	0
Carrigtwohill	0.005	2000	0	0	0	194	0	0	0
Cloyne	0.001	2000	0	0	0	194	0	0	0
Crosshaven	0.004	3571	0	0	0	484	0	0	0
Glanmire[a]	0.021	3571	0	0	0	484	0	0	0
Middleton	0.013	3571	0	0	0	484	0	0	0
Passage/Monkstown	0.01	3571	0	0	0	484	0	0	0
Tramore[a]	0.077	3571	0	0	0	484	0	0	0
Cobh	0.03	1286	2071	0	2071	161	290	0	0
Carrigaline/Ringaskiddy	0.044	1071	1857	0	1857	129	258	0	0
Carrigrennan	0.568	857	1357	0	1357	0	0	*3*	*5*

[a]Combined into Carrigrennan discharge following construction of treatment plant.

Chl, chlorophyll; DO, dissolved oxygen.

Table 2.4. Water quality characteristics at the tidal boundary for Cork Harbour Outer (Costello *et al.*, 2001) in the period prior to the commissioning of Carrigrennan WWTP

	Month											
Characteristic	Jan	Feb	Mar	Apr	May	Jun	Jul	Aug	Sep	Oct	Nov	Dec
Salinity (psu)	30	35	35	35	35	35	35	35	35	35	35	35
BOD ($mg l^{-1}$)	1.88	1.88	1.88	1.88	1.88	1.88	1.88	1.88	1.88	1.88	1.88	1.88
Organic N (µM)	0.71	9.93	19.4	26.1	29.4	27.4	21.1	11.9	2.43	0.00	0.00	0.00
NH_4 (µM)	1.29	1.29	1.29	1.29	1.29	1.29	1.29	1.29	1.29	1.29	1.29	1.29
NO_3 (µM)	23.0	21.4	17.7	13.0	8.36	5.00	3.93	5.36	8.86	9.29	18.3	21.8
DAIN (µM)	24.3	22.7	19.0	14.3	9.64	6.29	5.21	6.64	10.1	10.6	19.6	23.1
DO ($mg l^{-1}$)	8.77	8.77	8.77	8.77	8.77	8.77	8.77	8.77	8.77	8.77	8.77	8.77
Chl ($mg m^{-3}$)	1.72	2.42	3.87	6.21	8.85	10.27	1.72	1.72	4.32	2.67	1.83	1.53
Organic P (µM)	0.52	0.39	0.29	0.26	0.29	0.42	0.55	0.68	0.77	0.81	0.77	0.68
DAIP (µM)	0.74	0.71	0.61	0.48	0.35	0.23	0.19	0.23	0.32	0.45	0.58	0.71

Chl, chlorophyll; DO, dissolved oxygen; psu, practical salinity unit.

Table 2.5. Total riverine and nutrient loading characteristics for each of the water bodies in the Cork Harbour system

Water body	River flow ($m^3 s^{-1}$), annual average	River discharge ratio, (R_{SA})	Annual DAIN load ($kg y^{-1}$)	N load ratio, (R_{SA})	Annual DAIP load ($kg y^{-1}$)	P load ratio, (R_{SA})
Inner Cork Harbour	5.50	0.25	387,211	0.79	26,064	0.96
North Channel/ Owenacurra Estuary	3.10	0.25	317,150	0.51	4825	0.51
Lough Mahon	0.31	0.25	197,807	0.92	5412	0.96
Glashaboy Estuary	4.50	0.25	454,372	0.50	6828	0.50
Lower Lee Estuary	28.00	0.25	4,397,505	0.63	176,043	0.86

Annual average river flow, annual total nitrogen loads, annual total phosphorus loads and their corresponding summer/ annual ratios were determined based on Tables 2.1, 2.2 and 2.3.

Summer, April to September, inclusive.

Table 2.6. Tidal boundary conditions specified for Cork Harbour

Mean N concentration in adjacent seawater (mM)		Mean P concentration in adjacent seawater (mM)		Mean Chl concentration in adjacent seawater ($mg l^{-1}$)		Salinity in adjacent seawater (psu)
Winter	Summer	Winter	Summer	Winter	Summer	
19.87	8.70	0.63	0.30	2.34	5.52	34.0

Seasonal nutrient and chlorophyll concentrations are aggregated based on the data contained in Table 2.4.

Chl, chlorophyll; psu, practical salinity unit; summer, April to September, inclusive; winter, October to March, inclusive.

DCPM model inputs at the tidal boundary, taken from the equivalent MSN_WQ model in Table 2.4. Light attenuation values were derived for each water body using EPA Secchi disc monitoring data and the relation between Secchi disc readings and light attenuation given by Devlin *et al.* (2008).

2.3 Calibration

The MSN_WQ model as used here for comparison purposes was previously calibrated. Therefore, the reader is referred to Nash *et al*. (2011) for more information on model performance.

Calibration of the DCPM model of the Cork Harbour system entailed modification of the daily tidal exchange value, E (day^{-1}), to bring the salinity averages simulated by the DCPM model towards the averages derived from EPA monitoring data. Calibration proceeded from the tidal boundary towards the Lower Lee Estuary, and subsequently with consideration of the North Channel and Owenacurra Estuary.

Subsequently, the phytoplankton loss rate was modified from the default of $0.1\,day^{-1}$ to $0.125\,day^{-1}$ to bring the model-simulated seasonal averages closer to the observed values.

2.4 Comparison

Tables 2.7 and 2.8 summarise, respectively, DCPM and MSN_WQ model performance in the initial benchmarking test in Cork Harbour. In general, both models captured the variation in winter and summer nutrient concentration averages for each water body.

The most striking difference between the two models is the poor performance of the DCPM model with respect to summer average chlorophyll concentrations; the MSN_WQ model, in contrast, captured the order of magnitude of average chlorophyll concentrations from the Inner Cork Harbour upstream. The difference between the two models is possibly attributable to the following factors:

- In the MSN_WQ model, the relation between light attenuation and chlorophyll concentration would initially result in a rapid increase in chlorophyll concentration as conditions are favourable for growth of microalgae and phytoplankton. However, chlorophyll concentration becomes self-limiting as

Table 2.7. Comparison of seasonal average model nutrient loads in the Cork Harbour system prior to commissioning of Carrigrennan WWTP between EPA monitoring data and the DCPM model

	Mean DAIN (mM)				Mean DAIP (mM)				Mean Chl concentration (mg m^{-3})			
	Winter		Summer		Winter		Summer		Winter		Summer	
Water body	EPA	DCPM	EPA	DCPM	EPA	DCPM	EPA	DCPM	EPA	DCPM	EPA	DCPM
Outer Cork Harbour	28.57	11.90	3.57	4.10	0.65	0.72	0.17	0.18	1.00	2.70	6.62	6.20
Inner Cork Harbour	88.57	39.60	12.86	7.00	0.84	0.93	0.39	0.47	1.55	2.30	9.50	5.70
North Channel	70.00	63.20	36.40	54.70	0.94	1.08	0.84	1.03	5.64	1.70	12.00	2.40
Owenacurra Estuary	275.70	244.60	160.00	104.20	0.58	0.40	0.70	1.50	1.21	1.30	16.00	3.20
Lough Mahon	140.50	159.60	57.10	29.00	1.61	2.00	1.81	2.49	1.55	1.80	12.00	5.40
Glashaboy Estuary	468.20	327.40	229.30	49.20	1.61	2.10	1.87	2.61	1.21	0.60	7.50	1.90
Lower Lee Estuary	198.60	524.10	107.90	100.00	2.00	2.14	2.90	3.37	1.40	1.20	9.00	3.60

Chl, chlorophyll; Summer, April to September, inclusive; winter, October to March, inclusive.

Table 2.8. Comparison of seasonal average model nutrient loads in the Cork Harbour system prior to the commissioning of Carrigrennan WWTP between EPA monitoring data and the MSN_WQ model

	Mean DAIN (mM)				Mean DAIP (mM)				Mean Chl concentration (mg m^{-3})			
	Winter		Summer		Winter		Summer		Winter		Summer	
Water body	EPA	MSN_WQ	EPA	MSN_WQ	EPA	MSN_WQ	EPA	MSN_WQ	EPA	MSN_WQ	EPA	MSN_WQ
Outer Cork Harbour	28.57	11.80	3.57	5.60	0.65	0.61	0.17	0.20	1.00	0.80	6.62	5.50
Inner Cork Harbour	88.57	24.50	12.86	15.50	0.84	0.90	0.39	0.45	1.55	1.70	9.50	10.70
North Channel	70.00	55.90	36.43	34.20	0.94	1.10	0.84	0.80	5.64	4.30	12.00	10.30
Owenacurra Estuary	275.70	239.20	160.00	134.90	0.58	0.65	0.70	0.60	1.21	1.90	16.00	26.00
Lough Mahon	140.50	96.70	57.14	55.40	1.61	1.80	1.81	1.65	1.55	2.00	12.00	11.40
Glashaboy Estuary	468.20	402.60	229.20	225.20	1.61	1.70	1.87	2.10	1.21	1.50	7.50	8.40
Lower Lee Estuary	198.60	116.80	107.90	77.10	2.00	2.10	2.90	3.00	1.40	1.60	9.00	7.10

Chl, chlorophyll; Summer, April to September, inclusive; winter, October to March, inclusive.

it begins to build up in the water column. During suboptimal conditions caused by turbidity, growth still occurs, while advection of bloom chlorophyll could contribute to concentrations elsewhere. In the DCPM model, light attenuation coefficients were held constant and determined based on Secchi disc readings from the EPA.

- The DCPM model simulates growth of phytoplankton and macroalgae as a function of light, DAIN and DAIP, whereas in the MSN_WQ model, chlorophyll production is a function of NH_4, NO_3 and PO_4 as well as light, with an NH_4 preference factor included to partition growth due to NH_4 and NO_3.
- Owing to the extent of the Cork Harbour system and the complex exchanges that take place between neighbouring water bodies, the DCPM model may oversimplify exchange; the model disregards the physical constrictions on flow that exist between Lough Mahon and the North

Channel and the Inner Cork Harbour area. Although nutrient concentrations reflect solute transport, the physical exchange of chlorophyll may be incorrectly represented by the adopted exchange rates.

Both the DCPM model and the MSN_WQ model captured the spatial gradient between adjacent water bodies with respect to nitrogen and phosphorus concentrations, although chlorophyll concentrations were found to be more accurately simulated in the MSN_WQ model. Both models similarly underestimated winter DAIN towards the tidal boundary, in the Inner and Outer Cork Harbour areas. This is notable owing to the inclusion of winter DAIN in the trophic status assessment. The difference in the chlorophyll concentrations between the two sets of model results may be attributable to the more complex chlorophyll formulation in the MSN_WQ model, such as use of the site-specific light attenuation coefficient and the NH_4 preference factor. In the DCPM model, water is removed in bulk, as measured by the daily exchange coefficient, *E* (the fraction of the water body volume renewed on a daily basis), whereas the MSN_WQ model captures the exchange at local scale. Thus, chlorophyll at local scale may be retained in computational grid cells for longer, thereby allowing an increase in chlorophyll as a result of accumulation of nutrients by the same mechanism. The DCPM and MSN_WQ models are compared with EPA monitoring data in Tables 2.7 and 2.8. However, the EPA takes water samples at most three times during the summer and once during winter, whereas both models are run at time steps of the order of days or even seconds.

2.5 Conclusions

The proliferation of macroalgae in Cork Harbour is precluded by the infrequent exposure at spring low tide of the limited extent of suitable intertidal flats. Therefore, the Cork Harbour system and the associated complex exchange regime between neighbouring water bodies is ideal for benchmarking the simulation of chlorophyll growth in the DCPM tool. The DCPM tool simulates the growth of chlorophyll and macroalgae as a function of available DAIN, DAIP and light. The DCPM tool was benchmarked against the MSN_WQ water quality model, which has been iteratively improved and subjected to peer review. The nutrient loads and tidal boundary conditions attributed to the MSN_WQ model in Cork Harbour were applied to the DCPM model in a year-long benchmarking simulation. The results indicated that the MSN_WQ water quality model yielded a better representation of average water quality conditions, notably with respect to chlorophyll concentrations. The equivalent DCPM water quality model did not replicate the order of magnitude of chlorophyll concentrations in this application. We posit that this is due to the lack of a functional relationship between chlorophyll and light attenuation in the DCPM model. Moreover, chlorophyll concentration in the DCPM model is a function of DAIN, among other factors, whereas the MSN_WQ model simulates chlorophyll concentration as a function of both NO_3 and NH_4, with an NH_4 preference factor included.

3 DCPM Benchmark II: Dublin Bay and Adjoining Estuaries

3.1 Introduction

The DCPM model makes a number of trade-offs regarding macroalgae that restrict the relevance of the scenario simulations at local scale. Macroalgae are assumed to be retained in each box or subsystem in the DCPM model, whereas, in reality, macroalgae may be sloughed and advected. High bottom shear stress may make some sites unsuitable for establishment or ongoing survival of macroalgae patches (Aldridge and Trimmer, 2009). The areal extent of a macroalgae bloom, as a proportion of its available intertidal habitat, is central to compliance assessment, yet there is no functionality within the DCPM model to account for a change in the areal extent of the bloom as a consequence of changes in nutrient loads. The percentage of the area affected by macroalgae deposition above decaying macroalgae buried in excess of 3 cm into the sediment is also included in the compliance framework. This process is physically mediated and cannot be resolved within the DCPM model.

To proceed with benchmarking of the DCPM model against the MSN_WQ model, the interannual cycle of macroalgae growth and decay was incorporated into the pre-existing MSN_WQ model to allow comparison of the two models. The formulae adopted in the expanded MSN_WQ model were informed by a comprehensive literature review of previous macroalgae models. Further information on the MSN_WQ model and the macroalgae module formulae is included in Appendix 1. The resultant MSN_WQ model and the DCPM model were applied to Dublin Bay and the adjoining Tolka and Liffey estuaries, with applied loads pertaining to the period from 2010 to 2012.

Figure 3.1 presents Dublin Bay and the Liffey and Tolka estuaries. The Upper Liffey Estuary extends from Islandbridge Weir to Dublin City Custom House, and the downstream Lower Liffey Estuary extends from Dublin City Custom House to the mouth of the River Liffey adjacent to Poolbeg Lighthouse. The source of the River Liffey is Kippure in the Wicklow Mountains. The Liffey catchment comprises the majority of County

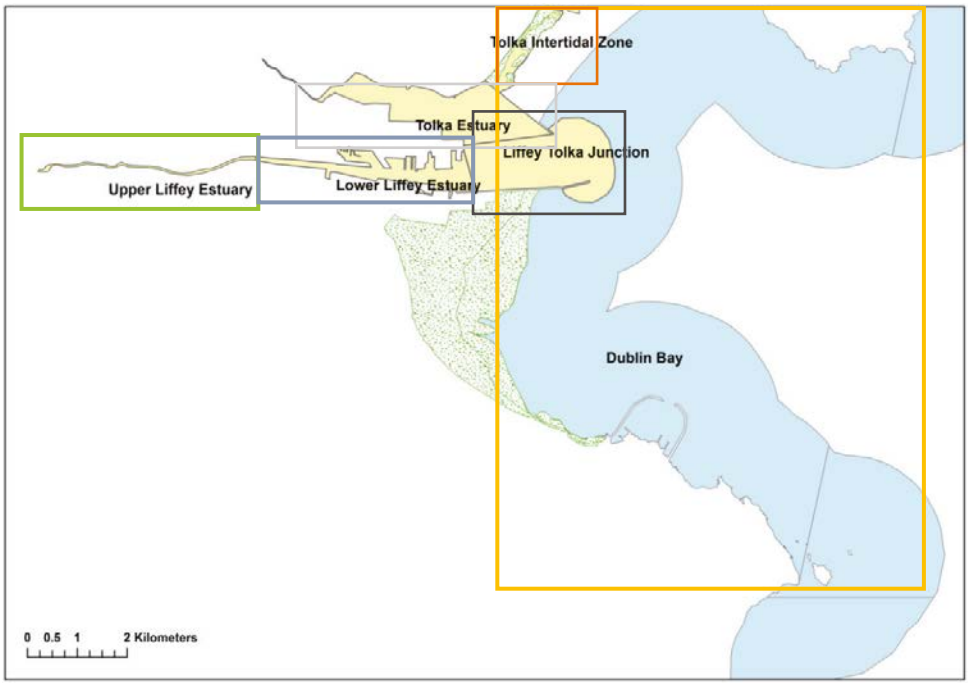

Figure 3.1. The Liffey and Tolka estuaries, their constituent subsections and Dublin Bay as defined for the DCPM model study.

Kildare, west County Wicklow, south County Dublin and the majority of Dublin City south of the River Tolka. The primary source of total nitrogen in the River Liffey is wastewater, followed by emissions from pasture (Ní Longphuirt *et al.*, 2016a). The Tolka Estuary spans from Fairview to the south of North Bull Island and north to the causeway that divides the north and south lagoons of North Bull Island. The River Tolka rises in Dunshaughlin, County Meath, and flows south-east towards the Tolka Estuary. Diffuse agriculture is the main contributor of nutrients north of the OSPAR monitoring point on the Tolka, while total nitrogen below the point is from diffuse urban sources (Ní Longphuirt *et al.*, 2016a).

Six water bodies have been defined, as labelled in Figure 3.1, for comparison purposes. The water body boundaries were a further development of the delineations used for the WFD. To accurately describe the growth of macroalgae in the Tolka Estuary, the intertidal zone of the Tolka Estuary, which is susceptible to annual opportunistic macroalgae blooms, was treated as a separate water body. The junction between the Liffey and the Tolka was also separated from the Lower Liffey Estuary as it receives flows from both streams.

3.2 MSN_WQ: Dublin

The expanded MSN_WQ model was applied to Dublin Bay to assess the functionality of the macroalgae growth module. As was the case with the Cork Harbour hydrodynamic model, the velocity, water elevation and wet/dry indices were averaged every half-hour throughout the spring–neap tidal cycle. A previously used MSN hydrodynamic model of Dublin Bay was carried over and modified such that the boundary hydrodynamic forcing at the north and south boundaries of the domain was tidal elevation with a temporal lag between high tides. The tidal lag between the north and south boundaries was tuned in order to match as closely as possible the tidal current data collected as part of the Dublin Bay Water Quality Management Plan (Mansfield, 1992). The optimum fit was established using a time lag of 6 minutes between Dun Laoghaire and Howth. The model bathymetry was discretised into 50-m grid cells. Figure 3.2 shows the tidal current direction and speed throughout the spring and neap ebb and flood tide at the current meter in Dublin Bay. The current speed and direction were better recreated by the model during the neap tide, with model and measurement following approximately the same path. During the spring tide, the model differed from the current meter data, with a longer ebb and shorter flood tide, while the magnitude of the current was lower within the model.

Floats were also released as part of the field studies completed for the Dublin Bay Water Quality Management Plan. Figure 3.3 presents the actual path taken by floats released on 3 May 1990 between 20 and 30 minutes before high tide. Figure 3.4 presents the path taken by particles released in the hydrodynamic model of Dublin Bay at the same stage of the tide. The prevailing conditions with respect to wind, tide and riverine inflow were recreated in the model. It can be seen in Figure 3.4 that the track followed by the particles released in the hydrodynamic model approximated the movements of the drogues presented in Figure 3.3.

The initial grid of water quality parameters for the MSN_WQ model was derived based on EPA monitoring data from throughout the Liffey and Tolka estuaries and Dublin Bay. Each water quality parameter was collated and regressed against collocated salinity values. The regression equations were derived for transitional and coastal waters, while the threshold salinity for using the coastal expression was identified by equating the expressions and solving for salinity. Table 3.1 gives the resultant expressions, which were subsequently applied to a salinity grid generated using the prevailing summer river flows.

The tidal boundary concentrations contained in Table 3.2 were also derived based on EPA monitoring data.

The treated effluent characteristics and discharge rates for Ringsend shown in Table 3.3 are averages taken from annual environment reports (AERs) for the facility for the years 2010, 2011, 2012 and 2014 (Dublin City Council, 2011, 2012, 2013; Irish Water, 2015b).

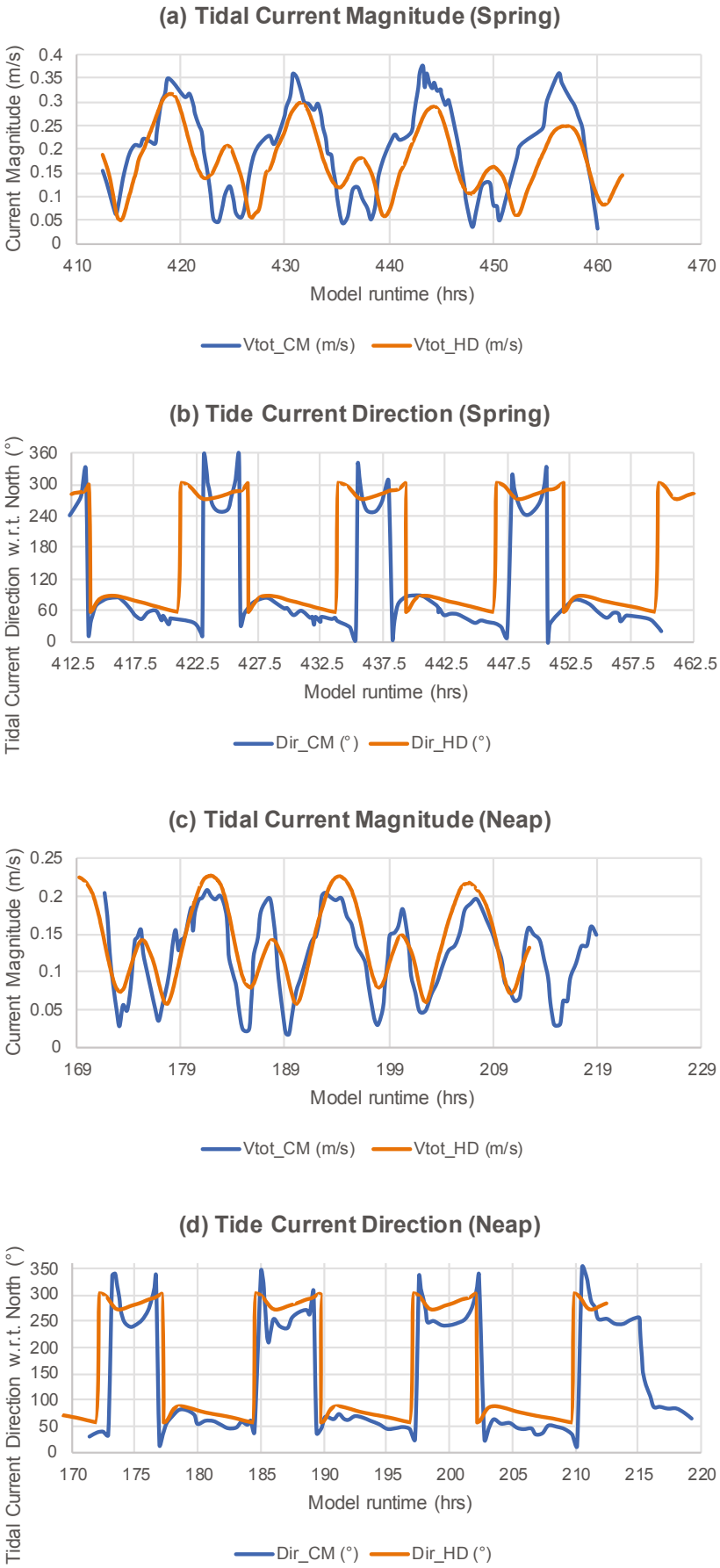

Figure 3.2. Spring and neap ebb and flood tidal current magnitude and direction, North Dublin Bay. The orange line indicates the numerical model result, while the blue line represents the tidal current meter data.

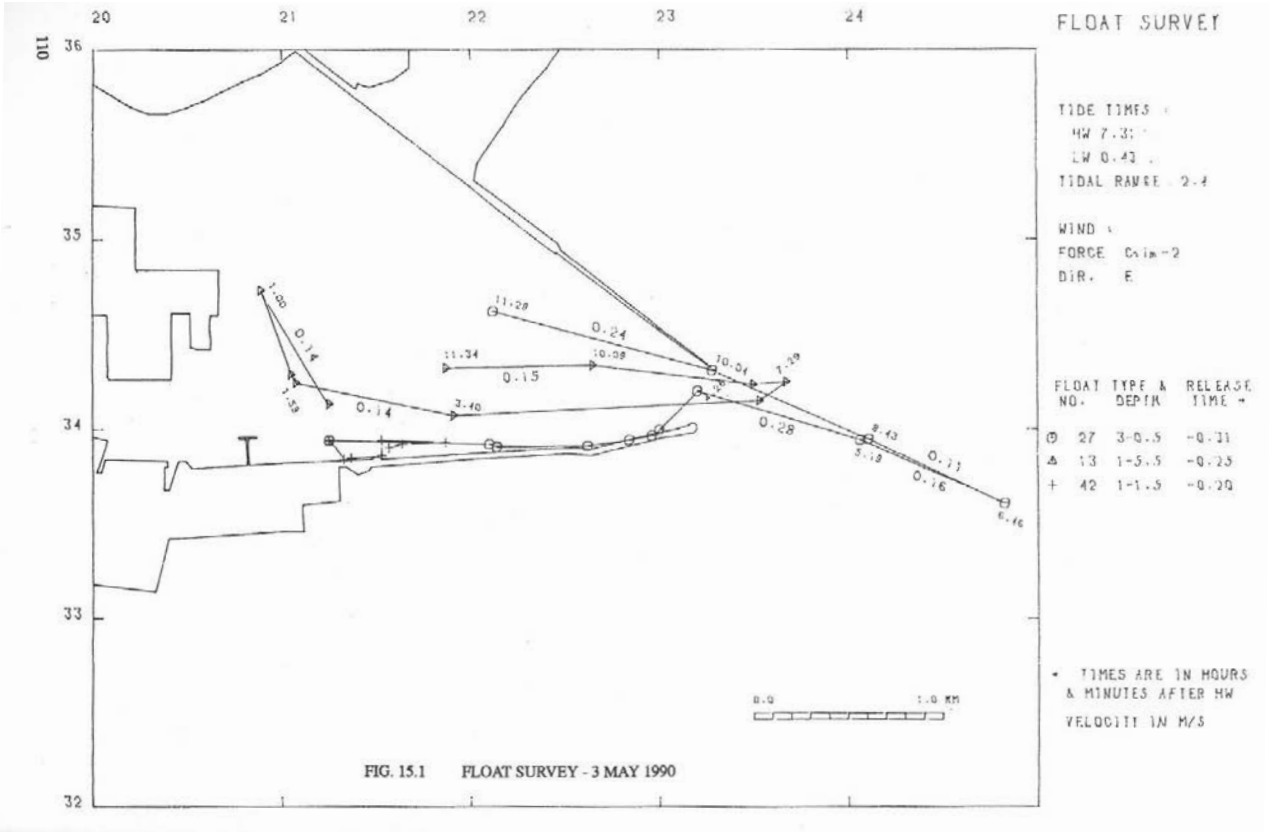

Figure 3.3. The path of three floats released on 3 May 1990 during fieldwork for the Dublin Bay Water Quality Management Plan.

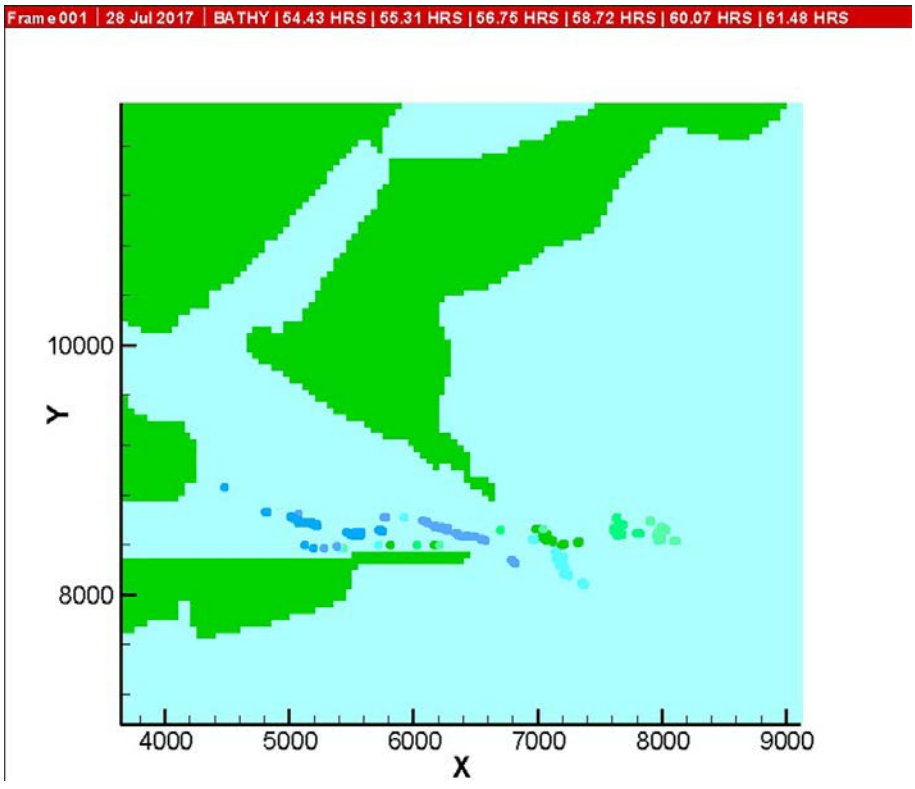

Figure 3.4. The path of particles released in the hydrodynamic model of Dublin Bay in a simulation of 3 May 1990. Atmospheric and riverine forcing conditions for the hydrodynamic simulation were taken from Mansfield (1992).

Table 3.1. The formulae utilised to generate the initial grid of water quality parameters for the Dublin Bay MSN_WQ model

Parameter	Freshwater → Transitional	Threshold (psu)	Transitional → Coastal
NH_4 (mg l^{-1})	0.097 – (SAL*0.00078)	20.5	0.1754 – (SAL*0.0046)
NO_3 (mg l^{-1})	2.4 – (SAL*0.07)	33.72	0.36 – (SAL*0.0095)
Chlorophyll (mg m^{-3})	12.19 – (SAL*0.24)	33.75	(SAL*0.276) – 5.23
DAIP (µg l^{-1})	48.4 – (SAL*0.27)	20.71	94.6 – (SAL*2.5)
BOD (mg l^{-1})	1.92 – (SAL*0.0244)		

The nine expressions were derived from monitoring data provided by the EPA for the Liffey and Tolka estuaries and Dublin Bay for the period spanning 2010–2012.

psu, practical salinity unit.

Table 3.2. The monthly tidal boundary conditions for the Dublin Bay MSN_WQ model

	Month											
Parameter	Jan	Feb	Mar	Apr	May	Jun	Jul	Aug	Sep	Oct	Nov	Dec
Salinity (psu)	33.5	33.5	33.5	33.8	33.8	33.8	33.8	33.8	33.8	33.5	33.5	33.5
BOD (mg l^{-1})	1.0	1.0	1.0	1.2	1.2	1.2	1.2	1.2	1.2	1.0	1.0	1.0
NH_4 (mg l^{-1})	0.05	0.05	0.05	0.01	0.01	0.01	0.01	0.01	0.01	0.05	0.05	0.05
NO_3 (mg l^{-1})	0.16	0.16	0.13	0.09	0.06	0.02	0.02	0.02	0.02	0.03	0.06	0.09
DO (mg l^{-1})	8.77	8.77	8.77	8.77	8.77	8.77	8.77	8.77	8.77	8.77	8.77	8.77
Chl (mg l^{-1})	0.0013	0.0018	0.0029	0.0059	0.0065	0.0025	0.0033	0.0058	0.0027	0.0012	0.0015	0.0012
DAIP (mg l^{-1})	0.0225	0.0220	0.0180	0.0130	0.0080	0.0030	0.0025	0.0025	0.0026	0.0042	0.0079	0.0130

Values were determined based on EPA monitoring data at DB510, DB540 and DB570 in Dublin Bay.

Chl, chlorophyll; DO, dissolved oxygen; psu, practical salinity unit.

Table 3.3. Details of average effluent characteristics for the WWTP discharging to Lower Liffey Estuary, determined from AERs

Flow rate ($m^3 s^{-1}$)	Salinity (psu)	BOD (mg l^{-1})	NH_4 (mg l^{-1})	NO_3 (mg l^{-1})	DO (mg l^{-1})	Chl (mg l^{-1})	DAIP (mg l^{-1})
5.00	0.00	15.23	8.40	5.04	0.00	0.00	2.50

Chl, chlorophyll; DO, dissolved oxygen; psu, practical salinity unit.

The riverine loadings to the system contained in Tables 3.4–3.8 were derived as follows:

- Liffey: hourly flow measurements at Leixlip provided by the Electricity Supply Board (ESB) were supplemented with EPA monitoring data collected at DB010.
- Tolka: daily flow measurements at the National Botanical Gardens in Glasnevin were supplemented with EPA monitoring data collected at DB300.
- Dodder: averaged annual OSPAR nutrient loading data from 2010 to 2014 were distributed throughout the year to follow the annual variation in nutrient loads and concentrations observed and interpolated for the Liffey.
- Camac and Poddle: Tolka monthly average flows were compared with flow percentiles made available by the EPA Hydrotools portal and the equivalent percentiles for each month were taken from the downloaded Camac and Poddle EPA Hydrotools spreadsheets. Nutrient concentrations for the Tolka were carried over.

Future refinements of the riverine inputs in Tables 3.4–3.8 for application in other modelling studies may include extrapolation of the nutrient loads from the

Table 3.4. Riverine inputs to the MSN_WQ model of the Liffey and Tolka estuaries and Dublin Bay from the River Liffey

	Parameter							
Month	Flow rate ($m^3 s^{-1}$)	Salinity (psu)	BOD ($mg l^{-1}$)	NH_4 ($mg l^{-1}$)	NO_3 ($mg l^{-1}$)	DO ($mg l^{-1}$)	Chl ($mg l^{-1}$)	DAIP ($mg l^{-1}$)
Jan	25.61	0.22	1.00	0.032	3.12	9.40	0.0008	0.022
Feb	24.62	0.26	1.00	0.032	3.12	9.40	0.0008	0.022
Mar	14.29	1.60	1.00	0.032	3.12	9.40	0.0008	0.022
Apr	6.26	3.00	1.00	0.025	3.38	8.12	0.0042	0.025
May	4.99	4.30	1.00	0.025	3.38	8.12	0.0042	0.025
Jun	3.64	8.30	1.00	0.025	3.38	8.12	0.0042	0.025
Jul	2.10	7.40	1.00	0.025	3.38	8.12	0.0042	0.025
Aug	2.58	3.80	1.00	0.025	3.38	8.12	0.0042	0.025
Sep	2.58	0.22	1.00	0.025	3.38	8.12	0.0042	0.025
Oct	4.99	0.22	1.00	0.032	3.12	9.40	0.0008	0.022
Nov	10.29	0.22	1.00	0.032	3.12	9.40	0.0008	0.022
Dec	20.40	0.22	1.00	0.032	3.12	9.40	0.0008	0.022

Data were derived from flow measurements provided by ESB International and the OSPAR Riverine Inputs and Direct Discharges (RID) programme and from EPA water quality measurements at the lowest salinity transitional monitoring point.

Chl, chlorophyll; DO, dissolved oxygen; psu, practical salinity unit.

Table 3.5. Riverine inputs to the MSN_WQ model of the Liffey and Tolka estuaries and Dublin Bay from the River Tolka

	Parameter							
Month	Flow rate ($m^3 s^{-1}$)	Salinity (psu)	BOD ($mg l^{-1}$)	NH_4 ($mg l^{-1}$)	NO_3 ($mg l^{-1}$)	DO ($mg l^{-1}$)	Chl ($mg l^{-1}$)	DAIP ($mg l^{-1}$)
Jan	2.72	0.00	1.00	0.032	2.38	9.40	0.0013	0.047
Feb	2.26	0.00	1.00	0.032	2.38	9.40	0.0013	0.047
Mar	1.25	0.00	1.00	0.032	2.38	9.40	0.0013	0.047
Apr	1.31	0.00	1.34	0.028	1.14	8.12	0.0039	0.088
May	1.05	0.00	1.34	0.028	1.14	8.12	0.0039	0.088
Jun	1.25	0.00	1.34	0.028	1.14	8.12	0.0039	0.088
Jul	1.20	0.00	1.34	0.028	1.14	8.12	0.0039	0.088
Aug	0.80	0.00	1.34	0.028	1.14	8.12	0.0039	0.088
Sep	1.46	0.00	1.34	0.028	1.14	8.12	0.0013	0.088
Oct	2.19	0.00	1.00	0.032	2.38	9.40	0.0013	0.047
Nov	2.67	0.00	1.00	0.032	2.38	9.40	0.0013	0.047
Dec	2.76	0.00	1.00	0.032	2.38	9.40	0.0013	0.047

Data were derived from flow measurements provided by ESB International and the OSPAR RID programme and from EPA water quality measurements at the lowest salinity transitional monitoring point.

Chl, chlorophyll; DO, dissolved oxygen; psu, practical salinity unit.

Table 3.6. Riverine inputs to the MSN_WQ model of the Liffey and Tolka estuaries and Dublin Bay from the River Camac

Month	Parameter							
	Flow rate ($m^3 s^{-1}$)	Salinity (psu)	BOD ($mg l^{-1}$)	NH_4 ($mg l^{-1}$)	NO_3 ($mg l^{-1}$)	DO ($mg l^{-1}$)	Chl ($mg l^{-1}$)	DAIP ($mg l^{-1}$)
Jan	2.14	0.00	1.00	0.032	2.38	9.40	0.0013	0.047
Feb	1.53	0.00	1.00	0.032	2.38	9.40	0.0013	0.047
Mar	0.81	0.00	1.00	0.032	2.38	9.40	0.0013	0.047
Apr	0.49	0.00	1.34	0.028	1.14	8.12	0.0039	0.088
May	0.39	0.00	1.34	0.028	1.14	8.12	0.0039	0.088
Jun	0.32	0.00	1.34	0.028	1.14	8.12	0.0039	0.088
Jul	0.16	0.00	1.34	0.028	1.14	8.12	0.0039	0.088
Aug	0.26	0.00	1.34	0.028	1.14	8.12	0.0039	0.088
Sep	0.26	0.00	1.34	0.028	1.14	8.12	0.0013	0.088
Oct	0.39	0.00	1.00	0.032	2.38	9.40	0.0013	0.047
Nov	0.65	0.00	1.00	0.032	2.38	9.40	0.0013	0.047
Dec	1.05	0.00	1.00	0.032	2.38	9.40	0.0013	0.047

Data were derived from flow measurements provided by ESB International and the OSPAR RID programme and from EPA water quality measurements at the lowest salinity transitional monitoring point.

Chl, chlorophyll; DO, dissolved oxygen; psu, practical salinity unit.

Table 3.7. Riverine inputs to the MSN_WQ model of the Liffey and Tolka estuaries and Dublin Bay from the River Poddle

Month	Parameter							
	Flow rate ($m^3 s^{-1}$)	Salinity (psu)	BOD ($mg l^{-1}$)	NH_4 ($mg l^{-1}$)	NO_3 ($mg l^{-1}$)	DO ($mg l^{-1}$)	Chl ($mg l^{-1}$)	DAIP ($mg l^{-1}$)
Jan	0.69	0.00	1.00	0.032	2.38	9.40	0.0013	0.047
Feb	0.45	0.00	1.00	0.032	2.38	9.40	0.0013	0.047
Mar	0.20	0.00	1.00	0.032	2.38	9.40	0.0013	0.047
Apr	0.14	0.00	1.34	0.028	1.14	8.12	0.0039	0.088
May	0.11	0.00	1.34	0.028	1.14	8.12	0.0039	0.088
Jun	0.09	0.00	1.34	0.028	1.14	8.12	0.0039	0.088
Jul	0.05	0.00	1.34	0.028	1.14	8.12	0.0039	0.088
Aug	0.07	0.00	1.34	0.028	1.14	8.12	0.0039	0.088
Sep	0.07	0.00	1.34	0.028	1.14	8.12	0.0013	0.088
Oct	0.11	0.00	1.00	0.032	2.38	9.40	0.0013	0.047
Nov	0.18	0.00	1.00	0.032	2.38	9.40	0.0013	0.047
Dec	0.28	0.00	1.00	0.032	2.38	9.40	0.0013	0.047

Data were derived from flow measurements provided by ESB International and the OSPAR RID programme and from EPA water quality measurements at the lowest salinity transitional monitoring point.

Chl, chlorophyll; DO, dissolved oxygen; psu, practical salinity unit.

Table 3.8. Riverine inputs to the MSN_WQ model of the Liffey and Tolka estuaries and Dublin Bay from the River Dodder

	Parameter							
Month	Flow rate ($m^3 s^{-1}$)	Salinity (psu)	BOD ($mg\,l^{-1}$)	NH_4 ($mg\,l^{-1}$)	NO_3 ($mg\,l^{-1}$)	DO ($mg\,l^{-1}$)	Chl ($mg\,l^{-1}$)	DAIP ($mg\,l^{-1}$)
Jan	8.30	0.00	1.00	0.025	0.83	9.40	0.0013	0.007
Feb	6.36	0.00	1.00	0.027	0.90	9.40	0.0013	0.007
Mar	3.06	0.00	1.00	0.031	1.03	9.40	0.0013	0.008
Apr	1.64	0.00	1.00	0.053	0.97	8.12	0.0039	0.031
May	1.28	0.00	1.00	0.054	0.99	8.12	0.0039	0.031
Jun	1.00	0.00	1.00	0.083	1.53	8.12	0.0039	0.048
Jul	0.27	0.00	1.00	0.090	1.65	8.12	0.0039	0.052
Aug	0.55	0.00	1.00	0.097	1.78	8.12	0.0039	0.056
Sep	0.55	0.00	1.00	0.177	3.24	8.12	0.0013	0.102
Oct	1.28	0.00	1.00	0.129	4.33	9.40	0.0013	0.035
Nov	2.39	0.00	1.00	0.085	2.84	9.40	0.0013	0.023
Dec	4.32	0.00	1.00	0.048	1.62	9.40	0.0013	0.013

Data were derived from flow measurements provided by ESB International and the OSPAR RID programme and from EPA water quality measurements at the lowest salinity transitional monitoring point.

DO, dissolved oxygen; psu, practical salinity unit.

Dodder to the Camac and Poddle, as the land use in the three catchments is similar. Flows from Office of Public Works station 09010 at Waldron's Bridge might also be used for monthly flow discharges for the River Dodder.

3.2.1 Sensitivity analysis

The expanded MSN_WQ model was run with different submodules activated to establish the importance of different functionalities. The reader is referred to Appendix 1 for further information on the equations referenced throughout this section. Tables 3.9 and 3.10 contain the default parameters which were utilised throughout the model sensitivity analysis. The model was run to represent an average summer. The time series of macroalgae wet weights throughout the summer are presented for comparison in the following subsections. Although the time series has not been compared with macroalgae monitoring data, each figure gives an indication of the impact of different expressions and parameters upon the evolution of the macroalgae bloom throughout an average summer.

Alternative temperature dependence formulae

Two temperature dependence formulae were implemented in the macroalgae module in the MSN_WQ model: equations A1.27 and A1.36. The values for ζ and θ used in equation A1.27 were 0.3 and 12.5, respectively, while the values for k_1, k_4, T_{opt}, T_{min}, T_{max}, Opt_{min} and Opt_{max} in equation A1.36 were 0.3, 0.01, 18°C, 6°C, 28°C, 21°C and 28°C, respectively. Figure 3.5 presents the effect of the two different expressions. Equation A1.36 results in a substantially larger bloom than equation A1.27. Parameters k_1 and k_4 control the shape of the growth function throughout the range of temperatures. Although accurate quantification of these parameters would necessitate detailed growth studies in controlled environments, nonetheless the expression has been built into the MSN_WQ model for later use. The bloom magnitude in the Tolka Estuary has generally been observed in the range of 40–100 tonnes in recent years. Using equation A1.27 brought the bloom magnitude closer to the expected order of magnitude.

Imposition of bed capacity limit

Figure 3.6 presents the impact of imposing an upper limit on the macroalgae bloom density, as implemented in the DCPM model. Applying a bed capacity limit of $150\,g\,dw\,m^{-2}$ further corrects the magnitude of the bloom towards the expected order of magnitude.

Table 3.9. The parameters and coefficients used in the Dublin Bay MSN_WQ model pertaining to the nitrogen and phosphorus cycles, dissolved oxygen production and uptake and photosynthetic properties in *Ulva* and phytoplankton

Value	Unit	Parameter
0.23	day^{-1}	Decay rate for BOD via deoxygenation
0.10	day^{-1}	Decay rate for BOD via settling loss
0.12	day^{-1}	Decay rate for biological oxidation of NH_4
6.36	mg N g^{-1} Chl	Nitrogen fraction of algal chlorophyll
0.06	mg l^{-1}	Phytoplankton half-saturation constant for nitrogen
0.08	mg l^{-1}	*Ulva* half-saturation constant for nitrogen
2.00	mg l^{-1}	Half-saturation DO-limiting constant
1.00	mg m^{-2} d^{-1}	Sediment oxygen demand rate
3.50	mg DO g^{-1} NH_4	Rate of oxygen uptake per unit of NH_4
0.13	mg DO g^{-1} Chl	DO production per unit of chlorophyll
0.10	mg DO g^{-1} Chl	DO uptake per unit of chlorophyll
2.00	day^{-1}	Maximum algae growth rate at reference temperature
22.00	W m^{-2}	Light level at which phytoplankton growth is half of the maximum rate
0.01	mg l^{-1}	Phytoplankton half-saturation constant for phosphorus
0.01	mg l^{-1}	*Ulva* half-saturation constant for phosphorus
0.16	day^{-1}	Rate of respiration plus excretion
0.20	m d^{-1}	Algae (chlorophyll) settling velocity
0.62	mg P g^{-1} Chl	Phosphorus fraction of algal chlorophyll
24.40	mg N g^{-1} dw	Nitrogen fraction of *Ulva*
1600.00	mg DO g^{-1} dw	DO production per unit of *Ulva*
1950.00	mg DO g^{-1} dw	DO uptake per unit of *Ulva*
0.45	day^{-1}	Maximum *Ulva* growth rate at reference temperature
25.00	W m^{-2}	Light level at which *Ulva* growth is half of the maximum rate
0.03	day^{-1}	Rate of *Ulva* respiration plus excretion (per day)
3.38	g ww g^{-1} dw	Conversion of dry weight to wet weight
5.00	g dw m^{-2}	Winter *Ulva* biomass density
1.49	mg P g^{-1} dw	Phosphorus fraction of *Ulva*
130.00	W m^{-2}	Saturation irradiance for phytoplankton
135.00	W m^{-2}	Saturation irradiance for *Ulva*
0.44	W m^{-2}	Compensation irradiance for *Ulva*
0.02	g C g^{-1} dw d^{-1} [(W m^{-2})$^{-1}$]	Photosynthetic efficiency of *Ulva*
0.03	mg Chl mg^{-1} C	Chlorophyll yield
3.33	g dw g^{-1} C	*Ulva* yield

DO, dissolved oxygen; dw, dry weight; ww, wet weight.

Macroalgae tissue nitrogen and phosphorus concentrations

To establish the impact of different initial tissue nitrogen and phosphorus concentrations on the evolution of the macroalgae bloom itself and the internal tissue nutrient concentrations, four permutations of maximum (38 mg N g^{-1} dw, 3.375 mg P g^{-1} dw) and minimum (17.5 mg N g^{-1} dw, 1.67 mg P g^{-1} dw) tissue nitrogen and phosphorus concentrations were tested alongside the default values (27.5 mg N g^{-1} dw, 2.5 mg P g^{-1} dw). Figures 3.7–3.9 present the impact. In summary, there is no impact on the bloom evolution, and the tissue nitrogen and phosphorus concentrations converge to approximately constant values after 6 weeks.

Table 3.10. The parameters and coefficients used in the Dublin Bay MSN_WQ model pertaining to the influence of salinity, dissolved oxygen, temperature, shear stress and tissue nitrogen and phosphorus concentrations on the growth of *Ulva*

Parameter no.	Unit	Description
20.00	psu	Optimum salinity (range: 20–30)
15.00	psu	Minimum salinity
34.00	psu	Maximum salinity
0.30	$°C^{-1}$	*Ulva* temperature coefficient
12.50	°C	*Ulva* reference temperature (optimum)
0.30	$°C\,d^{-1}$	Maximum magnitude of acclimatisation
0.00	None	Acclimatisation rate coefficient
0.50	None	Maximum temperature reduction factor
15.00	°C	Minimum optimum temperature for *Ulva*
21.00	°C	Maximum optimum temperature for *Ulva*
6.00	°C	Minimum tolerable temperature for *Ulva*
28.00	°C	Maximum tolerable temperature for *Ulva*
18.00	°C	Starting value for temperature dependence
0.30	None	K_1 temperature rate multiplier
0.01	None	K_4 temperature rate multiplier
150.00	$g\,dw\,m^{-2}$	K_b upper *Ulva* density limit
0.25	$N\,m^{-2}$	*Ulva* critical shear stress
0.10	None	Transition in inhibition of growth due to shear stress
17.5	$mg\,N\,g^{-1}\,dw$	Minimum tissue nitrogen concentration
38	$mg\,N\,g^{-1}\,dw$	Maximum tissue nitrogen concentration
1.67	$mg\,P\,g^{-1}\,dw$	Minimum tissue phosphorus concentration
3.375	$mg\,P\,g^{-1}\,dw$	Maximum tissue phosphorus concentration
3.13	$mg\,N\,g^{-1}\,d\,h^{-1}$	Maximum rate of NH_4 uptake in *Ulva*
1.10	$mg\,N\,g^{-1}\,d\,h^{-1}$	Maximum rate of NO_3 uptake in *Ulva*
0.66	$mg\,P\,g^{-1}\,dw\,h^{-1}$	Maximum rate of PO_4 uptake in *Ulva*
0.45	$mg\,N\,l^{-1}$	Half-saturation constant for NH_4 uptake
0.38	$mg\,N\,l^{-1}$	Half-saturation constant for NO_3 uptake
0.06	$mg\,P\,l^{-1}$	Half-saturation constant for PO_4 uptake
0.03	day^{-1}	Basal *Ulva* decay rate without oxygen stress
–0.16	None	Power rate of basal decay
0.15	None	Oxygen-related decay contribution
2.50	$mg\,DO\,g^{-1}\,dw\,h^{-1}$	*Ulva* respiration rate
2.00	None	Coefficient for temperature dependence of maximum growth
0.20	$°C^{-1}$	*Ulva* respiration temperature coefficient
10.00	°C	*Ulva* reference respiration temperature
20.00	°C	Reference temperature for maximum *Ulva* growth
10.00	°C	Reference temperature for maximum *Ulva* loss

DO, dissolved oxygen; dw, dry weight; psu, practical salinity unit.

Imposition of bed stress limits

Imposition of bed stress limits to the macroalgae growth function may reflect the influence on macroalgae growth of an inhospitable environment and conditions. To assess the potential impact of applying a bed stress limit, three values for the upper shear stress limit τ_{max} and growth inhibition coefficient δ were assessed. δ values can range from 0 to 1, with 0 indicating absolute growth inhibition, and 1 indicating no inhibition. The default τ_{max} and δ were $0.25\,N\,m^{-2}$ and 0.1, while the minimum and maximum

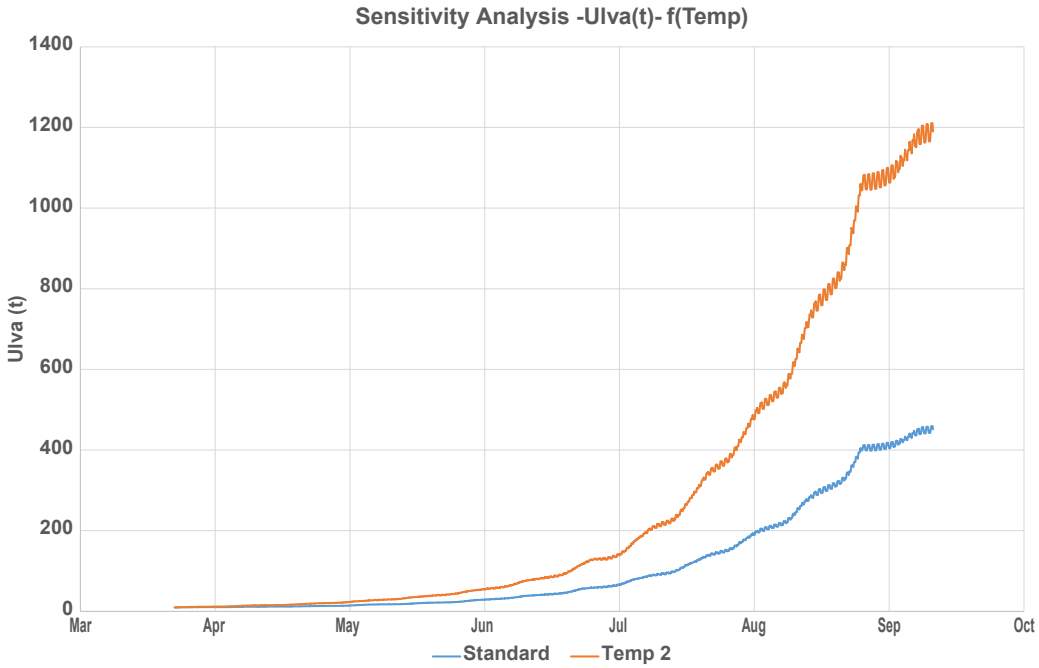

Figure 3.5. A comparison between the time series of macroalgae bloom in the Tolka Estuary simulated by the MSN_WQ model utilising equation A1.27 (Standard) and equation A1.36 (Temp2).

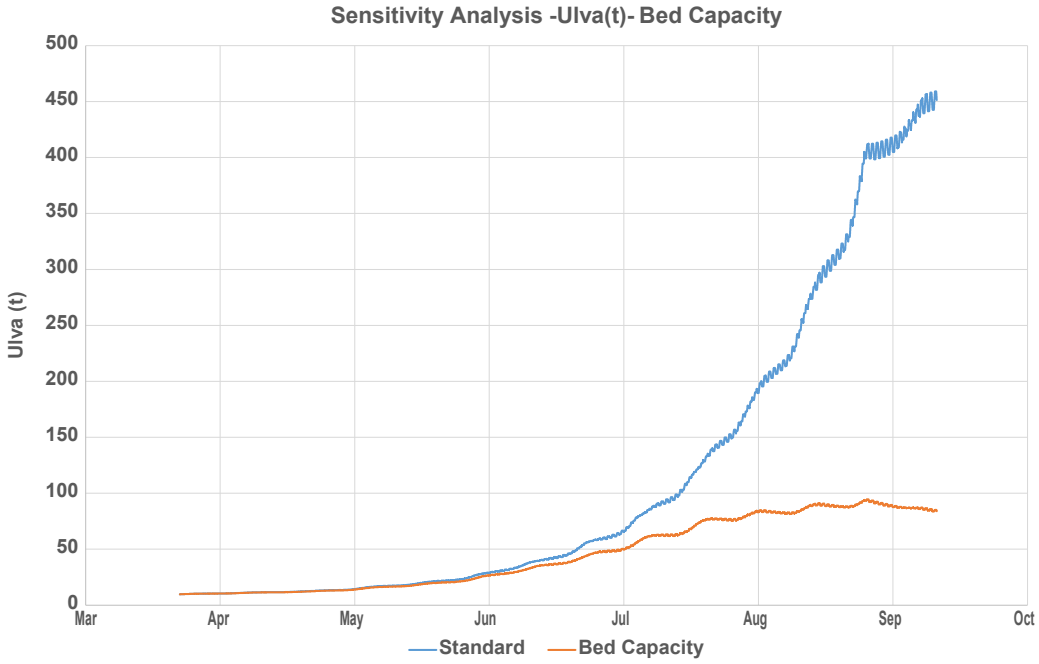

Figure 3.6. A comparison between the time series of macroalgae bloom simulated by the MSN_WQ model in the Tolka Estuary with and without imposition of a bed capacity limit of 150 g dw m^{-2}.

τ_{max} were 0.14 and 2.5, respectively, and the minimum and maximum δ values were 0.05 and 1, respectively. Figure 3.10 presents the impact of applying an upper bed stress limit to control macroalgae growth. Imposition of the bed stress limit function on macroalgae growth with the default parameters had a significant impact on bloom magnitude, while lowering the δ value to 0.05 reduced the macroalgae bloom further still. Increasing the bed stress limit to 2.5 N m^{-2} facilitated a large growth of macroalgae. Figures 3.11 and 3.12 give an indication of the consequences of different bed stress tolerances on tissue nutrient

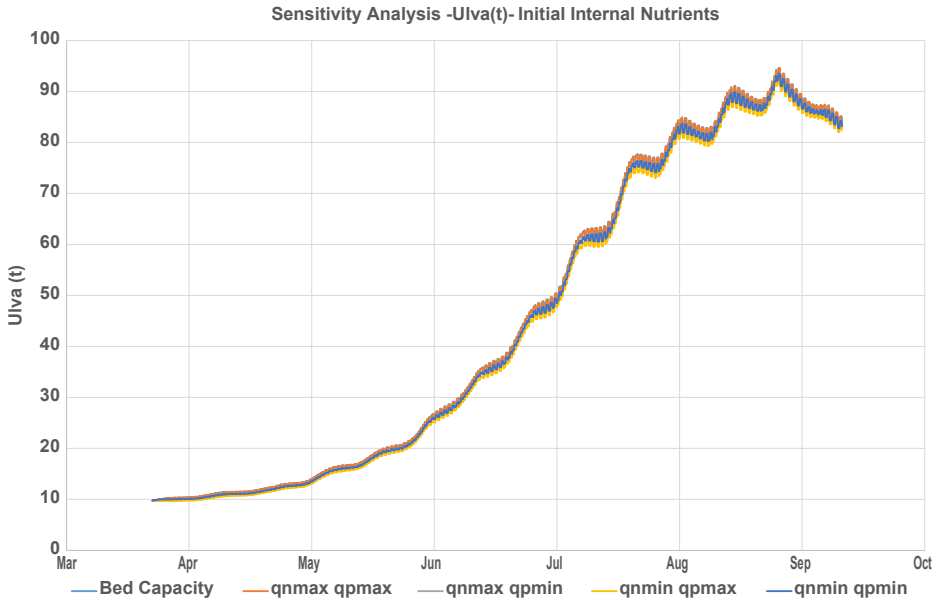

Figure 3.7. Comparison of the macroalgae blooms simulated by the MSN_WQ model at different initial tissue nitrogen and phosphorus concentrations. The "bed capacity" line, using average macroalgae nitrogen and phosphorus concentrations (27.5 mg N g^{-1} dw, 2.5 mg P g^{-1} dw), provides a baseline for comparison. The other four lines are permutations of tissue macroalgae nitrogen and phosphorus concentrations, where qnmin and qnmax are the lower and upper macroalgae tissue nitrogen concentrations taken from the literature (17.5 mg N g^{-1} dw, 38 mg N g^{-1} dw), and qpmin and qpmax are the lower and upper macroalgae tissue phosphorus concentrations taken from the literature (1.67 mg P g^{-1} dw, 3.37 mg P g^{-1} dw).

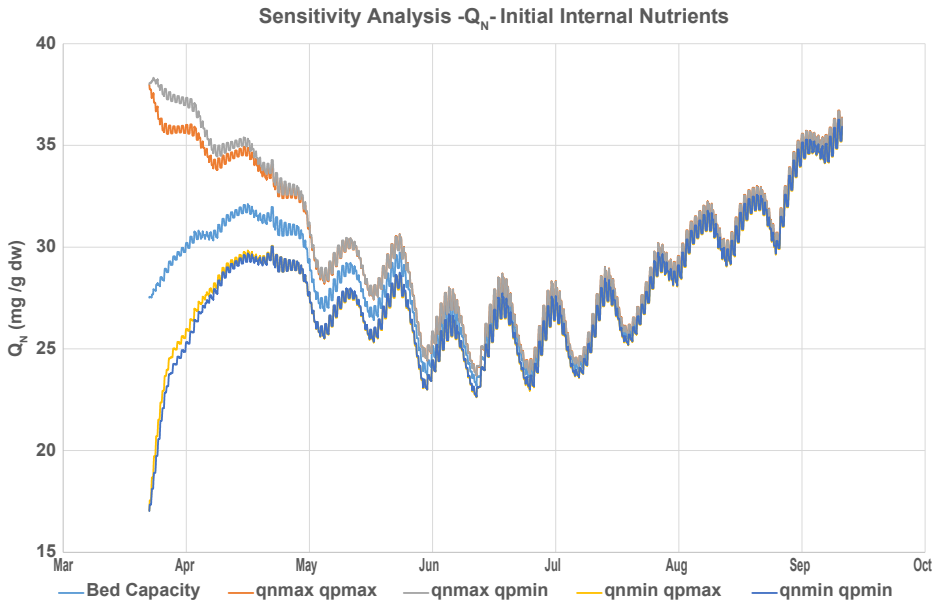

Figure 3.8. Comparison of the evolving tissue nitrogen concentrations in the macroalgae blooms simulated by the MSN_WQ model at different initial tissue nitrogen and phosphorus concentrations. The "bed capacity" line, using the average macroalgae nitrogen and phosphorus concentrations (27.5 mg N g^{-1} dw, 2.5 mg P g^{-1} dw), provides a baseline for comparison. The other four lines are permutations of tissue macroalgae nitrogen and phosphorus concentrations, where qnmin and qnmax are the lower and upper macroalgae tissue nitrogen concentrations taken from the literature (17.5 mg N g^{-1} dw, 38 mg N g^{-1} dw), and qpmin and qpmax are the lower and upper macroalgae tissue phosphorus concentrations taken from the literature (1.67 mg P g^{-1} dw, 3.375 mg P g^{-1} dw).

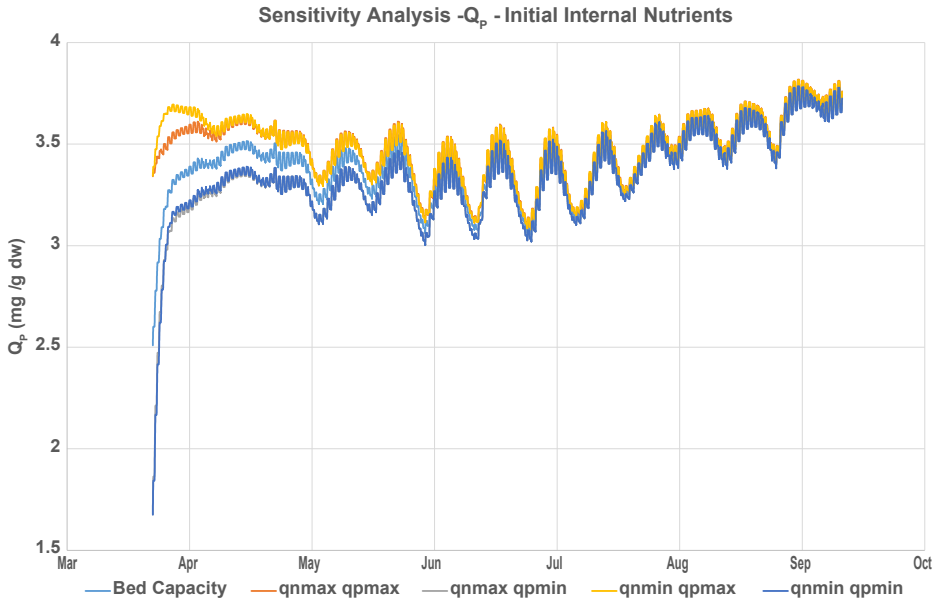

Figure 3.9. Comparison of the evolving tissue phosphorus concentrations in the macroalgae bloom simulated by the MSN_WQ model at different initial tissue nitrogen and phosphorus concentrations. The "bed capacity" line, using the average macroalgae nitrogen and phosphorus concentrations (27.5 mg N g^{-1} dw, 2.5 mg P g^{-1} dw), provides a baseline for comparison. The four other lines are four permutations of tissue macroalgae nitrogen and phosphorus concentrations, where qnmin and qnmax are the lower and upper macroalgae tissue nitrogen concentrations taken from the literature (17.5 mg N g^{-1} dw, 38 mg N g^{-1} dw), and qpmin and qpmax are the lower and upper macroalgae tissue phosphorus concentrations taken from the literature (1.67 mg P g^{-1} dw, 3.375 mg P g^{-1} dw).

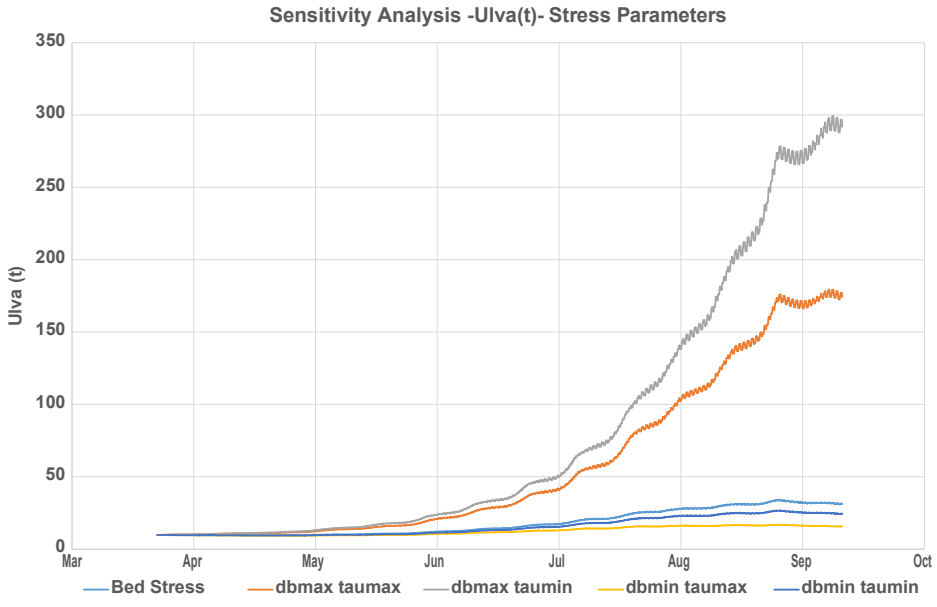

Figure 3.10. Comparison of the evolving macroalgae bloom tonnage simulated by the MSN_WQ model in the Tolka Estuary with varying bed stress limitation parameters. The "bed stress" line, using the default T_{max} (tau) and δ (db) values (0.25 N m^{-2}, 0.1), provides a baseline for comparison. The other four lines are permutations of higher and lower values for T_{max} and δ. The minimum and maximum τ_{max} values adopted were 0.14 N m^{-2} and 2.5 N m^{-2}, respectively, and the minimum and maximum δ values adopted were 0.05 and 1, respectively.

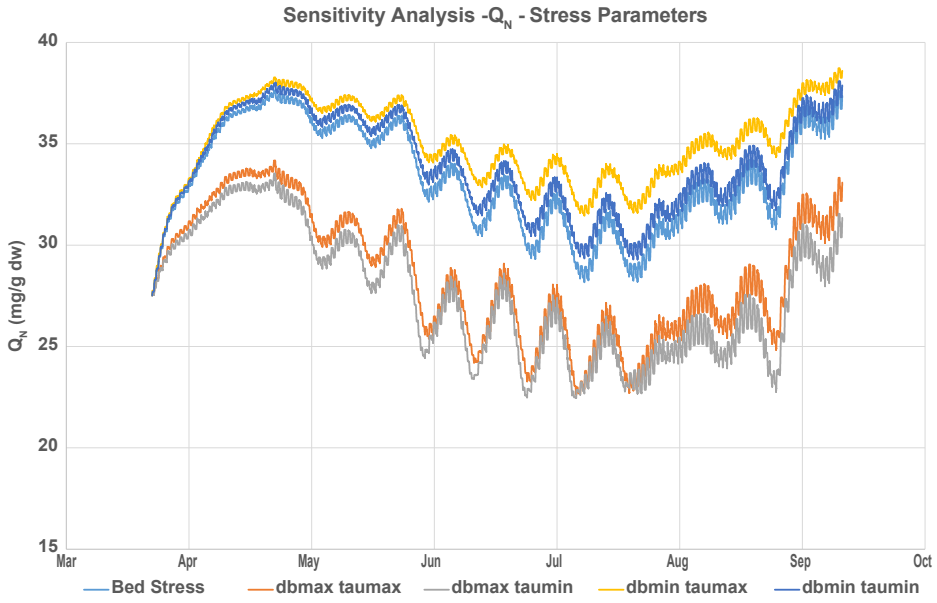

Figure 3.11. Comparison of the evolving macroalgae tissue nitrogen concentration time series simulated by the MSN_WQ model in the Tolka Estuary with varying bed stress limitation parameters. The "bed stress" line, using the default T_{max} (tau) and δ (db) values (0.25 N m^{-2}, 0.1), provides a baseline for comparison. The other four lines are permutations of higher and lower values for T_{max} and δ. The minimum and maximum τ_{max} values adopted were 0.14 N m^{-2} and 2.5 N m^{-2}, respectively, and the minimum and maximum δ values adopted were 0.05 and 1, respectively.

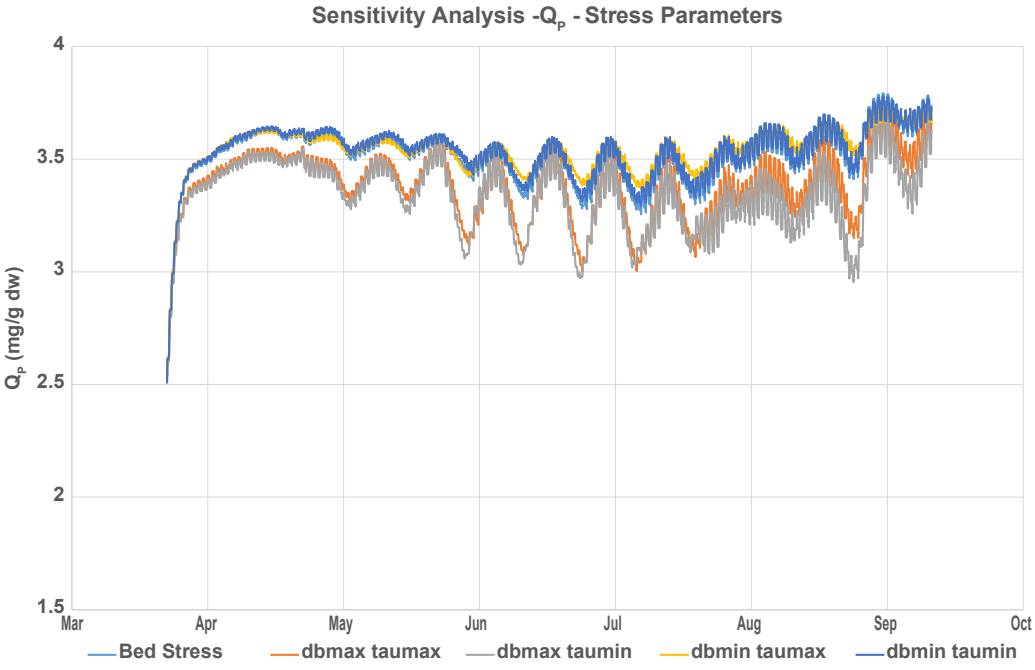

Figure 3.12. Comparison of the evolving macroalgae tissue phosphorus concentration time series simulated by the MSN_WQ model in the Tolka Estuary with varying bed stress limitation parameters. The "bed stress" line, using the default T_{max} (tau) and δ (db) values (0.25 N m^{-2}, 0.1), provides a baseline for comparison. The other four lines are permutations of higher and lower values for T_{max} and δ. the minimum and maximum τ_{max} values adopted were 0.14 N m^{-2} and 2.5 N m^{-2}, respectively, and the minimum and maximum δ values adopted were 0.05 and 1, respectively.

concentrations. Relatively uninhibited growth results in depletion of tissue nutrients, while tissue nutrients may accumulate when unsuitable bed stresses limit growth.

Imposition of salinity control

The rate of growth of macroalgae (Kamer and Fong, 2000) and macroalgae zoospores (Imchen, 2012) has been previously reported to be sensitive to ambient salinity concentrations (measured in practical salinity units, psu). Consequently, a functional expression to describe the limiting influence of salinity on macroalgae growth was built into the expanded MSN_WQ water quality model. To assess the impact of applying a salinity control on macroalgae growth, equations A1.44 and A1.45 were incorporated into the macroalgae growth function. The values for optimum salinity and upper and lower tolerable salinity were taken from Martins *et al.* (1999, 2007) and Martins and Marques (2002). In the absence of adequate peer-reviewed information on salinity sensitivity of *Ulva* spp., salinity sensitivity parameters relevant to a variant of *Ulva* spp., *Enteromorpha intestinalis*, were used. An optimum salinity of 20 psu was used, while the minimum and maximum tolerable salinities were taken as 15 psu and 34 psu, respectively. The expression was applied to the standard macroalgae growth function, without imposition of an upper bed capacity or bed stress limit. Figure 3.13 presents the outcome of applying such a salinity control.

Imposition of a salinity control on the growth of macroalgae reduced the size of the macroalgae bloom by an order of magnitude. Although the salinity sensitivity parameters were within the range of values that might reasonably be expected in most estuaries, there was a notable disparity between the summer average salinity concentrations generated by the MSN_WQ model (Table 3.10) and the average summer salinity concentrations determined from EPA monitoring data in each water body in the domain, with the exception of Dublin Bay.

3.2.2 MSN_WQ: seasonal average nutrient concentrations

Owing to the lack of information regarding macroalgae salinity sensitivity and optimum bed stress conditions, the accepted final MSN_WQ macroalgae model retained the growth expression as a function of internal tissue nitrogen and phosphorus, the bed carrying capacity and the standard temperature formulation. The resultant model was used for benchmarking against the DCPM model in Dublin Bay.

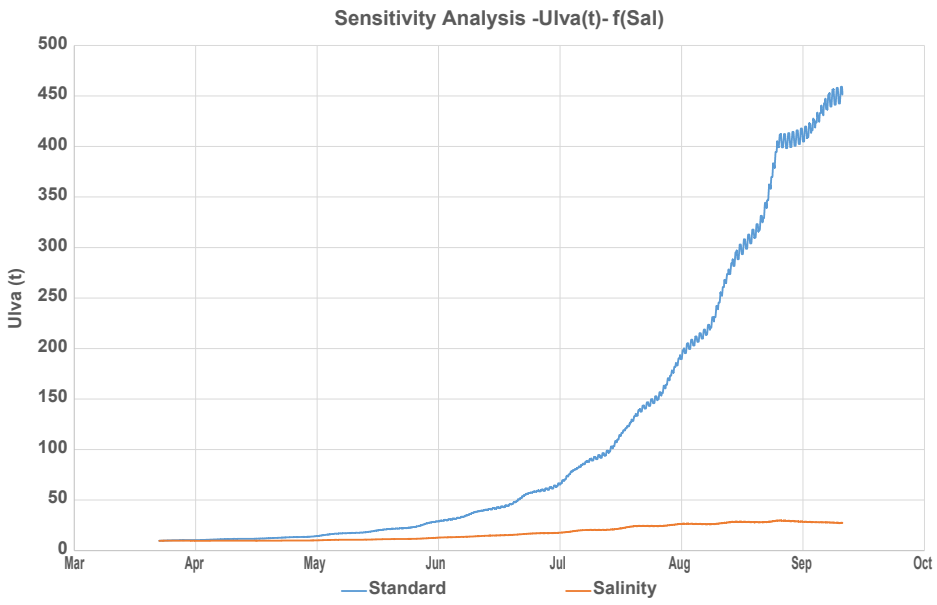

Figure 3.13. Comparison of the evolving simulated macroalgae bloom tonnage time series generated by the MSN_WQ model with and without imposing a growth-limiting salinity function on the macroalgae growth equation. The standard time series was generated using a macroalgae growth expression that was a function of internal tissue nitrogen and phosphorus concentrations and water column temperature.

Nutrients and chlorophyll were observed to accumulate upstream of the mouth of the Liffey Estuary, reflecting the limitations of applying the depth-integrated MSN_WQ model to the complex system comprising the Liffey and Tolka estuaries and their interface with Dublin Bay. The accumulation of the nutrients is reflected in the seasonal average concentrations as presented in Table 3.11. This may be attributed to depth integration of the Navier–Stokes equations, which is a characteristic of the MSN_WQ model. The main consequence of depth integration of the Navier–Stokes equations is that the vertical stratification and mixing that occurs at the interface of freshwater and saline waters is not resolved. As a result, the intensity of the incoming tidal current, which is assumed uniform throughout the water column, prevents the release of freshwater flow through the mouth of the Lower Liffey Estuary. The freshwater flows from the rivers entering Dublin Bay ought to remain in the upper stratum of the water column.

3.3 DCPM: Dublin

For benchmarking purposes, the six contiguous water bodies that were used for areal and seasonal averaging of parameter values in the preceding section were considered in the equivalent DCPM model. Digitised Admiralty chart data pertaining to Dublin Bay were used to derive the depth bins for each water body.

The riverine nutrient loadings as defined for the Dublin MSN_WQ model were summarised to the equivalent input data as required by the DCPM model. The relevant input data are given in Table 3.12. Nitrogen and phosphorus loads are described as annual average loadings, with the ratio of summer to annual loading, R_{SA}, specified to fit loadings to normalised annual curves, whilst river discharges are specified as long-term annual averages and, like the nutrient loadings, the summer to annual ratio is also specified.

Table 3.11. The summer average salinity, nutrient concentrations and macroalgae wet weight as simulated by the Dublin Bay MSN_WQ model

	Mean summer values									
	Salinity (psu)		DAIN (mM)		DAIP (mM)		Chl ($mg\,l^{-1}$)		Macroalgae (tonnes wet weight)	
Water body	EPA	MSN_WQ	EPA	MSN_WQ	EPA	MSN_WQ	EPA	MSN_WQ	EPA	MSN_WQ
Dublin Bay	33.1	33.6	3.0	7.5	0.3	0.5	4.4	5.2	–	–
Liffey–Tolka junction	31.7	26.4	32.9	57.6	2.4	2.9	3.6	5.1	–	–
Liffey Estuary Lower	27.8	12.9	43.5	111.8	1.3	2.0	4.1	5.9	–	–
Liffey Estuary Upper	11.2	5.1	130.7	133.5	1.6	0.7	14.2	5.2	–	–
Tolka Estuary	31.5	25.5	29.9	47.7	2.0	1.1	4.6	5.8	–	–
Tolka intertidal	32.5	28.9	14.6	29.6	1.9	0.7	2.5	5.3	104	81.5

Chl, chlorophyll.

Table 3.12. Annual average river discharges, annual DAIN and DAIP loadings and their corresponding summer to annual ratios for the period 2010–2012, which were applied to the DCPM model comprising Dublin Bay and the Liffey and Tolka estuaries

Water body	River flow ($m^3\,s^{-1}$), annual average	River discharge ratio, (R_{SA})	Annual N load ($kg\,y^{-1}$)	N load ratio, (R_{SA})	Annual P load ($kg\,y^{-1}$)	P load ratio, (R_{SA})
Liffey	10.73	0.80	825,947	0.81	10,776	0.97
Tolka	1.90	0.75	87,994	0.47	4353	0.98
Dodder	2.58	0.75	118,720	0.40	1460	0.93

Summer, April to September, inclusive.

Table 3.13 contains the point source loading from Ringsend WWTP. The loading data were derived from the available AER data for the facility from 2011 to 2014 to obtain a long-term average loading with respect to volumetric flow and the associated nutrient loading.

Table 3.14 contains the tidal boundary conditions, which were calculated from the monitoring points adjacent to Dublin Bay – DB510, DB540 and DB570.

Model calibration was carried out by tuning the residence time and seasonal river discharge ratio to match the simulated and observed salinity. Figure 3.14 compares the simulated time series for salinity in each water body with the seasonally averaged salinity conditions for 2010–2012. Better agreement with monitoring data is observed closer to the tidal boundary, with a greater disparity between simulated and monitoring data in the Upper Liffey Estuary.

The biological growth in the model is influenced by the light attenuation coefficient, k_d, the unit chlorophyll yields from nitrogen and phosphorus and the phytoplankton loss rate. Table 3.15 presents the order in which calibration of an earlier two-box model of the Lower Liffey Estuary and Dublin Bay was carried out with respect to summer chlorophyll. Upon expansion of the model to the six-box system presented here, the parameter values contained in Table 3.15 were carried over to initialise the model. The parameters were site-specific light attenuation rate, k_d, a chlorophyll nitrogen yield of 0.875 g Chl mmol^{-1} N and a daily phytoplankton loss rate of 0.18 day^{-1}. The expanded six-box DCPM model included the Tolka Estuary and the Upper Liffey Estuary, as well as averaged point loading (from the AER) from the Ringsend WWTP. Because the initial two-box system comprising the Lower Liffey Estuary and Dublin Bay did not account for the other four water bodies, it did not resolve the exchanges with, and growth and dilution within, the additional water bodies. Consequently, the combination of parameter values adopted at the conclusion of calibration of the two-box system compensated for the lack of resolution therein with respect to spatial and volumetric extent. Initialisation of the six-box DCPM model with the phytoplankton yield and phytoplankton loss rate of the two-box system generated seasonal average nutrient and phytoplankton concentrations that did not reflect EPA monitoring data.

Consequently, the phytoplankton yield per unit nitrogen, and the phytoplankton loss rate, were restored to default values. As a result, the model accuracy improved throughout the system, with the model estimating seasonal nutrient, phytoplankton and macroalgae monitoring averages to the correct order of magnitude. Where, previously, parameter modification was necessary to replicate the gradient in monitoring data, the natural gradient in monitoring data was restored to the model with all default model parameters, except for phytoplankton loss rate, which was increased throughout from 0.1 to 0.15 day^{-1}, and the site-specific light attenuation coefficients, k_d, which were retained. The disparity between the calibration process for the two-box and six-box DCPM models of the Dublin Bay system emphasises the importance of including the entire estuarine continuum from the freshwater limit to the tidal boundary in DCPM models.

Table 3.13. Nutrient and flow data for Ringsend WWTP

Ringsend WWTP	Q (m^3 s^{-1})	DAIN (kg y^{-1})	DAIP (kg y^{-1})
Current facilities (2 million PE)	4.86	2,680,900	437,256

Nutrient and flow data were averaged from AER data for the years 2010–2015.

Table 3.14. Tidal boundary concentrations of nitrogen, phosphorus and chlorophyll and salinity for the Dublin Bay DCPM model for 2010–2012

N concentration in adjacent seawater (mM)		P concentration in adjacent seawater (mM)		Chl concentration in adjacent seawater (mg l^{-1})		Salinity in adjacent seawater (psu)
Winter	Summer	Winter	Summer	Winter	Summer	
12.39	2.96	0.60	0.25	1.75	3.81	34.0

Concentrations are seasonal averages determined from EPA monitoring data from DB510, DB540 and DB570. Summer, April to September, inclusive; winter, October to March, inclusive.

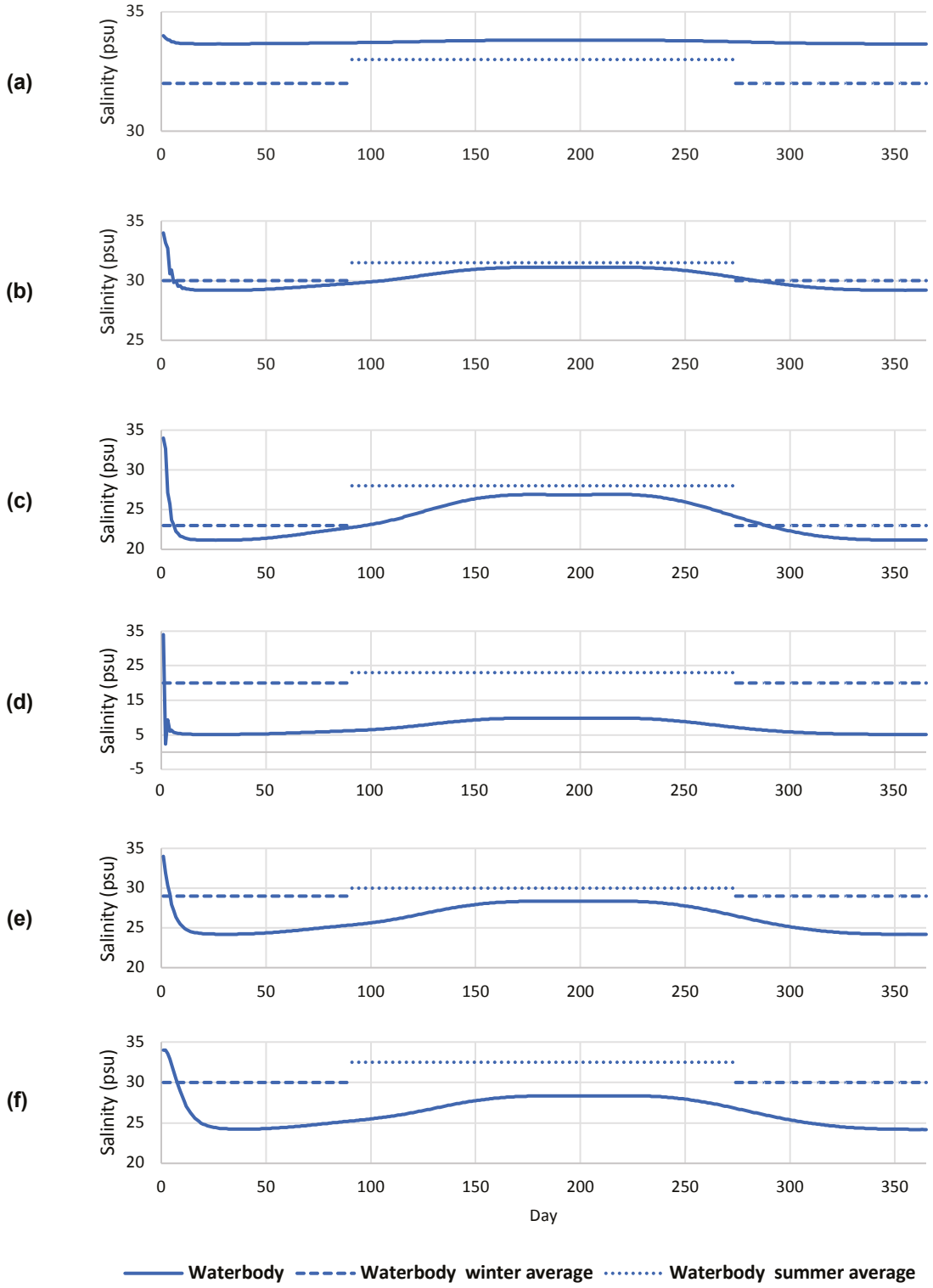

Figure 3.14. Salinity in the six constituent water bodies in the Dublin DCPM model for 2010–2012: (a) Dublin Bay, (b) the Liffey–Tolka junction, (c) the Lower Liffey Estuary, (d) the Upper Liffey Estuary, (e) the Tolka Estuary and (f) the intertidal zone of the Tolka Estuary.

Table 3.15. The steps taken to calibrate a DCPM model of the Lower Liffey Estuary and Dublin Bay with respect to chlorophyll

	Mean summer Chl (mg m^{-3})	
Calibration steps	**Dublin Bay**	**Lower Liffey**
EPA-provided values	4.36	3.55
(1) Default rates	3.84	4.05
(2) Site-specific K_d (m^{-1})	4.54	5.33
(3) Nitgrogen yield (2.2 → 1.5 g Chl $mmol^{-1}$ N)	4.49	5.27
(4) Nitrogen yield (1.5 → 1 g Chl $mmol^{-1}$ N)	4.34	5.07
(5) Nitrogen yield (1 → 0.95 g Chl $mmol^{-1}$ N)	4.32	5.04
(6) Nitrogen yield (0.95 → 0.875 g Chl $mmol^{-1}$ N)	4.28	5.00
(7) Phytoplankton loss rate (0.1 → 0.125 day^{-1})	4.17	4.50
(8) Phytoplankton loss rate (0.125 → 0.15 day^{-1})	4.07	4.07
(9) Phytoplankton loss rate (0.15 → 0.18 day^{-1})	3.95	3.62

Exclusion of any constituent water body may result in erroneous calibration, which would inadequately capture system behaviour in other simulations post calibration.

The performance of the calibrated DCPM model for 2010–2012 is presented in Table 3.16 in terms of seasonal averages of DAIN, DAIP, chlorophyll and macroalgae. Seasonal averages are calculated based on winter, spanning from October to March inclusive, and summer, spanning from April to September inclusive. Table 3.16 refers to percentage difference between the modelled seasonal averages and the monitoring averages. In general, the model is considered to have performed well if the percentage difference falls in the ±33% range. By this measure, the model performs best in Dublin Bay, the Liffey–Tolka junction and the Upper Liffey Estuary, whereas the model performs adequately in the Lower Liffey Estuary, where model values are of the correct order of magnitude. Simulated winter and summer DAIP averages are approximately double the monitored values, although it must be kept in mind that the averages are derived from monitoring data collected over a 3-year period, three times each summer and once each winter. The Lower Liffey Estuary may be influenced in this case by the effluent discharge from Ringsend WWTP. Owing to the arrangement of the boxes, the model may be simulating an exchange between the Liffey–Tolka junction and the Lower Liffey Estuary in excess of the prevailing exchange in reality. The main discrepancies in the Tolka Estuary and intertidal zone are related to DAIP and DAIN underestimation. Parameter averages are quite similar for the Tolka Estuary and the Liffey–Tolka junction, reflecting their proximity and also their relative volumes. The tidal portion of the Tolka Estuary is 4×10^6 m^3, while the Liffey–Tolka junction is 15×10^6 m^3. With daily tidal exchange, one might expect the parameter concentrations of the Tolka Estuary upstream of the junction to reflect the downstream parameter concentrations. The high summer chlorophyll concentrations in the Tolka Estuary may also reflect receipt of chlorophyll from the shallow, nitrogen-limited intertidal zone of the Tolka, which has very low light attenuation. The intertidal zone of the Tolka Estuary was simulated as nitrogen limited by the model, which is reflected in the high DAIN percentage difference of 91%, whereas the DAIP percentage difference is lower, at 50%, reflecting consumption of DAIP at a lower rate. The result also points to the possible role of nutrient cycling in sediment in providing the needed DAIN during summer. The calibrated model also accurately reproduces the peak summer macroalgae wet weight. The summer chlorophyll average for the intertidal zone is also taken from monitoring point LE350, which is on the most southerly point in the intertidal flat. Hence, the high simulated average of 27.32 g l^{-1} from the DCPM model cannot be objectively compared with the EPA average as it describes the full intertidal region and is possibly a better reflection of the average chlorophyll concentration in the area. An additional factor to consider is the relative infrequency of EPA water quality sampling, three times during summer and once during winter.

Table 3.16. Post-calibration performance of the Dublin Bay DCPM model in matching the EPA averaged data for the period spanning from 2010 to 2012

	Dublin Bay			Liffey–Tolka junction			Lower Liffey Estuary			Upper Liffey Estuary			Tolka Estuary			Tolka intertidal zone		
Parameter (mean)	EPA	DCPM	Difference (%)	EPA	DCPM	Difference (%)	EPA	DCPM	Difference (%)	EPA	DCPM	Difference (%)	EPA	DCPM	Difference (%)	EPA	DCPM	Difference (%)
Winter DAIN (µM)	14.29	14.02	–1.83	56.60	59.07	4.37	68.57	82.69	20.59	139.71	148.13	6.03	48.73	68.52	40.61	49.29	62.69	27.19
Summer DAIN (µM)	3.00	3.58	19.49	32.85	44.15	34.40	43.50	63.20	45.28	130.71	132.96	1.72	29.92	36.23	21.09	14.64	1.22	–91.68
Winter DAIP (µM)	0.67	0.69	2.26	3.84	3.03	–21.2	1.10	2.41	119.13	0.98	1.24	26.88	0.82	2.80	241.94	0.81	2.60	223.09
Summer DAIP (µM)	0.32	0.30	-6.73	2.40	2.73	13.92	1.34	2.41	80.12	1.62	1.35	–16.6	2.04	2.31	13.15	1.90	0.94	–50.18
Winter Chl ($mg\,m^{-3}$)	1.85	1.73	–6.75	1.32	1.60	20.78	1.36	1.43	5.46	1.63	2.09	28.24	1.48	2.15	45.13	1.60	3.25	103.24
Summer Chl ($mg\,m^{-3}$)	4.36	4.47	2.39	3.64	5.49	50.84	4.07	5.64	38.55	14.21	11.07	–22.1	4.56	13.17	188.55	2.50	27.32	993.00
Summer macro-algae ($mg\,m^{-3}$)	–	–	–	–	–	–	–	–	–	–	–	–	–	–	–	103.68	96.28	–7.14

Chl, chlorophyll.

Model results indicated that phytoplankton growth in the Upper Liffey Estuary, the Liffey–Tolka junction, the Lower Liffey Estuary and the Tolka Estuary was light limited, as the light-limited growth rate was consistently lower than the growth rate as a function of DAIN and DAIP. Phytoplankton growth in Dublin Bay was, however, determined to be nitrogen limited during the peak production season, as was macroalgae growth in the intertidal zone of the Tolka Estuary.

3.4 Comparative Model Performance

Based on each model's capability to replicate the seasonal water body average concentrations of nutrients and chlorophyll calculated from monitoring data, the DCPM model objectively performed better than the expanded MSN_WQ model in the Dublin Bay area.

The DCPM model is a simple box model that disregards physical restrictions in flow and vertical stratification, as it is a 0-D model. The MSN_WQ model of Dublin Bay outlined here is closer, in hydrodynamic terms, to the reality in Dublin Bay and at its interface with the Liffey and Tolka estuaries, although it does not resolve velocities vertically through the water column to reflect flow stratification. As a result, there is an apparent accumulation of freshwater at the junction between the estuaries and the inner Dublin Bay area.

3.5 DCPM Scenario Loading

To capitalise on the simplicity and relative performance of the calibrated DCPM model of Dublin Bay and its adjoining estuaries, several scenarios were considered.

Although nitrogen was the only nutrient deemed to limit growth in the baseline model simulation, in practical terms, efforts to reduce nitrogen loadings upstream may lead to reductions in both nitrogen and phosphorus loading. Moreover, phosphorus reduction is highly likely to improve the status of upstream river water bodies, which can be phosphorus limited. Thus, the three riverine nutrient load reduction scenarios considered were 25%, 50% and 75% reductions in riverine DAIN and DAIP loading. The sensitivity of the system to tidal nutrient concentrations was evaluated by applying lower and higher boundary concentration values. As 21% of at-risk rivers, 41% of at-risk transitional waters and 23% of at-risk coastal waters are subject to significant pressure from urban wastewater, it is clear that transitional waters near coastal cities are at greatest risk from urban wastewater (DHPLG, 2018). Urban wastewater accounts for 72% of DAIN entering the system and 96% of DAIP entering the system (Tables 3.12 and 3.13). Nutrient loading from urban wastewater is consistent throughout the year, whereas riverine nutrient loading varies seasonally, with greater inputs in spring and winter.

Ringsend WWTP serves the Greater Dublin agglomeration, and commenced operation in 2005 to treat a PE of 1.64 million. In terms of annual mean PE, AERs from 2010 to 2015 have identified that the plant has received anywhere between 50,000 PE and 300,000 PE above its design treatment capacity (Dublin City Council, 2011, 2012, 2013; Irish Water, 2015b, 2016). A 400,000 PE capacity upgrade is under construction at the plant. Irish Water is currently procuring a retrofit aerobic granular sludge (AGS) installation to bring the capacity to 2.4 million PE.

Two scenarios were evaluated to contextualise the outcome if the treatment plant was (1) not expanded, with excess influent discharge untreated, or (2) expanded, with the existing treatment standard maintained. To build upon the two scenarios related to population growth, further scenarios were simulated to determine the effect of three different types of AGS treatment technologies when applied to the expanded population equivalent of 1.94 million PE.

The three variants of AGS and their associated nutrient removal efficiencies, taken from Figdore *et al*. (2018), were:

- NIT: nitrifying granules with aerobic feeding;
- NDN-OHO: nitrifying–denitrifying granules with anoxic feeding;
- NDN-PAO: nitrifying–denitrifying, DAIP-accumulating granules with anaerobic feeding.

Alongside the three AGS scenarios, the prospect of the existing treatment method being applied to the expanded PE was considered as a fourth scenario. The expansion of Ringsend WWTP is primarily intended to (1) achieve compliance with the UWWTR and (2) provide adequate capacity to treat all wastewater from the Greater Dublin agglomeration. The final scenario reflected the treatment plant

meeting those two objectives, i.e. total nitrogen of 10 mg l^{-1}, total phosphorus of 1 mg l^{-1} and a PE of 1.94 million.

Table 3.17 presents the treatment efficiencies of AGS as set out by Figdore *et al.* (2018).

It should be noted that the largest operational retrofit AGS installation completed worldwide to date is 40,000 PE at Frielas, Libson, much smaller than the proposed 2.4 million PE capacity AGS upgrade and retrofit at Ringsend WWTP.

The three hypothetical AGS nutrient removal efficiencies used in the modelling scenarios are based on experiments using laboratory-scale AGS reactors. Assessment of the performance of the pilot full-scale AGS retrofit installation at Ringsend WWTP did not form part of this study. There is significant uncertainty as to the likely efficacy of the modelled treatment technologies at Ringsend WWTP owing to differences in physical setting, scale and influent characteristics between the laboratory experiments and the treatment plant. Therefore, further research, including full-scale process-proving of these alternative technologies at Ringsend, would be required to ascertain whether these treatment efficiencies could reliably be achieved through a retrofit installation at Ringsend WWTP.

When the upgrade is completed, Ringsend WWTP will be in full compliance with all relevant legislative requirements related to the primary discharges, i.e. UWWTR and Waste Water Discharge (Authorisation) Regulations.

The average influent nutrient characteristics from Ringsend AERs for 2010, 2011, 2012, 2014 and 2015 were calculated as 36 mg l^{-1} total nitrogen and 5.4 g l^{-1} total phosphorus. The ratios of DAIN to total nitrogen and of DAIP to total phosphorus for the influent were taken from Henze and Comeau (2008) as 0.75 and 0.66 respectively. All of the foregoing was taken into consideration in deriving the loading data presented in Table 3.18.

3.5.1 Riverine nutrient reductions

Three riverine nutrient load reduction scenarios were considered: annual average reductions in both DAIN and DAIP loadings of 25%, 50% or 75%. Reductions were considered based upon the 2010–2012 loading data, with the baseline for comparison being the seasonally averaged water column concentrations and macroalgae wet weights at calibration.

Figure 3.15 presents the percentage change in DAIN, DAIP, chlorophyll concentration and macroalgae resulting from the nitrogen load reductions considered for 2010–2012. The tiered riverine DAIN load reductions presented in Figure 3.15 yield tiered responses system-wide. In five of the six water bodies,

Table 3.17. The nutrient removal efficiency of three variants of AGS

	Removal efficiency (%), mean ± SD		
Nutrient	NIT	NDN-OHO	NDN-PAO
NH_4	96 ± 2	81 ± 7.9	98 ± 1
NO_2, NO_3	4 ± 2	30 ± 2.8	95 ± 2
PO_4-P	6 ± 2	9 ± 1	90 ± 9

SD, standard deviation. Reproduced from Table 2 of Figdore *et al.* (2018).

Table 3.18. The series of effluent loading scenarios at Ringsend WWTP that were simulated using the calibrated DCPM model for the system comprising the Liffey and Tolka estuaries and Dublin Bay

Scenario	*Q* ($m^3 s^{-1}$)	DAIN (kg y^{-1})	DAIP (kg y^{-1})
Existing treatment facilities and loading	4.86	2,680,900	437,256
Expansion by 20% with existing treatment	5.83	3,217,080	524,707
Expansion by 20% with additional load untreated	5.83	3,542,227	552,100
Expansion: plant refit with AGS NIT	5.83	4,976,556	650,780
Expansion: plant refit with AGS NDN-OHO	5.83	3,617,574	627,812
Expansion: plant refit with AGS NDN-PAO	5.83	258,398	66,992
Expansion compliant with UWWTR	5.83	1,435,545	126,328

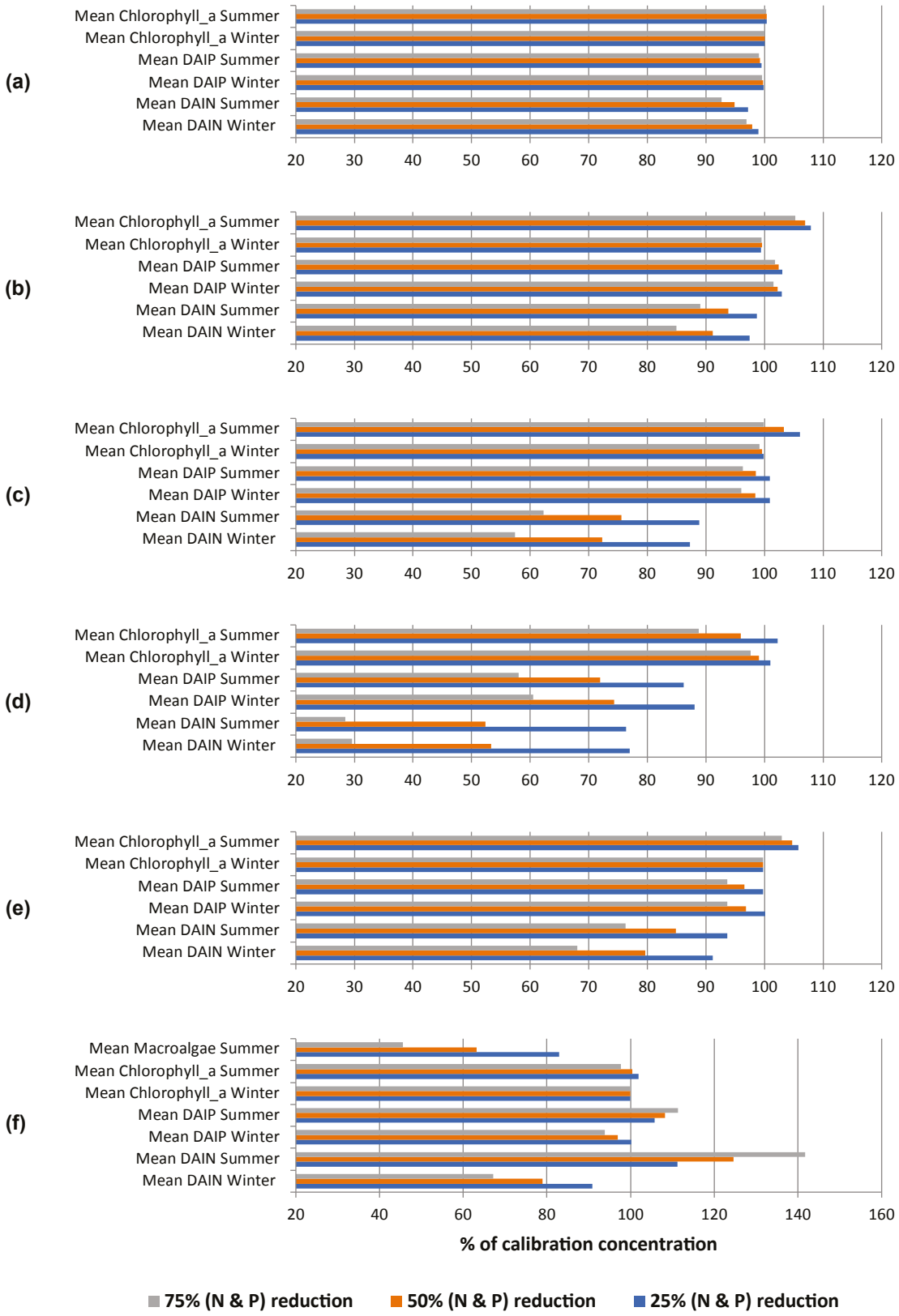

Figure 3.15. The change in DAIN, DAIP and chlorophyll concentrations and macroalgae tonnage simulated by a calibrated DCPM model comprising (a) Dublin Bay, (b) the Tolka–Liffey junction, (c) the Lower Liffey Estuary, (d) the Upper Liffey Estuary, (e) the Tolka Estuary and (f) the intertidal zone of the Tolka Estuary. The baseline (100%, i.e. calibration concentration) is taken from the DCPM columns of Table 3.16. The three nutrient reduction scenarios were based on 2010–2012 loading data.

an incremental reduction in the DAIN concentration was observed in tandem with incremental reduction in riverine nitrogen loading. In the case of the intertidal zone of the Tolka Estuary, however, incremental reduction in riverine nitrogen loading resulted in an increase in DAIN concentrations during the summer. This may be a response to the reduced assimilative capacity provided by macroalgae, which is presumed to be bound to the benthic zone and thus not subject to tidal exchange. There was a moderate increase in chlorophyll in summer throughout the system, which was postulated to be a response to more favourable nutrient concentrations for growth. The system-wide reduction in DAIP concentrations with a reduction in riverine nitrogen loading may be due to increased uptake of DAIP as a result of increased chlorophyll growth in the water column.

The area that benefited most from a reduction in riverine nitrogen loading, in terms of increased water quality, was the Upper Liffey Estuary, with nitrogen load reductions of greater than 25% inducing a reduction in chlorophyll concentrations of up to 11%. The same benefit was not replicated in the Tolka Estuary, where all riverine nitrogen load reductions result in an increase in chlorophyll concentrations. This is a consequence of the differing growth limitation in the system. Growth of macroalgae and chlorophyll in the intertidal zone of the Tolka was nitrogen limited during the summer, whereas the increase in chlorophyll concentration in all other water bodies was light limited. Consequently, reducing nitrogen loading to the system restricted the growth of macroalgae in the intertidal zone of the Tolka, thus allowing a moderate, albeit light-limited, increase in chlorophyll concentration in other water bodies. Reducing riverine nitrogen loading leads to a reduction in summer average macroalgae wet weight of 54%.

3.5.2 Population growth

Figure 3.16 outlines the consequences of Ringsend WWTP receiving an extra 20% PE, and whether the extra influent is treated, albeit limited to expansion of the existing treatment standard, or the extra influent is untreated and discharged raw. The scenarios assumed that the riverine and tidal forcing data remained at their 2010–2012 values. The baseline 100% calibration concentration for each water body in Figure 3.16 is taken from the columns corresponding to DCPM seasonal averages in Table 3.16.

Regarding the prospect of extending the existing treatment capacity by an extra 20% PE, the most notable observation with respect to primary producer growth was a 30% increase in the summer average macroalgae wet weight in the intertidal zone of the Tolka Estuary. The increase in chlorophyll in the same water body was negligible, and there was an increase in DAIP of 22% and a reduction in DAIN of 18%. In all other water bodies, summer average chlorophyll concentrations decreased by 2–8%. DAIP concentrations increased system-wide by 6–15%, whereas DAIN concentrations increased by 1–12%. The intertidal zone of the Tolka Estuary is the area that is light limited for the least time, only 45% of the year, with all other water bodies being light limited all year round. Therefore, the increased effluent loadings from the 20% population growth favoured the intertidal macroalgae in the Tolka Estuary over chlorophyll growth in all other water bodies, as a result of the shallowness of the intertidal zone and the lower light attenuation.

The impact of discharging the additional influent load untreated alongside treated effluent would be detrimental to water quality throughout the Liffey and Tolka estuaries and Dublin Bay. The summer macroalgae bloom weight would increase by in excess of 60%. Summer chlorophyll concentrations would increase by a maximum of 8% in the Upper Liffey Estuary, although summer chlorophyll in all other water bodies would increase by a maximum of 3%. The additional unassimilated nutrients in this scenario would lead to an increase in summer average DAIN of 2–26%, winter average DAIN of 3–18%, summer average DAIP of 8–32% and winter average DAIP of 3–21%.

3.5.3 Population growth including installation of AGS

Figure 3.17 presents the results of five scenarios pertaining to the level of treatment, or possible lack of treatment, at Ringsend WWTP to meet the needs of an expansion in loading of 20% PE. The baseline calibration concentration of 100% corresponds to the seasonal average concentrations generated by the DCPM model for the period 2010–2012 with the present riverine and wastewater loading.

In practical terms, the most pertinent scenario is the possibility of discharging the additional 20% loading to

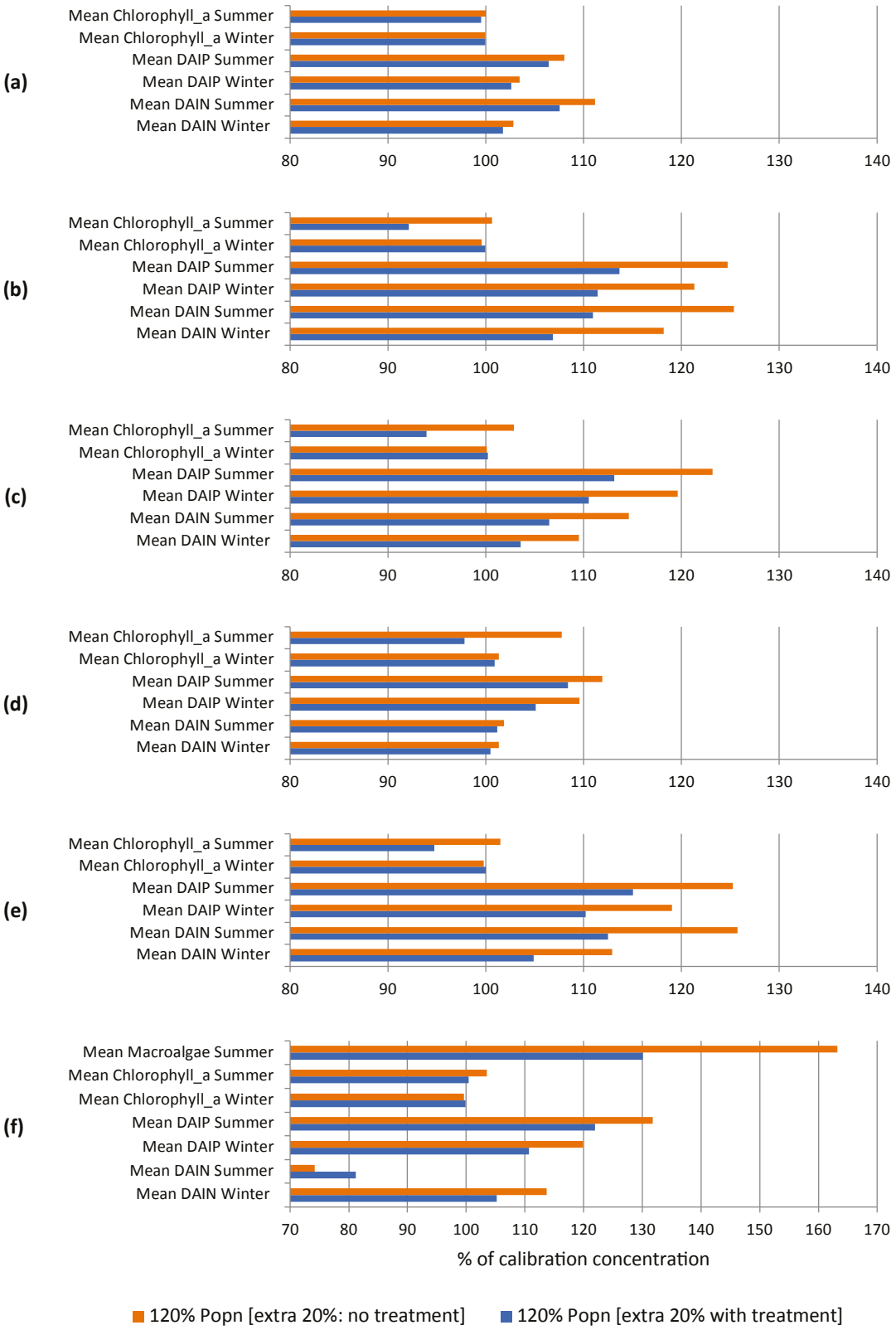

Figure 3.16. The change in DAIN, DAIP and chlorophyll concentrations and macroalgae tonnage due to a projected 20% population growth in the catchment of Ringsend WWTP based on 2010–2012 loading data, simulated by a calibrated DCPM model comprising (a) Dublin Bay, (b) the Tolka–Liffey junction, (c) the Lower Liffey Estuary, (d) the Upper Liffey Estuary, (e) the Tolka Estuary and (f) the intertidal zone of the Tolka Estuary. The baseline (100%, i.e. calibration concentration) is taken from the DCPM columns of Table 3.16. The two scenarios consider the consequences of the additional wastewater loading being untreated and discharged to overflow (orange bar) or the extension of the existing treatment standard to the additional loading.

Ringsend untreated. This scenario has been included for comparison purposes but was discussed in section 3.5.2.

Referring to Table 3.17, each variant of AGS removes DAIN and DAIP in differing amounts. The most effective scenario in Figure 3.17 is NDN-PAO, which has the effect of reducing summer average DAIN concentrations by up to 70%, and by a minimum of 4% in the Upper Liffey Estuary. Summer average DAIP concentrations also decreased by up to 78% in the Tolka–Liffey junction area and the Tolka Estuary under the NDN-PAO scenario. The combination of reduced DAIN and DAIP loading leads to a simulated decrease in summer average chlorophyll concentrations of up to 51%. Under the same circumstances, the summer macroalgae bloom weight in the intertidal zone of the Tolka Estuary would decrease by 72%, leading to a collocated increase of 49% in DAIN concentration resulting from a drop in the assimilative capacity.

Delivery of a 20% expansion of treatment capacity and a standard of treatment capable of meeting the UWWTR effluent criteria for total nitrogen and total phosphorus would improve water quality parameters throughout the system with the exception of the intertidal zone of the Tolka Estuary, where summer average DAIN concentrations would increase by 112%. This would occur in response to a loss of assimilative capacity as a result of a disproportionately small increase in the summer macroalgae weight.

The two other variants of AGS treatment, named NIT and NDN-OHO here, would not meet the requirements of the UWWTR based upon the treatment efficiencies declared by Figdore *et al.* (2018), leading to a large percentage increase in seasonal average DAIN and DAIP concentrations and macroalgae bloom weight, and a corresponding but lower increase in summer chlorophyll concentrations.

3.5.4 Tidal nutrient boundary conditions

Two scenarios were also considered to establish the sensitivity of the model domain to changes in coastal nutrient concentrations exchanged with the system. The scenarios were compared with the baseline scenario of 100% of the riverine nutrient loads and a 20% population increase reflected in Ringsend effluent discharges. As coastal DAIN and DAIP concentrations have been observed to increase and decrease in parallel, summer tidal boundary nutrient concentrations were considered at 90% and 125% of their values for 2010–2012. Figure 3.18a indicates that the summer DAIP and DAIN concentrations in Dublin Bay increased or decreased approximately in line with the change in tidal boundary conditions, although there was no change in the average simulated summer chlorophyll concentrations. In the other five water bodies, there was a slight increase in chlorophyll, DAIN and DAIP concentrations during summer of 2–10%, irrespective of whether the tidal nutrient concentrations had increased or decreased. This was counter to expectations. One might have expected a reduction in coastal nutrient concentrations to result in a decrease in primary productivity due to a reduction in the availability of the limiting nutrient, and the reverse to occur with increasing nutrient concentrations at the tidal boundary. However, the authors postulate that the reason for this is that the seasonal average winter and summer coastal chlorophyll concentrations were kept at the original baseline concentration, although, in real-world scenarios, the relation between winter and summer coastal nutrient concentrations and chlorophyll concentrations would vary depending upon the prevailing conditions offshore, and the wider oceanic circulation.

3.6 Discussion

Simple 0-D water quality box models such as the DCPM model cannot by their nature account for physical inhibition of macroalgae growth due to bed stress, or describe the local-scale water advection, which may facilitate growth at one site and deprive macroalgae spores of nutrients elsewhere. The DCPM model has been benchmarked against two versions of hydrodynamic, solute transport and water quality model MSN_WQ – the pre-existing version, as applied to Cork Harbour and environs, and an expanded version that describes macroalgae growth as a function of internal tissue nutrient concentrations, bed capacity, bed stress and salinity.

The MSN_WQ model as applied to Cork Harbour performed better than the equivalent DCPM model. This may be attributed to the inherent skill in the MSN_WQ model with respect to hydrodynamics and solute transport. The prevailing circulation in Cork Harbour is complex as a result of the spatially heterogeneous residence time. The DCPM model

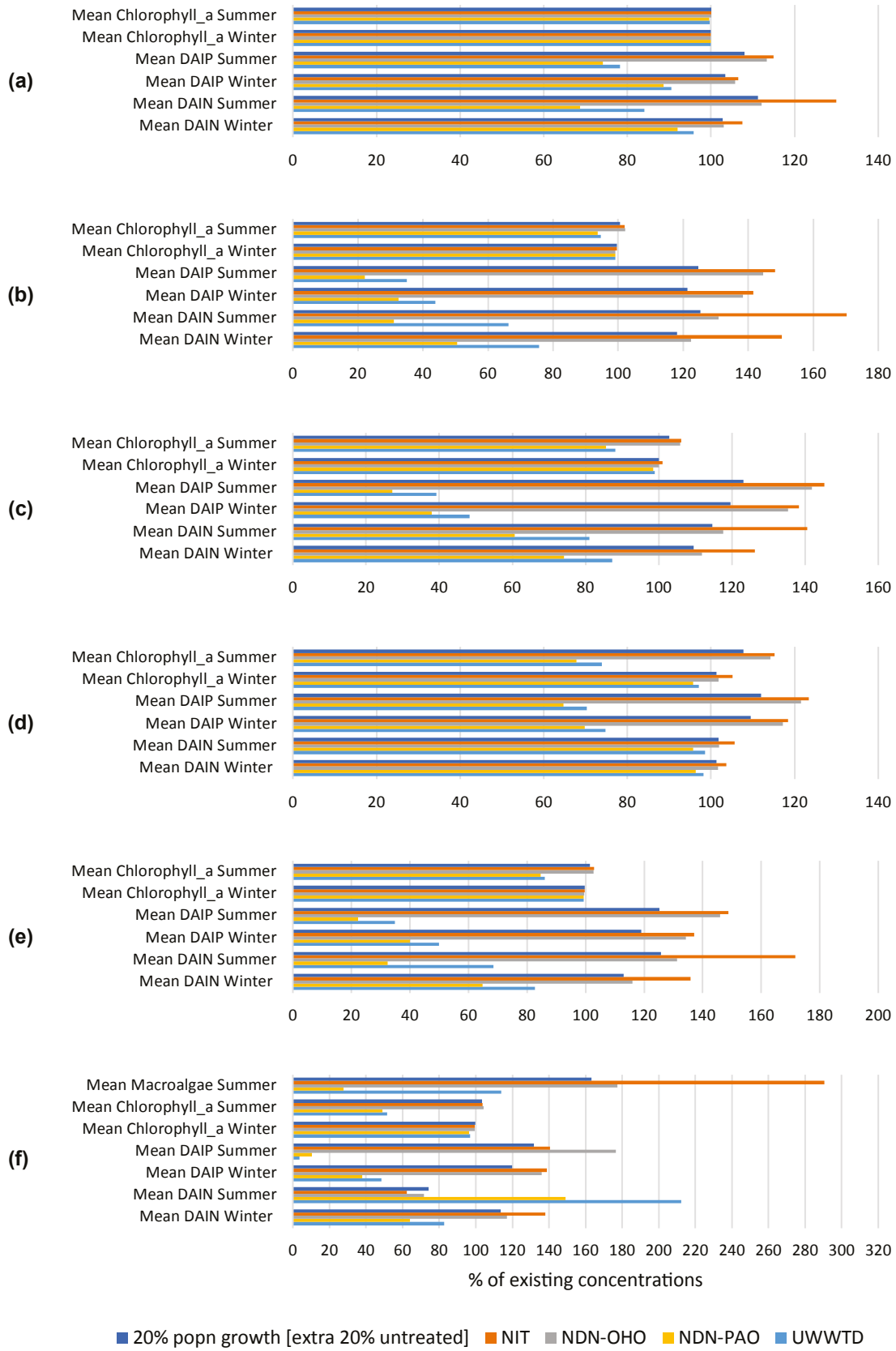

Figure 3.17. The change in DAIN, DAIP and chlorophyll concentrations and macroalgae tonnage caused by different types of wastewater treatment at Ringsend WWTP, simulated by a calibrated DCPM model comprising (a) Dublin Bay, (b) the Tolka–Liffey junction, (c) the Lower Liffey Estuary, (d) the Upper Liffey Estuary, (e) the Tolka Estuary and (f) the intertidal zone of the Tolka Estuary. The baseline (100%, i.e. calibration concentration) is taken from the DCPM columns of Table 3.16, and refers to existing levels of riverine and wastewater effluent loading.

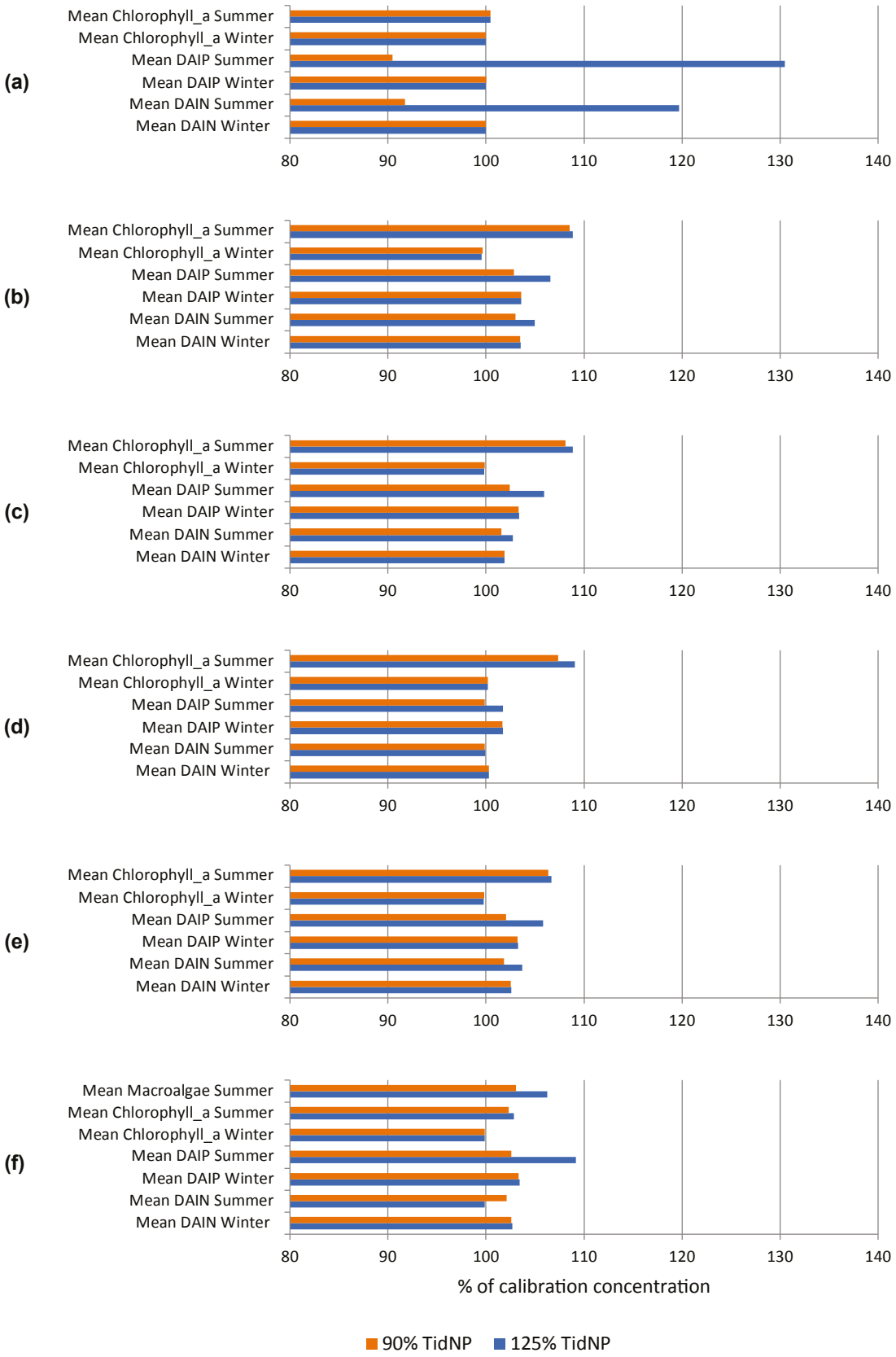

Figure 3.18. The change in DAIN, DAIP and chlorophyll concentrations and macroalgae tonnages due to an increase or decrease in summer tidal nutrient concentrations based on 2010–2012 loading data, simulated by a calibrated DCPM model comprising (a) Dublin Bay, (b) the Tolka–Liffey junction, (c) the Lower Liffey Estuary, (d) the Upper Liffey Estuary, (e) the Tolka Estuary and (f) the intertidal zone of the Tolka Estuary. The baseline (100%, i.e. calibration concentration) is taken from the DCPM columns of Table 3.16.

approximates exchange between water bodies without consideration of the shape or orientation of different water bodies, or the interface between neighbouring water bodies.

The expanded MSN_WQ model of Dublin Bay, incorporating a macroalgae life cycle module, did not perform as well as the equivalent DCPM model. Circulation in Dublin Bay is simpler than in Cork Harbour in the horizontal sense, although, owing to the magnitude of the flows into the Liffey and Tolka estuaries, and their proximity to the coast, vertical stratification is a feature of the estuaries. Owing to vertical integration of the continuity and Navier–Stokes equations, vertical stratification has been disregarded, and all volumes are assumed to have the same density. During the flood tide, the consequence of this simplification is that riverine flow and the incoming tide are two opposing forces. The outcome in the Dublin Bay MSN_WQ model is retention of freshwater behind the mouth of Dublin Bay. In contrast, owing to the simplicity of the DCPM model, a proportion of the volume in each water body transfers with a daily time step to the adjacent downstream water body.

The results outlined here indicate that the macroalgae life cycle module has been developed to the stage of "proof of concept" in the MSN_WQ model. Furnishing the module with relevant site-specific parametrisation is beyond the scope and time frame of this project. The full capability and potential of the code are, however, restricted by the assumption of a uniform vertical velocity distribution in the MSN_WQ model. Although depth integration of the Navier–Stokes equations reduces computational expense, in this context depth integration disregards the potential for vertical stratification of flows.

The WFD-UKTAG Opportunistic Macroalgae Bloom Tool (OBMT) (Wells *et al.*, 2009) determines the ecological quality ratio (EQR) of transitional and coastal water bodies based on:

- percentage cover of the available intertidal habitat (AIH);
- average biomass of the AIH;
- average biomass of the affected area (AA);
- size of the AA;
- ratio of AA/AIH;
- percentage of sampled areas with macroalgae entrained within the sediment to a depth of at least 3 cm.

The DCPM model cannot resolve the relocation of the boundary of the AA in response to nutrient enrichment or curtailment of nutrient loads. Burial of macroalgae into underlying sediment was not accounted for in the current study. Nonetheless, the burial process is physically mediated and thus cannot be described by the DCPM model. Such factors are included in macroalgae compliance assessment. The DCPM model also disregards physical factors such as bottom shear stress, which will influence the distribution of macroalgae at local scales. Therefore, although the DCPM model has been calibrated and validated for three Irish transitional/coastal systems, the response of each system to the recommended nutrient load reductions in terms of change in EQR cannot be determined in advance. However, it is possible to utilise the DCPM model to determine the nutrient load reduction that would cause the average biomass density in the AIH to fall below the threshold for good or high status. The values of 100 and 500 g ww m^{-2} may be used as preliminary indicators in the DCPM model for the possibility of high and good status, respectively. Thus, the DCPM model is useful as a screening tool for identifying the order of magnitude of nutrient reductions necessary to trigger the good or high status threshold for one of the six WFD-UKTAG OBMT criteria. Further work is recommended to identify the correlation between achievement of compliance with the good and high status criterion for average biomass in the AIH and achievement of compliance with the other five criteria. Neither the DCPM nor the MSN_WQ model can determine in its current format what nutrient load reduction will result in a good or high EQR as determined by the WFD-UKTAG macroalgae compliance parameters.

Integration of the macroalgae growth module, which has been developed here into a high-resolution 3-D hydrodynamic, solute transport and water quality model such as the Regional Ocean Modelling System (ROMS), is necessary to address the aforementioned shortcomings in the DCPM model.

The urban system comprising the Liffey and Tolka estuaries and Dublin Bay is in close proximity to the Irish Sea, heavily modified, and subject to point and non-point pressures from a large catchment area. Replication of the water renewal regime that occurs in response to tidal exchange is particularly challenging for a box model such as the DCPM model, not least because of the presence of the

sea walls north and south of the Liffey Estuary as it discharges to Dublin Bay. The prevailing salinity concentrations provide a proxy for solute transport. Although the model approximated the seasonal salinity values in the polyhaline and saline waters, it performed inadequately in the oligohaline Upper Liffey Estuary. This may reflect the inability of the model to account for the cross-sectional area that facilitates tidal exchange. In addition, the Upper Liffey Estuary is some 4 km long, approximately 5 m deep at its most downstream point and 50 m wide at its widest. Therefore, bottom friction and the law of the wall (Schlichting, 1979) must be considered as but two factors contributing to mixing inaccuracy upstream in the DCPM model. Accurate river soundings up to the estuarine limit with respect to the lowest astronomical tide, including their flood banks where practicable, would greatly benefit model accuracy and facilitate more realistic simulations where real flow measurements are available. As a counterpoint, the model performs well with respect to matching the seasonal nutrient and average chlorophyll concentrations obtained by monitoring in the Upper Liffey Estuary. In spite of the complex exchanges that take place between the downstream water bodies, the DCPM model consistently achieves the correct order of magnitude for relevant parameters.

This gives credence to the DCPM model, the application of site-specific light attenuation data, the adopted tidal boundary data, the calculated and extrapolated riverine nutrient loading data, and the reported effluent concentrations in the Ringsend AER.

The various simulated scenarios reflect the complexities of nutrient load modification. Reductions in the riverine DAIN and DAIP loads resulted in moderate increases in chlorophyll concentration in some water bodies, which was a combined effect of more favourable molar concentrations, due to the reduction in riverine nutrient loads and a reduction in the assimilated nutrients in some water bodies, and thus a lesser reduction in concentrations than might be expected.

Model sensitivity to changes in tidal nutrient concentrations is unclear owing to uncertainty about the relationship between the seasonal chlorophyll concentrations and nutrient concentrations. In the event of an increase in tidal nutrient concentrations due to upwelling, this may be accompanied by low chlorophyll concentrations from deeper cooler waters. Therefore, a full exposition of the sensitivity of a calibrated DCPM model to tidal boundary nutrient concentrations may be possible using data from operational models of the adjacent coastal shelf. Differences between the nearshore and open seas would also need to be accounted for.

The depth-wise difference in density between riverine and tidal inputs and the vertical gradient of horizontal currents due to river and tidal influences are the primary causes of stratification in estuaries. As large riverine freshwater inputs are the cause of vertical stratification, a stratified estuary is thus also a recipient of large nutrient inputs. Therefore, incorporation of the macroalgae model developed for this study into a 3-D hydrodynamic model would add significantly to national biogeochemical modelling capacity and allow for detailed forecasting and scenario modelling (Skerratt *et al.*, 2013) or carbon and nitrogen budgeting in coastal shelf regions (Plus *et al.*, 2015). Benchmarking of the expanded MSN_WQ model against the DCPM model has highlighted the shortcomings of applying a depth-integrated model to stratified systems such as Dublin Bay. The expanded MSN_WQ model developed as part of this study has achieved a similar level of capability as other models (Coffaro and Sfriso, 1997; Solidoro *et al.*, 1997a,b; Martins and Marques, 2002; de Guimaraens *et al.*, 2005; Aveytua-Alcázar *et al.*, 2008; Aldridge and Trimmer, 2009; Port, 2016). Alongside the macroalgae life cycle, the model also describes the life cycle of phytoplankton, the nitrogen and phosphorus cycles and the production and consumption of dissolved oxygen. The model is suitable for application to well-mixed systems that do not receive large riverine inputs. One such suitable domain relevant within the context of this study is Courtmacsherry Bay.

Future use of this model must be contextualised in terms of the gains and shortcomings of modelling efforts elsewhere. Haverson *et al.* (2017) utilised a 2-D depth-integrated hydrodynamic model and the DCPM model at separate stages of a case study, without explicitly building the macroalgae life cycle into a high-resolution hydrodynamic model. In this study of Poole Harbour, favourable hydrodynamic conditions (water velocity $< 0.13\,m\,s^{-1}$, water depth $< 1.05\,m$) were identified by cross-referencing mean velocity fields and water depths with macroalgae maps. The expanded

MSN_WQ model developed as part of this study aimed to encompass both hydrodynamic and ecological factors within one model. The newly expanded MSN_WQ model has the inbuilt functionality to spatially restrict macroalgae growth to areas subjected to low bed shear stress. As shear stress is proportional to velocity, the resultant model has addressed the question of hydrodynamic control of macroalgae in a complete end-to-end ecohydrodynamic model.

Beyond the functionality of the expanded MSN_WQ model, Perrot *et al.* (2014) included percentage emersion as a factor in macroalgae mortality, to reflect the influence of desiccation on survival of macroalgae.

The growth of macroalgal early-life spores was precluded from the expanded MSN_WQ model. It has been incorporated in a number of other studies (Martins *et al.*, 2007, 2008). In the context of climate change and increasingly extreme metocean conditions, precipitation and riverine discharge extremes, it is possible that macroalgal spores may be advected to neighbouring sheltered intertidal zones, thus leading to establishment of new macroalgae bloom sites.

Species-specific macroalgal self-shading was considered by Trancoso *et al.* (2005) and Ren *et al.* (2014). In the expanded MSN_WQ model, it was assumed that macroalgae were non-buoyant, thus rendering self-shading irrelevant. This is another aspect for future consideration in any further adaptation or use of the macroalgae module of the MSN_WQ model.

The work of Brush and Nixon (2010) is considered the most detailed macroalgae life cycle model, owing to the detailed description of macroalgae growth as layers of thalli. Light attenuation is accounted for through each macroalgal layer, and consequently primary production of each layer of macroalgae is scaled based on available light. Additionally, carbon, nitrogen and phosphorus uptake are modelled separately. Imposition of a bed capacity limit within the expanded MSN_WQ model provides an upper limit on primary production throughout the macroalgal mat, and hence on bloom weight. It is concluded here that the approach adopted is more computationally efficient than the Brush and Nixon model, and thus more suitable for timely scenario modelling in an Irish context. Additional computation would be necessary to resolve processes occuring in each macroalgae layer, whereas in the present work, all macroalgae layers are simplified to a single layer with an upper weight limit.

3.7 Summary

- The DCPM model was applied to the system comprising Dublin Bay and the Liffey and Tolka estuaries for 2010–2012, to establish the order of magnitude of reduction in seasonal average concentrations of nutrients and chlorophyll and macroalgae weight resulting from:
  - three incremental reductions in both DAIP and DAIN loading: 25%, 50% and 75%;
  - higher and lower DAIP and DAIN concentrations (90% and 125% of the ambient summer average concentrations for 2010–2012) at the tidal boundary;
  - expansion of treatment capacity by 20% PE at Ringsend WWTP and:
    - the effect of no expansion of treatment capacity (additional wastewater discharged untreated);
    - implementation of different types of AGS treatment;
    - implementation of treatment standards to comply with the UWWTR.
- Site-specific light attenuation coefficients and exchange rates were calculated for each water body based on Secchi disc readings from 2010 to 2012.
- Physical mixing was calibrated by modifying the calculated exchange rates and seasonal river discharge ratio to match the salinity time series generated by the DCPM model with the salinity observations gathered by the EPA.
- Calibration of biological growth entailed modification of the phytoplankton loss rate.
- Based on 2010–2012 average riverine inputs, a 75% reduction in riverine inputs of nitrogen and phosphorus to the system would significantly reduce the macroalgae bloom magnitude by over 50%.
- Retention of the existing treatment capacity and treatment technology in Ringsend WWTP would result in:
  - an increase in summer average DAIN concentrations of 3–23% in all water bodies except the intertidal zone of the Tolka Estuary, where concentrations would fall by 25%, and an

increase in winter average DAIN concentrations of 1–18%;
  - an increase in summer average DAIP concentrations of 4–31% and an increase in winter average DAIP concentrations of 3–20%;
  - an increase in summer average chlorophyll concentrations of 3–8% and a negligible increase in winter average chlorophyll concentrations;
  - an increase in summer average macroalgae bloom tonnage of 60%.
- Expansion of the treatment capacity at Ringsend WWTP by 20% without any improvement in treatment technology would result in a reduction in summer average chlorophyll concentrations of up to 8%, although summer and winter DAIN and DAIP concentrations would increase by up to 20%. The macroalgae bloom tonnage would increase by 30%.
- Based on the treatment efficiencies quoted in Table 3.17 (adopted from Figdore *et al.*, 2018), adopting NIT (nitrifying granules with aerobic feeding) or NDN-OHO (nitrifying–denitrifying granules with anoxic feeding) in an expansion and refitting of Ringsend WWTP would result in an increase in DAIN and DAIP concentrations during winter and summer, ranging from 6% to 70%. The summer average macroalgae tonnage would increase by 80–180%.
- Expansion of the treatment capacity of Ringsend WWTP by 20% and refitting with NDN-PAO (nitrifying–denitrifying, DAIP-accumulating granules with anaerobic feeding) would lead to a substantial reduction in seasonal average concentrations of DAIN (30–70%), DAIP (25–75%) and chlorophyll (5–25%), except at the intertidal zone of the Tolka Estuary. The Tolka Estuary would see a reduction in both the summer average macroalgae tonnage and the summer average chlorophyll concentration, of 70% and 50%, respectively, owing to the nitrogen limitation of macroalgae and chlorophyll in the Tolka Estuary. The loss of assimilative capacity within the macroalgae would result in an increase in DAIN and DAIP concentrations.
- Summer average chlorophyll concentrations were found to increase by 1–10% as a result of both a decrease of 10% and increase of 25% in tidally exchanged offshore DAIN and DAIP concentrations. The increase in chlorophyll concentrations observed in response to a reduction in offshore nutrient concentrations is attributed to less favourable bloom-forming conditions, thus resulting in a slower, steady increase in chlorophyll concentration. The increase in chlorophyll concentrations in response to higher offshore nutrient concentrations is attributed to conditions more suitable for bloom formation, causing a greater peak chlorophyll concentration and thus increasing the seasonal average chlorophyll concentration.
- The magnitude of macroalgae bloom increases in response to both increases and decreases in offshore DAIN and DAIP. The increase in bloom magnitude in response to lower offshore concentrations may be due to less competition with chlorophyll. The chlorophyll concentration would increase more slowly, with chlorophyll concentrations largely attributable to circulation of existing chlorophyll.

3.8 Conclusion

The macroalgae module that has been assembled as part of this study and integrated into the 2-D depth-integrated MSN_WQ model has been progressed to the stage of "proof of concept". Although the MSN_WQ model is significantly more complex and more numerically expensive to run than the DCPM model, depth integration of hydrodynamics limits the applicability of the model to Dublin Bay. To fully capitalise on the developments made as part of this study, it is recommended that the macroalgae module is adapted to ROMS, which is a 3-D hydrodynamic model, as operational ROMS coastal and ocean models are maintained by the Marine Institute. Therefore, the eventual ROMS model could be run on a weekly basis to determine the likely trajectory of macroalgae blooms. In a national context, the resultant model would be applicable to all transitional and coastal waters, subject to availability of bathymetry and site-specific nutrient loading data.

A DCPM model of Dublin Bay and its adjoining estuaries was developed as part of the benchmarking process. After calibration, a range of scenarios were simulated to consider the outcome of lowering riverine nitrogen and phosphorus loading, a 20% population growth, improvements in wastewater treatment

technology at Ringsend and the influence of higher or lower tidal nutrient concentrations.

Owing to the predominantly light-limited pelagic primary production, the greatest benefit wrought by a reduction in riverine DAIN and DAIP loading is a substantial reduction in the macroalgae bloom magnitude, by up to 54% in the case of 75% riverine nutrient load reduction. Moderate changes in chlorophyll concentrations are induced by changes in nutrient loadings.

Because of the proximity of Ringsend to the intertidal zone of the Tolka Estuary, a reduction in the wastewater nutrient load due to technology upgrades at Ringsend yields the greatest reduction in simulated macroalgae wet weight.

The scenario that restores DAIN, DAIP and chlorophyll concentrations throughout the system to compliance with salinity-referenced conditions under the Trophic Status Assessment Scheme (TSAS) is implementation of the NDN-PAO AGS treatment at Ringsend. The same scenario also restored macroalgae wet weight density to below 100 $g\,m^{-2}$, although the lesser scenario of reducing riverine DAIN loading by 50% would also bring the macroalgae wet weight density within the range of good/high status.

4 DCPM Performance with Varying Data Resolution: Rural Case Studies

4.1 Introduction

According to the Irish River Basin Management Plan 2018–2021 (DHPLG, 2018), 1460 water bodies are at risk of not achieving their environmental objectives, of which 1184 are rivers, 56 are transitional waters and 13 are coastal waters. Agricultural waste provides the principal pressure in over 53% of at-risk water bodies, while 20% are at risk from urban wastewater pressures and a further 11% are at risk from domestic wastewater.

The proportion of at-risk water bodies subject to significant pressure from agriculture increases along the catchment-to-coast continuum, from 53% of at-risk rivers, through 57% of at-risk transitional water to 61% of at-risk coastal waters. The increasing susceptibility to agricultural pressure towards coastal waters reflects the concentration of agricultural runoff in the coastal and transitional receiving waters.

In addition to the urban case study and scenario modelling of the Liffey and Tolka estuaries included in the benchmarking process, two systems subject to agricultural pressures, namely Clonakilty Harbour/Clonakilty Bay and Argideen Estuary/Courtmacsherry Bay, were selected in this research project to assess the practicality of applying the DCPM model to Irish transitional and coastal waters. The quality and resolution of input data varied between the systems. Data gaps and future research needs were identified upon conclusion of modelling activities.

The two systems differ not only in their geographical spread and shape, but also with respect to the resolution of nutrient loading data available. Clonakilty Bay in the years 2010 and 2011 was, therefore, considered as an example of what can be achieved given basic inputs such as knowledge of annual average riverine loading and sparse monitoring data. Courtmacsherry Bay was used to showcase the possibilities of high-resolution sub-hourly riverine nutrient monitoring and flow measurement at a river inlet. Four separate years were analysed specifically in terms of the summer riverine nutrient loads and necessary reductions thereof.

4.2 Rural Catchment A: Courtmacsherry

Figure 4.1 presents the receiving waters of the Argideen Estuary/Courtmacsherry Bay system, a rural catchment of approximately 180 km^2. The Argideen Estuary/Courtmacsherry Bay system receives five rivers: (1) the East Cruary and (2) the Timoleague, both of which enter the Timoleague Receiving Waters; (3) the Argideen; (4) the Flaxfort stream, entering at Flaxfort Strand; and (5) the Kilbrittain, entering at Courtmacsherry Bay North.

The receiving waters were divided into seven subsections, namely the inner portion of Courtmacsherry Bay, Courtmacsherry Bay North, the Lower Argideen Estuary, Flaxfort Strand, Argideen Macroalgae, the Timoleague Receiving Waters and the Upper Argideen Estuary, as presented in Figure 4.1. As in the case of the urban catchments, the water body boundaries were a further development of the delineations used for the WFD.

Owing to the similarity between the five river subcatchments, in terms of catchment slope, subsoil, groundwater connectivity and land use practices, freshwater discharges and associated DAIN and DAIP loadings for the Argideen (135 km^2), East Cruary (9.7 km^2), Flaxfort (5.4 km^2) and Kilbrittain (23.2 km^2) rivers have been scaled up from area-normalised data derived from the Agricultural Catchments Programme (ACP) data for the Timoleague catchment (5.2 km^2). In addition, outgoing nutrient loads at Courtmacsherry and Timoleague prior to construction and operation of the upgraded facility at Courtmacsherry were based on information on wastewater treatment at Courtmacsherry and conveyancing at Timoleague from Wastewater Discharge Authorisation Application D0294-02 (Courtmacsherry and Timoleague).

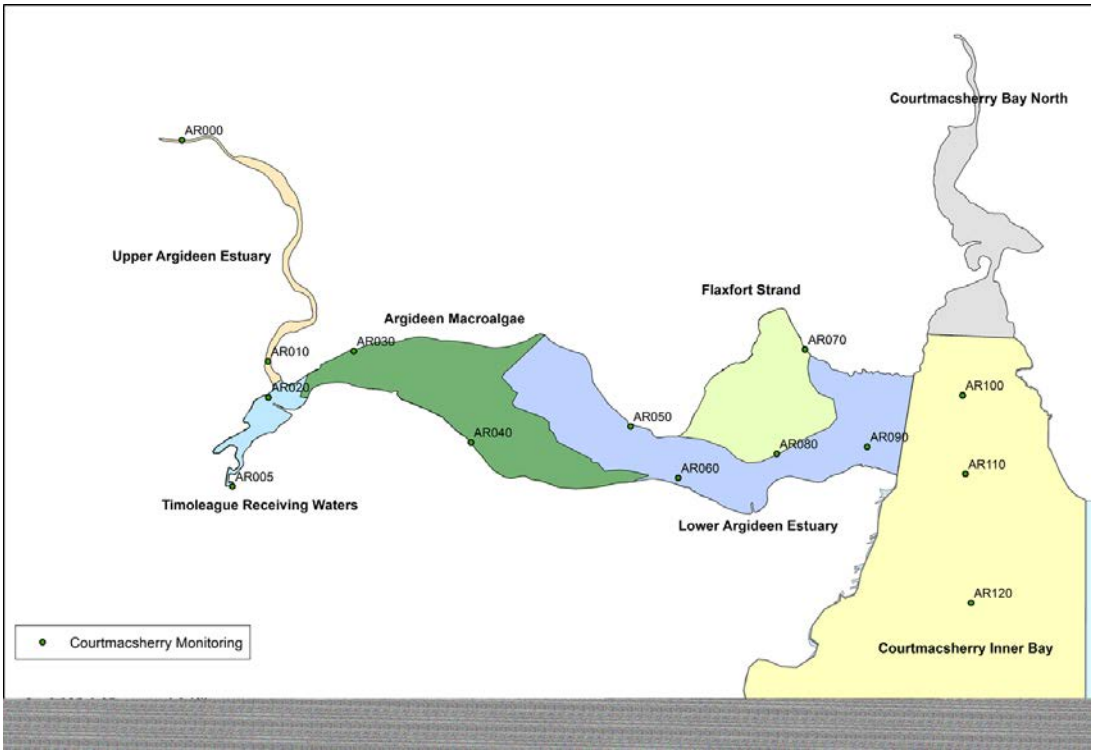

Figure 4.1. The seven water bodies that constitute the DCPM model domain spanning Courtmacsherry Bay and the Argideen Estuary from monitoring points AR000 to AR120. Copyright © 2019 McGovern, Nash and Hartnett. This is an open-access article distributed under the terms of the Creative Commons Attribution License (CC BY). The use, distribution or reproduction in other forums is permitted, provided the original author(s) and the copyright owner(s) are credited and that the original publication in this journal is cited, in accordance with accepted academic practice.

River discharge and nutrient load data for the Timoleague River for years 2010, 2011, 2015 and 2016 were provided by Per-Erik Mellander and Sara Vero of the Teagasc ACP (Shortle and Jordan, 2017). These data provided an opportunity to assess year-to-year differences in the prevailing nutrient loadings and the consequences thereof.

The main research objectives of DCPM modelling of the Courtmacsherry/Argideen system were:

- to characterise each water body with respect to the limiting factor for phytoplankton and macroalgae growth;
- to quantify the benefit of nutrient load reduction for primary production;
- to establish the influence of summer hydrological conditions relative to average conditions upon nutrient transfer and thus eutrophication;
- to identify any improvement in water quality due to better agricultural practice, as endorsed by the Good Agricultural Practice Regulations, also known as Nitrates Action Plans (DOEHLG, 2006, 2009, 2010b, 2014), utilising detailed runoff data for the Timoleague catchment collected by the ACP.

4.2.1 Baseline nutrient loading

Tables 4.1 and 4.2 present the DAIN, DAIP and chlorophyll loadings that were used in the model for the four years studied. These data are a summation of all extrapolated ACP data and wastewater loadings. In the absence of more accurate data, the annual average chlorophyll loads for the periods 2010–2011 and 2015–2016 were used for each of the constituent years. Nutrient loading to the Timoleague/East Cruary includes effluent released from the secondary discharge points in Timoleague. Considering the estimated summer DAIN and DAIP loadings for the four years, the total loads were most similar for 2010, 2011 and 2016, and the higher loads in 2015 reflect a markedly higher annual average flow and R_{SA}.

Table 4.1. River discharge and nutrient loading data applied to the DCPM model of the Courtmacsherry Bay/Argideen Estuary system for 2010, 2011, 2015 and 2016

	Annual average river flow ($m^3 s^{-1}$)	River discharge ratio (R_{SA})	Annual N load ($kg y^{-1}$)	N load ratio (R_{SA})	Annual P load ($kg y^{-1}$)	P load ratio (R_{SA})	Annual Chl load ($kg y^{-1}$)	Chl load ratio (R_{SA})
2010[a]								
Argideen	3.12[b]	0.61	550,092.25[b]	0.55	5579.13[b]	0.61	353.02[c]	1.05
Timoleague/East Cruary	0.35[b]	0.61	61,369.93[b]	0.55	733.30[b]	0.67	33.29[c]	1.10
Kilbrittain	0.54[b]	0.61	94,646.54[b]	0.55	959.92[b]	0.61	60.74[c]	1.05
Flaxfort Strand	0.13[b]	0.61	22,029.80[b]	0.55	223.43[b]	0.61	–[d]	–
Total			728,138.52		7495.78			
Summer			199,763.42		2328.87			
Winter			528,375.10		5166.91			
2011								
Argideen	3.03[b]	0.34	574,394.59[b]	0.26	5542.04[b]	0.33	353.02[c]	1.05
Timoleague/East Cruary	0.34[b]	0.34	64,055.37[b]	0.27	729.20[b]	0.44	33.29[c]	1.10
Kilbrittain	0.52[b]	0.34	98,827.90[b]	0.26	953.54[b]	0.33	60.74[c]	1.05
Flaxfort Strand	0.12[b]	0.34	23,003.05[b]	0.26	221.94[b]	0.33	–[d]	–
Total			760,280.91		7446.73			
Summer			101,505.35		1346.23			
Winter			658,775.55		6100.50			
2015								
Argideen	6.01[b]	0.56	1,221,587.23[b]	0.58	17,092.90[b]	0.6	411.47[c]	0.77
Timoleague/East Cruary	0.66[b]	0.56	135,571.02[b]	0.58	2005.59[b]	0.62	50.96[c]	0.93
Kilbrittain	1.03[b]	0.56	181,167.23[b]	0.58	2940.93[b]	0.6	70.80[c]	0.77
Flaxfort Strand	0.24[b]	0.56	42,168.23[b]	0.58	684.53[b]	0.6	–[d]	–
Total			1,580,493.72		22,723.95			
Summer			460,588.70		6865.16			
Winter			1,119,905.01		15,858.79			
2016								
Argideen	4.04[b]	0.40	784,224.00[b]	0.35	10,787.00[b]	0.54	411.47[c]	0.77
Timoleague/East Cruary	0.45[b]	0.40	85,828.66[b]	0.36	1222.89[b]	0.52	50.96[c]	0.93
Kilbrittain	0.71[b]	0.40	134,930.00[b]	0.35	1856.00[b]	0.54	70.80[c]	0.77
Flaxfort Strand	0.16[b]	0.40	31,406.00[b]	0.35	432.00[b]	0.54	–[d]	–
Total			1,036,388.66		14,297.89			
Summer			182,375.27		3829.21			
Winter			854,013.39		10,468.68			

[a]Between January and April 2010, flow data were available but nitrogen and phosphorus data were not available; hence, nitrogen and phosphorus data were extrapolated from the flow–load curve derived from other years.

[b]Q, N, and P scaled from Teagasc ACP data.

[c]Load calculation from monitoring/flow estimates.

[d]No data were available, used or estimated.

Chl, chlorophyll.

4.2.2 Flow–load relationships

Table 4.3 and Figure 4.2 present in detail the annual and seasonal flow characteristics of the Timoleague River, which were used as a basis for flow and nutrient estimates for the entire system. The driest of the four years was 2011. In general, the net summer nutrient mass transfer from each river was proportional to the average summer discharge from the Timoleague. The summer flow exceedance curves in Figure 4.2 indicate

Table 4.2. Characteristics of the effluent from the existing Courtmacsherry WWTP, which discharges to the Lower Argideen Estuary

Average discharge ($m^3 s^{-1}$)	Wastewater discharge ratio (R_{SA})	Annual N load ($kg y^{-1}$)	N load ratio (R_{SA})	Annual P load ($kg y^{-1}$)	P load ratio (R_{SA})
0.003	1.00	1,=460.00	1.00	113.15	1.00

R_{SA} is the ratio of the total summer discharge, or mass, to the annual sum.

Table 4.3. Comparison of the average annual, summer and winter discharges ($m^3 s^{-1}$) from the River Timoleague for the years 2010, 2011, 2015 and 2016 compared with the 4-year averages

	Year				
Discharge	2010–2016	2010	2011	2015	2016
$Q_{AV\ YR}$	0.151	0.127	0.125	0.258	0.210
$Q_{AV\ SUMM}$	0.075	0.065	0.040	0.131	0.062
$Q_{AV\ WINT}$	0.271	0.181	0.189	0.345	0.306

$Q_{AV\ YR}$ is the average of the entire dataset of hourly discharge measurements, while $Q_{AV\ SUMM}$ is the average of the values measured from April to September, inclusive, and $Q_{AV\ WINT}$ is the average of values measured from October to March, inclusive.

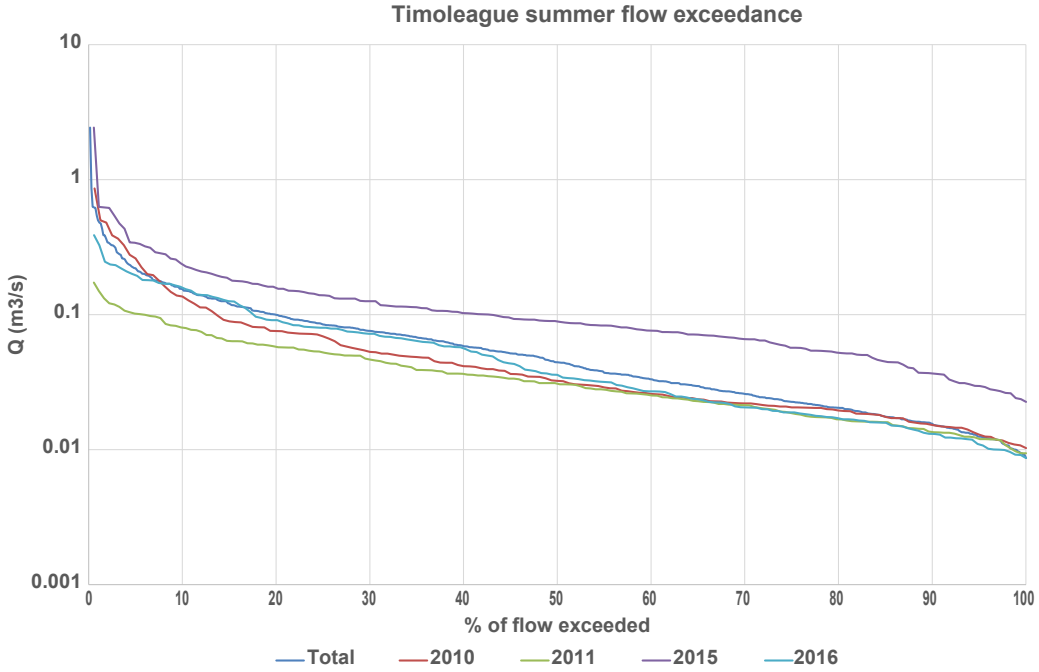

Figure 4.2. Comparison of the summer flow exceedance distributions in the Timoleague River for each of the years 2010, 2011, 2015 and 2016 compared with the overall summer flow exceedance distribution for the four years combined.

that the summer of 2011 was, for the most part, distinctly drier than the other three summers. Summer 2011 was drier than an average year, or indeed the year 2016, but with higher flows at lower percentiles. Hence, higher than Q_{50} (median) flows in 2016 delivered a sustained higher nutrient transfer, which is borne out in figures presented in Table 4.3.

Figure 4.3 presents the DAIN (Figure 4.3a) and DAIP (Figure 4.3b) flow–load relations for the four summers under examination. Although the full range of observed flows was used for derivation of flow–load relations for each nutrient and year, in Figure 4.3 the derived relations were applied to the 4-year averaged flow percentiles only for comparison purposes. Note

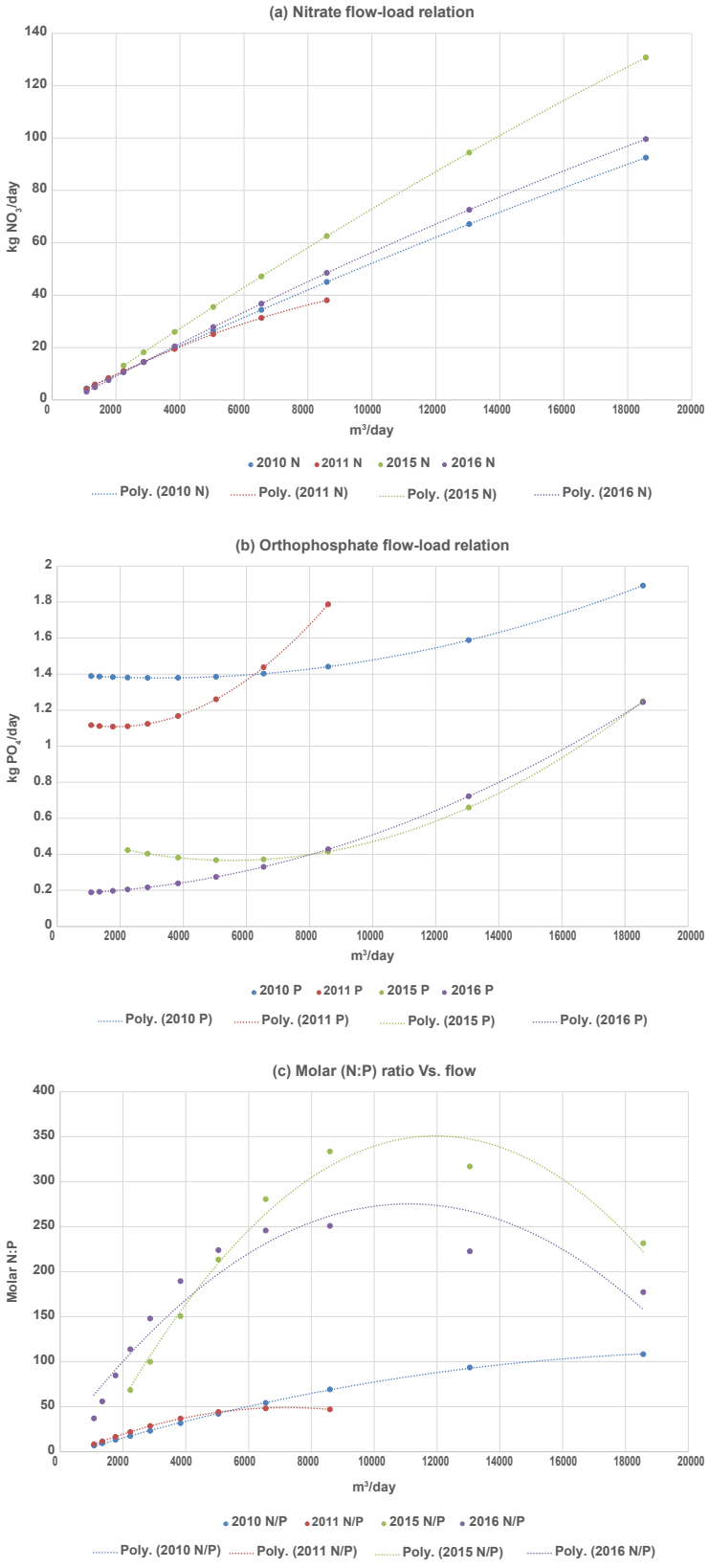

Figure 4.3. The relation between summer flow in the Timoleague River and (a) NO_3 load, (b) PO_4 load and (c) molar N:P ratio. The relations were derived for the summers of 2010, 2011, 2015 and 2016 based on data provided by the Teagasc ACP. Flow values are long-term summer flow percentiles Q_{05}–Q_{95}.

that in the cases of 2011 and 2015, the ranges of percentiles used for comparison were restricted to the range of observations. Figure 4.3c presents the molar ratio of summer N:P loading values, taken from Figure 4.3a and b. The shape of the curve of the projected N:P ratio versus flow for the years 2015 and 2016, towards the high-flow/low-percentile situation, is similar, although the summers were different with respect to the average flows. The flow value at which the N:P ratio begins to decline in 2015 and 2016 was determined, by differentiation of the fitted trendline, to be 11,059 $m^3 d^{-1}$ and 11,923 $m^3 d^{-1}$, which falls in the range of Q_{05} and Q_{10}. The implication of this trend is that, at higher flows, phosphorus limitation of the system is offset by increasing DAIP loading relative to DAIN, the consequence of which would be higher potential growth of primary producers after higher rainfall.

Table 4.4 shows the tidal boundary conditions, which were calculated by averaging monitoring data from the monitoring point AR120 at the outer edge of Courtmacsherry Inner Bay for 2010, 2015 and 2016; in the absence of coastal monitoring data in 2011, the 2010 boundary data were adopted. Considering the nutrient loading regime presented in Tables 4.1 and 4.2 and Figure 4.3, and the flow data presented in Table 4.3 and Figure 4.2, the lower summer chlorophyll concentration in 2010 and 2011 may be due to the lower than average but sustained flow in both years transferring less DAIN and DAIP throughout the peak production season. The lower summer DAIP concentration and higher summer chlorophyll concentration in 2015 and 2016, matched by lower salinities, may reflect a higher freshwater loading to the coastal zone, with DAIP depleted because of higher growth of phytoplankton.

Table 4.5 presents the final exchange rates for the water bodies. For each water body the final exchange rates for all four years fell within a narrow range, with the greater variation in values from year to year occurring further upstream, reflecting greater exchange due to higher flushing because of higher freshwater flows. Preliminary values for the exchange rates for each of the seven water bodies were determined using equations A2.24 and A2.25 (see Appendix 2).

Figure 4.4 compares the seasonal averaged salinity for 2010, 2011, 2015 and 2016 with the DCPM model-derived salinity time series for each year. In general, for each water body, the calibrated water body averaged salinity curves lie between the summer and winter average salinities.

Site-specific k_d values were determined for each water body using Secchi depth readings together with the separate expressions given by Devlin *et al.* (2008) for transitional and coastal waters. Secchi disc recordings were available only for 2010 and 2011. Using all site-specific values for parameters such as light attenuation coefficients, exchange rate and seasonal ratios for river discharge and nutrient loading brought all DCPM observations to the right order of magnitude. The main differences between the final calibrated models for each year are highlighted in Table 4.6. The only other differences between the four models were the nutrient loads, tidal boundary conditions, the exchange rates in Table 4.6 and the river discharge.

Table 4.7 presents a comparison between seasonally averaged monitoring data and the DCPM model estimates for the four years. The most notable observation from Table 4.7 is the imprecision of the model for 2011 with respect to the summer

Table 4.4. Tidal boundary concentrations of DAIN, DAIP, chlorophyll and salinity used for the DCPM model of the Courtmacsherry Bay/Argideen Estuary system for each of the four years considered in this case study

	N concentration in adjacent seawater (mM)		P concentration in adjacent seawater (mM)		Chl concentration in adjacent seawater (mg l^{-1})		Salinity in adjacent seawater (psu)
Year	Winter	Summer	Winter	Summer	Winter	Summer	
2010	32.14	2.85	0.63	0.25	1.57	0.85	34.89
2011	32.14	2.85	0.63	0.25	1.57	0.85	34.89
2015	19.60	2.95	0.81	0.13	1.23	3.38	34.51
2016	15.82	1.98	0.82	0.08	0.90	3.38	34.51

Chl, chorophyll; summer, April to September, inclusive; winter, October to March, inclusive.

Table 4.5. Final tidal exchange rates for 2010, 2011, 2015 and 2016 applied to the DCPM model of the Courtmacsherry Bay/Argideen Estuary system

	Exchange rate (day^{-1})			
Water expanse	**2010**	**2011**	**2015**	**2016**
Courtmacsherry Inner Bay	0.50	0.50	0.50	0.50
Lower Argideen Estuary	0.75	0.75	0.75	0.80
Argideen Macroalgae	0.44	0.44	0.54	0.50
Timoleague Receiving Waters	0.44	0.44	0.25	0.20
Upper Argideen Estuary	0.22	0.22	0.30	0.11
Courtmacsherry Bay North	0.30	0.30	0.30	0.35
Flaxfort Strand	0.35	0.35	0.35	0.40

Exchange rates were the result of calibration for each year. At the outset of calibration for the year 2010, the initial exchange rates for the system were determined after Hartnett *et al.* (2011b). The calibration exchange rate for each year was initially taken as the exchange rate for the previous year.

Table 4.6. Parameters that were modified from the default values during biological calibration of the DCPM model of the Courtmacsherry Bay/Argideen Estuary system

			Year			
Parameter	**Default**	**Range**	**2010**	**2011**	**2015**	**2016**
Macroalgae turnover rate (day^{-1})	0.033	0.02–0.1[a]	–	–	0.05	0.05
Macroalgae wet weight to dry weight ratio	7	–	5	–	–	4.9
Phytoplankton loss rate (day^{-1})	0.10	0–0.8[a]	0.08	0.08	0.08	0.08

Non-default phytoplankton loss rates were used only for Timoleague Receiving Waters and the Upper Argideen Estuary.
[a]From Porcella *et al.* (1985).

macroalgae standing stock. The authors postulate that there are two possible reasons for this anomaly:

1. Growth of macroalgae, in suitable intertidal areas, and of phytoplankton is generally noted to have been phosphorus limited in the years 2010, 2015 and 2016. The DCPM model results indicate that, in 2011, primary production from the Lower Argideen Estuary to Courtmacsherry Inner Bay was phosphorus limited at the beginning and end of the summer, and nitrogen limited at the peak of summer. Table 4.3 shows that the summer of 2011 was notably dry. Figure 4.3a and b indicates that, in terms of modelled flow–load relations, DAIP transfer from the catchments was much higher at median summer flow values, whereas nitrogen transfer was relatively linear throughout the observed flow range. Figure 4.3c captures the flat molar N:P ratio projection with increasing flow, indicating the possibility that, although the molar ratio suited growth, the overall lack of nutrients transferred to the catchment via agricultural runoff from rainfall events inhibited growth. The higher DAIP load at median flows may reflect the effect of first flushing of DAIP at the initiation of a rainfall event.
2. The lack of available coastal monitoring data for AR100, AR110 and AR120 led to the adoption of 2010 tidal boundary data. The combined effect of accurate freshwater loading and uncertain tidal boundary conditions may explain the apparent nitrogen limitation in the DCPM model. If the boundary nutrient concentrations in 2011 were like those in 2010, there is a possibility that nitrogen limitation would have been offset by an intertidal flux of ammonia into the water column in the lower reaches of the estuary.

Figure 4.5a presents the limiting factors for primary producer growth in 2010, which were similar to those prevailing in 2015 and 2016. The Upper Argideen Estuary and the Timoleague Receiving Waters were both light limited throughout the year. Primary production in all other water bodies was light limited during the early spring, and then phosphorus limited

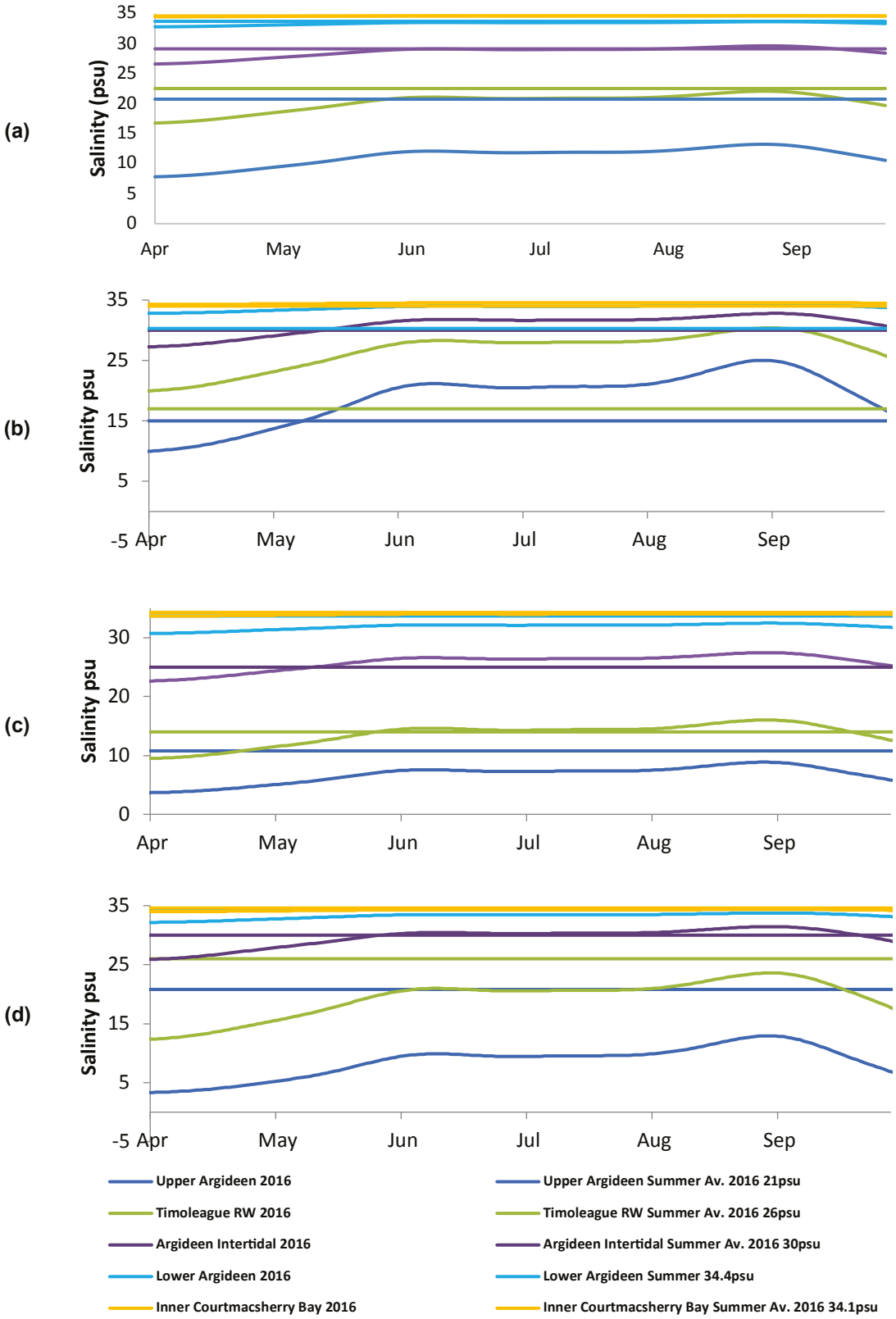

Figure 4.4. Comparison of the salinity in the Argideen Estuary/Courtmacsherry Bay system simulated by the DCPM model and the summer average salinity concentrations determined from EPA monitoring data for (a) 2010, (b) 2011, (c) 2015 and (d) 2016.

Table 4.7. Observations of seasonal DAIN, DAIP, phytoplankton and macroalgae concentrations in the Argideen Estuary/Courtmacsherry Bay system area compared with DCPM model-simulated seasonal averages after calibration for 2010, 2011, 2015 and 2016

	DAIN (µM)				DAIP (µM)				Chlorophyll (mg m^{-3})				Macroalgae (tonnes wet weight)	
	Winter		Summer		Winter		Summer		Winter		Summer		Summer	
Water body	EPA	DCPM	EPA	DCPM	EPA	DCPM	EPA	DCPM	EPA	DCPM	EPA	DCPM	EPA	DCPM
2010														
Courtmacsherry Inner Bay	40.07	37.31	4.64	4.21	0.65	0.63	0.23	0.20	1.00	1.59	1.14	1.92	–	0.00
Lower Argideen Estuary	109.29	63.86	10.00	13.37	0.78	0.71	0.22	0.13	1.60	1.77	3.89	3.41	–	0.00
Argideen Macroalgae	250.36	155.43	30.71	52.29	0.92	0.99	0.12	0.04	2.25	2.05	10.70	5.83	794.00	784.97
Timoleague Receiving Waters	322.86	280.37	108.83	137.96	1.35	1.40	0.25	0.40	3.76	2.15	15.90	9.16	–	0.00
Upper Argideen Estuary	357.14	373.73	96.00	231.80	1.28	1.71	0.73	0.88	1.90	2.37	19.38	10.48	–	0.00
Courtmacsherry. Bay North	–	70.28	–	12.32	–	0.70	–	0.03	–	2.44	–	3.02	–	365.39
Flaxfort Strand	–	75.57	–	16.02	–	0.70	–	0.03	–	2.33	–	3.93	102.00	116.76
2011														
Courtmacsherry Inner Bay	40.07	37.31	4.64	4.21	0.65	0.63	0.23	0.20	1.00	1.59	1.14	1.92	–	0.00
Lower Argideen Estuary	109.29	63.86	10.00	13.37	0.78	0.71	0.22	0.13	1.60	1.77	3.89	3.41	–	0.00
Argideen Macroalgae	250.36	155.43	30.71	52.29	0.92	0.99	0.12	0.04	2.25	2.05	10.70	5.83	794.00	784.97
Timoleague Receiving Waters	322.86	280.37	108.83	137.96	1.35	1.40	0.25	0.40	3.76	2.15	15.90	9.16	–	0.00
Upper Argideen Estuary	357.14	373.73	96.00	231.80	1.28	1.71	0.73	0.88	1.90	2.37	19.38	10.48	–	0.00
Courtmacsherry Bay North	–	70.28	–	12.32	–	0.70	–	0.03	–	2.44	–	3.02	–	365.39
Flaxfort Strand	–	75.57	–	16.02	–	0.70	–	0.03	–	2.33	–	3.93	102.00	116.76

Table 4.7. Continued

Water body	DAIN (µM)				DAIP (µM)				Chlorophyll (mg m^{-3})				Macroalgae (tonnes wet weight)	
	Winter		Summer		Winter		Summer		Winter		Summer		Summer	
	EPA	DCPM	EPA	DCPM	EPA	DCPM	EPA	DCPM	EPA	DCPM	EPA	DCPM	EPA	DCPM
2015														
Courtmacsherry Inner Bay	40.07	37.31	4.64	4.21	0.65	0.63	0.23	0.20	1.00	1.59	1.14	1.92	–	0.00
Lower Argideen Estuary	109.29	63.86	10.00	13.37	0.78	0.71	0.22	0.13	1.60	1.77	3.89	3.41	–	0.00
Argideen Macroalgae	250.36	155.43	30.71	52.29	0.92	0.99	0.12	0.04	2.25	2.05	10.70	5.83	794.00	784.97
Timoleague Receiving Waters	322.86	280.37	108.83	137.96	1.35	1.40	0.25	0.40	3.76	2.15	15.90	9.16	–	0.00
Upper Argideen Estuary	357.14	373.73	96.00	231.80	1.28	1.71	0.73	0.88	1.90	2.37	19.38	10.48	–	0.00
Courtmacsherry Bay North	–	70.28	–	12.32	–	0.70	–	0.03	–	2.44	–	3.02	–	365.39
Flaxfort Strand	–	75.57	–	16.02	–	0.70	–	0.03	–	2.33	–	3.93	102.00	116.76
2016														
Courtmacsherry Inner Bay	40.07	37.31	4.64	4.21	0.65	0.63	0.23	0.20	1.00	1.59	1.14	1.92	–	0.00
Lower Argideen Estuary	109.29	63.86	10.00	13.37	0.78	0.71	0.22	0.13	1.60	1.77	3.89	3.41	–	0.00
Argideen Macroalgae	250.36	155.43	30.71	52.29	0.92	0.99	0.12	0.04	2.25	2.05	10.70	5.83	794.00	784.97
Timoleague Receiving Waters	322.86	280.37	108.83	137.96	1.35	1.40	0.25	0.40	3.76	2.15	15.90	9.16	–	0.00
Upper Argideen Estuary	357.14	373.73	96.00	231.80	1.28	1.71	0.73	0.88	1.90	2.37	19.38	10.48	–	0.00
Courtmacsherry Bay North	–	70.28	–	12.32	–	0.70	–	0.03	–	2.44	–	3.02	–	365.39
Flaxfort Strand	–	75.57	–	16.02	–	0.70	–	0.03	–	2.33	–	3.93	102.00	116.76

during the peak of summer. Owing to low flow conditions, the limiting factor for chlorophyll growth in 2011 varied between light, nitrogen and phosphorus, as presented in Figure 4.5b. From Figure 4.5c it can be seen that macroalgae growth was nitrogen limited during the summer of 2011, in contrast to other summers, when the system was strictly phosphorus limited.

There was generally good agreement between the DCPM model-simulated averages and seasonal average observations for the other three years, with respect to nutrients, phytoplankton and macroalgae. The same gradient observed in monitoring data throughout the continuum from freshwaters to the coastal zone was replicated in the equivalent results generated by the DCPM model. It is important to emphasise that the averages generated by the DCPM

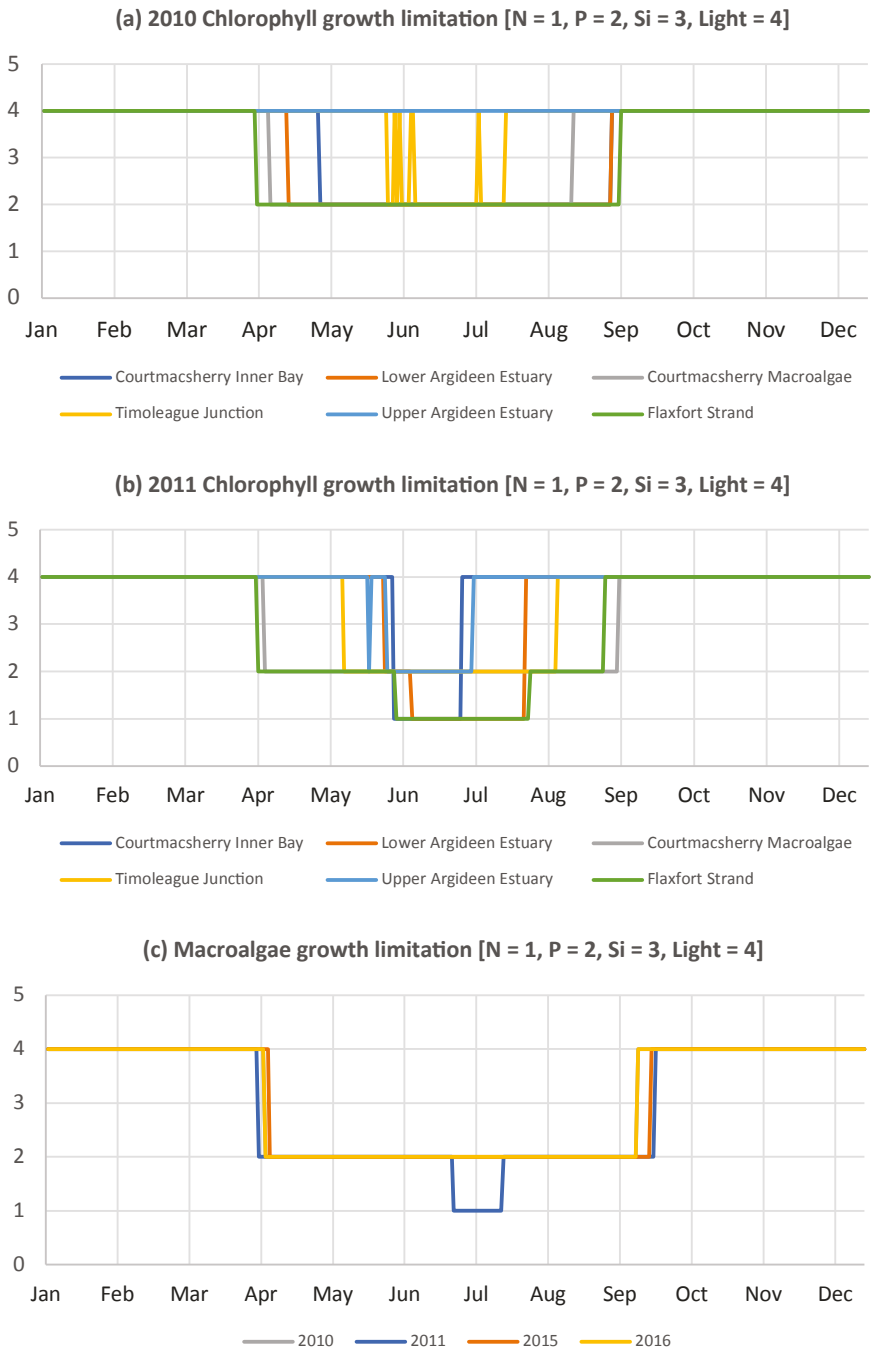

Figure 4.5. Limiting factors for chlorophyll growth in the water bodies of the Courtmacsherry Bay/ Argideen Estuary, as indicated by the DCPM model, in (a) 2010 and (b) 2011. (c) Limiting factors for macroalgae growth in 2010, 2011, 2015 and 2016.

model are based on daily resolution outputs over the full summer from April to September inclusive, whereas the EPA monitoring data are collected at three time points during the summer.

The performance of the calibrated DCPM model for both periods is presented in Tables 4.8 and 4.9 in terms of percentage difference between the seasonal averages of DAIN, DAIP and chlorophyll concentration and macroalgae and the simulated averages. The objective of calibration was to achieve a percentage difference of at most ±30%. Taking the year 2010, for example, the winter averages are generally within the range of ±40%. As winter is a time of low productivity, the averages reflect the model performance with respect to mixing. Bearing in mind that the models for the four years were calibrated for mixing by tuning the exchange rate to match observed salinity averages, the performance of the model for winter 2010 suggests that model calibration has been successful with respect to mixing.

The averages determined by the DCPM model are based on estimated water depth distributions derived from Admiralty charts. It may be noted that there is a reduction in the model accuracy towards the freshwater end of the Upper Argideen Estuary and the Timoleague Receiving Waters. As concentrations are determined as mass per unit volume, the consequence of under- or overestimation of volume must be kept in mind when interpreting the percentage difference. A lack of knowledge with respect to how the river reaches and their adjacent flood banks interact under high flows must also be considered. Under- or overestimation of water body volumes also influences the modelled exchange for each daily time step.

4.2.3 Scenario loading

Owing to the observed system-wide trend of phosphorus limitation during the peak primary production season, the nutrient load reduction scenarios were primarily focused on further DAIP reduction. Table 4.10 summarises the nine scenarios considered. Additional DAIP reduction may be brought about by:

- sustained improvement in soil phosphorus management (scenarios 2 and 3);
- improved wastewater infrastructure (scenario 9).

Although the system was predominantly phosphorus limited during the four years, for a brief period in 2011 the system switched to nitrogen limited because of the dry conditions. As a result of this dry period, the outcome of a joint reduction in DAIN and DAIP was also considered, hereafter referred to as a coupled reduction; scenarios 4 and 5 apply this case. Coupled reductions and DAIP reduction alone have been considered in two steps of 33% of the initial diffuse nutrient loading.

Opportunistic macroalgae growth occurs in the intertidal zone in the Argideen Estuary. Consequently, the impact of lower tidally exchanged coastal nutrient concentrations was considered in scenarios 6 and 7, with coupled reductions. As previously noted, the years 2010 and 2016 were similar with respect to summer flow exceedance distributions and averages. For this reason, the 2010 flow–load relationship for DAIN and DAIP was applied to 2016 flows (scenario 8), and vice versa (scenario 1), to establish the improvements in water quality due to better catchment management practice between 2010 and 2016.

The availability of winter nutrient monitoring data (NH_4, NO_3, NO_2 and PO_4) for the Western Celtic Seas for 2015, allied with an estimate of the ratio of winter to summer nutrients, facilitated the inclusion of an additional DCPM box representing Courtmacsherry Outer Bay with tidal boundary conditions. Thus, the potential impact of nutrient load reductions on the outer coastal waters was investigated.

Finally, scenario 9 investigated the effect of centralising the wastewater from Timoleague and Courtmacsherry, expanding the treatment capacity from 500 PE to 2500 PE, and treating in compliance with current regulations and associated amendments (DOEHLG, 2001, 2004, 2010a) and then discharging into the Courtmacsherry Harbour area.

Coupling of 2010 flows and 2016 flow–load relationship

Figure 4.6 presents the implications of scenario 1, considering the flow–load relation for NO_3 and PO_4 in 2016 occurring in tandem with the 2010 flow, i.e. the flow–load relations for 2016 were applied to the flow observations of 2010. This resulted in an increase of 31% in summer phosphorus loading, whereas there was effectively no change in nitrogen loading.

Table 4.8. Post-calibration performance of the DCPM model of the Courtmacsherry Bay/Argideen Estuary system for 2010 and 2011

Parameter (mean)	Courtmacsherry Inner Bay			Lower Argideen Estuary			Argideen Macroalgae			Timoleague Receiving Waters			Upper Argideen Estuary			Flaxfort Strand		
	EPA	DCPM	Difference (%)	EPA	DCPM	Difference (%)	EPA	DCPM	Difference (%)	EPA	DCPM	Difference (%)	EPA	DCPM	Difference (%)	EPA	DCPM	Difference (%)
2010																		
DAIN (µM)																		
Winter	40.07	37.31	–6.90	109.29	63.86	–41.57	250.36	155.43	–37.92	322.86	280.37	–13.16	357.14	373.73	4.65	–	75.57	–
Summer	4.64	4.21	–9.39	10.00	13.37	33.73	30.71	52.29	70.24	108.83	137.96	26.77	96.00	231.80	141.46	–	16.02	–
DAIP (µM)																		
Winter	0.65	0.63	–3.09	0.78	0.71	–9.80	0.92	0.99	7.91	1.35	1.40	3.58	1.28	1.71	33.57	–	0.70	–
Summer	0.23	0.20	–13.90	0.22	0.13	–42.15	0.12	0.04	–69.09	0.25	0.40	57.36	0.73	0.88	21.50	–	0.03	–
Chlorophyll ($mg m^{-3}$)																		
Winter	1.00	1.59	59.01	1.60	1.77	10.45	2.25	2.05	–9.00	3.76	2.15	–42.80	1.90	2.37	24.58	–	2.33	–
Summer	1.14	1.92	68.24	3.89	3.41	–12.28	10.70	5.83	–45.53	15.90	9.16	–42.40	19.38	10.48	–45.93	–	3.93	–
Summer macroalgae (tonnes wet weight)							794.00	784.97	–1.14							102.00	116.76	14.47
2011																		
DAIN (µM)																		
Winter	–	38.47	–	71.25	71.13	–0.16	–	179.16	–	323.00	296.06	–8.34	352.00	416.45	18.31	–	85.72	–
Summer	–	4.82	–	20.71	9.00	–56.53	–	28.48	–	38.57	66.89	73.42	99.71	135.75	36.14	12.92	8.52	–34.07
DAIP (µM)																		
Winter	–	0.64	–	0.68	0.72	6.58	–	1.04	–	1.36	1.41	3.99	0.69	1.80	161.45	–	0.72	–
Summer	–	0.25	–	0.21	0.18	–11.48	–	0.05	–	0.19	0.18	–8.44	0.27	0.47	75.92	0.08	0.05	–36.63
Chlorophyll ($mg m^{-3}$)																		
Winter	–	1.58	–	1.64	1.74	6.04	–	2.00	–	3.76	2.06	–45.10	4.32	2.30	–46.84	–	2.28	–
Summer	–	1.56	–	9.75	2.91	–70.16	–	5.27	–	8.93	7.90	–11.47	25.80	12.02	–53.40	3.40	3.93	15.58
Summer macroalgae (tonnes wet weight)								814.46	–54.83							236.00	161.42	–31.60

Table 4.9. Post-calibration performance of the DCPM model of the Courtmacsherry Bay/Argideen Estuary system for 2015 and 2016

Parameter (mean)	Courtmacsherry Inner Bay			Lower Argideen Estuary			Argideen Macroalgae			Timoleague Receiving Waters			Upper Argideen Estuary			Flaxfort Strand		
	EPA	DCPM	Difference (%)	EPA	DCPM	Difference (%)	EPA	DCPM	Difference (%)	EPA	DCPM	Difference (%)	EPA	DCPM	Difference (%)	EPA	DCPM	Difference (%)
2015																		
DAIN (µM)																		
Winter	21.28	31.41	47.59	36.43	87.57	140.38	93.57	222.41	137.69	282.14	391.23	38.67	267.14	451.88	69.15	–	98.43	–
Summer	4.86	6.48	33.34	11.79	28.13	138.71	72.71	95.73	31.66	255.71	275.62	7.78	183.57	378.69	106.29	–	31.30	–
DAIP (µM)																		
Winter	0.78	0.85	8.44	1.24	1.10	–11.38	1.83	1.74	–4.94	1.65	2.56	55.53	1.47	2.86	94.69	–	1.14	–
Summer	0.12	0.09	–22.96	0.09	0.07	–26.75	0.28	0.10	–66.29	1.14	1.41	23.45	0.74	2.22	202.49	–	0.05	–
Chlorophyll ($mg\,m^{-3}$)																		
Winter	1.52	1.40	–8.02	2.82	1.66	–41.27	5.76	1.89	–67.22	3.93	1.88	–52.00	3.95	1.94	–50.86	–	1.88	–
Summer	4.21	4.30	2.21	6.50	5.42	–16.63	15.65	7.08	–54.79	13.43	7.76	–42.21	15.38	6.30	–59.04	–	5.83	–
Summer macroalgae (tonnes wet weight							1332.00	1,31.03	–0.07							96.00	63.52	–33.83
2016																		
DAIN (µM)																		
Winter	17.48	24.83	42.02	43.17	65.94	52.74	98.57	187.84	90.56	147.86	377.54	155.34	154.29	473.66	207.00	–	83.54	–
Summer	1.64	2.98	81.57	2.29	11.09	385.09	20.14	43.41	115.51	44.29	145.61	228.80	62.86	262.09	316.95	–	14.44	–
DAIP (µM)																		
Winter	0.75	0.84	11.60	1.60	0.98	–38.71	2.99	1.45	–51.67	2.84	2.24	–21.16	2.65	2.66	0.60	–	1.01	–
Summer	0.08	0.08	0.41	0.11	0.06	–44.57	0.45	0.11	–75.54	0.60	0.72	21.14	1.03	1.90	83.68	–	0.03	–
Chlorophyll ($mg\,m^{-3}$)																		
Winter	1.28	1.10	–13.94	3.30	1.42	–57.06	–	1.93	–	3.60	2.34	–34.99	5.50	2.64	–52.02	–	1.90	–
Summer	4.83	4.21	–12.82	4.60	5.71	24.19	9.23	9.86	6.83	24.40	19.89	–18.47	30.00	22.06	–26.48	–	6.32	–
Summer macroalgae (tonnes wet weight)							380.00	380.84	0.22							20.00	42.02	110.12

Table 4.10. Scenarios considered in nutrient load scenario simulations

Year(s)	Scenario number	Scenario description
2010	1	2016 flow–load relationships (N and P) × 2010 flows
2011, 2015, 2016	2	–33% freshwater phosphorus loading
	3	–66% freshwater phosphorus loading
	4	–33% freshwater phosphorus loading and −33% freshwater nitrogen loading
	5	–66% freshwater phosphorus loading and −66% freshwater nitrogen loading
	6	–33% tidal phosphorus concentration and −33% tidal nitrogen concentration
	7	–66% tidal phosphorus concentration and −66% tidal nitrogen concentration
2016	8	2010 flow–load relationships (N and P) × 2016 flows
	9	Upgrading of wastewater infrastructure

Scenarios 1 and 8 lead to a discussion of improvements in catchment management between 2010 and 2016.

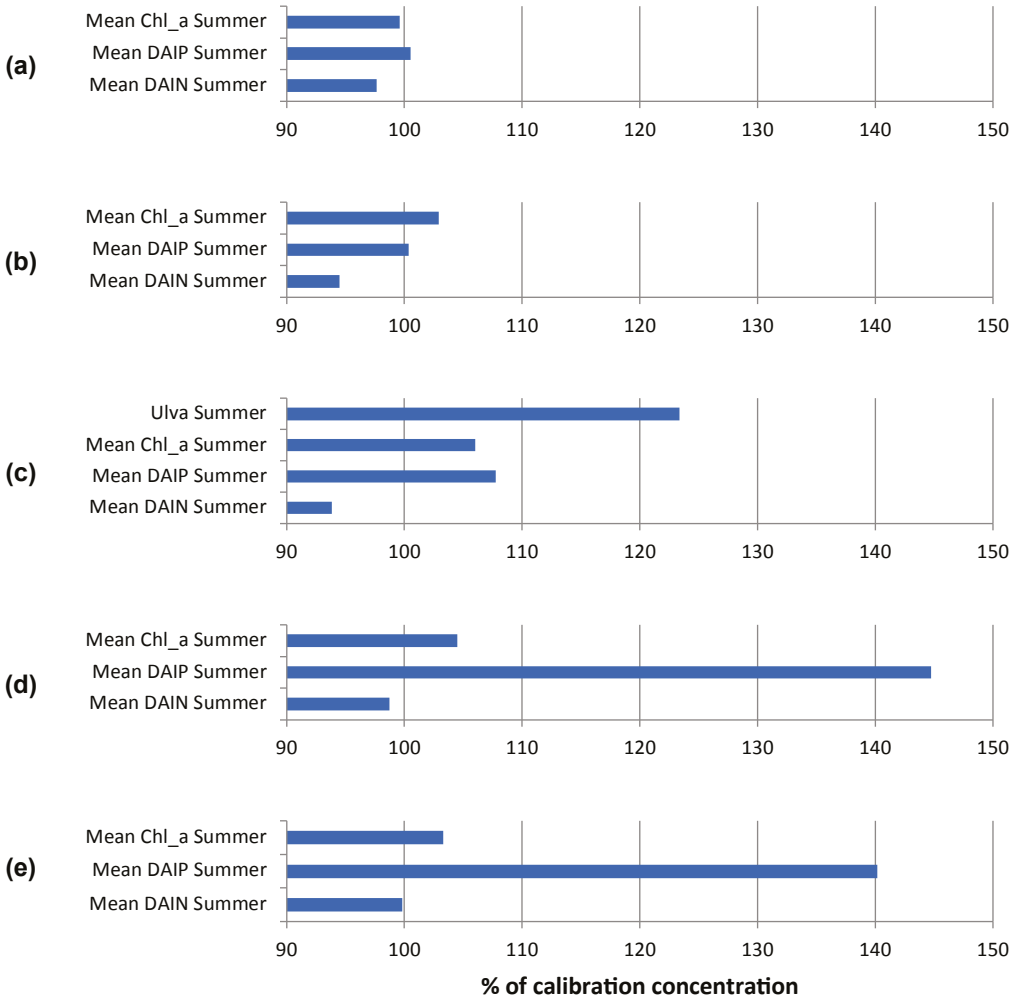

Figure 4.6. Percentage change in the average concentrations of DAIN, DAIP and chlorophyll and in macroalgae tonnage simulated by the DCPM model of the Courtmacsherry Bay/Argideen Estuary system due to imposition of flow–load relations for 2016 on 2010 flow data (scenario 1). The DCPM model of the system comprises (a) Courtmacsherry Inner Bay, (b) the Lower Argideen Estuary, (c) Argideen Macroalgae, (d) the Timoleague Receiving Waters and (e) the Upper Argideen Estuary.

A moderate 5% increase in summer chlorophyll concentration in the freshwater Upper Argideen Estuary and Timoleague Receiving Waters reflects light limitation in these waters in early and late summer. A 40–50% increase in the DAIP concentration in both reflects the greater availability of phosphorus. This increase in DAIP concentration has a greater impact in the downstream Argideen Macroalgae zone, where there was an observed increase in the *Ulva* tonnage of approximately 25%, an increase in the summer average chlorophyll concentration of 5% and an increase in DAIP concentration of 7–8%. System-wide, there was a reduction in summer DAIN concentrations, which reflects greater uptake of DAIN by primary producers, as application of the 2016 flow–load relation results in a negligible increase in DAIN loading during the summer.

2011

Scenarios 2–7 were simulated for the year 2011. The effects of the scenarios are summarised in Figure 4.7. Firstly, scenarios 2 and 3 were considered. Application of the two reductions, in a stepwise manner, resulted in a system-wide increase in DAIN of between 2% and 10%, and a reduction of 5–30% in the summer average chlorophyll concentration. A slight reduction in the net macroalgae tonnage was observed in response to scenarios 2 and 3.

Scenarios 4 and 5 were subsequently simulated to investigate the outcome of intensive nutrient management during the drier than average summer of 2011. The results indicated that the coupled reductions could lead to a decrease in *Ulva* bloom magnitudes of up to 40%, although there was no additional reduction in phytoplankton bloom magnitudes in the freshwater Upper Argideen Estuary and Timoleague Receiving Waters beyond what was observed with scenarios 2 and 3.

A complex effect of scenarios 4 and 5 was a substantial increase in DAIP concentrations of 2–160% in waters downstream of and including Timoleague Receiving Waters. This increase, due to lower DAIP assimilation in primary producers, was indicated throughout the system. There was also a decrease in DAIN concentrations, which reflects a combination of the reduction in the DAIN load and a reduction in the assimilative capacity.

To establish the sensitivity of primary producers to coastal nutrient concentrations, scenarios 6 and 7 were considered. The two simulated reductions had a greater impact on primary producers in brackish waters, although the effect did propagate through to the two freshwater water bodies, with an increase in DAIN and DAIP due to a reduction in primary producers. Comparing the effect of coupled nutrient reduction at the tidal boundary versus coupled reduction from freshwater loading, it is clear from Figure 4.7c that there was a similar impact on *Ulva* bloom magnitudes, yet the coupled reduction in freshwater nutrient loadings leads to a large increase in unassimilated DAIP in the intertidal macroalgae zone in the Argideen Estuary.

2015

The same loading scenarios considered for summer 2011 were also applied to summer 2015. Figure 4.8a–f summarises the outcomes of scenarios 2–7.

Scenarios 2 and 3 resulted in an increase in DAIN concentration of 10–15% throughout the system. There was a reduction in average chlorophyll concentration of 2–20%, induced by a 66% reduction in DAIP loading, although scenario 2 resulted in a negligible change in average chlorophyll concentration. Both scenarios resulted in a reduction in the summer average *Ulva* bloom magnitude of 62–83%.

Scenarios 4 and 5 affected DAIP concentrations and primary producers to the same extent as scenarios 2 and 3, with the sole difference between scenarios 2 and 3 and scenarios 4 and 5 being a reduction in DAIN concentrations throughout, as would be expected in line with the reduction in DAIN loading.

Scenarios 6 and 7 had a moderate impact on the average chlorophyll concentration of 3–10%, but there was no corresponding reduction in summer macroalgae bloom magnitudes. Whilst the zone of impact with respect to nutrient concentrations extended from Courtmacsherry Inner Bay (Figure 4.8a) to the large macroalgae patch (Figure 4.8c), the reduction in chlorophyll concentration extended to the freshwater water bodies upstream (Figure 4.8d and e).

As winter monitoring data for the Celtic Sea adjacent to Courtmacsherry Bay were available, Courtmacsherry

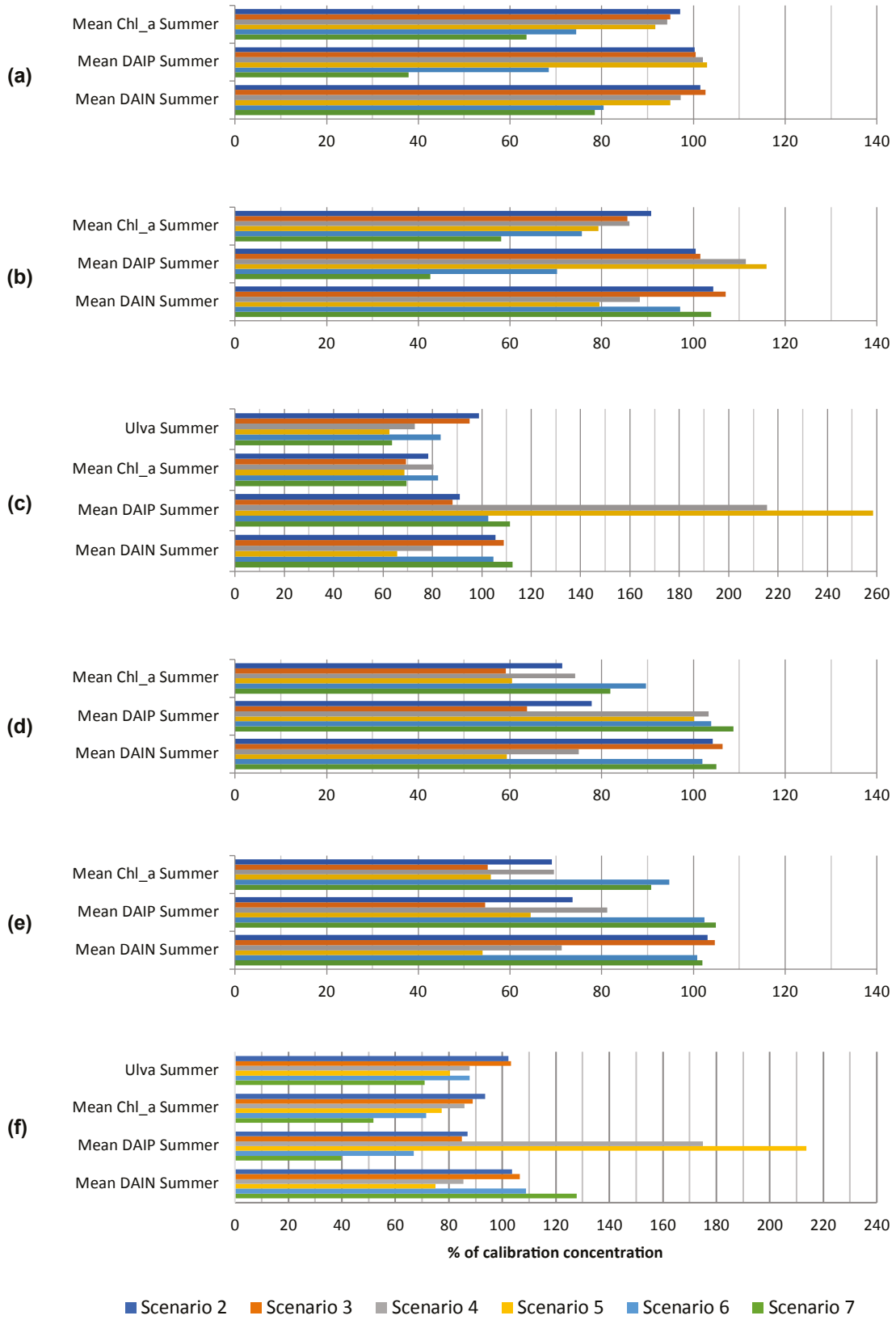

Figure 4.7. Percentage change in the concentrations of DAIN, DAIP and chlorophyll and in macroalgae tonnage due to riverine nutrient load reduction or boundary reduction based on 2011 loading data, for the DCPM model comprising (a) Courtmacsherry Inner Bay, (b) the Lower Argideen Estuary, (c) Argideen Macroalgae, (d) Timoleague Receiving Waters, (e) the Upper Argideen Estuary and (f) Flaxfort Strand.

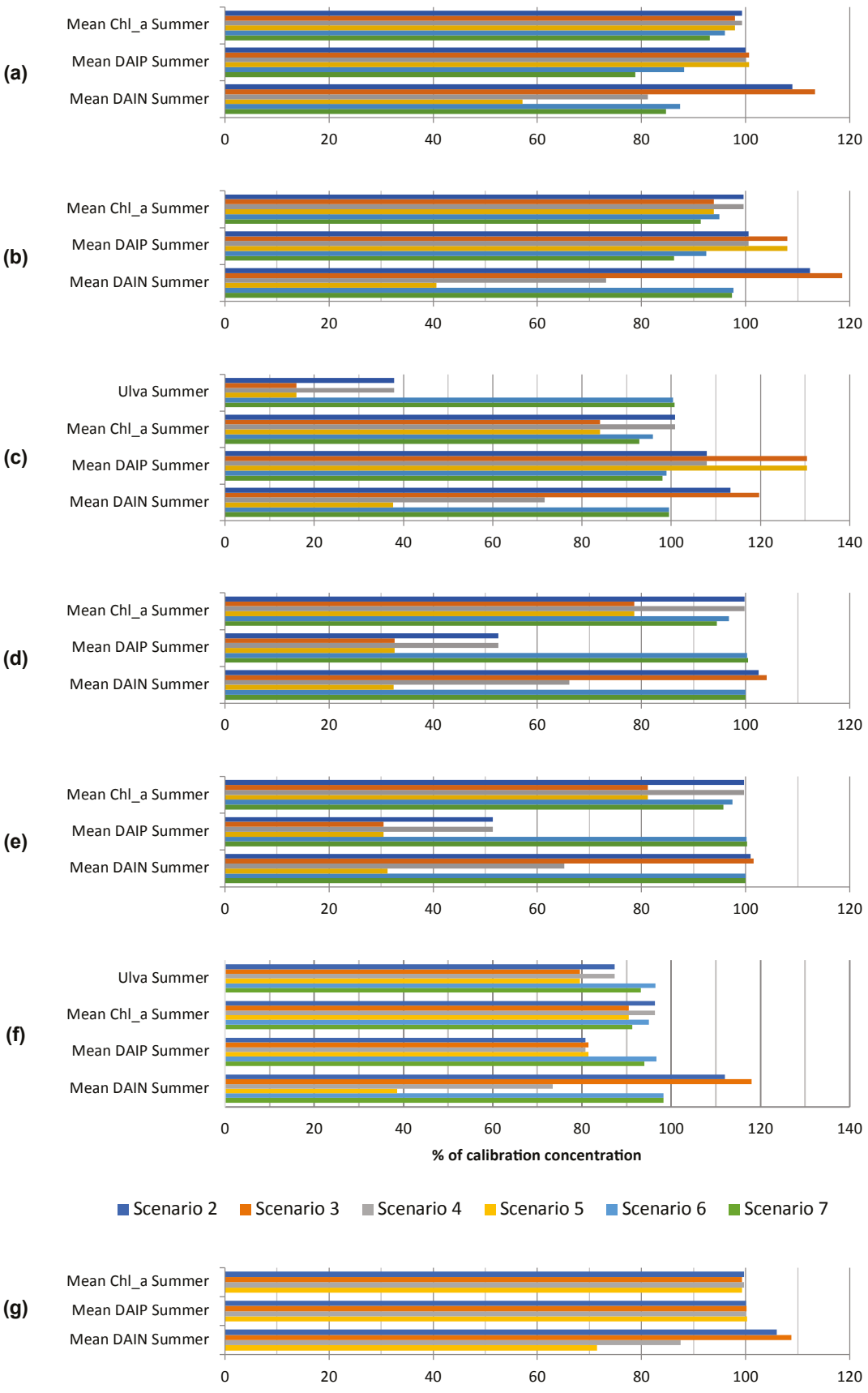

Figure 4.8. Percentage change in the concentrations of DAIN, DAIP and chlorophyll and in macroalgae tonnage due to riverine nutrient load reduction or boundary reduction based on 2015 loading data, for the DCPM model comprising (a) Courtmacsherry Inner Bay, (b) the Lower Argideen Estuary, (c) Argideen Macroalgae, (d) Timoleague Receiving Waters, (e) the Upper Argideen Estuary and (f) Flaxfort Strand.

Outer Bay was included to establish the impact of freshwater nutrient regime modification on the adjacent coastal waters during summer, i.e. scenarios 2 to 5 were applied. As a result of the phosphorus limitation of the system throughout, scenarios 2 and 3 led to a 5–7% increase in DAIN concentrations in the deeper expanses of Courtmacsherry Bay. Scenarios 4 and 5 resulted in a 0.5% reduction in DAIP concentrations and a 1% reduction in chlorophyll concentration, and a reduction of 16–28% in DAIN concentrations.

2016

The same six scenarios considered for 2011 and 2015 have been applied to 2016, with Figure 4.9 summarising the effects of each possible modification to nutrient loading.

As demonstrated elsewhere, application of scenarios 2 and 3 resulted in an increase in DAIN concentrations throughout the system, of 2–17% in this case, with a linear response increasing in proportion to the DAIP load reduction applied. An associated reduction in average DAIP concentrations of 4-66% throughout the system was also induced. Owing to the phosphorus limitation of primary producers, summer average chlorophyll concentrations reduced by 2-66% in response to freshwater DAIP load reduction, with the greatest effect observed in the freshwater reaches of the system. Macroalgae standing stock declined by up to 50% in response to freshwater DAIP reduction of 66%.

Scenario 4 had a greater impact than scenario 2 on chlorophyll concentrations in the freshwater Timoleague Receiving Waters and Upper Argideen Estuary, reflecting the delicate balance of nutrient limitation within the system. Scenario 5, however, had a similar impact throughout the system to scenario 3. No additional benefit with respect to *Ulva* bloom abatement was derived from scenarios 4 and 5 above that observed with scenarios 2 and 3.

Scenarios 6 and 7 were also considered. As was the case for 2011 and 2015, there was a minor reduction in chlorophyll, DAIN and DAIP concentrations in the brackish-saline reaches of the system, with the effect diminishing with distance from the tidal boundary.

Couplimg of 2016 flows and 2010 flow–load relationship

Owing to the hydrological similarity of the summers of 2010 and 2016 (see Figure 4.2 and Table 4.3), here, as a counterpoint to scenario 1 (see 'Coupling of 2010 flows and 2016 flow–load relationship' above), in which the summer 2016 flow–load relationships for DAIN and DAIP are applied to summer 2010 flows, scenario 8 was simulated. The net product of combining 2016 flows and 2010 flow–load relations was a reduction in DAIN loading of 5% and an increase in DAIP loading of 133%.

One of the most notable observations from scenario 8 was an increase of 25–185% in the limiting nutrient of DAIP in the Argideen Macroalgae zone (Figure 4.10c), Timoleague Receiving Waters (Figure 4.10d) and Upper Argideen Estuary (Figure 4.10e), with excesses increasing with distance upstream; there was a moderate reduction in DAIP in the remaining water bodies of 0.5–2%. As availability of DAIP was greater during the peak primary production period, there was an increase of 6–65% in summer average chlorophyll concentrations, and an increase of 265% in summer *Ulva* standing stock.

The increase in available DAIP reflects an increase of approximately 150% in summertime freshwater DAIP loading over and above baseline summer 2016 loading. DAIN loading remained static in comparison with the baseline summer 2016 DAIN loading. Therefore, the reduction in observed summer average DAIN concentrations throughout the system in Figure 4.10 reflects a greater uptake of DAIN by primary producers.

Upgrading of wastewater infrastructure

At present, wastewater infrastructure in the hinterlands of the Argideen Estuary and Courtmacsherry Bay comprises:

- a septic tank in Courtmacsherry with a 500 PE capacity with 12 hours retention time for average flows, which discharges to the Argideen Estuary; and
- collection and conveyance of untreated wastewater for discharge to Timoleague Receiving Waters.

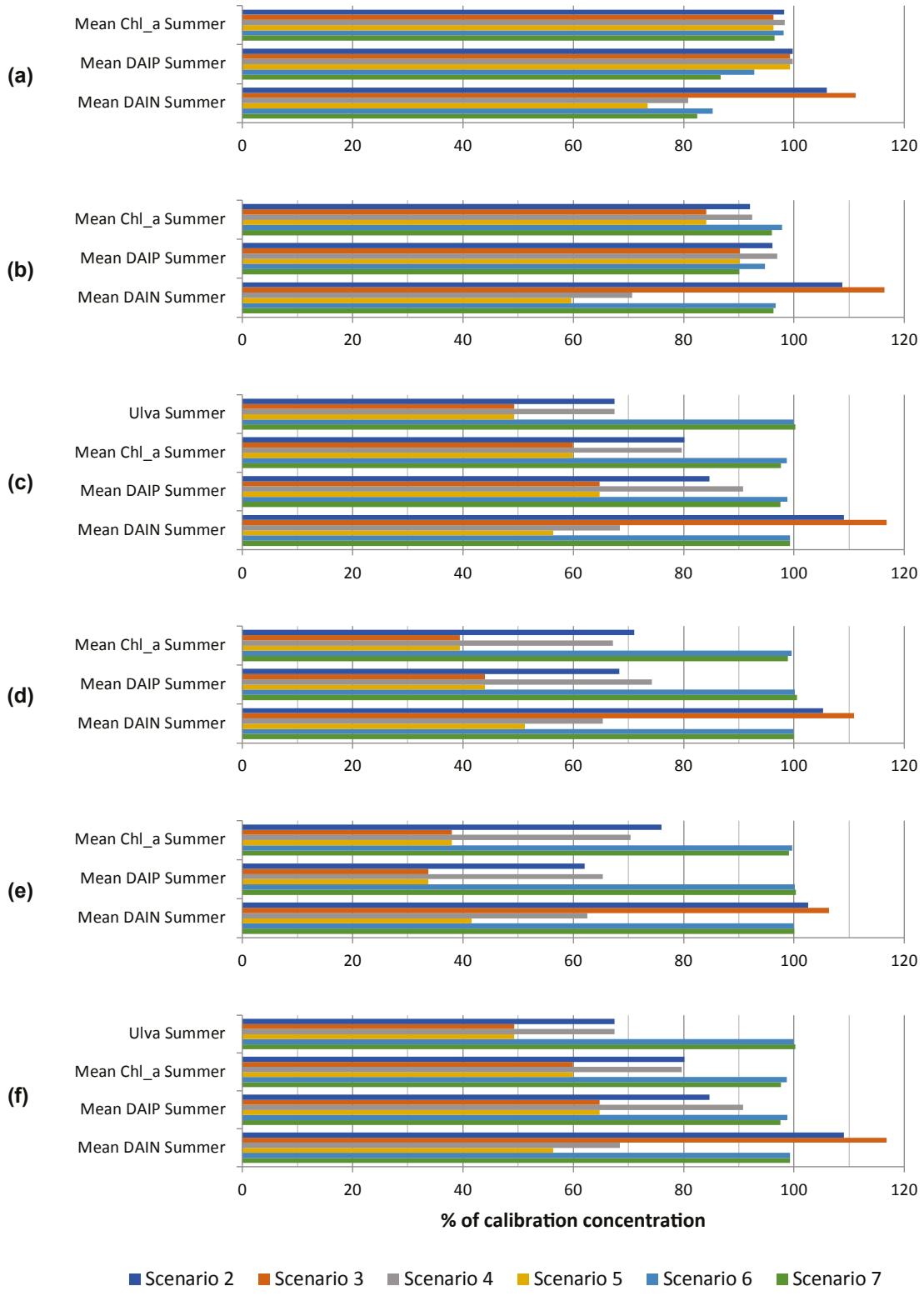

Figure 4.9. Percentage change in the concentrations of DAIN, DAIP and chlorophyll and in macroalgae tonnage due to riverine nutrient load reduction or boundary reduction based on 2016 loading data, for the DCPM model comprising (a) Courtmacsherry Inner Bay, (b) the Lower Argideen Estuary, (c) Argideen Macroalgae, (d) Timoleague Receiving Waters, (e) the Upper Argideen Estuary and (f) Flaxfort Strand.

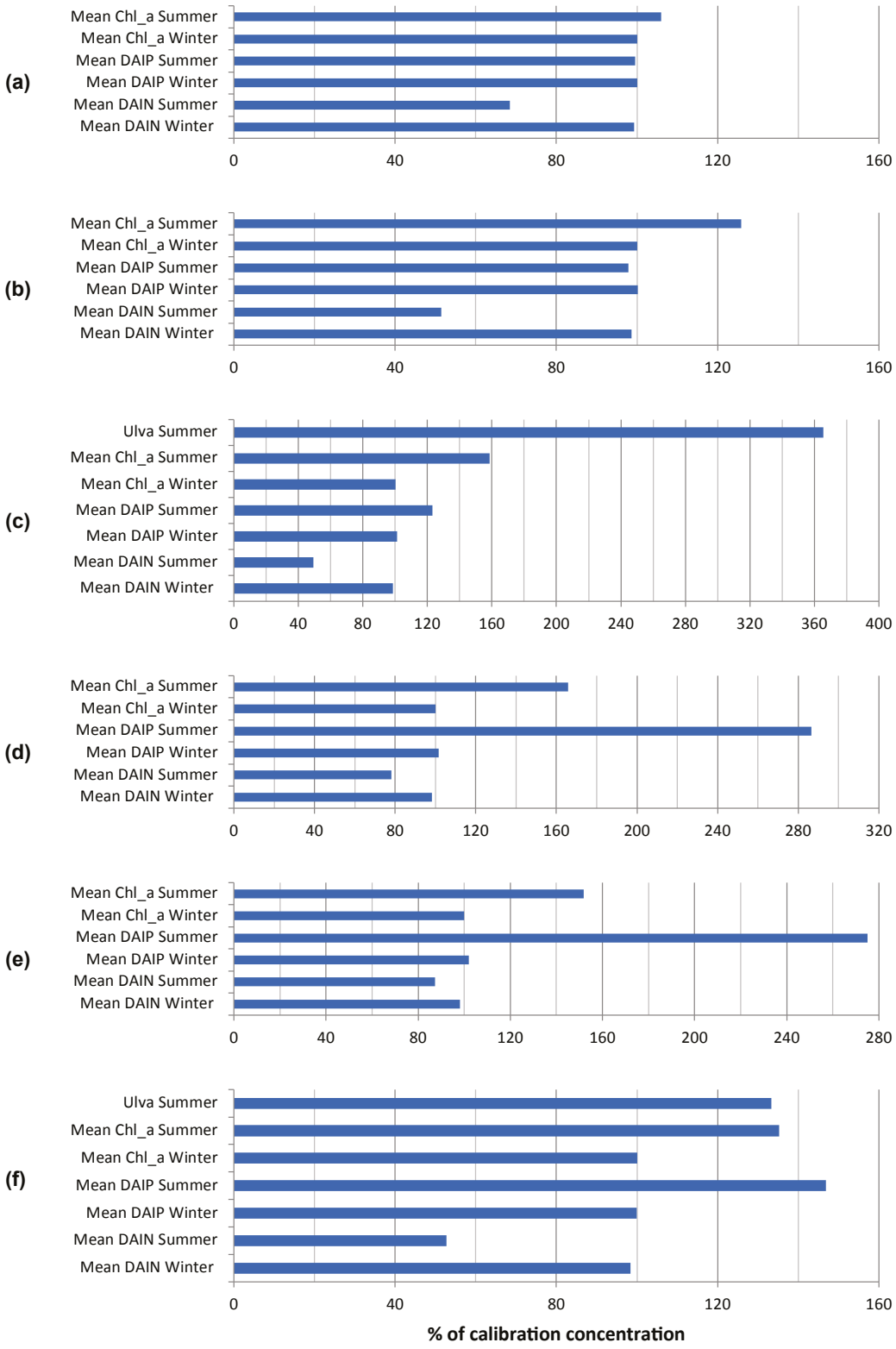

Figure 4.10. Percentage change in the average concentrations of DAIN, DAIP and chlorophyll and in macroalgae tonnage simulated by the DCPM model of the Courtmacsherry Bay/Argideen Estuary system due to imposition of flow–load relations for 2010 on 2016 flow data (scenario 8). The DCPM model of the system comprises (a) Courtmacsherry Inner Bay, (b) the Lower Argideen Estuary, (c) Argideen Macroalgae, (d) the Timoleague Receiving Waters and (e) the Upper Argideen Estuary.

The potential improvement in water quality resulting from centralisation of treatment, and treatment of wastewater in accordance with UWWTR for a 2500 PE, has been considered in scenario 9, through removal of the existing wastewater discharge to the Timoleague Receiving Waters, and discharge of the projected licence volumes, and nutrient concentrations, as set out in licence application D0294-02.

Figure 4.11 summarises the projected effects, assuming that the plant is operating at full capacity. The baseline for comparison, representing 100% of calibration concentrations, is taken from Table 4.9 (2011 data).

Although there was no notable improvement in Courtmacsherry Inner Bay (Figure 4.11a), Figure 4.11b suggests that there would be a slight increase in summer DAIN and DAIP concentrations in the Lower Agrideen Estuary. Further upstream, owing to cessation of the discharge of untreated wastewater to Timoleague Receiving Waters, there would be a reduction in the summer macroalgae standing stock and summer average chlorophyll and DAIP concentrations. All changes induced by the improvement in wastewater infrastructure lie in the range of ±3%.

4.2.4 Discussion[5]

A high-level overview of the summertime hydrological patterns in 2010, 2011, 2015 and 2016 reveals differing conditions in each year, although the summers of 2010 and 2016 were closest to the 4-year average discharge and flow exceedance curve. The summer of 2011 was notably dry, whereas the lowest observed flow, during summer 2015, was approximately equivalent to the median flow in summer 2011. Therefore, assuming "business as usual", i.e. that no remedial measures were applied between 2010 and 2016, the outcomes of the nutrient load reduction scenarios considered here may be interpreted as the potential outcomes for average (2010, 2016), dry (2011) and wet (2015) summers.

Referring to Figure 4.3a, NO_3 transfer from the Timoleague catchment was linear with increasing rainfall/river flow for the years 2010, 2011 and 2016, while in summer 2015 the trend was steeper, signifying increasing NO_3 transfer from the catchment with increasing precipitation. In a study of the NO_3 dynamics between surface water and groundwater from 2010 to 2012 in the Timoleague, Mellander *et al.* (2014) suggested that there was a possibility of nitrogen limitation in the catchment because of the capacity for physical and chemical attenuation, and chemical and hydrological buffering in the grasslands of the Timoleague. The highest observed groundwater NO_3 concentration in 2011 was not reflected in the associated surface waters until 2012, which was the wettest year on record. Therefore, in terms of NO_3 delivery, system response may not be an immediate reflection of prevailing rainfall volumes. Thus, whilst the flow–load relationships for DAIN have been derived separately for all four summers, with each relationship ostensibly reflecting different prevailing climatic conditions, there may be interannual linkages and lags between DAIN loading to the catchment and discharge of DAIN to watercourses.

Figure 4.3b indicates that orthophosphate transfer increased with increasing river discharge across the flow percentiles, indicating greater transfer with increasing precipitation. The shape of the curve is similar for the years 2010, 2015 and 2016, while the curve for 2011 apparently reflects a "first-flush" effect: when rainfall events are fewer or precipitation overall is lower, nutrient transfer in each event is higher. The most notable observation in Figure 4.3b is the year-on-year reduction in orthophosphate transfer across the range of flow percentiles. There has been a sustained improvement in phosphorus balance in the Timoleague catchment since the Nitrates Action Plans (DOEHLG, 2006) were introduced in 2006, evidenced by a gradual reduction in DAIP surplus and a convergence of soil DAIP indices towards optimum values (Murphy *et al.*, 2015). However, although the predominant source of DAIP within the Timoleague catchment is storm runoff from agriculture, Shore *et al.* (2017) suggested that point source pressures, such as domestic wastewater from one-off dwellings, play a significant role in baseflow DAIP concentrations; an increase in total reactive phosphorus concentrations

5 Some of the text in sections 4.2.4 and 4.2.5 has been previously published in McGovern *et al.* (2019).

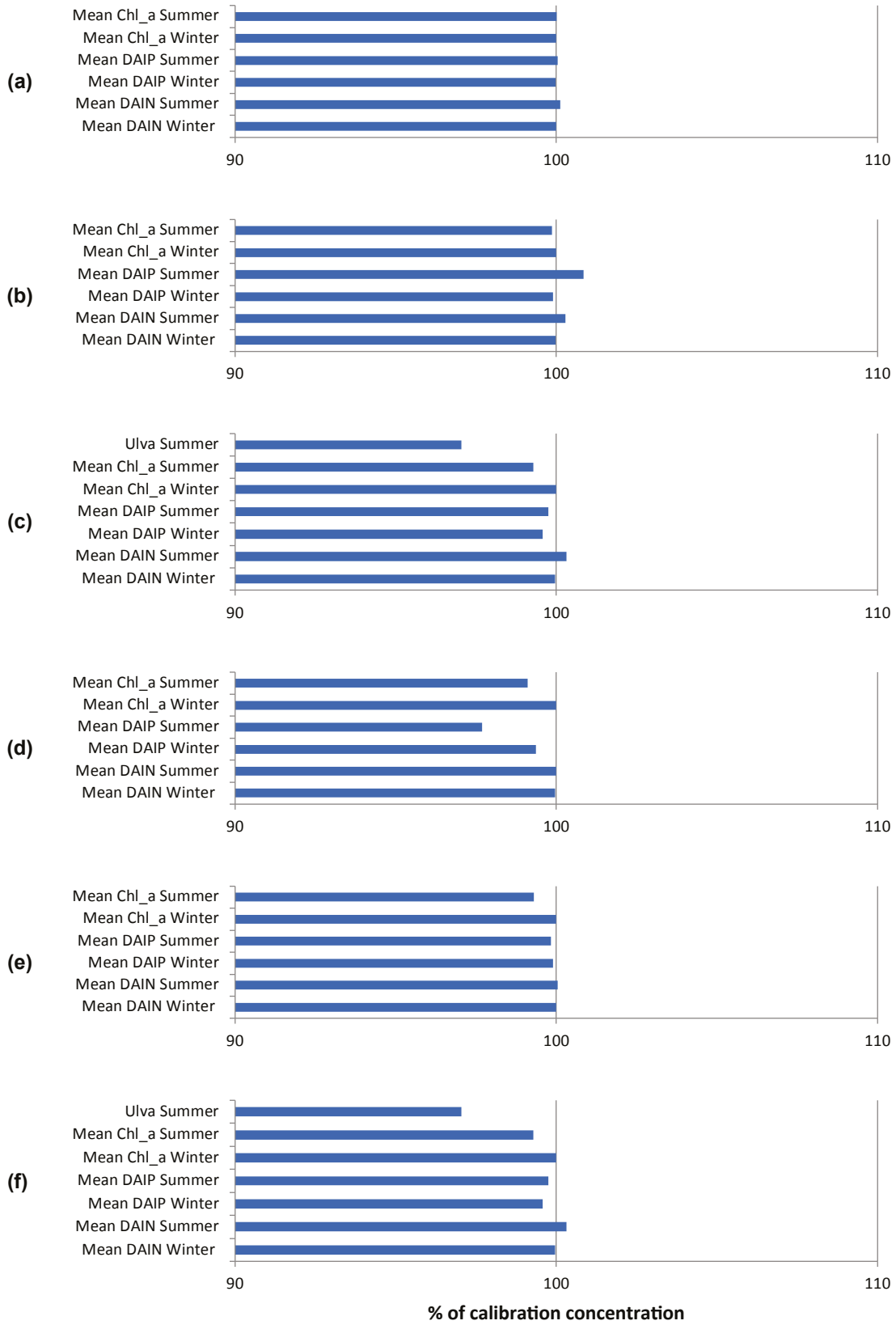

Figure 4.11. Percentage change in the average concentrations of DAIN, DAIP and chlorophyll and macroalgae tonnage simulated by the DCPM model of the Courtmacsherry Bay/Argideen Estuary system due to relocation and centralisation of WWTP facilities, with licensed capacity for 2500 PE (scenario 9). The DCPM model of the system comprises (a) Courtmacsherry Inner Bay, (b) the Lower Argideen Estuary, (c) Argideen Macroalgae, (d) the Timoleague Receiving Waters and (e) the Upper Argideen Estuary.

observed during very low flow in the Timoleague was attributed to baseflow point source pressures. In the same catchment, Jordan *et al.* (2012) also remarked upon significant DAIP transfer from baseflow during summer. A study by Jarvie *et al.* (2006) of seven catchments in the UK came to the same conclusion, i.e. that point source effluent discharge during spring and summer low flows contributed significantly to phosphorus loading even though agriculture was a major contributor to nutrient loading in these catchments.

Figure 4.3c reflects the combined emerging trend in the molar N:P ratio that developed between 2010 and 2016. In the summers of 2010 and 2011, the molar ratio was much lower than in 2015 and 2016, reflecting a suitable nutrient loading ratio for primary producer proliferation. In the summers of 2015 and 2016, the molar ratio curve indicated increasing nutrient limitation with increasing flow, up to approximately Q_{10} flows. Thereafter, higher rainfall and resultant runoff would contain DAIN and DAIP concentrations closer to the optimum N:P Redfield ratio of 16:1. Dupas *et al.* (2017) deduced from the apparent chemostasis[6] in the Timoleague catchment that there was a large phosphorus store in the catchment. The same publication noted the same patterns in nutrient flow–load curves, namely a downwards inflection in the flow–NO_3 curve above 6 mm d^{-1} rainfall and an upwards inflection in the flow–phosphate curve above 6 mm d^{-1} rainfall. These patterns were linked to the combined influence of shallow flow and overland flow that connect regions of low NO_3 and PO_4, thus explaining a reduction in the N:P ratio under high-flow conditions. The authors postulated that the reason for low NO_3 transfer was better retention of nitrogen in grasslands such as the Timoleague catchment because the grass growing phase lasts longer than other land use activities. In contrast, the risk of phosphorus mobilisation increases in grassland (Haygarth *et al.*, 1998).

Changes in the nutrient flow–load relations from 2010 to 2016 suggest that the conditions prevailing in the Timoleague catchment in an average year have improved (2010 vs 2016), potentially as a result of better agricultural practices. Growth of benthic and pelagic primary producers has been almost consistently phosphorus limited in recent years, suggesting that continued improvements in phosphorus management and retention in the Timoleague catchment may result in a considerable reduction in macroalgae and phytoplankton bloom magnitudes. However, Mellander *et al.* (2018) observed a strong positive correlation between annual average in-stream DAIN ($R^2 = 0.57$) and DAIP ($R^2 = 0.82$) concentrations in the Timoleague and the intensity of the North Atlantic Oscillation (NAOi). The same study also identified a strong correlation ($R^2 = 0.86$) between the number of Irish rain days exceeding 25 mm and the NAOi. Therefore, although improvements in land management practices may yield dividends by helping to reduce eutrophication, the influence of the NAOi may either diminish or accentuate the effects of programme measures aimed at improving trophic status. Figure 4.12 presents the NAOi time series for the summers of 2010–2017; in northern Europe, a positive value implies drier weather, whereas a negative value implies greater rainfall and higher temperatures. Noting the deviation from zero, it can be seen that the NAOi deviated considerably further from zero in summer 2015 than in 2010, 2011 and 2016, thus reflecting the observed high riverine flows in 2015 noted in Table 4.3 and Figure 4.2.

The two largest observed macroalgae blooms of the four years considered here were in 2011 and 2015. Whilst the NAOi values in each year vary, the area enclosed by the x-axis and the curve for 2011 indicate a consistency to the score for summer of that year.

Given the hydrological differences between 2015 and 2016, the scenario loads for each year give an insight into the differing extent of nutrient load reductions necessary in the case of a wet or dry summer.

For example, in 2015 the total *Ulva* wet weight observed was 1330 tonnes. This tonnage was matched by the calibrated DCPM model for that year. Of the two different DAIP load reductions considered, the greater, a 66% reduction, would have resulted in a total wet weight of 330 tonnes, which is only slightly lower than the observed tonnage of 380 tonnes for the substantially drier summer of 2016. Therefore, to effectively maintain a low bloom magnitude of

6 Chemostasis is the observation of a lower coefficient of variation in flow-weighted nutrient concentrations (nitrogen and phosphorus) than in the discharge itself, reflecting a legacy of high nutrient storage in the catchment.

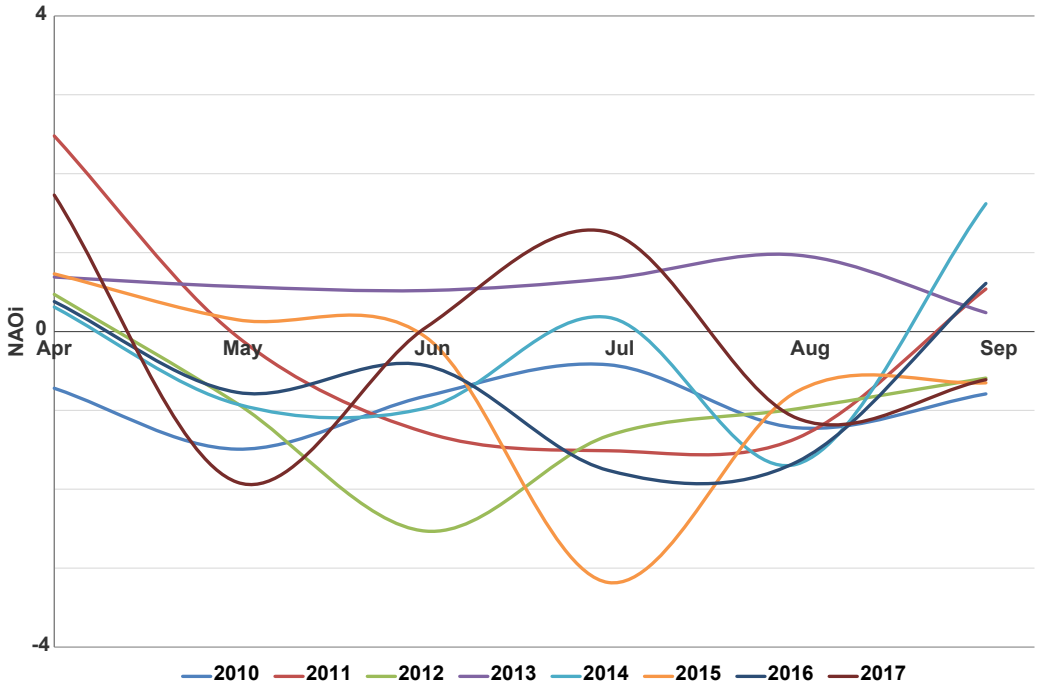

Figure 4.12. The evolving NAOi in summers 2010–2017. Data provided by the National Oceanic and Atmospheric Administration (NOAA) Climate Prediction Centre (www.noaa.gov).

300–400 tonnes, no further effort may be required in dry summers, but a significant effort, of the order of a 60–70% reduction in phosphorus transfer, may be required in a wet summer such as 2015.

A 66% reduction in DAIP loading in 2016 would have resulted in a reduction of 50% in the total wet weight, to 190 tonnes. The details of practical measures necessary to cause such a reduction in DAIP load during a wet (2015) and dry (2016) summer are beyond the scope of this research. However, overland flow connectivity in a catchment such as the Timoleague significantly contributes to DAIP transfer to watercourses during storm events. Meanwhile, during drier periods, baseflow DAIP is responsible for a disproportionate increase in total reactive phosphate concentrations in watercourses; reducing the contribution from point sources should be considered in practice (not modelled) for drier summers.

A substantial error was observed in the simulated *Ulva* wet weight in the DCPM model results for 2011. Based on the nutrient loadings and tidal boundary fluxes for 2011, the system was nitrogen limited during the peak growth season in summer 2011. Therefore, additional sources of the limiting nutrient, nitrogen, must be considered, such as intertidal fluxes of NH_4 from the benthic zone.

Courtmacsherry Bay has exhibited large *Ulva* blooms across the four years discussed here, with tonnages varying between 380 and 1800 tonnes. Decay and burial of *Ulva* in the months after bloom formation results in the incorporation of considerable amounts of organic nitrogen into the benthic zone, which is available for mineralisation and subsequent release in the following summer. Therefore, there is a possibility that there is an interannual link between bloom formations in Courtmacsherry, resulting in large blooms such as the 2011 recording.

Notwithstanding the differing hydrological conditions, the results of applying the 2010 flow–load relationships for DAIN and DAIP to 2016, and vice versa, suggest that there was an improvement in phosphorus retention within the Timoleague catchment between 2010 and 2016; the combination of 2010 flows and 2016 flow–load relationships led to an increase in the simulated *Ulva* tonnage from 784 tonnes to 968 tonnes. However, applying the 2010 flow–load relationships to the 2016 flows resulted in an even greater increase, from 380 tonnes to 1391 tonnes. Other factors may have diminished the extent of improvements that would otherwise be possible, such as the NAOi and the potential lag times between implementation of measures and catchment response. However, there was a clear improvement

in flow-normalised DAIP transfer between 2010 and 2016, as evidenced by the flow–DAIP load curves in Figure 4.3b. Therefore, the improvements already observed in *Ulva* bloom magnitudes between 2010 and 2016 may continue with sustained improvement in farm phosphorus management in the Timoleague catchment.

Table 4.11 compares the molar N:P ratio in the freshwater loading to the system and the tidal boundary waters in the summers of 2010 and 2016. Whilst the 2016 N:P ratio for the total summer loading is closer to the Redfield ratio of 16:1 than the 2010 value, the tidal molar N:P ratio in 2016 represents a state of phosphorus limitation. Simulated *Ulva* tonnages in the Argideen Estuary are sensitive to tidal boundary nutrient forcing during the summer. While the total diffuse freshwater DAIN loads for 2010 and 2016 were quite similar, the total diffuse freshwater DAIP load in summer 2016 was 64% greater than in summer 2010. Consequently, had the tidal DAIP concentration in 2016 (0.08 µM) been the same as 2010 (0.25 µM), a greater bloom would have occurred. Therefore, the authors recommend incorporating ocean nutrient hindcast data in all future modelling activities, to increase confidence in model veracity.

There were two sources of uncertainty pertaining to annual and summer nutrient loads:

1. Although the availability of hourly nutrient and flow data for the Timoleague Estuary has reduced the uncertainty pertaining to freshwater nutrient loadings, additional uncertainty remains owing to the extrapolation of the nutrient and flow data from the Timoleague catchment to the other four river systems that enter the Argideen Estuary/ Courtmacsherry Bay system. However, the descriptors of the five catchments are similar, as can be seen from Table 4.12.

Table 4.11. Molar N:P ratio in freshwater and tidal boundary waters in the summers of 2010 and 2016 in the system comprising the Argideen Estuary and Courtmacsherry Bay

	N:P ratio	
Year	Freshwater	Tidal boundary waters
2010	190:1	12:1
2016	105:1	25:1

Table 4.12. Comparison of catchment descriptors across the Argideen Estuary/Courtmacsherry Bay system

	Catchment				
Descriptor	Burrane	Owenkeagh	Kilbrittain	East Cruary	Flaxfort
General					
Area (km^2)	10.9	41.2	23.2	9.7	5.4
Average annual rainfall ($mm\,y^{-1}$)	1252	1330	1255	1164	1222
Stream length (km)	9.8	38.7	20.6	9.7	3
Drainage density ($km\,km^{-2}$)	0.9	0.9	0.9	1	0.6
Slope (%)	9.4	7.8	10.6	7.5	7
FARL Index	1	1	1	1	1
Soil code (% of catchment)					
Poorly drained	4.2	1.4	1.3	2	1
Well drained	95.8	91.3	97.7	98	99
AlluvMIN	0	7.1	1	0	0
Peat	0	0.2	0	0	0
Water	0	0.1	0	0	0
Made	0	0	0	0	0

FARL, Flood Attenuation by Rivers and Lakes.

Table 4.13. Comparison of nutrient loads derived from SLAM and data provided by the Teagasc ACP and scaled up from the Timoleague subcatchment to the entire catchment

Nutrient load estimates	DAIN (kg)	%SLAM	DAIP (kg)	%SLAM
SLAM annual (total)	798,933		4590	
SLAM summer (total)	399,466		2295	
SLAM summer (inorganic)	331,557		1400	
ACP summer 2010	199,763	60	2328	166
ACP summer 2011	101,505	31	1346	96
ACP summer 2015	460,588	139	6865	490
ACP summer 2016	182,375	55	3829	274

2. Table 4.13 compares the nutrient loads generated by the national Source Load Apportionment Model (SLAM) (Mockler *et al.*, 2017) and the loads derived from locally available stream monitoring data. In the absence of high-resolution data, such as those provided by the ACP, SLAM nutrient loads were adopted for DCPM modelling, without reference to the prevailing hydrological conditions. Summer nutrient loads were assumed to be half of the annual loads; the inorganic fraction of nitrogen, taken from OSPAR loading data for the Tolka, was assumed to be 83%; and the inorganic fraction of phosphorus, taken from Jordan *et al.* (2012), was assumed to be 61%. The ratio of the estimated DAIN and DAIP loads relative to the load derived by SLAM, denoted %SLAM in Table 4.13, varies between summers. Both 2010 and 2016 represent an average summer, when the estimated nirogen load is 55–60% of the SLAM loading, and the phosphorus loads are 160–280% of the SLAM loading. The dry (2011) and wet (2015) summers differ yet again, with loads undershooting (dry) or exceeding (wet) the SLAM estimates for both nitrogen and phosphorus. Therefore, to reduce the uncertainty associated with adopting SLAM loading in DCPM simulations, six reliable ratios or factors akin to "%SLAM" must be identified, in order to scale SLAM loadings to a wet, dry or average summer, and the winter equivalents. This would facilitate the simulation in the DCPM model of the effect of nine combinations of three potential types of hydrological summer and three potential types of hydrological winter on *Ulva* and phytoplankton blooms.

The water bodies with the greatest discrepancy between modelling and monitoring averages are those with the greatest measured chlorophyll concentration, possibly a reflection of nutrient limitation. Furthermore, the greatest deficit in terms of DAIP averages lies in sections with significant growth of primary producers, all of which are phosphorus limited. Several factors have been cited as important for accurate prediction of the evolution of chlorophyll concentrations in response to varying ambient conditions.

Cerco *et al.* (2004) incorporated Droop kinetics for algal biomass into EFDC (Environmental Fluid Dynamics Code), resulting in the model better simulating the observed combination of phosphorus and algal biomass concentrations, where previously phosphorus concentrations had been overestimated, although algal biomass concentrations were robustly predicted; thus, the Droop kinetic allows for a more accurate prediction of nutrient concentrations in the water column, although its influence on the algal biomass growth rate is negligible. Bonachela *et al.* (2011) proposed a cell-level model for phytoplankton growth that was capable of reflecting the resilience of phytoplankton under extreme nutrient limitation, unlike the classic Michaelis–Menten approach, which does not reflect dynamic increasing nutrient affinity with decreasing nutrient concentrations.

Malone *et al.* (1988) observed that NO_3 transfer from the Susquehanna River to Chesapeake Bay fuelled the spring bloom, with excess NO_3 transferred downstream and assimilated. Later, during summer, smaller summertime blooms were observed that correlated with the magnitude of the spring bloom, which in turn was dependent upon the magnitude of the freshwater loading during spring. The definite advection of downstream chlorophyll to the upper reaches was another discussion point, given the implication that the chlorophyll undergoing ammonification in late spring may consist of tidal

chlorophyll transferred upstream, in addition to growth induced by freshwater NO_3. In summary, the authors noted that "the annual cycle of riverine nutrient inputs is in phase with phytoplankton biomass but out of phase with phytoplankton productivity".

Regarding the fate of freshwater phytoplankton in estuaries, Joint (1981) cited different outcomes for freshwater species in estuaries, such as mass mortality of halophobic freshwater phytoplankton at salinities of below 1 psu in the Tamar Estuary, England (Morris *et al.*, 1978), and an abundance of "dead or almost dead" freshwater phytoplankton in the Rhone (Blanc *et al.*, 1969). Joint (1981) also singled out the work of Forester (1973), who pointed out that survival is species dependent and that some freshwater phytoplankton adapt to brackish waters, although some others die at salinities greater than 10 psu.

In a study of the Weser Estuary, Germany, Schuchardt *et al.* (1993) identified a community of riverine and local phytoplankton and zooplankton, without any marine species, suggesting that survivability of freshwater phytoplankton may be site dependent, or more specifically dependent upon the combination of freshwater and tidal boundary influences.

Roegner *et al.* (2011) identified a seasonal variation in the influence of freshwater and oceanic boundaries in the Columbia River Estuary, with fluvial chlorophyll concentrations up to nine times higher than the oceanic concentrations in spring, and oceanic chlorophyll concentrations up to seven times greater than the fluvial concentration in summer.

In this research the annual riverine phytoplankton loading has been estimated based on the seasonal average flows and phytoplankton concentrations at freshwater monitoring sites. The contribution of riverine phytoplankton loading to the water column concentration in the downstream brackish waters is unknown. These questions must be addressed in an Irish context to improve confidence in trophic water quality modelling, beyond the research described here. Likewise, seasonal variation in chlorophyll concentrations must be more accurately described so that its influence on upstream estuarine average chlorophyll concentrations can be accounted for. The resilience of tidally exchanged phytoplankton in brackish waters must also be elucidated, in much the same manner as suggested for riverine chlorophyll loading.

Throughout the calibration process, parameters were kept to physiologically meaningful ranges from the literature. The summer average wet tonnage of *Ulva* provides a good indicator of model accuracy, as the assumption is made that there is no advection of *Ulva* between adjacent water bodies. Thus, although some percentage error statistics suggest a poor model performance, nutrients and phytoplankton are freely advected throughout the system, with monitoring carried out three times during summer and once during winter. Therefore, comparison with monitoring data may lead to flawed interpretation of model performance. A better measure of model performance in this case is comparison of the model with (1) monitored salinity values, as salinity is a conservative tracer, or (2) monitored *Ulva* wet weights, as these better reflect the net primary production potential during the summer because of the poorer advection of macroalgae, which is often bound to underlying sediment.

4.2.5 Summary

- The DCPM model was applied to the system comprising the Argideen Estuary and Courtmacsherry Bay for 2010, 2011, 2015 and 2016, to establish the order of magnitude of reduction in seasonal average nutrients, chlorophyll and macroalgae resulting from:
  - two incremental reductions in DAIP loading, of 33% and 66%;
  - two incremental reductions in both DAIP and DAIN loading, of 33% and 66;
  - two incremental reductions in both DAIP and DAIN concentrations, of 33% and 66%, at the tidal boundary;
  - the inclusion of Courtmacsherry Outer Bay in nutrient load reduction scenario modelling for the year 2015;
  - upgrading of wastewater treatment to the standards set out in the UWWTR, to handle a projected capacity of 2500 PE.
  - application of 2010 flow–nutrient load relationships to 2016, and of 2016 flow–nutrient load relationships to 2010, to determine the improvements caused by implementation of Nitrates Action Plan activities in the intervening years.
- Site-specific light attenuation coefficients and exchange rates were calculated for each water body based on Secchi disc readings from 2010

and 2011. The same light attenuation coefficients were carried over to 2015 and 2016, which proved sufficient with respect to model accuracy.
- Physical mixing was calibrated by modifying the calculated exchange rates and seasonal river discharge ratio to match the salinity time series generated by the DCPM model with the salinity observations gathered by the EPA.
- Calibration of biological growth entailed modification of the macroalgae turnover rate, the macroalgae dry weight to wet weight ratio and the phytoplankton loss rate.
- For summer 2011, which was the driest of the four years, a reduction in DAIP alone led to a small increase in DAIN throughout the system and a minor reduction in chlorophyll, with a negligible decrease in macroalgae, while a reduction in both DAIN and DAIP load resulted in a decrease in the *Ulva* bloom magnitude of up to 40%. Owing to the complex swapping of nutrient limitation between DAIN and DAIP, a reduction in both yielded the greatest dividends.
- For summer 2015, which was the wettest of the four years, a reduction in DAIP loading alone affected primary production to the same extent as combined DAIN and DAIP load reduction.
  - Reducing freshwater DAIP loading alone would result in a slight increase in DAIN concentrations in the deep outer portion of Courtmacsherry Bay. Coupled reduction of DAIN and DAIP would have a greater influence on DAIN concentrations than on DAIP concentrations, with a net reduction of DAIN of up to 28% possible with a 66% reduction in freshwater DAIN and DAIP loads.
- Although the hydrological conditions during the summers of 2010 and 2016 differed, the overall flows were similar. The main distinction between the summers was a difference with respect to flow duration, with more high flows observed in summer 2010. Flow–load curves were derived for both summers, and the flow–load curves were swapped to quantify the improvement, if any, brought about by improvements in agricultural practices within the catchment.
  - Applying the 2016 flow–load relationships for DAIN and DAIP to 2010 flows resulted in an increase in the simulated *Ulva* tonnage of 24%.
  - Applying the 2010 flow–load relationships for DAIN and DAIP to 2016 flows resulted in an almost fourfold increase in the simulated *Ulva* tonnage.
- The differing flow–nutrient load curves between 2010 and 2016 indicate that there was a reduction between 2010 and 2016 in transfer of DAIP from the Timoleague catchment to surface waters between 2010 and 2016. Given the phosphorus limitation of primary production for summer 2010, a reduction in the phosphorus transfer rate between the hydrologically similar summers of 2010 and 2016 would ostensibly indicate that a reduction in *Ulva* magnitudes would be induced. A reduction in the monitored *Ulva* tonnages in the main macroalgae patch of Courtmacsherry from from 784 tonnes in 2010 to 391 tonnes in 2016 would bear out this hypothesis. In an effort to confirm this improvement, application of the flow–load relationships from each year to the other indicates that a dramatic increase in *Ulva* tonnages would have been caused were the nutrient management regime in 2010 to remain in place in 2016.
- It is necessary to consider the possibility that the unique evolution of rainfall patterns from day to day, coupled with groundwater–surface water interactions, contributed to the difference between the two years.
- Several aspects pertaining to riverine phytoplankton/chlorophyll loading pose additional sources of uncertainty when applying the DCPM model. These are:
  - the quantity of riverine phytoplankton entering the system;
  - the associated age and viability of same in brackish waters;
  - the size/cross-sectional area of the phytoplankton mass in the water column, which affects water transparency and the suitability of the water column for additional phytoplankton growth.
- Consolidation and improvements in wastewater conveyance and treatment were found to have a negligible effect on water quality, with all observed changes falling within the range of ±3%.

4.3 Rural Catchment B: Clonakilty

The following case study details the influence of estimated DAIN and DAIP loadings, and reductions thereof, on the simulated ambient summer and winter

average DAIN, DAIP and chlorophyll concentrations and summer average macroalgae wet weight derived by the DCPM box model (Aldridge *et al.*, 2013). The system comprises four sections, namely the inner portion of Clonakilty Bay, the Ashgrove Receiving Waters, the inner portion of Clonakilty Harbour and the intertidal macroalgae zone, as presented in Figure 4.13.

The main objectives of this case study were to establish:

- the characteristics of the water bodies with respect to the limiting factor for phytoplankton growth and macroalgae;
- the benefit of nutrient load reduction on primary production.

The case study of Courtmacsherry Bay and the Argideen Estuary was completed with high-resolution riverine loading data provided by the Teagasc ACP. Similarly, in Chapter 3, riverine loading data for the Dublin Bay model were derived from the OSPAR RID monitoring programme for the Tolka, while the Liffey nutrient loading data were determined from high-resolution flow data and interpolated water quality data from the most upstream monitoring point in the transitional monitoring regime there. A more realistic application of the DCPM model elsewhere may be run based on ungauged flow estimates such as the flow percentiles provided by EPA Hydrotools or nutrient load estimates from source load apportionment models such as SLAM; alternatively, nutrient loads may be derived as for the Liffey in Chapter 3, where daily or monthly estimates of flow are combined with interpolated sparse monitoring data to determine annual or seasonal nutrient loads.

Two streams entering the Clonakilty Harbour/Bay system have been included: the Clonakilty and Ashgrove streams. The Clonakilty stream enters Clonakilty Harbour at monitoring point CY000, draining a catchment of 24.8 km^2. The Ashgrove stream enters Clonakilty Harbour at the downstream end, adjacent to Clonakilty Inner Bay, receiving runoff from 18 km^2 of predominantly agricultural lands.

Generalised annual total nitrogen and total phosphorus loading values for the Clonakilty and Ashgrove streams were generated using SLAM (Ní Longphuirt *et al.*, 2016a). The nutrient loading estimates generated by SLAM indicate that the Clonakilty stream accounts for almost two-thirds of the total phosphorus loading to Clonakilty Harbour (Table 4.14), while the total nitrogen

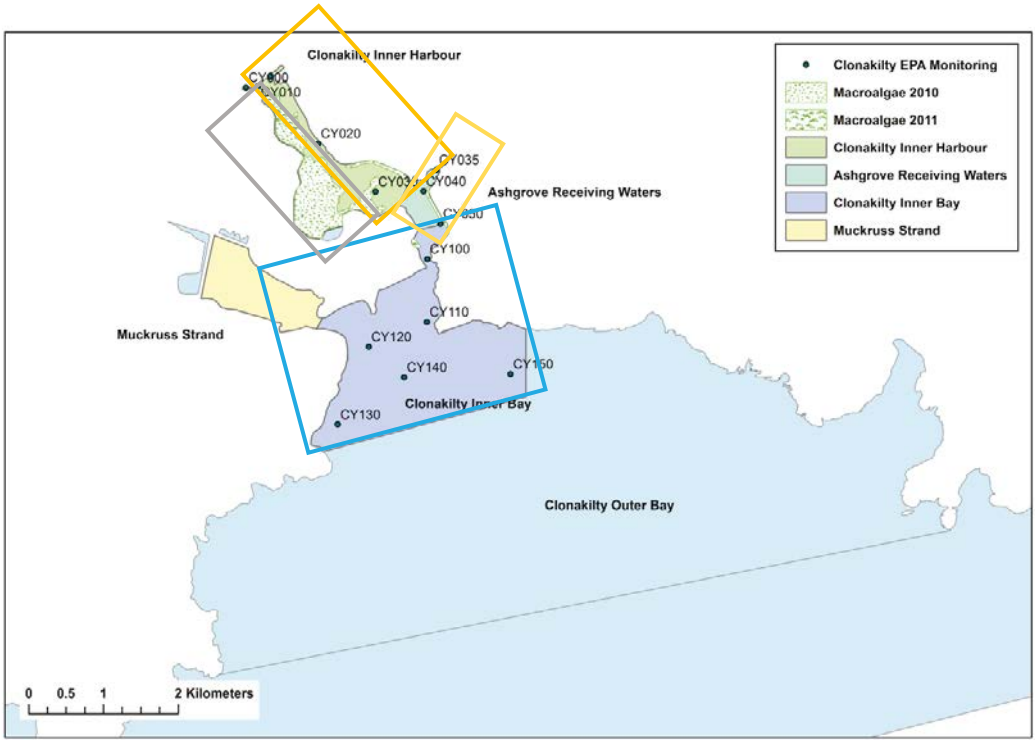

Figure 4.13. The four water bodies that constitute the DCPM model domain spanning the Clonakilty Bay and Clonakilty Harbour from monitoring points CY000 to CY150.

Table 4.14. Comparison of estimated inorganic nutrient loading to Clonakilty Harbour derived from SLAM and nutrient loading estimates derived using flow data and inorganic nutrient monitoring observations

	SLAM						Monitoring calculation	
Stream	Total N load ($kg\,y^{-1}$)	Ratio of inorganic to total N	Inorganic N load ($kg\,y^{-1}$)	Total P load ($kg\,y^{-1}$)	Ratio of inorganic to total P	Inorganic P load ($kg\,y^{-1}$)	Inorganic N load ($kg\,y^{-1}$)	Inorganic P load ($kg\,y^{-1}$)
Clonakilty	72,070.23	0.83	59,457.94	402.38	0.43	171.01	10,359.68	338.25
Ashgrove	62,964.47	0.83	51,945.69	221.58	0.43	94.17	5533.19	184.24

loading is approximately evenly split between the two streams. Ninety-eight per cent of total nitrogen loading to Clonakilty Harbour is of agricultural origin, from pasture and arable land. Twenty-seven per cent of total phosphorus is derived from diffuse urban runoff, with the remainder attributed to pasture and arable lands. The inorganic fractions of total nitrogen and total phosphorus given in SLAM are unknown.

The period spanning 2010–2011 was the focus of this case study. Estimates of Q_{50} were obtained from the EPA WFD Hydrotools site, while the ratio of summer to annual flow was approximated by using Q_{30} and Q_{70} as the winter and summer flow, respectively.

Table 4.14 presents the total nitrogen and total phosphorus loadings available from SLAM for the Ashgrove and Clonakilty streams, multiplied by the ratios of inorganic to total nitrogen and inorganic to total phosphorus determined from OSPAR RID data for the River Tolka. The ratios of inorganic to total nitrogen and phosphorus, 0.81 and 0.64 respectively, were used because of the similarity in catchment use, with the Tolka catchment comprising mainly agricultural land. DAIN and DAIP loadings were also calculated separately based on monitoring data at the most upstream monitoring point for each stream, which is CY000 for the Clonakilty stream and CY035 for the Ashgrove stream. Average seasonal DAIN and DAIP concentrations at each monitoring point were multiplied by the winter and summer flow estimates and the resultant value was scaled up to a 6-month period; these loading values are based on sampling at a maximum of three occasions during summer and once during winter. These calculated values are also presented on the right-hand side of Table 4.14. There is a clear disparity between both DAIN and DAIP loading estimates, with the DAIN loading data derived from monitoring data 10–20% of the estimates determined from SLAM. The equivalent DAIP loading data are approximately twice the inorganic phosphorus loading data estimated from SLAM total phosphorus data. The ratio of summer to annual DAIN and DAIP loading was determined using monitoring data from the same two monitoring points for each stream.

The model was provisionally set up using the inorganic nitrogen and phosphorus loading estimates from SLAM contained in Table 4.14. A value of 0.83 was initially adopted for the ratio of DAIN to total nitrogen. The initial model simulation indicated average seasonal DAIN concentrations in the Inner Harbour and Ashgrove Receiving Waters of almost twice the average concentration calculated from monitoring data, while the corresponding DAIP values were 20–40% of calculated averages. Subsequently, the DAIN/total nitrogen ratio was reduced in steps of 0.1, resulting in a lowering of the observed seasonal DAIN ratios in Clonakilty Inner Bay, Ashgrove and Clonakilty Inner Harbour towards the observed seasonal averages. The final ratio of 0.43 was adopted, resulting in seasonal average DAIN concentrations close to the observed averages for five of the six values. The final annual inorganic nitrogen loading was approximately halfway between the initial load determined by applying the DAIN/total nitrogen ratio in the Tolka catchment to the annual total nitrogen loading data from SLAM, and the loading determined using assumed seasonal discharge data from flow rating curves and monitoring data at the upstream monitoring points. The equivalent inorganic phosphorus load calculated using monitoring data and estimated seasonal discharge data was adopted because of the low seasonal average DAIP concentrations returned using the estimated inorganic phosphorus fraction of total phosphorus from SLAM. Table 4.15 presents the final riverine freshwater discharge and nutrient discharge values applied to the Clonakilty DCPM

Table 4.15. Q_{50}, annual DAIN and DAIP loadings and the corresponding summer to annual ratios for both streams entering Clonakilty Harbour

Stream	River flow (Q_{50}) ($m^3 s^{-1}$)	River discharge ratio (R_{SA})	DAIN load ($kg y^{-1}$)	N load ratio (R_{SA})	DAIP load ($kg y^{-1}$)	P load ratio (R_{SA})
Clonakilty	0.40	0.65	30,629.75	0.75	338.25	1.03
Ashgrove	0.16	0.65	26,759.70	0.75	184.24	1.17

Summer, April to September, inclusive.

model. Estimates of Q_{50} were obtained from the EPA WFD Hydrotools site, while the ratio of summer to annual flow was approximated by using the Q_{30} and Q_{70} as winter and summer flow, respectively. The ratio of summer to annual DAIN and DAIP loading was determined using monitoring data from the most upstream monitoring location for each stream, while the light attenuation coefficient was determined from Secchi disc readings. Owing to the very high transparency in the Inner Clonakilty Harbour, the light attenuation coefficient was taken to be 0.05.

Bathymetry data for the Clonakilty Bay/Harbour and the Argideen Estuary/Courtmacsherry Bay area were extracted by digitising Admiralty charts. These data served two purposes, providing depth bins for the DCPM model and also providing a basis for the calculation of the tidal prism ratio as a means of determining a meaningful residence time and, thus, exchange rate. Eighty-six per cent of the inner portion of Clonakilty Harbour is intertidal, with the majority of the intertidal zone covered by macroalgae blooms on an annual basis.

Using all site-specific values for parameters such as exchange rate, light attenuation and seasonal ratios for river discharge and nutrient loading brought all DCPM observations near to calibrated. The only calculated parameter that required subsequent modification was the R_{SA} value for DAIN for the Ashgrove stream, which was reduced from the calculated value of 0.96 to 0.75, the corresponding value for the Clonakilty stream.

Table 4.16 presents a comparison between seasonally averaged monitoring data and the equivalent provided by the DCPM model. There is a considerable deficit in summer and winter DAIP throughout the system. This is reflected in the phosphorus limitation of the Clonakilty Bay and Harbour areas. Phytoplankton growth in the receiving waters for the Ashgrove stream is light limited.

Owing to the phosphorus limitation of the Inner Bay and Inner Harbour, three DAIP load reduction scenarios were applied to the Clonakilty and Ashgrove streams: 25%, 50% and 75%. Catchment management measures aimed at reducing DAIP transfer to receiving waters may result in an unintended reduction in DAIN. Hence, three additional scenarios were considered, in which both DAIN and DAIP freshwater loads were reduced by 25%, 50% and 75%.

Figure 4.14 presents the percentage change in DAIN, DAIP and chlorophyll concentrations and macroalgae tonnage due to the load reductions considered, for 2010–2011.

There was a marked response in all four water bodies in terms of DAIN and chlorophyll concentrations in response to the reduction in DAIP loading from each stream, aside from the drop in DAIP concentrations, ranging from 1% to 70%, which was expected. In Clonakilty Bay there was a net increase in the average DAIN and chlorophyll concentrations in summer of 1%. Similarly, in the Ashgrove Receiving Waters, there was an increase in the mean summer DAIN concentration of 3–10%. A 25% DAIP load reduction induced a 2% increase in chlorophyll concentration while DAIP load reductions of 50% and 75% caused a decrease in chlorophyll concentrations of 5% and 27%. The Inner Clonakilty Harbour was similarly influenced by a reduction in DAIP loading, with a 25% reduction increasing chlorophyll concentrations by 3%, while reductions of 5% and 35% were induced by DAIP load reductions of 50% and 75%, respectively. The increase in DAIN concentrations in response to DAIP load reduction, due to lower assimilation, ranged from 5% to 15%. A greater increase in DAIN concentrations was caused in the intertidal zone in response to the same DAIP load reductions, with increases ranging from 8% to 24%. Chlorophyll concentrations in the Inner Clonakilty Harbour increased by 5% under a

Table 4.16. Seasonal DAIN, DAIP and phytoplankton concentrations observed in the Clonakilty Harbour–Clonakilty Bay system area compared with DCPM model-simulated seasonal averages after calibration

	Water body			
	Clonakilty Inner Bay	Ashgrove	Clonakilty Inner Harbour	Clonakilty Intertidal
DAIN (µM)				
Winter				
EPA	24.13	87.29	127.21	–
DCPM model	20.93	113.39	136.64	135.06
Summer				
EPA	3.87	132.70	104.62	-
DCPM model	2.24	77.25	96.10	87.77
DAIP (µM)				
Winter				
EPA	0.58	0.78	0.96	–
DCPM model	0.58	0.72	0.72	0.70
Summer				
EPA	0.20	0.27	0.46	-
DCPM model	0.15	0.27	0.26	0.02
Chlorophyll ($mg\,m^{-3}$)				
Winter				
EPA	1.37	2.83	2.23	–
DCPM model	1.17	0.78	0.58	0.66
Summer				
EPA	2.33	2.63	4.32	–
DCPM model	2.16	3.60	4.23	4.42
Macroalgae (tonnes wet weight)				
Summer				
EPA	0.00	0.00	0.00	110.00
DCPM model	0.00	0.00	0.00	89.91

25% DAIP load reduction, while greater increases caused a reduction in chlorophyll concentrations of 4–33%. There was a consistent reduction in summer macroalgae blooms by 32–81% in response to DAIP load reductions of 25–75%.

Coupled reduction in both DAIN and DAIP riverine loads had differing effects on coastal and transitional waters, presented in Figure 4.15. There was an increase of 1–3% in phosphorus in Clonakilty Inner Bay in response to the three coupled load reduction scenarios, matched by a reduction of 2–6% in nitrogen and chlorophyll. Further inland, there was a slightly smaller reduction in DAIP in response to coupled load reductions, of approximately 1%, although DAIN concentrations reduced approximately in line with load reductions. There was also a greater reduction in chlorophyll concentrations, of 2–3%, caused by coupled riverine nutrient load reductions. The decrease in the mean macroalgae bloom tonnage in the Intertidal zone of Clonakilty Harbour with reduction of both nitrogen and phosphorus loadings was approximately in line with the decrease induced by reduction of phosphrus alone.

4.3.1 Discussion

Three of the four water bodies in the Clonakilty Harbour–Clonakilty Bay system were deemed to be phosphorus limited with respect to eutrophication. As a consequence, riverine load reduction scenario modelling focused on reductions in inorganic phosphorus loading. The six load scenarios comprised three incremental 25% reductions in inorganic phosphorus loading, ranging from 25% to 75%, and

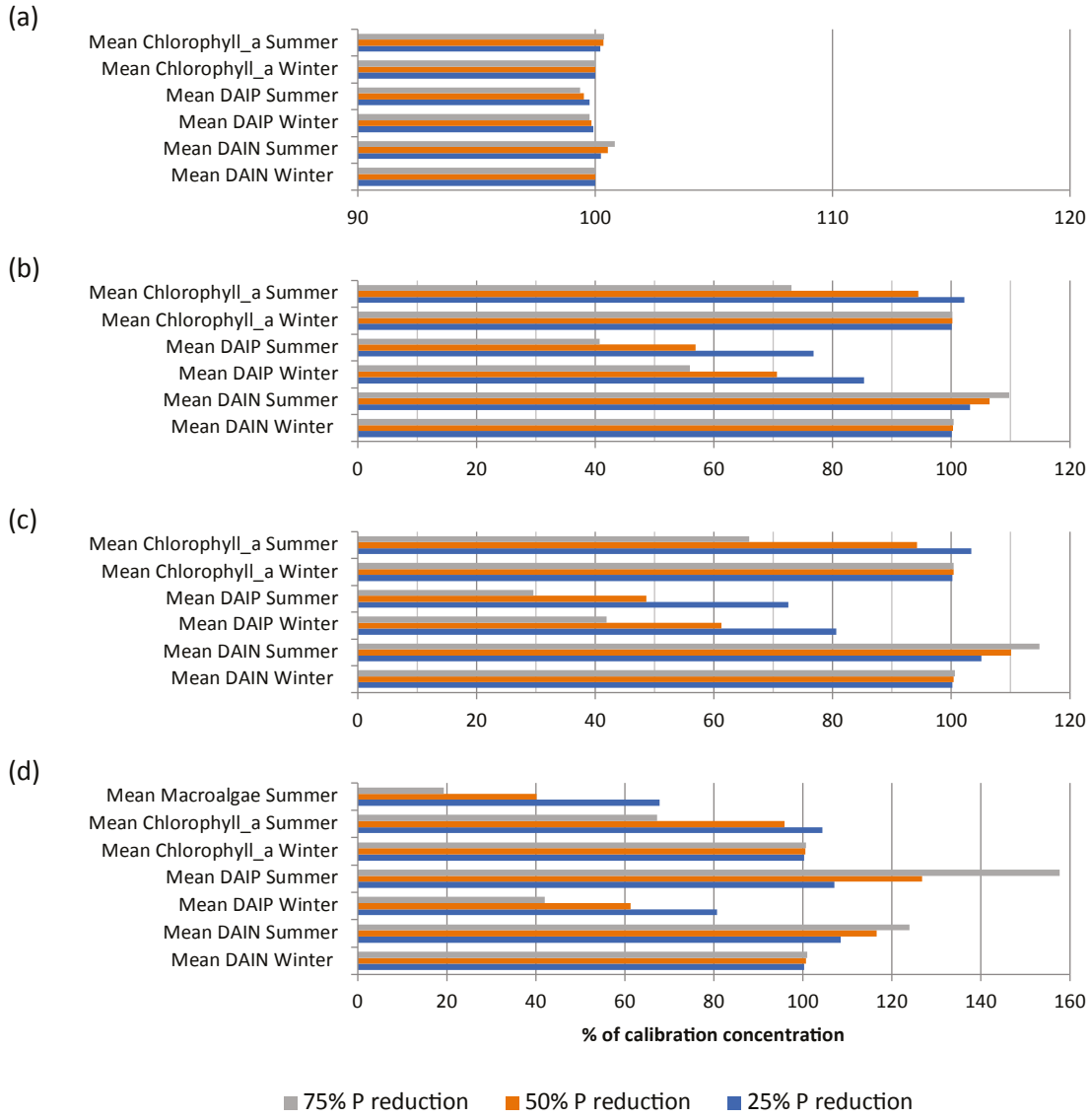

Figure 4.14. Percentage reduction in the concentrations of DAIN, DAIP and chlorophyll and macroalgae tonnage simulated by the Clonakilty DCPM model, due to phosphorus reduction scenarios based on 2010–2011 loading data. The model comprises (a) Clonakilty Inner Bay, (b) Ashgrove Receiving Waters, (c) Clonakilty Inner Harbour and (d) Clonakilty Intertidal Macroalgae zone.

three incremental coupled reductions in inorganic nitrogen and phosphorus loading, of 25%, 50% and 75%. The DCPM model was calibrated for the 2010–2011 period.

The three scenarios considering stepped 25% reductions in both nitrogen and phosphorus from riverine sources had largely the same effects as phosphorus load reduction alone; the main difference was a slightly greater reduction in summer average chlorophyll concentrations, by an additional 2–3%.

As macroalgae growth was phosphorus limited, reductions in riverine DAIP loading across the six simulated scenarios resulted in a significant and linear decrease in summer macroalgae standing stock of 31–81%. Reducing the riverine loading of both nitrogen and phosphorus had the same effect on macroalgae tonnages as reducing riverine phosphorus loading alone. Within the scope of the nutrient load reduction scenarios considered here, the macroalgae in Clonakilty Harbour are consistently phosphorus limited, with no nitrogen limitation induced by changing loads of both nutrients. Nitrogen limitation of macroalgae may be theoretically possible if a disproportionate excess of nitrogen was removed relative to phosphorus. However, the exact level of nitrogen load reduction necessary to cause nitrogen limitation has not been considered here.

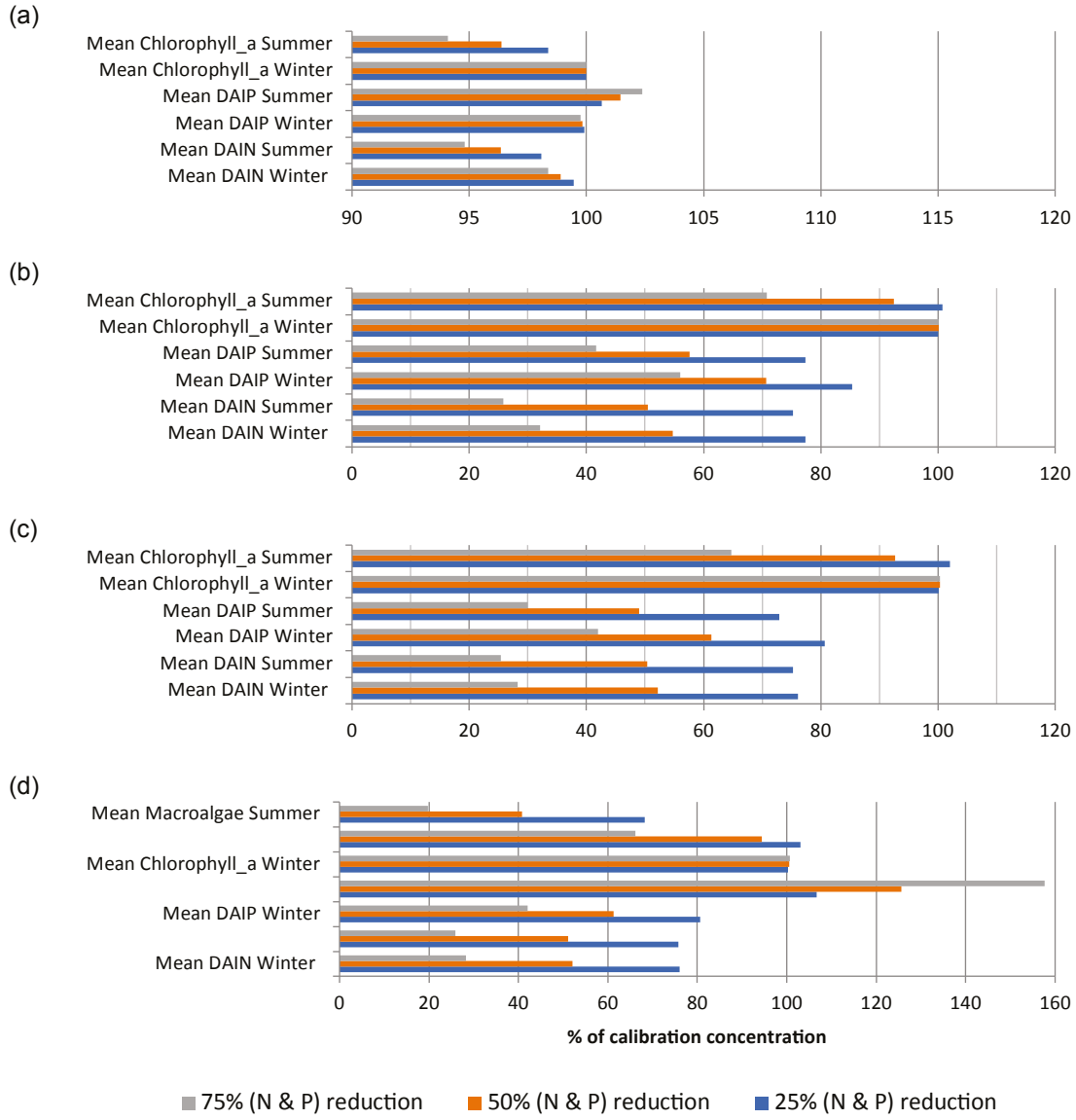

Figure 4.15. Percentage reduction in the concentrations of DAIN, DAIP and chlorophyll and macroalgae tonnage simulated by the Clonakilty DCPM model resulting from various coupled nitrogen and phosphorus reduction scenarios based on 2010–2011 loading data. The model comprises (a) Clonakilty Inner Bay, (b) Ashgrove Receiving Waters, (c) Clonakilty Inner Harbour and (d) Clonakilty Intertidal Macroalgae zone.

The calibrated exchange rates for the transitional water bodies were in the range of 0.32–0.37 day^{-1}, which is equivalent to a residence time of 3.2–3.6 days. The high rate of daily flushing has the consequence of suppressing chlorophyll concentrations, while a short residence time also favours macroalgae growth in water bodies with a large intertidal zone as a result of high light availability and high nutrient renewal rates.

The uncertainty pertaining to the timing, intensity and magnitude of nitrogen and phosphorus loading from the Ashgrove and Clonakilty streams to Clonakilty Harbour propagates through to the confidence in the accuracy of model results and loading scenarios. Neither the annual loads provided by SLAM coupled with available ratios of inorganic to total nitrogen and inorganic to total phosphorus nor the rudimentary load calculations projected from sparse monitoring data and river percentile data taken from the EPA Hydrotools Service could be accepted and presumed representative of the actual average loading for the years 2010 and 2011.

In order to calibrate the DCPM model with the available data, it was deemed necessary to adopt the SLAM annual total nitrogen loading data. Furthermore,

it was necessary to lower the DAIN/total nitrogen ratio from 0.83 to 0.43 in the calibration process to bring the DCPM model results in line with observations; the final value was outside the range of observed DAIN/total nitrogen ratios in the Tolka, which was 0.55–0.97 in the period 1990–2015. These actions fall outside the procedure followed for the Dublin Bay and Courtmacsherry Bay systems.

The results of the three scenarios that focused on riverine phosphorus load reductions highlighted the potential for an increase in DAIN throughout the estuarine system due to a drop in the assimilative capacity. To offset this prospect, the authors suggest that a reduction in riverine phosphorus loading should be allied to a smaller reduction in riverine nitrogen loading to avoid advection of unassimilated DAIN to the coastal shelf.

The differing response of estuarine chlorophyll to 25% and 50% riverine phosphorus load reduction, whereby the lesser reduction causes an increase in chlorophyll but the larger reduction causes a decrease in chlorophyll, suggests that an intermediate riverine phosphorus load reduction would result in no net change in the summer average chlorophyll. Both of the riverine phosphorus load reductions induce a reduction in the magnitude of the summer average *Ulva* bloom, of 32–59%. Therefore, it stands to reason that an intermediate riverine phosphorus load reduction can maintain existing chlorophyll concentrations but substantially reduce the magnitude of the macroalgae bloom.

4.3.2 Summary

A DCPM model was assembled and calibrated for the receiving waters comprising Clonakilty Inner Bay, Ashgrove Receiving Waters and Clonakilty Inner Harbour and its adjacent intertidal zone. The main objective was to establish the order of magnitude of reduction in seasonal average nutrient and chlorophyll concentrations and macroalgae summer wet weight resulting from a series of riverine nutrient load reduction scenarios.

Site-specific light attenuation coefficients and exchange rates were calculated for each water body. Exchange rates were based on estimated residence times determined using an expression derived by Hartnett *et al.* (2011b). In the absence of flow measurements for the Clonakilty and Ashgrove streams, flow estimates were taken from flow percentile curves provided by the EPA Hydrotools Service. Physical mixing was calibrated by modifying the calculated exchange rates and seasonal river discharge ratio to match the salinity time series generated by the DCPM model with the salinity observations gathered by the EPA. Calibration of biological growth was achieved through either increasing or reducing the phytoplankton loss rate, with final values ranging from 0.065 to 0.15 day^{-1}.

Six nutrient load reduction scenarios were considered. Firstly, three scenarios considered reductions in riverine inorganic phosphorus in steps of 25%. The percentage reduction in the observed seasonal average DAIP in each transitional water body was approximately in line with the percentage reduction in inorganic loading. A slight increase in estuarine chlorophyll concentration, of 2–4%, was caused by a 25% phosphorus load reduction, which may be a consequence of more favourable steady-state molar N:P ratios throughout, due to lower assimilation of DAIN in tandem with phosphorus load reduction. A decrease of 4–34% in chlorophyll was induced by a corresponding increase in DAIN concentrations of 2–25% with 50% and 75% riverine phosphorus load reductions.

The small changes in DAIN, DAIP and chlorophyll concentrations in the Inner Bay in response to the six scenarios reflect the scale of the bay and its assimilative capacity. Reducing annual total phosphorus loads results in an associated increase in DAIN concentrations as a result of a reduction in assimilative capacity in the system. This has the potential to negatively impact on any nearby nitrogen-limited coastal water bodies as a result of increased DAIN concentrations in coastal waters.

4.4 Discussion: Practicalities of Realistic Application of the DCPM Model

Application of the DCPM box model to the Courtmacsherry Bay and Clonakilty Bay systems has highlighted a number of aspects that require further endeavour and clarification, to reinforce the validity of the conclusions drawn from scenario simulations, and thus the measures and actions taken to restore trophic status and recreational and amenity value in Irish transitional and coastal waters. Assembly,

calibration and validation of each of the three models entailed using whatever data were readily available, irrespective of spatial or temporal resolution. This would be the case with intensive operational application of the model.

Apparent summer tidal boundary nutrient concentrations taken from coastal monitoring data naturally vary between years as a result of offshore and oceanic processes. As a result of deep-water upwelling, cold nutrient-rich waters with low phytoplankton concentrations may be delivered to the estuarine intertidal zone, thus providing the necessary nutrient concentrations or indeed restoring the molar N:P concentration towards the Redfield ratio. Therefore, analysis of the range of likely nutrient concentrations and chlorophyll concentrations in summer, and the expected variations possible throughout the year, is necessary.

Riverine chlorophyll loading can be specified in the DCPM model, and riverine chlorophyll will invariably contribute to water column concentrations and subsequently to remineralised nutrients in the system. However, this functionality can be used with confidence only if there is greater knowledge of the annual variation in riverine chlorophyll concentrations, and the influence of stream order, catchment slope, and groundwater nutrient efflux on chlorophyll concentrations. The resilience of riverine chlorophyll in brackish waters must also be quantified, in order to apply a relevant loss rate.

Although chlorophyll concentrations can be replicated in the DCPM model to the same order of magnitude as in the sampling data, underestimation of the limiting nutrient is often a consequence because of the simulated overconsumption of the limiting nutrient within the model as a result of the fixed Michaelis–Menten formulation. A cell-level growth formulation that reflects the increasing affinity of chlorophyll for nutrients with decreasing availability of nutrients should be trialled to investigate if this would improve DCPM model accuracy with respect to the limiting nutrient.

Notwithstanding restrictions relating to depth specification in oligohaline waters, extensive efforts to calibrate physical mixing in the DCPM model, by comparing model-simulated salinity with measurements, leads to quicker calibration of biological growth, given accurate nutrient and chlorophyll loading data. Calibration must always proceed from the coastal waters moving upstream. Deviation of biological growth parameters from default values is rarely necessary with the exception of phytoplankton loss rates.

Knowledge of salinity and macroalgae bloom wet weights gives an insight into physical mixing processes and trophic growth potential due to nutrient loading. Therefore, in estuaries where accurate nutrient loading data are available, and where intertidal zones exist and macroalgae proliferate, there is a greater likelihood of the eventual model being accurate with respect to chlorophyll and nutrient concentrations if the DCPM model accurately simulates salinity concentrations and macroalgae tonnages.

The interannual difference in the nutrient loading data made available by the Teagasc ACP for the years 2010, 2011, 2015 and 2016 indicated that annual total nitrogen and total phosphorus loads derived from SLAM can be adopted henceforth only with greater knowledge of their likely deviation from the declared loading during wet, dry or average summers and winters. Otherwise, given that observed DAIN and DAIP loads are threefold higher in wet summers than in dry summers, DCPM models may be incorrectly calibrated, as it is possible to iteratively calibrate them until the model-simulated values converge towards measurements, to the extent that the applied loading permits. Knowledge of the scaling factor that should be applied to the SLAM loading data to derive a wet, dry or average winter and summer would facilitate a more robust series of the nine scenarios run. Greater knowledge of the proportion of total nitrogen and total phosphorus loads declared by SLAM that comprises DAIN and DAIP, respectively, for each point and non-point source of pressure would also increase confidence in SLAM loadings. Additionally, if the ratio of inorganic to total nutrients changes throughout the year, characterisation of the annual variation would also be beneficial.

The tendency of the non-limiting nutrient to build up in the upper reaches of estuaries results in a high model error, which is compounded by the often underestimated depths declared for these same reaches. Owing to the sensitivity of the DCPM model to the declared bathymetric depths in the upper reaches of estuaries, the model may be unsuitable at present for compliance purposes; model error in

upper reaches was in the range of ±50% in many cases. Accurate estimation of oligohaline waters is therefore central to increasing confidence in the results simulated by the DCPM model.

The EPA transitional and coastal monitoring team currently use the UKTAG OMBT to identify status under the WFD (Wan *et al.*, 2017). The compliance metric is based on percentage cover of AIH, biomass per square metre of AIH, biomass per square metre of AA, percentage entrained in AA, the size of the AA and the ratio of AA to AIH. The DCPM model has the capability to simulate biomass per square metre of both AIH and AA, although AIH and AA are input parameters. Therefore, the model cannot simulate a change in the AA, although the AIH is constant and describes the area exposed between high and low tide. The AA is considered as the area within which macroalgae wet weight densities exceed 100 g m^{-2}.

Entrainment is included in the blooming tool as it provides a proxy for the interannual potential regeneration; entrainment is defined by the blooming tool as the presence of buried macroalgae to a depth of greater than 3 cm beneath the sediment surface. This is another aspect of the DCPM model that precludes its application for compliance purposes. The influence of the physical actions of the tide on macroalgae cannot be described by a 0-D box model such as the DCPM model.

The ability of the DCPM model to accurately replicate the summer average bloom magnitude in terms of wet weight is reliant upon correct specification of the ratio of macroalgae wet weight to dry weight. Although species-specific ratios of dry weight to wet weight have been identified (Wickham *et al.*, 2019), the ratios vary as a result of ageing or intermittent desiccation. In this research, the ratio was varied between 4.9 and 7 g ww g^{-1} dw. Uncertainty must be attributed to these values, considering that the ratio that best reflects the prevailing conditions from year to year will depend on the frequency and extent of desiccation. The effects of desiccation on species are not universal, as *Gracilaria vermiculophylla* has been identified as resistant to desiccation (Thomsen and McGlathery, 2007). Desiccation suppresses the maximum quantum yield, and therefore the fixation rate and the carbon content, in a manner that is dependent upon the relative water content (Holzinger and Karsten, 2013; Holzinger *et al.*, 2015). Desiccation can also be the cause of *in situ* macroalgae death when the relative water content drops below 50% (Gupta and Kushwaha, 2017). Further research to elucidate the intricacies of desiccation, and thus oxidation and the subsequent rate of mortality, would greatly benefit future scenario modelling activities and increase confidence in eventual model results.

4.5 Conclusions: Necessary Point and Non-point Nutrient Load Reductions to Irish Estuaries

Two transitional/coastal systems with predominantly non-point agricultural loading have been considered in the context of possible, achievable gains in estuarine water quality. The DCPM model provided reasonable estimates of prevailing salinity, nutrient and chlorophyll concentrations and macroalgae bloom magnitudes. The differences between the simulated seasonal averages and the monitored seasonal averages may preclude the use of the model for assessment purposes against TSAS (see McGarrigle *et al.*, 2010) or UKTAG macroalgae criteria. However, adopting the calibrated model set-up here, and considering the simulated water column concentrations and macroalgae wet weights as representative of real-world conditions, the following conclusions can be drawn from the scenarios simulated:

- Argideen Estuary/Courtmacsherry Bay system: in order to improve the likelihood of compliance with summer TSAS parameter limits and UKTAG upper wet macroalgae density limits, the following observations were made with respect to nutrient load reductions:
  - Average summer conditions are represented by the year 2016. None of the scenarios considered for 2016 restored macroalgae wet densities to less than 100 g ww m^{-2}. DAIN compliance in Courtmacsherry Inner Bay was restored by reducing the riverine nitrogen and phosphorus load by 33%. A 66% reduction in riverine nitrogen and phosphorus load was necessary to restore DAIN and chlorophyll concentrations to compliance in Timoleague Receiving Waters and to restore DAIN, DAIP and chlorophyll concentrations to compliance in the Upper Argideen Estuary.
  - Wet summer conditions are represented by the year 2015. None of the scenarios considered for 2015 restored macroalgae wet densities to less than 100 g ww m^{-2}. A 33% riverine

nitrogen load reduction was necessary to restore compliance of DAIN in the Lower Argideen Estuary. A 66% riverine nitrogen load reduction was necessary to restore DAIN compliance in the intertidal zone of the Argideen Estuary. A 66% riverine nitrogen and phosphorus load reduction was necessary to restore compliance with DAIN and chlorophyll limit criteria in the Timoleague Receiving Waters. A 66% riverine nitrogen load reduction was necessary to restore compliance with DAIN limit criteria in the Upper Argideen Estuary.

– Consolidation of wastewater treatment and conveyance in the Argideen Estuary and Courtmacsherry Bay was found to have a negligible effect on water quality parameters, with simulated changes in seasonal average concentrations falling within ±3%.

- Clonakilty Harbour/Bay system: for the period 2010–2011, a 50% riverine nitrogen load reduction would have restored compliance of winter/summer DAIN exceedance in Ashgrove Receiving Waters. A 25% reduction in riverine nitrogen load would restore winter DAIN compliance in Clonakilty Inner Harbour and the adjacent intertidal zone of Clonakilty Harbour, whereas a 25% riverine phosphorus load reduction would restore macroalgae wet densities to less than 100 g ww m^{-2}.

5 Conclusions

5.1 The Nature and Magnitude of Necessary Load Reductions to Eliminate Problematic Macroalgae

Dublin Bay and the Tolka and Liffey estuaries were modelled for the period 2010–2011. Wastewater pressures accounted for 72% of DAIN loading and 96% of DAIP loading. To reduce macroalgae bloom magnitudes to a compliance wet weight density (< 100 g m^{-2}) (Wells *et al.*, 2009), riverine nutrient loading would need to be reduced by 50%, or the treatment plant at Ringsend could be upgraded to the NDN-PAO (nitrifying-denitrifying, DAIP-accumulating granules with anaerobic feeding) variant of AGS treatment. This would reduce the weight of the macroalgae bloom by 72%. Considering the individual impacts of riverine nutrient load reduction and wastewater infrastructure improvement, a combination of both measures may deliver synergistic results.

The system comprising the Argideen Estuary and Courtmacsherry Bay is subject primarily to diffuse nutrient pressures from agriculture. Owing to the availability of high-resolution monitoring data for the Argideen River, it was possible to scale up the nutrient loads and flow observations to the entire system catchment by extrapolating nutrient loads to the other rivers entering the Argideen Estuary and Courtmacsherry Bay. Hourly nutrient concentration and flow data were made available for the years 2010, 2011, 2015 and 2016. Scenario modelling focused on summer of each year. The years 2015 and 2016 were identified as representative of wet and average summers, respectively. For both years, a coupled 66% reduction in the riverine nitrogen and phosphorus loading was found to restore the constituent water bodies to compliance for TSAS parameters, although none of the scenarios restored the macroalgae wet density to below 100 g ww m^{-2}. DCPM model simulations for 2015 and 2016 indicated that, if the riverine nitrogen and phosphorus loads to the Argideen Estuary and Courtmacsherry Bay were reduced by 66%, the mean summer macroalgae blooms would have been 212 and 187 tonnes, respectively, with the macroalgae wet density for both years in the range of 180–190 g ww m^{-2}. Macroalgae wet density is the sole opportunistic macroalgae compliance parameter that can be simulated in the DCPM model. Consolidation of wastewater conveyance and centralisation of wastewater treatment was found to have a negligible effect on seasonal water quality parameters in the Argideen Estuary/Courtmacsherry Bay system, with all changes within ±3% of the calibration concentrations.

The Clonakilty Harbour/Bay system was modelled based on nitrogen load estimates generated by SLAM and phosphorus loads calculated from monitoring data and freshwater flow estimates, while freshwater loading was estimated based on flow percentiles provided by the EPA Hydrotools Service. For the period 2010–2011, a moderate 25% phosphorus load reduction was deemed necessary to restore macroalgae bloom density to below the threshold value (100 g m^{-2}).

The magnitude of nutrient load reductions necessary to improve water quality and the relevant pressure differs between estuaries, not least due to factors such as residence time, estuary shape, width and length and the proximity of each subsidiary water body to the adjacent coastal shelf, which ultimately receives all waters.

The DCPM model was applied to a detailed study of the Argideen Estuary/Courtmacsherry Bay system during four different summers with respect to nutrient load magnitudes and the resultant ambient water quality conditions. The four years reflect wet, dry and average summers. The primary observation from the 4-year study is the manner in which prevailing rainfall patterns impact the efficacy of nutrient load reduction scenarios. Expectations from nutrient load reductions ought to be greater or lesser from year to year dependent upon the prevailing rainfall. The year 2011 was notably drier than 2010, 2015 and 2016. The lack of rainfall in 2011 induced outright nutrient limitation as the shortage of rain prevented the transfer of nutrients from the catchment to receiving waters.

The results from the DCPM model studies in this project indicate the influence of proximity to coastal

waters, and offshore coastal nutrient concentration, on macroalgae blooms in estuarine intertidal zones. Tidal renewal of nutrient-depleted estuarine waters replenishes the limiting nutrient during peak bloom-forming conditions. This observation has been previously made in the Argideen Estuary (Ní Longphuirt *et al.*, 2016b); the results of this project corroborate the finding.

Population growth places pressure on estuarine and coastal water quality, not least due to the concentration of population growth around urban coastal centres. The effects of population growth in Dublin City and environs, and the range of possible responses in terms of expansion of wastewater treatment, were considered in this report. A 20% PE increase in nutrient loading to Ringsend WWTP without any additional treatment capacity would result in a 63% increase in the weight of the macroalgae bloom in the Tolka Estuary. However, expansion of treatment capacity and treatment in compliance with the UWWTR would result in a minor increase of 14% in the macroalgae bloom, despite an increase in loading of 20% PE. Further reductions in riverine non-point nutrient loading to the Liffey and Tolka estuaries may further compound the benefits of improved wastewater treatment facilities.

5.2 Role of a High-resolution Coupled Hydrodynamic, Water Quality and Macroalgae Model

A pre-existing depth-integrated 2-D hydrodynamic, solute transport and water quality model, MSN_WQ, was modified to incorporate macroalgae growth and decay as a function of water column nutrient concentrations, macroalgae tissue nutrient concentrations, bottom stress, bed capacity, salinity and oxygen concentrations. Initial benchmarking of the DCPM model against MSN_WQ in Cork Harbour indicated that the models estimated *in situ* nutrient concentrations equally well, although chlorophyll concentrations were more accurately simulated by the MSN_WQ model.

In the expanded MSN_WQ model, the state variables of macroalgae dry weight, tissue nitrogen and tissue phosphorus were added alongside BOD, salinity, NH_4, NO_3, dissolved oxygen, chlorophyll and orthophosphate. The model was applied to the system comprising the Liffey and Tolka estuaries and Dublin Bay, and run from April to September, inclusive.

The MSN_WQ model performed just as well as the DCPM model with respect to the summer average macroalgae bloom magnitude, with the simulated value approximating the monitored value. Inclusion of the macroalgae life cycle and its biogeochemical interactions in the MSN_WQ model as part of this study progresses the task of high-resolution macroalgae modelling in Ireland to the point of proof of concept. The updated MSN_WQ model, as a consequence of incorporating the Droop cellular model, reflected the expected reduction in tissue nitrogen and phosphorus throughout peak growth in summer and the subsequent accumulation of nitrogen and phosphorus as growth reduced towards the end of the summer. Inclusion of an average nutrient flux from Jennings (1996) also influenced throughout the summer cycle by increasing the macroalgae bloom magnitude.

In comparison with the DCPM model, average water column concentrations of nitrogen, phosphorus and chlorophyll were observed to be higher than monitored values. This is due to the adoption of depth-integrated Navier–Stokes equations in the MSN_WQ model. Therefore, riverine inputs are presumed fully vertically mixed. Significant freshwater discharges to the system should be released to the coastal zone, although in this instance the freshwater discharges were mixed with incoming tidal waters and retained in the Liffey–Tolka junction. A fully 3-D model such as ROMS or EFDC would resolve vertical velocity distribution, such that the dominant surface flows out of the mouth of the Liffey would exceed the inflows from the tide, leading to a net flow out of the mouth of the Liffey. Thus, the vertical and horizontal salinity–temperature boundary would move with the ebb and flood of the tide to reflect reality in the Liffey–Tolka junction.

6 Recommendations

6.1 DCPM Model Application

The recommended default DCPM model parameters have proven robust in all applications of the model as part of this study. The values are largely reliable, and the model reflects the seasonal variation that would be expected, such as nutrient limitation and bloom formation during optimum growth conditions. The authors propose that the ability of the DCPM model to match summer macroalgae bloom wet weight and seasonally varying salinity provides a good proxy for overall model performance as long as all riverine nutrient loads and tidal nutrient concentrations have been accurately specified and the variation thereof throughout the year has been adequately described via the R_{SA} value and the forcing curves provided in the model. To expedite model sign-off, calibration of physical mixing and the prevailing salinity in the DCPM model by tuning R_{SA} and the daily exchange rate, E, should proceed methodically inland from coastal boxes. Adopting water body boundaries as classified by the WFD proved to be unwieldy and complicated calibration somewhat, especially with respect to calibration of the model against observed macroalgae bloom magnitudes. Intertidal zones must be treated as separate water bodies, positioned upstream in the network of the tidal waters adjacent.

6.2 Recommended Large-scale Modelling Activities

The expanded MSN_WQ model correctly estimated the order of magnitude of the macroalgae bloom for the period 2010–2011, thus providing proof of concept that the interactions and formulations within the model are correct. Owing to thermohaline stratification at the junction between the Liffey and Tolka estuaries and Dublin Bay, the 2-D depth integration of Navier–Stokes equations in MSN_WQ results in apparently restricted exchange between the junction and the open coastal waters. The resultant ebb and flood pattern in the 2-D hydrodynamic model underpinning the MSN_WQ model provides a high-level overview of the prevailing exchange, although the vertical velocity distribution around the mouth of the Lower Liffey Estuary is not resolved.

To account for the stratification at the junction between the Lower Liffey Junction and Dublin Bay, a full 3-D hydrodynamic, solute transport and water quality model is recommended, such as ROMS. The developed code and parametrisation of the macroalgae life cycle is transferable to ROMS with minor modification. The Marine Institute runs an operational ROMS model of the North-East Atlantic, which would facilitate running the resultant 3-D model of Dublin Bay on a semi-operational basis, such that hindcast data would be readily available to run the high-resolution water quality model on a weekly basis. The Copernicus Marine Environment Monitoring Service (CMEMS) has made available a reanalysis biogeochemical dataset generated by the NEMO (Nucleus for European Modelling of the Ocean) model for the period from 2002 to 2014, which would provide offshore coastal shelf nutrient, phytoplankton, chlorophyll and oxygen boundary conditions.

The bathymetry of two additional systems, namely Clonakilty Harbour and Bay and the Argideen Estuary and Courtmacsherry Bay, was digitised as part of this study. The availability of these data would also facilitate the application of the newly expanded MSN_WQ model to either system. Owing to the availability of subhourly nutrient and flow monitoring data for the Argideen River from the Teagasc ACP, the Argideen Estuary/Courtmacsherry Bay system is preferred. The resultant model would facilitate scenario analyses of the impact of different catchment measures on trophic status in the transitional and coastal waters, while multiyear model runs would also be possible.

The current iteration of the MSN_WQ model has provided for a single generic macroalgae species, while the model has been populated with parameters pertaining to *Ulva* spp. It would be straightforward to expand the model to describe the broader community of macroalgae species, with knowledge of the maximum daily growth rate, NH_4 and NO_3 uptake rates and half-saturation constants, and the saturation and half-saturation light intensity pertaining to each species. This may potentially assist with detangling the causes for domination and succession

of different species throughout the summer. Projects such as SeaMat have been purposed with elucidating the factors influencing the sequencing of different macroalgae species such as *Gracilaria*, *Ulva* and *Ectocarpus*. Thus, the future modelling permutations stemming from this study and the SeaMat project are manifold.

6.3 Knowledge Gaps: Future Research Requirements

A number of knowledge gaps have been identified; addressing the knowledge gaps would increase the accuracy of both simple box models such as DCPM and detailed high-resolution models such as MSN_WQ.

An annual chlorophyll load in kilograms per year can be specified in the DCPM model. Inevitably there will be a riverine contribution to chlorophyll concentrations in transitional and coastal waters. The chlorophyll loads that were applied in the DCPM model were derived based on rudimentary calculations. All modelling activities in this context would greatly benefit from detailed knowledge of the annual variation in chlorophyll concentrations, as a function of (1) non-point nitrogen and phosphorus loading to the catchment throughout the year, (2) the resultant DAIN and DAIP concentrations in the catchment itself, (3) the number of lakes or reservoirs in the catchment to facilitate growth of chlorophyll, and their physical characteristics, (4) rainfall and (5) the daily irradiance. This would enable more detailed scenario modelling of the influence of wetter or drier seasons on nutrient transfer, or changes in nutrient transfer due to catchment management practice on trophic status in transitional and coastal waters.

Annual nutrient loading values were made available for this study from SLAM. When the approximate annual load was compared with loads derived from subhourly monitoring data, a disparity was observed between the SLAM-derived loads and the calculated loads transferred to waterways during a wet, dry or average summer or winter. Therefore, the authors recommend the derivation of scaling factors to modify SLAM loads to represent a wet, dry or average summer and winter.

Annual nutrient loads taken from SLAM are quoted as total nitrogen and total phosphorus. The inorganic fractions of nitrogen and phosphorus are needed as input for DCPM. Therefore, knowledge of the ratio of inorganic to total nitrogen and total phosphorus for each nutrient source in SLAM, plus the likely variation thereof throughout the year, would greatly increase confidence in model results. OSPAR RID data collected monthly at OSPAR sites since 1990 reveal the variation in the ratio of inorganic to total nitrogen and phosphorus in each catchment. However, the equivalent ratios are not readily available for individual sources of nutrients such as wastewater, pasture and forestry. Ratios determined based on annually aggregated data for the Dodder, Liffey and Tolka indicate substantial interannual variation (Figures 6.1 and 6.2).

Knowledge of the survivability, or decay rate, of riverine plankton classes in brackish waters would also improve understanding of nutrient cycling at the interface between rivers and transitional waters.

Macroalgae calculations in the DCPM and MSN_WQ models are executed based on macroalgae dry weight. The dry weight to wet weight ratio is an input parameter that converts the resultant bloom from dry weight to wet weight. The parameter varies between 4 and 10, although a fixed value is generally used in macroalgae modelling. The ratio of wet weight to dry weight is influenced by desiccation and oxidation amongst other environmental factors; the value has a large bearing on the accuracy of the model. Therefore, a detailed analysis of the topic and associated analysis would greatly benefit modelling activities.

Application of an average NH_4 flux throughout the intertidal zone of the Tolka Estuary in the MSN_WQ model resulted in an increase in the bloom wet weight. Release of nutrients from the intertidal sediment beneath macroalgae has been previously proven to fuel growth of macroalgae during nutrient limitation. Intertidal nutrient release is generally hypothesised to be caused by burial of macroalgae under their own weight into the sediment beneath. Macroalgae have the potential to return annually in perpetuity, as a result of their ability to sequester nutrients during conditions that are unfavourable for growth. Decay of macroalgae subsequently results in sequestration of the same nutrients in intertidal sediment.

The factors that influence intertidal nutrient fluxes into the water column are a function of location and elevation. Therefore, spatially resolved models such as MSN_WQ and ROMS are preferable for detailed modelling of intertidal nutrient fluxes and

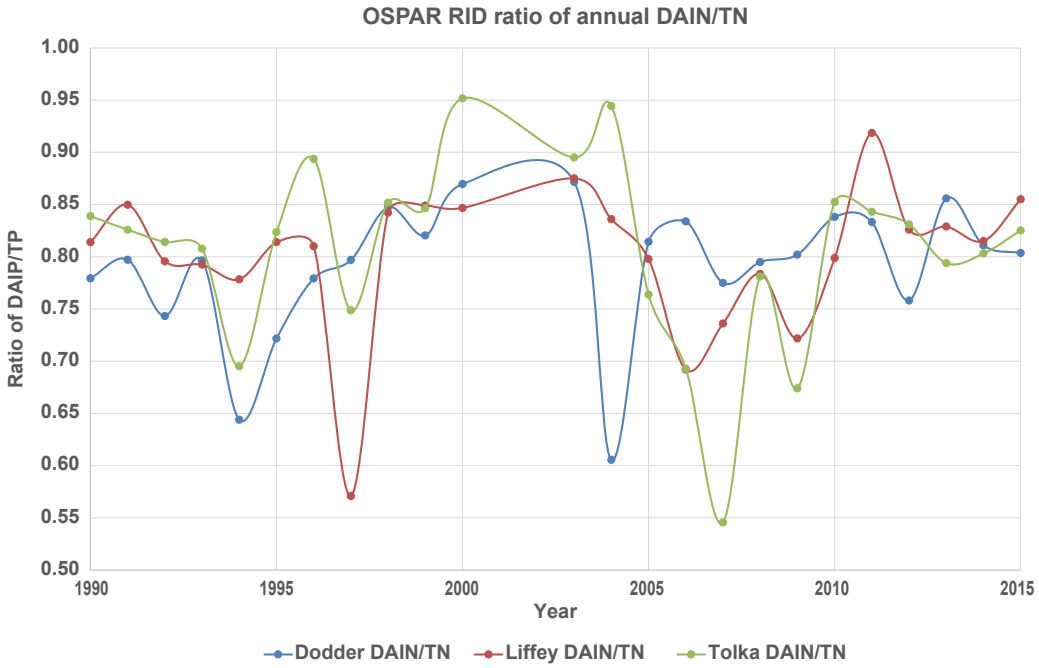

Figure 6.1. The ratio of DAIN to total nitrogen (TN) in the rivers Dodder, Liffey and Tolka determined on an annually aggregated basis from OSPAR RID data spanning 1990–2015 (with thanks to the EPA Transitional and Coastal team).

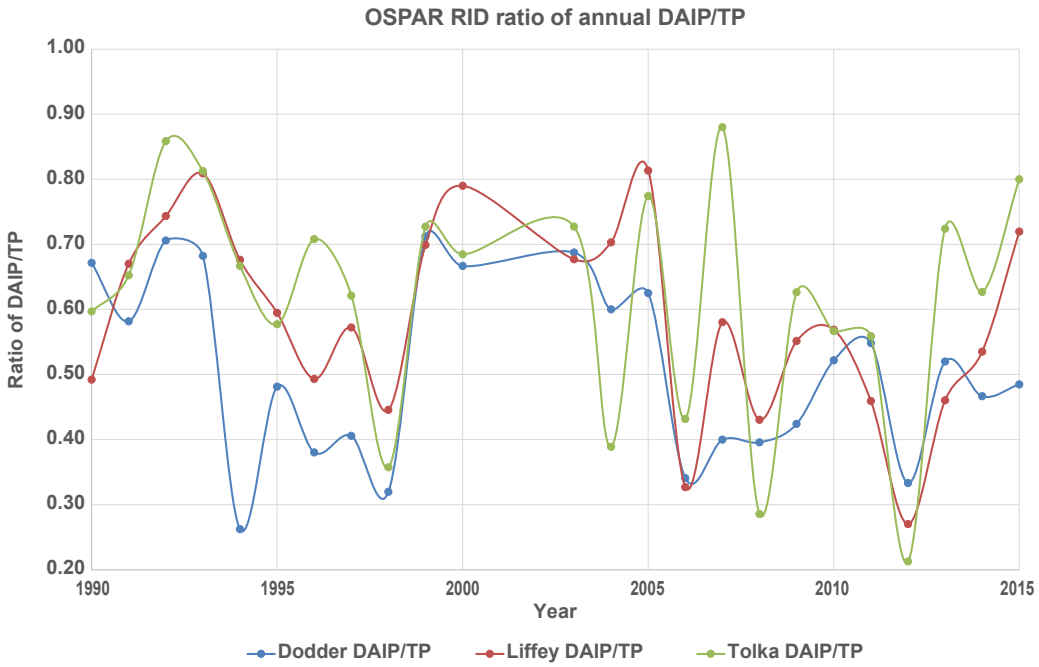

Figure 6.2. The ratio of DAIP to total phosphorus (TP) in the rivers Dodder, Liffey and Tolka determined on an annually aggregated basis from OSPAR RID data spanning 1990–2015 (with thanks to the EPA Transitional and Coastal team).

the interaction between macroalgae and intertidal sediment. Physical factors such as bottom shear stress also influence the eventual site for establishment and proliferation of macroalgae. Therefore, although the DCPM model is suitable for scenario modelling, the MSN_WQ and ROMS models must be adopted for compliance assessment modelling. The burial depth of macroalgae is included in the macroalgae assessment framework adopted nationally, as is the affected area and the ratio of the AA and the AIH. Variation in these

factors cannot be adequately described in the DCPM model. The authors recommend further detailed modelling of the role of intertidal sediment in either of the aforementioned spatially resolved hydrodynamic and water quality models.

The performance of the DCPM model with respect to estimation of winter chlorophyll values was affected by adoption of the same light attenuation coefficient, k_d, for the entire year, although light attenuation will change throughout the year depending upon nutrient and sediment loading and the resultant chlorophyll concentrations. Where feasible, a detailed regression model of k_d values, derived from Secchi disc readings, against chlorophyll concentrations and suspended sediment concentrations would greatly improve model performance during winter.

References

Aldridge, J.N. and Trimmer, M., 2009. Modelling the distribution and growth of “problem” green seaweed in the Medway estuary, UK. In Andersen, J.H. and Conley, D.J. (eds), *Eutrophication in Coastal Ecosystems: Towards Better Understanding and Management Strategies*. Springer, Dordrecht, the Netherlands, pp. 107–122.

Aldridge, J.N., Tett, P., Painting, S.J., Capuzzo, E. and Mills, D.K., 2010. *The Dynamic Combined Phytoplankton and Macroalgae (CPM) Model*. *Technical Report.* Contract C3290 Report. Environment Agency, Bristol, UK.

Aldridge, J., van der Molen, J. and Forster, R., 2012. *Wider Ecological Implications of Macroalgal Cultivation*. The Crown Estate, London.

Aldridge, J.N., Painting, S., Tett, P., Capuzzo, E. and Mills, D.K., 2013. *The Dynamic Combined Phytoplankton and Macroalgae (CPM) Model, version 2.0*. Centre for Environment, Fisheries and Agriculture Science, Lowestoft, UK.

Aveytua-Alcázar, L., Camacho-Ibar, V.F., Souza, A.J., Allen, J.I. and Torres, R., 2008. Modelling *Zostera marina* and *Ulva* spp. in a coastal lagoon. *Ecological Modelling* 218: 354–366. https://doi.org/10.1016/j.ecolmodel.2008.07.019

Blanc, F., Leveau, M. and Szekielda, K.H., 1969. Effets eutrophiques au débouché d’un grand fleuve (Grand Rhône). *Marine Biology* 3: 233–242. https://doi.org/10.1007/bf00360956

Bonachela, J.A., Raghib, M. and Levin, S.A., 2011. Dynamic model of flexible phytoplankton nutrient uptake. *Proceedings of the National Academy of Sciences of the United States of America* 108: 20633–20638. https://doi.org/10.1073/pnas.1118012108

Brown, L.C. and Barnwell, T.O., 1985. *Computer program Documentation for the ENHANCED Stream Water Quality Model QUAL2E* (No. EPA/600/3-85/065). United States Environmental Protection Agency, Washington, DC.

Brush, M.J. and Nixon, S.W., 2010. Modeling the role of macroalgae in a shallow sub-estuary of Narragansett Bay, RI (USA). *Ecological Modelling* 221: 1065–1079. https://doi.org/10.1016/j.ecolmodel.2009.11.002

Burkholder, J.M., Tomasko, D.A. and Touchette, B.W., 2007. Seagrasses and eutrophication. *Journal of Experimental Marine Biology and Ecology* 350: 46–72. https://doi.org/10.1016/j.jembe.2007.06.024

Cerco, C.F., Noel, M.R. and Tillman, D.H., 2004. A practical application of Droop nutrient kinetics (WR 1883). *Water Research* 38: 4446–4454. https://doi.org/10.1016/j.watres.2004.08.027

Chen, B., Zou, D. and Jiang, H., 2015. Elevated CO_2 exacerbates competition for growth and photosynthesis between *Gracilaria lemaneiformis* and *Ulva* lactuca. *Aquaculture* 443: 49–55. https://doi.org/10.1016/j.aquaculture.2015.03.009

Coffaro, G. and Sfriso, A., 1997. Simulation model of *Ulva* rigida growth in shallow water of the Lagoon of Venice. *Ecological Modelling* 102: 55–66. https://doi.org/10.1016/S0304-3800(97)00094-X

Costello, M.J., Hartnett, M., Mills, P., O’Mongain, E., Collier, L., Johnson, M., Nash, S., Leslie, R., Berry, A., Emblow, C., Collins, A. and McCrea, M., 2001. *Nutrient Dynamics of Two Estuaries in Ireland: Wexford and Cork Harbours*. Environmental Protection Agency, Johnstown Castle, Ireland.

DAF (Department of Agriculture, Fisheries and Food), 2010. *Food Harvest 2020. A Vision for Irish Agri-food and Fisheries*. Department of Agriculture, Food and the Marine, Dublin.

DECLG (Department of the Environment, Community and Local Government), 2015. *Public Consultation Document on the Significant Water Management Issues in Ireland*. DECLG, Dublin.

de Guimaraens, de Moraes Paiva, A. and Coutinho, R., 2005. Modeling *Ulva* spp. dynamics in a tropical upwelling region. *Ecological Modelling* 188: 448–460. https://doi.org/10.1016/j.ecolmodel.2005.04.023

Devlin, M.J., Barry, J., Mills, D.K., Gowen, R.J., Foden, J., Sivyer, D. and Tett, P., 2008. Relationships between suspended particulate material, light attenuation and Secchi depth in UK marine waters. *Estuarine, Coastal and Shelf Science* 79: 429–439. https://doi.org/10.1016/j.ecss.2008.04.024

Devlin, M.J., Barry, J., Mills, D.K., Gowen, R.J., Foden, J., Sivyer, D., Greenwood, N., Pearce, D. and Tett, P., 2009. Estimating the diffuse attenuation coefficient from optically active constituents in UK marine waters. *Estuarine, Coastal and Shelf* Science 82: 73–83. https://doi.org/10.1016/j.ecss.2008.12.015

DHPLG (Department of Housing, Planning and Local Government), 2018. *River Basin Management Plan for Ireland 2018–2021*. DHPLG, Dublin.

DOEHLG (Department of the Environment, Heritage and Local Government), 2001. *S.I. No. 254 of 2001 Urban Waste Water Treatment Regulations*. Stationery Office, Dublin.

DOEHLG (Department of the Environment, Heritage and Local Government), 2004. *S.I. No. 440 of 2004 Urban Waste Water Treatment (Amendment) Regulations*. Stationery Office, Dublin.

DOEHLG (Department of the Environment, Heritage and Local Government), 2006. *S.I. No. 378 of 2006 European Communities (Good Agricultural Practice for Protection of Waters) Regulations*. Stationery Office, Dublin.

DOEHLG (Department of the Environment, Heritage and Local Government), 2009. S*.I. No. 101 of 2009 European Communities (Good Agricultural Practice for Protection of Waters) Regulations*. Stationery Office, Dublin.

DOEHLG (Department of the Environment, Heritage and Local Government), 2010a. S*.I. No. 48 of 2010 Urban Waste Water Treatment (Amendment) Regulations*. Stationery Office, Dublin.

DOEHLG (Department of the Environment, Heritage and Local Government), 2010b. *S.I. No. 610 of 2010 European Communities (Good Agricultural Practice for Protection of Waters) Regulations*. Stationery Office, Dublin.

DOEHLG (Department of the Environment, Heritage and Local Government), 2014. *S.I. No. 31 of 2014 European Communities (Good Agricultural Practice for Protection of Waters) Regulations*. Stationery Office, Dublin.

Duarte, C.M., 1995. Submerged aquatic vegetation in relation to different nutrient regimes. *Ophelia* 41: 87–112. https://doi.org/10.1080/00785236.1995.10422039

Dublin City Council, 2011. *Annual Environmental Report, 2011. Greater Dublin Area Agglomoration. Waste Water Discharge Licence No D0034-01*. Available online: http://www.epa.ie/licences/lic_eDMS/090151b2804307e1.pdf (accessed 9 November 2020).

Dublin City Council, 2012. *Annual Environmental Report, 2012. Greater Dublin Area Agglomoration. Waste Water Discharge Licence No D0034-01*. Available online: http://www.epa.ie/licences/lic_eDMS/090151b280480302.pdf (accessed 9 November 2020).

Dublin City Council, 2013. *Annual Environmental Report, 2013. Greater Dublin Area Agglomoration. Waste Water Discharge Licence No D0034-01*. Available online: http://www.epa.ie/licences/lic_eDMS/090151b2804dbf44.pdf (accessed 9 November 2020).

Dupas, R., Mellander, P.-E., Gascuel-Odoux, C., Fovet, O., McAleer, E.B., McDonald, N.T., Shore, M. and Jordan, P., 2017. The role of mobilisation and delivery processes on contrasting dissolved nitrogen and phosphorus exports in groundwater fed catchments. *Science of the Total Environment* 599–600: 1275–1287. https://doi.org/10.1016/j.scitotenv.2017.05.091

Dupas, R., Minaudo, C., Gruau, G., Ruiz, L. and Gascuel-Odoux, C., 2018. Multidecadal trajectory of riverine nitrogen and phosphorus dynamics in rural catchments. *Water Resources Research* 54: 5327–5340. https://doi.org/10.1029/2018WR022905

EEA (European Environment Agency), 2018. *European Waters: Assessment of Status and Pressures*. EEA Report No. 7/201. European Environment Agency, Copenhagen.

EPA (Environmental Protection Agency), 2018. *Urban Waste Water Treatment in 2017*. Environmental Protection Agency, Johnstown Castle, Ireland.

Falconer, R.A., Lin, B., Wu, Y. and Harris, E., 2001. *DIVAST Reference Manual*. Hydro-Environmental Research Centre, Cardiff University, Cardiff.

Fanning, A., Craig, M., Webster, P., Bradley, C., Tierney, D., Wilkes, R., Mannix, A., Treacy, P., Kelly, F., Geoghegan, R., Kent, T. and Mageean, M., 2017. *Water Quality in Ireland 2010–2015*. Environmental Protection Agency, Johnstown Castle, Ireland.

Farrelly, P., Crosse, S., O'Donoghue, P., Whyte, S., Farrelly, P.B., Burn, T., Byrne, D., Holmes, O., Maklin, R., McKearney, J.J. and Salley, F., 2014. *Food Harvest 2020 Environmental Analysis Report*. Final Report – January 2014. Department of Agriculture, Food and the Marine, Dublin.

Figdore, B.A., Stensel, H.D. and Winkler, M.-K.H., 2018. Comparison of different aerobic granular sludge types for activated sludge nitrification bioaugmentation potential. *Bioresource Technology* 251: 189–196. https://doi.org/10.1016/j.biortech.2017.11.004

Fong, P., Boyer, K.E., Desmond, J.S. and Zedler, J.B., 1996. Salinity stress, nitrogen competition, and facilitation: what controls seasonal succession of two opportunistic green macroalgae? *Journal of Experimental Marine Biology and Ecology* 206: 203–221. https://doi.org/10.1016/S0022-0981(96)02630-5

Forester, J.W., 1973. The fate of freshwater algae entering an estuary. In Stevensen, L. and Colwell, R. (eds), *Estuary Microbial Ecology*. University of South Carolina Press, Columbia, SC, p. 22.

Gao, Z., Xu, D., Meng, C., Zhang, X., Wang, Y., Li, D., Zou, J., Zhuang, Z. and Ye, N., 2014. The green tide-forming macroalga *Ulva linza* outcompetes the red macroalga *Gracilaria lemaneiformis* via allelopathy and fast nutrients uptake. *Aquatic Ecology* 48: 53–62. https://doi.org/10.1007/s10452-013-9465-9

Green-Gavrielidis, L., MacKechnie, F., Thornber, C. and Gomez-Chiarri, M., 2018. Bloom-forming macroalgae (*Ulva* spp.) inhibit the growth of co-occurring macroalgae and decrease eastern oyster larval survival. *Marine Ecology Progress Series* 595: 27–37.

Gupta, V. and Kushwaha, H.R., 2017. Metabolic regulatory oscillations in intertidal green seaweed *Ulva lactuca* against tidal cycles. *Scientific Reports* 7: 16430. https://doi.org/10.1038/s41598-017-15994-2

Hartnett, M. and Nash, S., 2004. Modelling nutrients and chlorophyll-a dynamics in an Irish brackish water body. *Environmental Modelling and Software* 19: 47–56. https://doi.org/10.1016/S1364-8152(03)00109-9.

Hartnett, M., Nash, S. and Olbert, I., 2011a. An integrated approach to trophic assessment of coastal waters incorporating measurement, modelling and water quality classification. *Estuarine, Coastal and Shelf Science* 112: 126–138. https://doi.org/10.1016/j.ecss.2011.08.012

Hartnett, M., Dabrowski, T. and Olbert, A., 2011b. A new formula to calculate residence times of tidal waterbodies. *Proceedings of the Institution of Civil Engineers – Water Management* 164: 243–256.

Haverson, D., Aldridge, J. and Edwards, K., 2017. Assessment of nutrients and macroalgae growth in Poole Harbour, UK. In *Proceedings of the XXIVth TELEMAC-MASCARET User Conference*, Graz University of Technology, Austria, 17–20 October.

Haygarth, P.M., Hepworth, L. and Jarvis, S.C., 1998. Forms of phosphorus transfer in hydrological pathways from soil under grazed grassland. *European Journal of Soil Science* 49: 65–72. https://doi.org/doi:10.1046/j.1365-2389.1998.00131.x

Henze, M. and Comeau, Y., 2008. Wastewater characterisation. In Henze, M., van Loosrecht, M.C.M., Ekama, G.A. and Brdjanovic, D. (eds), *Biological Wastewater Treatment: Principles Modelling and Design*. IWA Publishing, London.

Holzinger, A. and Karsten, U., 2013. Desiccation stress and tolerance in green algae: consequences for ultrastructure, physiological and molecular mechanisms. *Frontiers in Plant Science* 4: 327. https://doi.org/10.3389/fpls.2013.00327

Holzinger, A., Herburger, K., Kaplan, F. and Lewis, L.A., 2015. Desiccation tolerance in the chlorophyte green alga *Ulva compressa*: does cell wall architecture contribute to ecological success? *Planta* 242: 477–492. https://doi.org/10.1007/s00425-015-2292-6

Imchen, T., 2012. Recruitment potential of a green alga *Ulva flexuosa* Wulfen dark preserved zoospore and its development. *PLoS ONE* 7: e32651. https://doi.org/10.1371/journal.pone.0032651

Irish Water, 2015a. *Water Services Strategic Plan. Ervia.* Irish Water, Dublin.

Irish Water, 2015b. *Annual Environmental Report, 2014. Agglomoration: Ringsend. Licence Register No.: D0034-01*. Irish Water, Dublin.

Irish Water, 2016. *Annual Environmental Report, 2015. Agglomoration: Ringsend. Licence Register No.: D0034-01*. Irish Water, Dublin.

Irvine, K., Mills, P., Bruen, M., Walley, W., Hartnett, M., Black, A., Tynan, S., Duck, R., Bragg, O., Rowan, J., Wilson, J., Johnston, P. and O'Toole, C., 2004. The use of mathematical models to support the implementation of the Water Framework Directive in Ireland. 5th National Hydrology Seminar 2004: The Water Framework Directive – Monitoring & Modelling Issues for River Basin Management, Tullamore, Ireland, 16 November.

Jarvie, H.P., Neal, C. and Withers, P.J.A., 2006. Sewage-effluent phosphorus: a greater risk to river eutrophication than agricultural phosphorus? *Science of the Total Environment* 360: 246–253. https://doi.org/10.1016/j.scitotenv.2005.08.038

Jennings, E., 1996. *Sediment–Water Nitrogen Exchange in the Intertidal Areas of Dublin Bay*. University of Dublin, Dublin.

Joint, I.R., 1981. Growth and survival of estuarine microalgae. In Jones, N.V. and Wolff, W.J. (eds), *Feeding and Survival Srategies of Estuarine Organisms. Marine Science*, Vol. 15. Springer, Boston, MA, pp. 17–28. https://doi.org/10.1007/978-1-4613-3318-0_2

Jordan, P., Melland, A.R., Mellander, P.E., Shortle, G. and Wall, D., 2012. The seasonality of phosphorus transfers from land to water: implications for trophic impacts and policy evaluation. *Science of the Total Environment* 434: 101–109. https://doi.org/10.1016/j.scitotenv.2011.12.070

Kamer, K. and Fong, P., 2000. A fluctuating salinity regime mitigates the negative effects of reduced salinity on the estuarine macroalga, *Enteromorpha intestinalis* (L.) link. *Journal of Experimental Marine Biology and Ecology* 254: 53–69. https://doi.org/10.1016/S0022-0981(00)00262-8

McGarrigle, M., Lucey, J. and O'Cinneide, M., 2010. *Water Quality in Ireland 2007–2009*. Environmental Protection Agency, Johnstown Castle, Ireland.

McGovern, J.V., Nash, S. and Hartnett, M., 2019. Interannual improvement in sea lettuce blooms in an agricultural catchment. *Frontiers in Marine Science*, 18 March. https://doi.org/10.3389/fmars.2019.00064

Malone, T.C., Crocker, L.H., Pike, S.E. and Wendler, B.W., 1988. Influences of river flow on the dynamics of phytoplankton production in a partially stratified estuary. *Marine Ecology Progress Series* 48: 15. https://doi.org/10.3354/meps048235

Mansfield, M.J., 1992. *Dublin Bay Water Quality Management Plan*. Environmental Research Unit, Dublin.

Martins, I. and Marques, J.C., 2002. A model for the growth of opportunistic macroalgae (*Enteromorpha* sp.) in tidal estuaries. *Estuarine, Coastal and Shelf Science* 55: 247–257. https://doi.org/10.1006/ecss.2001.0900

Martins, I., Oliveira, J.M., Flindt, M.R. and Marques, J.C., 1999. The effect of salinity on the growth rate of the macroalgae *Enteromorpha intestinalis* (Chlorophyta) in the Mondego estuary (west Portugal). *Acta Oecologica* 20: 259–265. https://doi.org/10.1016/S1146-609X(99)00140-X

Martins, I., Lopes, R.J., Lillebø, A.I., Neto, J.M., Pardal, M.A., Ferreira, J.G. and Marques, J.C., 2007. Significant variations in the productivity of green macroalgae in a mesotidal estuary: implications to the nutrient loading of the system and the adjacent coastal area. *Marine Pollution Bulletin* 54: 678–690. https://doi.org/10.1016/j.marpolbul.2007.01.023

Martins, I., Marcotegui, A. and Marques, J.C., 2008. Impacts of macroalgal spores on the dynamics of adult macroalgae in a eutrophic estuary: high versus low hydrodynamic seasons and long-term simulations for global warming scenarios. *Marine Pollution Bulletin* 56: 984–998. https://doi.org/10.1016/j.marpolbul.2008.01.025

Melland, A.R., Fenton, O. and Jordan, P., 2018. Effects of agricultural land management changes on surface water quality: a review of meso-scale catchment research. *Environmental Science & Policy* 84: 19–25. https://doi.org/10.1016/j.envsci.2018.02.011

Mellander, P.E., Melland, A.R., Murphy, P.N.C., Wall, D.P., Shortle, G. and Jordan, P., 2014. Coupling of surface water and groundwater nitrate-N dynamics in two permeable agricultural catchments. *Journal of Agricultural Science* 152: 107–124. https://doi.org/10.1017/S0021859614000021

Mellander, P.-E., Jordan, P., Bechmann, M., Fovet, O., Shore, M.M., McDonald, N.T. and Gascuel-Odoux, C., 2018. Integrated climate-chemical indicators of diffuse pollution from land to water. *Scientific Reports* 8: 944. https://doi.org/10.1038/s41598-018-19143-1

Menesguen, A. and Salamon, J., 1987. Eutrophication modeling as a tools for fighting against *Ulva* coastal mass blooms. *Proceedings of the International Conference on Computer Modelling in Ocean Engineering*, Venice, Italy, 19–23 September, pp. 443–450.

Mockler, E.M., Deakin, J., Archbold, M., Gill, L., Daly, D. and Bruen, M., 2017. Sources of nitrogen and phosphorus emissions to Irish rivers and coastal waters: estimates from a nutrient load apportionment framework. *Science of the Total Environment* 601–602: 326–339. https://doi.org/10.1016/j.scitotenv.2017.05.186

Morris, A.W., Mantoura, R.F.C., Bale, A.J. and Howland, R.J.M., 1978. Very low salinity regions of estuaries: important sites for chemical and biological reactions. *Nature* 274: 678. https://doi.org/10.1038/274678a0

Murphy, P.N.C., Mellander, P.E., Melland, A.R., Buckley, C., Shore, M., Shortle, G., Wall, D.P., Treacy, M., Shine, O., Mechan, S. and Jordan, P., 2015. Variable response to phosphorus mitigation measures across the nutrient transfer continuum in a dairy grassland catchment. *Agriculture, Ecosystems & Environment* 207: 192–202. https://doi.org/10.1016/j.agee.2015.04.008

Nash, S., Hartnett, M. and Dabrowski, T., 2011. Modelling phytoplankton dynamics in a complex estuarine system. *Proceedings of the Institution of Civil Engineers – Water Management* 164: 35–54. https://doi.org/10.1680/wama.800087

Nelson, T.A. and Lee, A., 2001. A manipulative experiment demonstrates that blooms of the macroalga *Ulva*ria obscura can reduce eelgrass shoot density. *Aquatic Botany* 71: 149–154. https://doi.org/10.1016/S0304-3770(01)00183-8

Nelson, T.A., Haberlin, K., Nelson, A.V., Ribarich, H., Hotchkiss, R., Alstyne, K.L.V., Buckingham, L., Simunds, D.J. and Fredrickson, K., 2008. Ecological and physiological controls of species composition in green macroalgal blooms. *Ecology* 89: 1287–1298. https://doi.org/10.1890/07-0494.1

Ní Longphuirt, S., Mockler, E.M., O'Boyle, S., Wynne, C. and Stengel, D.B., 2016a. Linking changes in nutrient source load to estuarine responses: an Irish perspective. *Biology and Environment: Proceedings of the Royal Irish Academy* 116B: 295–311. https://doi.org/10.3318/bioe.2016.21

Ní Longphuirt, S., O'Boyle, S., Wilkes, R., Dabrowski, T. and Stengel, D.B., 2016b. Influence of hydrological regime in determining the response of macroalgal blooms to nutrient loading in two Irish estuaries. *Estuaries and Coasts* 39: 478–494. https://doi.org/10.1007/s12237-015-0009-5

O'Boyle, S., Wilkes, R. and Dabrowski, T., 2011. Ireland's report on "distance to target"; a quantitative estimate of the amount of nutrient reduction required to reach non-problem area status with regard to eutrophication. OSPAR Convention, Meeting of the Intersessional Correspondence Group on Eutrophication, Dessau, Germany, November 2011.

O'Boyle, S., Wilkes, R., McDermott, G., Ní Longphuirt, S. and Murray, C., 2015. Factors affecting the accumulation of phytoplankton biomass in Irish estuaries and nearshore coastal waters: a conceptual model. *Estuarine, Coastal and Shelf Science* 155: 75–88. https://doi.org/10.1016/j.ecss.2015.01.007

O'Boyle, S., Quinn, R., Dunne, N., Mockler, E.M. and Ni Longphuirt, S., 2016. What have we learned from over two decades of monitoring riverine nutrient inputs to Ireland's marine environment? *Biology and Environment*: *Proceedings of the Royal Irish Academy* 116B: 313–327. https://doi.org/10.3318/bioe.2016.23

O'Boyle, S., Wilkes, R., McDermott, G. and Ní Longphuirt, S., 2017. Will recent improvements in estuarine water quality in Ireland be compromised by plans for increased agricultural production? A case study of the Blackwater estuary in southern Ireland. *Ocean & Coastal Management* 143: 87–95. https://doi.org/10.1016/j.ocecoaman.2016.12.020

OSPAR Commission, 2013. *Revised JAMP Eutrophication Monitoring Guideline: Nutrients*. OSPAR Commission, London.

Painting, S.J., Devlin, M.J., Malcolm, S.J., Parker, E.R., Mills, D.K., Mills, C., Tett, P., Wither, A., Burt, J., Jones, R. and Winpenny, K., 2007. Assessing the impact of nutrient enrichment in estuaries: susceptibility to eutrophication. *Marine Pollution Bulletin* 55: 74–90. https://doi.org/10.1016/j.marpolbul.2006.08.020

Parages, M., Figueroa, F., Conde-Álvarez, R. and Jiménez, C., 2014. Phosphorylation of MAPK-like proteins in three intertidal macroalgae under stress conditions. *Aquatic Biology* 22: 213–226.

Perrot, T., Rossi, N., Ménesguen, A. and Dumas, F., 2014. Modelling green macroalgal blooms on the coasts of Brittany, France to enhance water quality management. *Journal of Marine Systems* 132: 38–53. https://doi.org/10.1016/j.jmarsys.2013.12.010

Philip Farrelly & Co. 2015. *Food Wise 2025 Environmental Analysis Report*. Final Report – November 2015. Department of Agriculture, Food and the Marine, Dublin.

Plus, M., Auby, I., Maurer, D., Trut, G., Del Amo, Y., Dumas, F. and Thouvenin, B., 2015. Phytoplankton versus macrophyte contribution to primary production and biogeochemical cycles of a coastal mesotidal system. A modelling approach. *Estuarine, Coastal and Shelf Science* 165: 52–60. https://doi.org/10.1016/j.ecss.2015.09.003

Porcella, D.B., Mills, W.B. and Bowie, G.L., 1985. *Rates, Constants and Kinetics Formulations in Surface Water Quality Modelling*, 2nd edn. United States Environmental Protection Agency Office of Research and Development, Washington, DC.

Port, M.A., 2016. Measuring and modelling estuarine macroalgae blooms and water column nutrients. PhD Thesis. The University of Waikato, Hamilton, New Zealand.

Portilla, E., Tett, P., Gillibrand, P.A. and Inall, M., 2009. Description and sensitivity analysis for the LESV model: water quality variables and the balance of organisms in a fjordic region of restricted exchange. *Ecological Modelling* 220: 2187–2205. https://doi.org/10.1016/j.ecolmodel.2009.05.004

Ren, J.S., Barr, N.G., Scheuer, K., Schiel, D.R. and Zeldis, J., 2014. A dynamic growth model of macroalgae: application in an estuary recovering from treated wastewater and earthquake-driven eutrophication. *Estuarine, Coastal and Shelf Science* 148: 59–69. https://doi.org/10.1016/j.ecss.2014.06.014

Roegner, G.C., Seaton, C. and Baptista, A.M., 2011. Climatic and tidal forcing of hydrography and chlorophyll concentrations in the Columbia River Estuary. *Estuaries and Coasts* 34: 281–296. https://doi.org/10.1007/s12237-010-9340-z

Schlichting, H., 1979. *Boundary Layer Theory*. McGraw Hill, New York, NY.

Schuchardt, B., Haesloop, U. and Schirmer, M., 1993. The tidal freshwater reach of the Weser estuary: riverine or estuarine? *Netherland Journal of Aquatic Ecology* 27: 215–226. https://doi.org/10.1007/bf02334785

Schulte, R.P.O., Melland, A.R., Fenton, O., Herlihy, M., Richards, K. and Jordan, P., 2010. Modelling soil phosphorus decline: expectations of Water Framework Directive policies. *Environmental Science & Policy* 13: 472–484. https://doi.org/10.1016/j.envsci.2010.06.002

Shore, M., Murphy, S., Mellander, P.-E., Shortle, G., Melland, A.R., Crockford, L., O'Flaherty, V., Williams, L., Morgan, G. and Jordan, P., 2017. Influence of stormflow and baseflow phosphorus pressures on stream ecology in agricultural catchments. *Science of the Total Environment* 590–591: 469–483. https://doi.org/10.1016/j.scitotenv.2017.02.100

Shortle, G. and Jordan, P., 2017. *Agricultural Catchments Programme Phase 2 Report*. Teagasc ACP, Dublin.

Skerratt, J., Wild-Allen, K., Rizwi, F., Whitehead, J. and Coughanowr, C., 2013. Use of a high resolution 3D fully coupled hydrodynamic, sediment and biogeochemical model to understand estuarine nutrient dynamics under various water quality scenarios. *Ocean & Coastal Management* 83: 52–66. https://doi.org/10.1016/j.ocecoaman.2013.05.005

Solidoro, C., Brando, V.E., Dejak, C., Franco, D., Pastres, R. and Pecenik, G., 1997a. Long term simulations of population dynamics of *Ulva r*. in the lagoon of Venice. *Ecological Modelling* 102: 259–272. https://doi.org/10.1016/S0304-3800(97)00060-4

Solidoro, C., Pecenik, G., Pastres, R., Franco, D. and Dejak, C., 1997b. Modelling macroalgae (*Ulva rigida*) in the Venice lagoon: model structure identification and first parameters estimation. *Ecological Modelling* 94: 191–206. https://doi.org/10.1016/S0304-3800(96)00025-7

Thomsen, M.S. and McGlathery, K.J., 2007. Stress tolerance of the invasive macroalgae *Codium fragile* and *Gracilaria vermiculophylla* in a soft-bottom turbid lagoon. *Biological Invasions* 9: 499–513. https://doi.org/10.1007/s10530-006-9043-3

Thornton, K.W. and Lessem, A.S., 1978. A temperature algorithm for modifying biological rates. *Transactions of the American Fisheries Society* 107: 284–287. https://doi.org/10.1577/1548-8659(1978)107<284:ataf mb>2.0.co;2

Trancoso, A.R., Saraiva, S., Fernandes, L., Pina, P., Leitão, P. and Neves, R., 2005. Modelling macroalgae using a 3D hydrodynamic-ecological model in a shallow, temperate estuary. *Ecological Modelling* 187: 232–246. https://doi.org/10.1016/j.ecolmodel.2005.01.054

Trodd, W. and O'Boyle, S., 2018. W*ater Quality in 2017; An Indicators Report*. Environmental Protection Agency, Johnstown Castle, Ireland.

Valiela, I., McClelland, J., Hauxwell, J., Behr, P.J., Hersh, D. and Foreman, K., 2003. Macroalgal blooms in shallow estuaries: controls and ecophysiological and ecosystem consequences. *Limnology and Oceanography* 42: 1105–1118. https://doi.org/10.4319/lo.1997.42.5_part_2.1105

Van Alstyne, K.L., Nelson, T.A. and Ridgway, R.L., 2015. Environmental chemistry and chemical ecology of "green tide" seaweed blooms. *Integrative and Comparative Biology* 55: 518–532. https://doi.org/10.1093/icb/icv035

Wan, A.H.L., Wilkes, R.J., Heesch, S., Bermejo, R., Johnson, M.P. and Morrison, L., 2017. Assessment and characterisation of Ireland's green tides (*Ulva* species). *PLoS ONE* 12: e0169049. https://doi.org/10.1371/journal.pone.0169049

Wells, E., Best, M., Scanlan, C. and Foden, J., 2009. *Water Framework Directive Development of Classification Tools for Ecological Assessment: Opportunistic Macroalgae Blooming*. Water Framework Directive – United Kingdom Technical Advisory Group (WFD-UKTAG). Available online: https://wfduk.org/sites/default/files/Media/Characterisation%20of%20the%20water%20environment/Biological%20Method%20Statements/Opportunistic%20Macroalgae%20Blooming%20Technical%20Report.pdf (accessed 9 November 2020).

Whitehouse, L.N.A. and Lapointe, B.E., 2015. Comparative ecophysiology of bloom-forming macroalgae in the Indian River Lagoon, Florida: *Ulva lactuca*, *Hypnea musciformis*, and *Gracilaria tikvahiae*. *Journal of Experimental Marine Biology and Ecology* 471: 208–216. https://doi.org/10.1016/j.jembe.2015.06.012

Wickham, S.B., Darimont, C.T., Reynolds, J.D. and Starzomski, B.M., 2019. Species-specific wet-dry mass calibrations for dominant Northeastern Pacific Ocean macroalgae and seagrass. *Aquatic Botany* 152: 27–31. https://doi.org/10.1016/j.aquabot.2018.09.006

Young, C.S. and Gobler, C.J., 2017. The organizing effects of elevated CO_2 on competition among estuarine primary producers. *Scientific Reports* 7: 7667. https://doi.org/10.1038/s41598-017-08178-5

Zhang, X., Xu, D., Mao, Y., Li, Y., Xue, S., Zou, J., Lian, W., Liang, C., Zhuang, Z., Wang, Q. and Ye, N., 2010. Settlement of vegetative fragments of *Ulva prolifera* confirmed as an important seed source for succession of a large-scale green tide bloom. *Limnology and Oceanography* 56: 233–242. https://doi.org/10.4319/lo.2011.56.1.0233

Abbreviations

AA	Affected area
ACP	Agricultural Catchments Programme
AER	Annual environmental report
AGS	Aerobic granular sludge
AIH	Available intertidal habitat
BOD	Biochemical oxygen demand
CPM	Combined phytoplankton and macroalgae
DAIN	Dissolved available inorganic nitrogen
DAIP	Dissolved available inorganic phosphorus
DCPM	Dynamic Combined Phytoplankton and Macroalgae
DIVAST	Depth Integrated Velocity and Solute Transport
DO	Dissolved oxygen
EFDC	Environmental Fluid Dynamics Code
EPA	Environmental Protection Agency
EQR	Ecological quality ratio
ESB	Electricity Supply Board
LAT	Lowest astronomical tide
MSN_WQ	Multi-scale Nesting and Water Quality
NAOi	North Atlantic Oscillation
NDN-OHO	Nitrifying–denitrifying granules with anoxic feeding
NDN-PAO	Nitrifying–denitrifying, DAIP-accumulating granules with anaerobic feeding
NIT	Nitrifying granules with aerobic feeding
OBMT	Opportunistic Macroalgae Bloom Tool
OSPAR	(from Oslo and Paris) Convention for the Marine Environment of the North-East Atlantic
PAR	Photosynthetically active radiation
PE	Population equivalent
psu	Practical salinity unit
RID	Riverine Inputs and Direct Discharges
ROMS	Regional Ocean Modelling System
R_{SA}	Summer to annual ratio
SLAM	Source Load Apportionment Model
SWAT	Soil & Water Assessment Tool
TPR	Tidal prism ratio
TSAS	Trophic Status Assessment Scheme
UWWTR	Urban Waste Water Treatment Regulations
WFD	Water Framework Directive
WWTP	Wastewater treatment plant

Glossary

Aerobic	In reference to biological processes, requiring oxygen
Anaerobic	In reference to biological processes, occurring in the absence of oxygen
Annual Environment Report	A document describing the environmental performance of an EPA-licensed facility, including any incidents during the reporting period and scheduled improvements. All EPA-licensed facilities are required to publish such a report each year
Anoxic	In reference to an environment, lacking oxygen
Assimilation	The process of absorption into tissue and retention thereafter
Benchmark	To compare with a consistent standard or the considered state of the art
Bloom	An abundant growth or production; in the context of eutrophication, a bloom is a luxuriant growth of algae that occurs in response to optimum growth conditions
Chlorophyll	A green pigment found in algae and plants
Diffuse pressure	In the context of water quality, pollution that occurs over a broad area via the available pathways
Ebb	In reference to tidal circulation, the outgoing tide
Effluent	Discharged waste liquids; may refer to treated or untreated wastewater
Estuary	The tidal semi-enclosed coastal waters that receive riverine inflow from the catchment(s) upstream
Eutrophication	Excess enrichment of waters with nutrients that are necessary for growth of algae. Eutrophication may coincide with (1) the excess growth of algae, thus reflecting the presence of excess nutrients; (2) fluctuating dissolved oxygen, due to alternating primary production and cellular respiration; and (3) reduced water transparency, due to the presence of algae in the water column
Flood	In reference to tidal circulation, the incoming tide
Hydrodynamics	The study of the movement of fluids and the forces that cause or are caused by movement of fluids
Influent	Raw waste liquids, prior to treatment
Limiting nutrient	In the context of eutrophication, the nutrient that is scarcest and thus throttles potential bloom conditions
Macroalgae	A large form of algae that grows tethered to the benthic zone (the bottom of the water column). Opportunistic bloom-forming macroalgae species include *Gracilaria* spp. and *Ulva* spp
Mesohaline	Waters with a salinity between 5 and 18 psu (practical salinity units)
Oligohaline	Waters with salinity between 0.5 and 5 psu
OSPAR Commission	A commission that addresses the objectives of the Oslo Convention of 1972 (to reduce dumping of waste at sea) and the Paris Convention of 1974 (to reduce land-based pollution of the marine environment) The OSPAR Commission was established under the OSPAR Convention as an agreement between 15 governments and the European Union

Phytoplankton	Microscopic algae suspended in the water column
Point pressure	A pressure to water quality that is released from a clearly identifiable location such as a wastewater effluent outfall from a wastewater treatment facility
Polyhaline	Waters with a salinity between 18 and 30 psu
Residence time	The time required for the entire volume of a water body to be replaced by freshwater and tidal inputs
Secchi disc	A plain white, circular disc, 30 cm in diameter, used to determine the transparency, or light attenuation, in the water column. The disc is extended beneath the water column until it is no longer visible, that depth being defined as the Secchi depth
Transitional	Waters that lie between freshwater and coastal saline waters, and thus another term for estuarine waters (see Estuary)
Yield	In the context of eutrophication, the tissue weight of phytoplankton or macroalgae gained per unit of nutrients (usually nitrogen or phosphorus)

Appendix 1 MSN_WQ

A1.1 MSN_WQ

The MSN_WQ model is a 2-D finite difference hydrological model developed at NUI Galway from the DIVAST (Depth Integrated Velocity and Solute Transport) model, which was originally derived by Falconer *et al.* (2001). The original code and the scope of the model have been further developed by the Marine Modelling Group in NUI Galway to the extent that it is now considered a separate entity. The MSN_WQ model allows multiscale modelling of coastal water bodies by using nested grids. The MSN_WQ model solves the depth-integrated continuity and Navier–Stokes equations (equations A1.3–A1.5), yielding current velocities and water surface elevations, while the advection diffusion equation (equation A1.6) forms the basis for solute transport and water quality modules. The MSN_WQ model has been applied extensively in industry and has been continually improved, all of which is fully documented in many journal publications and reports. The MSN_WQ model of Cork Harbour has been thoroughly calibrated and validated against laboratory and field data (Hartnett *et al*., 2011a; Nash *et al*., 2011). The detailed model of Cork Harbour developed by Nash *et al*. (2011) incorporated monthly average input data for a number of parameters, comprising mean river inflows for eight rivers, including the rivers Lee, Owenacurra, Owenbuidhe and Glashaboy; nutrient influxes at the seaward boundaries; temperature, light intensity and photoperiod for chlorophyll calculations; and domestic and industrial effluent discharges at 19 outfalls in the model domain.

Depth integration reduces the governing equations from three dimensions to two, as shown in Figure A1.1, which reduces the computational complexity of the solution scheme. Depth integration is allowable in shallow, vertically well-mixed waters because vertical velocities are negligible compared with the horizontal orthogonal components and vertical accelerations are negligible compared with gravity. In a stratified water body, the vertical velocity profile is parabolic (Schlichting, 1979), whereas depth integration in a vertically well-mixed water body assumes a constant velocity with depth.

The orthogonal horizontal velocity components, U and V, which are depth integrated over depth H in the vertical, Z, direction are given by equations A1.1 and A1.2, where h is the water depth below mean water level and ζ is the water elevation above or below mean water level, as depicted in Figure A1.2.

$$U = \frac{1}{H}\sum_{-h}^{\zeta} u \, dZ \tag{A1.1}$$

$$V = \frac{1}{H}\sum_{-h}^{\zeta} v \, dZ \tag{A1.2}$$

The continuity equation A1.3 considers that the mass entering a finite space must be equal to the mass leaving that space. In the X or Y direction momentum equations (equations A1.4 and A1.5, respectively), the momentum terms on the left-hand side are local and advective accelerations, while the terms on the right-hand side

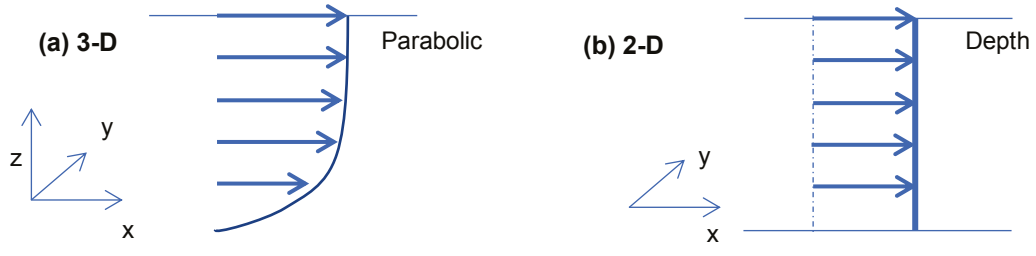

Figure A1.1. Velocity profile with depth in (a) a 3-D stratified model and (b) a shallow, depth-integrated model.

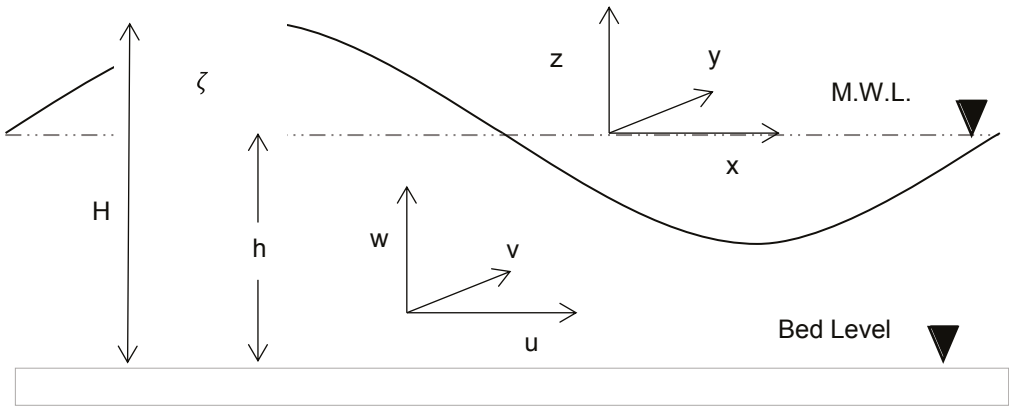

Figure A1.2. A shallow, well-mixed water body. MWL, mean water level. *ζ* is the water elevation above or below MWL and *h* is the water depth below MWL.

represent the momentum of the causative forces, which consist of the Coriolis effect, pressure gradients, wind shear stress, bed resistance and turbulence.

The depth-integrated hydrodynamic equations are given by Falconer *et al*. (2001):

Continuity equation

$$\frac{\partial \zeta}{\partial t} + \frac{\partial q_x}{\partial x} + \frac{\partial q_y}{\partial y} = 0 \tag{A1.3}$$

X direction momentum equation

$$\frac{\partial q_x}{\partial t} + \beta\left[\frac{\partial U q_x}{\partial x} + \frac{\partial U q_y}{\partial y}\right] = f q_y - gH\frac{\partial \zeta}{\partial x} + \frac{\rho_a C W_x \left(W_x^2 + W_y^2\right)^{\frac{1}{2}}}{\rho} - \frac{gU\left(U^2+V^2\right)^{\frac{1}{2}}}{C^2} + 2\frac{\partial}{\partial x}\left[\varepsilon H\frac{\partial U}{\partial x}\right] + \frac{\partial}{\partial y}\left[\varepsilon H\left[\frac{\partial U}{\partial y} + \frac{\partial V}{\partial x}\right]\right] \tag{A1.4}$$

Y direction momentum equation

$$\frac{\partial q_y}{\partial t} + \beta\left[\frac{\partial V q_x}{\partial x} + \frac{\partial V q_y}{\partial y}\right] = f q_x - gH\frac{\partial \eta}{\partial y} + \frac{\rho_a C W_y \left(W_x^2 + W_y^2\right)^{\frac{1}{2}}}{\rho} - \frac{gV\left(U^2+V^2\right)^{\frac{1}{2}}}{C^2} + 2\frac{\partial}{\partial y}\left[\varepsilon H\frac{\partial V}{\partial y}\right] + \frac{\partial}{\partial y}\left[\varepsilon H\left[\frac{\partial V}{\partial x} + \frac{\partial U}{\partial y}\right]\right] \tag{A1.5}$$

Advection diffusion equation

$$\frac{\partial H_\phi}{\partial t} + \frac{\partial H U_\phi}{x} + \frac{\partial H V_\phi}{y} = \frac{\partial}{\partial x}\left[D_{xx} H\frac{\partial \phi}{x} + D_{xy} H\frac{\partial \phi}{y}\right] + \left[D_{yx} H\frac{\partial \phi}{x} + D_{yy} H\frac{\partial \phi}{y}\right] + \Phi_\phi \tag{A1.6}$$

$$D_{xx} = \frac{\left(k_p U^2 + k_l V^2\right) H\sqrt{g}}{c\sqrt{U^2+V^2}} + D_w \tag{A1.7}$$

$$D_{yy} = \frac{\left(k_p V^2 + k_l U^2\right) H\sqrt{g}}{c\sqrt{U^2+V^2}} + D_w \tag{A1.8}$$

$$D_{yy} = \frac{\left(k_p V^2 + k_l U^2\right) H\sqrt{g}}{c\sqrt{U^2+V^2}} + D_w \tag{A1.9}$$

where:

u and v are the X and Y direction velocities;

U and V are the X and Y direction depth-integrated velocities;

ζ is the water elevation above/below mean water level;

q_x and q_y are depth-integrated volumetric fluxes in X and Y directions ($q_x = UH$; $q_y = VH$);

β is the momentum correction factor for non-uniform vertical velocity profile;

$f = 2\sin\theta$ is the Coriolis parameter;

ω is the angular velocity of the earth's rotation;

θ is the geographic latitude;

C is the Chezy bed roughness coefficient;

ρ_a is the density of air ($1.292\,\mathrm{kg\,m^{-3}}$);

ρ is the fluid density;

ε is the depth-mean eddy viscosity;

g is the gravitational acceleration;

W_X, W_Y and W_Z are wind velocity in the X, Y and Z directions;

H is the total water depth;

ϕ is the depth-averaged solute concentration;

D_{XX}, D_{XY}, D_{YX} and D_{YY} are dispersion coefficients in the X and Y directions;

k_p is the longitudinal depth-averaged dispersion constant;

k_i is the depth-averaged turbulent diffusion constant;

D_w is the wind-induced dispersion coefficient;

c is the Chezy coefficient; and

Φ_ϕ is all other sources and sinks: outfalls, rivers, chemical and biological transformations.

A1.2 Water Quality Modelling

The water quality equations used in the MSN_WQ model originate from the QUAL2E water quality model (Brown and Barnwell, 1985). Up to 10 water quality parameters may be simulated in the MSN_WQ model: biochemical oxygen demand (BOD), dissolved oxygen (DO), organic nitrogen, NH_4, NO_3, organic phosphorus, orthophosphate, chlorophyll, temperature and salinity. Figure A1.3 presents the interactions between each of the water quality parameters in the most recent version of the MSN_WQ model.

Chlorophyll concentration is used as a proxy measure of overall phytoplankton growth with no explicit consideration of individual species of phytoplankton. The phosphorus and nitrogen nutrient cycle, phytoplankton cycle and DO cycle are fully interactive, as can be seen in equations A1.10 and A1.11, which share a number of terms. Decay of phytoplankton generates phosphorus and nitrogen by-products.

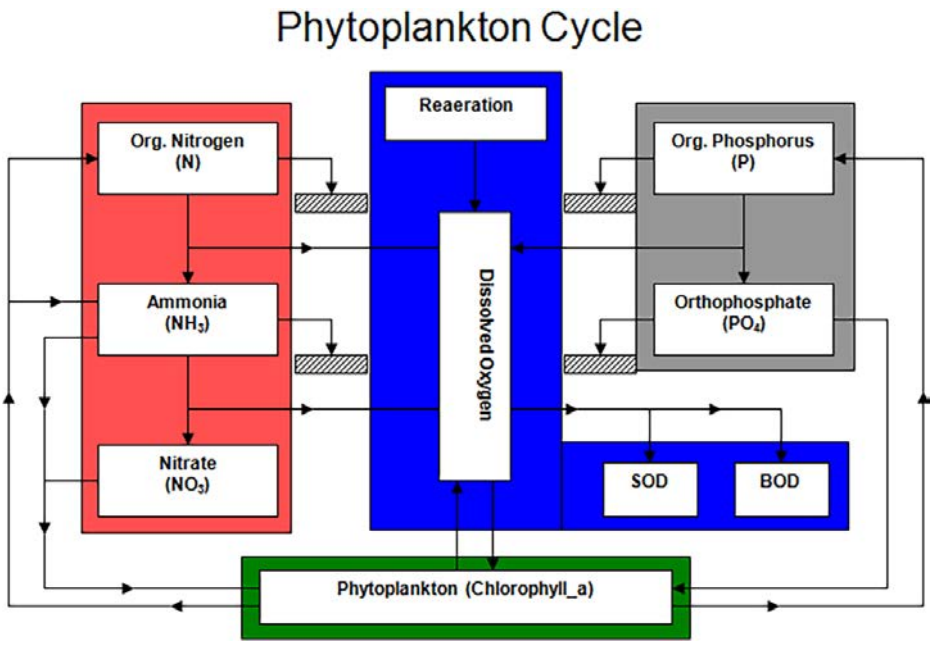

Figure A1.3. Schematic of MSN_WQ model components and processes. SOD, sediment oxygen demand.

A1.2 Phytoplankton Kinetics

The chlorophyll growth rate is defined in equation A1.10, and takes into account growth, decay and the settling velocity of phytoplankton. The growth rate is a lumped term that is a product of individual adjustment or limitation factors which describe the constraint of chlorophyll growth by available nutrients, temperature and light. Equation A1.12 describes the light-limiting factor G_L, which accounts for photoperiod f, the light attenuation coefficient K_A and the relative intensity of surface lighting. An example of a site-specific light attenuation coefficient previously derived by Hartnett and Nash (2004) is presented in equation A1.13, which was derived using Secchi disc data. It can be seen in equations A1.12 and A1.13 that, intuitively, the growth of chlorophyll at depth is hampered by the attenuation of light by existing chlorophyll in the water column. Thus, the light-limiting growth factor, G_L, is inversely related to the concentration of chlorophyll, C_p.

$$\frac{\partial C_P}{\partial t} = \left(G_{PI} - D_{PI} - V_{S4}\right)C_P \tag{A1.10}$$

$$G_{PI} = \left(G_{PI}\right)_{max} G_T G_N G_L \tag{A1.11}$$

$$G_L = \left[\log\left(\frac{I_H + I_O}{I_H + I_O^{-K_A H}}\right)\right]\frac{f}{K_A H} \tag{A1.12}$$

$$K_A = 0.79012 + 0.004296(C_P) \tag{A1.13}$$

where:

C_{PI} is the phytoplankton population;

G_{PI} is the growth rate constant;

D_{PI} is the death plus respiration rate constant;

V_{S4} is the settling velocity;

D is the total water depth;

$(G_{PI})_{max}$ is the maximum growth rate under optimum lighting and nutrient conditions;

G_T is the temperature adjustment factor;

G_N is the nutrient limitation factor;

G_L is the growth-limiting factor;

I_H is the light level that results in a growth rate of half of $(G_{PI})_{max}$;

I_O is the surface light intensity;

f is the fraction of day exposed to sunlight; and

K_A is the light attenuation coefficient.

A1.3 Phosphorus Cycle

The simplified phosphorus cycle model in MSN_WQ considers phytoplankton phosphorus, organic phosphorus and orthophosphate phosphorus. Equation A1.14 presents the rate of phytoplankton phosphorus accumulation, which is directly proportional to the phytoplankton-specific growth and decay rates and the phytoplankton settling velocity. Phytoplankton phosphorus is recycled to the organic phosphorus pool.

Phytoplankton phosphorus

$$\frac{\partial}{\partial t}\left(C_P A_{PC}\right) = \left(G_{PI} - D_{PI} - \frac{V_{S4}}{D}\right) C_P A_{PC} \tag{A1.14}$$

Organic phosphorus

$$\frac{\partial}{\partial t}\left(C_{OP}\right) = D_{PI} C_P A_{PC} - k_{83}\theta_{83}^{T-20} X_{PRC} C_{OP} - \frac{V_{S3}\left(1-f_{D8}\right)}{D} C_{OP} \tag{A1.15}$$

Orthophosphate phosphorus

$$\frac{\partial}{\partial t}\left(C_{IP}\right) = k_{83}\theta_{83}^{T-20} X_{PRC} C_{OP} - G_{PI} C_P A_{PC} - \frac{V_{S3}\left(1-f_{D8}\right)}{D} C_{IP} \tag{A1.16}$$

$$X_{PRC} = \frac{C_P}{K_{MPC} + C_P} \tag{A1.17}$$

where:

G_{PI} is the phytoplankton growth rate;

D_{PI} is the phytoplankton loss rate;

A_{PC} is the phosphorus to chlorophyll ratio;

k_{83} is the dissolved organic phosphorus mineralisation rate;

θ_{83} is the temperature coefficient;

X_{PRC} is the Michaelis–Menten expression for phosphorus uptake dynamics;

K_{MPC} is the Michaelis–Menten dynamic half-saturation constant for phytoplankton limitation of phosphorus recycling;

f_{D3} is the fraction of dissolved inorganic phosphorus in the water column;

f_{D8} is the fraction of dissolved organic phosphorus;

V_{S3} is the organic matter settling velocity; and

V_{S4} is the inorganic sediment settling velocity.

A1.4 Nitrogen Cycle

Four forms of nitrogen are modelled in the MSN_WQ model. The simplified nitrogen cycle describing the interaction between the four forms is summarised by equations A1.18–A1.21. Decay of phytoplankton returns a fraction of phytoplankton nitrogen to the organic nitrogen pool. Ammonification of the organic nitrogen converts organic nitrogen to NH_4. NH_4 subsequently undergoes transformation to NO_3 via nitrification in the presence of oxygen. Denitrification of NO_3 to free nitrogen gas (N_2) is an additional sink for nitrogen.

Phytoplankton nitrogen

$$\frac{\partial}{\partial t}\left(C_P A_{NC}\right) = \left(G_{PI} - D_{PI} - \frac{V_{S4}}{D}\right) C_P A_{NC} \tag{A1.18}$$

Organic nitrogen

$$\frac{\partial}{\partial t}\left(C_{ON}\right) = D_{PI} C_P A_{NC} f_{ON} - k_{71}\theta_{71}^{T-20} X_{PRC} C_{ON} - \frac{V_{S3}\left(1-f_{D7}\right)}{D} C_{ON} \tag{A1.19}$$

NH_4

$$\frac{\partial}{\partial t}\left(C_{NH4}\right) = k_{71}\theta_{71}^{T-20} X_{PRC} C_{ON} - G_{PI} P_{NH4} C_P A_{NC} - k_{12}\theta_{12}^{T-20}\left(\frac{C_{DO}}{k_{NIT} + C_{DO}}\right) C_{NH4} + D_{PI} C_P A_{NC}\left(1-f_{ON}\right) \tag{A1.20}$$

NO_3

$$\frac{\partial}{\partial t}\left(C_{NO3}\right) = k_{12}\theta_{12}^{T-20}\left(\frac{C_{DO}}{k_{NIT} + C_{DO}}\right) C_{NH4} - G_{PI}\left(1-P_{NH4}\right) C_P A_{NC} - k_{12}\theta_{12}^{T-20}\left(\frac{K_{NO3}}{k_{NIT} + C_{DO}}\right) C_{NH4} \tag{A1.21}$$

where:

A_{NC} is the nitrogen to chlorophyll ratio;

C_{DO} is the dissolved oxygen concentration;

k_{12} is the nitrification rate; and

C_{NH4} is the NH_4 concentration.

A1.5 Dissolved Oxygen Modelling

DO modelling must take account of nitrification, the presence of a carbonaceous BOD, the consumption and production of DO by phytoplankton and the *in situ* oxygen concentration. Equation A1.22 accounts for these processes and is used in the MSN_WQ model for DO modelling.

$$\frac{\partial}{\partial t}\left(C_{DO}\right) = k_r\theta_a^{T-20}\left(C_S - C_{DO}\right) - k_d\theta_d^{T-20}\left(\frac{C_{DO}}{k_{BOD} + C_{DO}}\right) C_{BOD} - \frac{64}{12} k_{12}\theta_{12}^{T-20}\left(\frac{C_{DO}}{k_{NIT} + C_{DO}}\right) C_{NH4}$$
$$- \frac{SOD}{D} + G_{PI} C_P\left(A_{OC} + \frac{48}{14} A_{NC}\left(1-P_{NH4}\right)\right) - A_{OC} k_{ir}\theta_{ir}^{T-20} C_P \tag{A1.22}$$

where:

C_s is the dissolved oxygen saturation concentration;

C_{BOD} is the BOD concentration;

k_r is the reaeration rate;

k_d is the deoxygenation rate;

k_{BOD} is the half-saturation constant for BOD;

k_{NIT} is the half-saturation constant for nitrogen;

SOD is the sediment oxygen demand;

D is the depth;

G_{PI} is the phytoplankton growth rate;

A_{oc} is the oxygen to chlorophyll ratio;

P_{NH4} is the NH_4 preference factor; and

k_{ir} is the rate of dissolved oxygen uptake through phytoplankton respiration and excretion.

A1.6 Modelling of Macroalgae in Transitional and Coastal Waters

Although the pre-existing MSN_WQ model described the nitrogen and phosphorus cycles, BOD, DO and chlorophyll, the life cycle of macroalgae was not included.

This section summarises the state of the art with respect to macroalgae modelling and identifies the expressions that were incorporated into the MSN_WQ model.

The study by Solidoro *et al.* (1997b) was the most comprehensive initial effort to model the growth of *Ulva rigida*. A two-step kinetic scheme was used to describe the non-linear relationship between nitrogen uptake and subsequent growth. Internal nitrogen quota or intratissual nitrogen concentration became a state variable in that case owing to the sensitivity of the growth to the presence or absence of nitrogen. Equation A1.23 describes net growth of macroalgae as a function of gross growth, μ, dependent upon incident light, I, temperature T, internal nitrogen concentration, Q, external phosphorus concentration and mortality, f_{death}:

$$\frac{dB}{dt} = \left(\mu - f_{death}\right)B \tag{A1.23}$$

$$\mu\left(I,T,Q,\left[P\right]\right) = \mu_{max}\left(g_1\left(Q\right)g_2\left(\left[P\right]\right)g_3\left(I\right)g_4\left(T\right)\right) \tag{A1.24}$$

Modification of growth to account for internal tissue nitrogen concentration is described by equation A1.25: nitrogen is assimilated prior to growth and growth occurs only once the minimum cell quotient, Q_{min}, is exceeded. The term k_c is the half-saturation constant of internal tissue concentration. In the case of phosphorus, uptake and growth of external phosphorus were assumed to be equal, and thus modelled using a Monod kinetic, as presented in equation A1.26:

$$g_1\left(Q\right) = \frac{Q - Q_{min}}{Q - Q_{min} + k} = \frac{Q - Q_{min}}{Q - k_c} \tag{A1.25}$$

$$g_2\left(\left[P\right]\right) = \frac{\left[P\right]}{k_P + \left[P\right]} \tag{A1.26}$$

The influence of temperature on growth was described by the S-type formulation of Menesguen and Salamon (1987), with growth inhibited at any temperature in excess of ϑ_p, as presented in equation A1.27:

$$g_4(T) = \left(1 + \exp\left[-\zeta_p\left(T - \theta_p\right)\right]\right)^{-1} \tag{A1.27}$$

Solidoro *et al.* (1997b) used a descriptor for *Ulva* mortality that consisted of two parts, the first describing the *Ulva* death rate as a consequence of proliferation and the second describing death due to stress caused by oxygen depletion:

$$f_{\text{death}}\left(DO\right) = k_d B^{\beta} + k_t \frac{\max\left[f_{\text{resp}} B - DO, 0\right]}{f_{\text{resp}} B} \tag{A1.28}$$

Primary production was modelled in an analogous manner to growth of *Ulva*, as presented in equations A1.29 and A1.30. Respiration as a function of temperature is described by equation A1.31, in the same manner as growth inhibition due to extreme temperatures is described in equation A1.27:

$$\frac{dDO}{dt} = \left(\varphi\left(I,T,Q,\left[P\right]\right) - f_{\text{resp}}\left(T\right)\right)B \tag{A1.29}$$

$$\varphi\left(I,T,Q,\left[P\right]\right) = \varphi_{\max}\left(g_1\left(Q\right)g_2\left(\left[P\right]\right)g_3\left(I\right)g_4\left(T\right)\right) \tag{A1.30}$$

$$f_{\text{resp}}\left(T\right) = k_{\text{resp}}\left(1 + \exp\left[-\zeta_{\text{resp}}\left(T - \theta_{\text{resp}}\right)\right]\right)^{-1} \tag{A1.31}$$

The rate of change of *Ulva* tissue nitrogen was described as a function of the maximum uptake rates of NH_4 and NO_3, existing tissue nitrogen values and the *Ulva* growth rate, as presented in equations A1.32–A1.35:

$$\frac{dQ}{dt} V_{\text{NH}}\left(\left[\text{NH}_4\right],Q\right) + V_{\text{NO}}\left(\left[\text{NO}_x\right],Q\right) - \left[\mu\left(I,T,Q,\left[P\right]\right)\right]Q \tag{A1.32}$$

$$V_{\text{NX}}([\text{NX}], Q) = V_{\text{mNX}} f_1(\text{NX}) f_2(Q) \tag{A1.33}$$

$$f_1\left(\text{NX}\right) = \frac{\left[\text{NX}\right]}{k_{\text{NX}} + \left[\text{NX}\right]} \tag{A1.34}$$

$$f_2\left(Q\right) = \frac{Q_{\max} - Q}{Q_{\max} - Q_{\min}} \tag{A1.35}$$

where V_{NH} and V_{NO} are the NH_4 and NO_3 uptake rate, respectively, V_{mNX} is the maximum uptake rate for nitrogen species NX, Q is the internal tissue concentration and k_{NX} is the half-saturation coefficient for nitrogen species NX.

Coffaro and Sfriso (1997) described the temperature dependence of macroalgae growth by a detailed curve (equation A1.36), parametrised by K_a, K_b, γ_1 and γ_2 in equations A1.37–A1.40, after Thornton and Lessem (1978). Temperature acclimatisation was allowed for by modifying the optimum temperature, T_{opt}, based on T_{avg}, the average temperature in the previous 2 weeks. Light attenuation was described by a depth-integrated saturation curve (equation A1.43):

$$f\left(T\right) = K_a K_b g_x \tag{A1.36}$$

$$K_a = \frac{k_1 \exp\left(\gamma_1 \left(T - T_{min}\right)\right)}{1 + k_1 \left(\exp\left(\gamma_1 \left(T - T_{min}\right)\right) - 1\right)} \tag{A1.37}$$

$$K_b = \frac{k_4 \exp\left(\gamma_2 \left(T_{max} - T\right)\right)}{1 + k_4 \left(\exp\left(\gamma_2 \left(T_{max} - T\right)\right) - 1\right)} \tag{A1.38}$$

$$\gamma_1 = \frac{1}{T_{opt} - T_{min}} \ln\left(\frac{0.98\left(1 - k_1\right)}{0.02 k_1}\right) \tag{A1.39}$$

$$\gamma_2 = \frac{1}{T_{max} - T_{opt}} \ln\left(\frac{0.98\left(1 - k_4\right)}{0.02 k_4}\right) \tag{A1.40}$$

$$T_{opt} = T_{opt} + Ac\left(1 - \exp\left(-k_T \left(T_{avg} - T_{opt}\right)\right)\right) \tag{A1.41}$$

$$g_x = 1 - T_{rid} \frac{T_{opt} - Opt_{min}}{Opt_{max} - Opt_{min}} \tag{A1.42}$$

$$f\left(L\right) = \frac{1}{K_{ext} z} \ln\left(\frac{k_L + L\left(0\right)}{k_L + L\left(0\right) \exp\left(-K_{ext} z\right)}\right) \tag{A1.43}$$

where Ac is the maximum magnitude of acclimatisation, k_T is the acclimatisation coefficient, Opt_{min} and Opt_{max} are the minimum and maximum optimum temperatures, k_L is the half-saturation coefficient of light intensity, z is the depth of the water column, K_{ext} is the light extinction coefficient and $L(0)$ is the light intensity at the water surface.

Martins and Marques (2002) modelled the net *Enteromorpha* production in the Mondego Estuary in Portugal. Growth was modelled as a function of light, temperature and internal nutrient concentrations, as in other modelling studies. A novel aspect of the work of Martins and Marques (2002) was the consideration of an optimum salinity range within which *Enteromorpha* thrives. For salinity greater than 5 psu, equation A1.44 was used, while salinity under 5 psu was modelled using equation A1.45:

$$f\left(S\right) = 1 - \left(\frac{S - S_{opt}}{S_{opt} - S_{opt}}\right)^m \tag{A1.44}$$

$$f\left(S\right) = \frac{S - S_{opt}}{S_{opt} - S_{opt}} \tag{A1.45}$$

where S_{opt} is the salinity at which maximum growth occurs and S_x is S_{min} when salinity is less than S_{opt} and S_{max} when greater than S_{opt}; m is 2.5 for $S < S_{opt}$ and 2 for $S > S_{opt}$.

De Guimaraens *et al.* (2005) modelled macroalgae in a similar manner to others with respect to internal nutrient quota, light availability and temperature, but additionally incorporated algae carrying capacity as a limiting parameter on growth; the expression contained in equation A1.46 describes the restriction of growth as biomass concentration, B, approaches the carrying capacity, K:

$$f\left(K\right) = 1 - \frac{B}{K} \tag{A1.46}$$

A factor not considered elsewhere was that ammonium uptake is proportional to the ratio of NO_3 to NH_4 in the water column, as presented in equation A1.47. The NH_4 proportion was then incorporated in the equations for NH_4 and NO_3 uptake (equations A1.49 and A1.50). Orthophosphate uptake was modelled in an analogous manner, as presented in equations A1.51 and A1.52:

$$NH_{pro} = \frac{NH}{NO + NH} \tag{A1.47}$$

$$N_{rep} = \frac{Q_{Nmax} - N}{Q_{Nmax} - Q_{Nmin}} \tag{A1.48}$$

$$NH_{upt} = \frac{V_{mNH} N_{rep} NH_{pro} NH}{NH + K_{mNH}} \tag{A1.49}$$

$$NO_{upt} = \frac{V_{mNO} N_{rep} \left(1 - NH_{pro}\right) NO}{NO + K_{mNO}} \tag{A1.50}$$

$$PO_{upt} = \frac{V_{mPO} P_{rep} PO}{NH + K_{mNH}} \tag{A1.51}$$

$$P_{rep} = \frac{Q_{Pmax} - P}{Q_{Pmax} - Q_{Pmin}} \tag{A1.52}$$

where NH_{pro} is the ammonium proportion, NH and NO are the water column concentrations of NH_4 and NO_3 respectively, V_{mX} and K_{mX} are the maximum uptake rate and half-saturation constant for of nutrient species NX and Q_{Xmax} and Q_{Xmin} are the maximum and minimum internal nutrient concentrations for nutrient X.

Aldridge and Trimmer (2009) applied a 2-D depth-integrated finite element hydrodynamic, water quality and macroalgae model to the Medway Estuary. A suitability index was derived to (a) reflect the proportion of the time that photosynthesis was possible and (b) limit growth when the maximum bed stress exceeded the critical bed shear stress, as presented in equations A1.53 and A1.54:

$$G_{\gamma} = \gamma P_{>D^*} \left(1 - P_{>0}\right) \tag{A1.53}$$

$$\gamma = \frac{1}{1 + \exp\left[\frac{\tau_{max} - \tau_c}{\delta}\right]} \tag{A1.54}$$

where $P_{>D^*}$ is the proportion of time that the depth is greater than the depth of the photic zone D^*, $P_{>0}$ is the proportion of the time that the cell is wet, γ is the bed stress dependence index, τ_{max} is the maximum bed stress at a location, τ_c is the critical shear stress and δ controls the transition between no effect and growth inhibition.

A1.7 Incorporating Macroalgae Cycling into the MSN_WQ model

A comprehensive review of macroalgae modelling suggested that the following factors should be taken into account when modifying the MSN_WQ model to describe macroalgae growth:

- growth as a function of:
  - internal nitrogen and phosphorus stores;
  - temperature;
  - incident light;
  - salinity;
  - carrying capacity and bed stress;

- death as a function of:
  - temperature;
  - stress due to depletion of DO from respiration of macroalgae blooms.

The following modifications were made to the MSN_WQ model:

- Macroalgae growth was included in an analogous manner to phytoplankton and a Droop kinetic was incorporated to describe internal tissue nutrient levels, to simulate the non-linear uptake of nutrients and subsequent growth.
- A salinity function was introduced.
- The loss function was adapted to account for death resulting from oxygen depletion and desiccation during drying.
- The effect of different temperature dependence curves on growth and decay was explored.
- A bed stress dependence index was added.
- A carrying capacity (upper limit of macroalgae dry weight beyond which growth cannot occur) was added.

A1.8 Existing Biological Growth Functions in the MSN_WQ model

Phytoplankton growth

$$\frac{\partial C_P}{\partial t} = \left(G_{PI} - D_{PI} - \frac{V_{S4}}{D} \right) C_P \tag{A1.55}$$

Growth

$$G_{PI} = \left(G_{PI} \right)_{max} G_T G_N G_L \tag{A1.56}$$

$$G_L = \left[\log \frac{I_H + I_O}{I_H + I_O^{-K_A H}} \right] \frac{f}{K_A H} \tag{A1.57}$$

$$K_A = 0.79012 + 0.004296(C_P) \tag{A1.58}$$

$$G_N = \frac{\left(C_{NH3} + C_{NO3} \right)}{K_N + \left(C_{NH3} + C_{NO3} \right)} \tag{A1.59}$$

$$G_P = \frac{C_{IP}}{K_P C_{IP}} \tag{A1.60}$$

$$G_N = G_P + G_N \tag{A1.61}$$

Phytoplankton phosphorus

$$\frac{\partial}{\partial t}\left(C_P A_{PC} \right) = \left(G_{PI} - D_{PI} - \frac{V_{S4}}{D} \right) C_P A_{PC} \tag{A1.62}$$

Organic phosphorus

$$\frac{\partial}{\partial t}\left(C_{OP} \right) = D_{PI} C_P A_{PC} - k_{83} \theta_{83}^{T-20} X_{PRC} C_{OP} - \frac{V_{S3}\left(1 - f_{D8} \right)}{D} C_{OP} \tag{A1.63}$$

Orthophosphate phosphorus

$$\frac{\partial}{\partial t}\left(C_{\mathrm{IP}}\right)=k_{83}\theta_{83}^{T-20}X_{\mathrm{PRC}}C_{\mathrm{OP}}-G_{\mathrm{PI}}C_{\mathrm{P}}A_{\mathrm{PC}}-\frac{V_{\mathrm{S3}}\left(1-f_{\mathrm{D8}}\right)}{D}C_{\mathrm{IP}} \tag{A1.64}$$

$$X_{\mathrm{PRC}}=\frac{C_{\mathrm{P}}}{K_{\mathrm{MPC}}+C_{\mathrm{P}}} \tag{A1.65}$$

Phytoplankton nitrogen

$$\frac{\partial}{\partial t}\left(C_{\mathrm{P}}A_{\mathrm{NC}}\right)=\left(G_{\mathrm{PI}}-D_{\mathrm{PI}}-\frac{V_{\mathrm{S4}}}{D}\right)C_{\mathrm{P}}A_{\mathrm{NC}} \tag{A1.66}$$

Organic nitrogen

$$\frac{\partial}{\partial t}\left(C_{\mathrm{ON}}\right)=D_{\mathrm{PI}}C_{\mathrm{P}}A_{\mathrm{NC}}f_{\mathrm{ON}}-k_{71}\theta_{71}^{T-20}X_{\mathrm{PRC}}C_{\mathrm{ON}}-\frac{V_{\mathrm{S3}}\left(1-f_{\mathrm{D7}}\right)}{D}C_{\mathrm{ON}} \tag{A1.67}$$

NH_4

$$\frac{\partial}{\partial t}\left(C_{\mathrm{NH4}}\right)=k_{71}\theta_{71}^{T-20}X_{\mathrm{PRC}}C_{\mathrm{ON}}-G_{\mathrm{PI}}P_{\mathrm{NH4}}C_{\mathrm{P}}A_{\mathrm{NC}}-k_{12}\theta_{12}^{T-20}\left(\frac{C_{\mathrm{DO}}}{k_{\mathrm{NIT}}+C_{\mathrm{DO}}}\right)C_{\mathrm{NH4}} \tag{A1.68}$$

NO_3

$$\frac{\partial}{\partial t}\left(C_{\mathrm{NO3}}\right)=k_{12}\theta_{12}^{T-20}\left(\frac{C_{\mathrm{DO}}}{k_{\mathrm{NIT}}+C_{\mathrm{DO}}}\right)C_{\mathrm{NH4}}-G_{\mathrm{PI}}\left(1-P_{\mathrm{NH4}}\right)C_{\mathrm{P}}A_{\mathrm{NC}} \tag{A1.69}$$

Dissolved oxygen

$$\begin{aligned}\frac{\partial}{\partial t}\left(C_{\mathrm{DO}}\right)=&k_{\mathrm{r}}\theta_{\mathrm{a}}^{T-20}\left(C_{\mathrm{S}}-C_{\mathrm{DO}}\right)-k_{\mathrm{d}}\theta_{\mathrm{d}}^{T-20}\left(\frac{C_{\mathrm{DO}}}{k_{\mathrm{BOD}}+C_{\mathrm{DO}}}\right)C_{\mathrm{BOD}}-\frac{64}{14}k_{12}\theta_{12}^{T-20}\left(\frac{C_{\mathrm{DO}}}{k_{\mathrm{NIT}}+C_{\mathrm{DO}}}\right)C_{\mathrm{NH4}}-\frac{\mathrm{SOD}}{D}\\&+G_{\mathrm{PI}}C_{\mathrm{P}}\left(A_{\mathrm{OC}}+\frac{48}{14}A_{\mathrm{NC}}\left(1-P_{\mathrm{NH4}}\right)\right)-A_{\mathrm{OC}}k_{\mathrm{ir}}\theta_{\mathrm{ir}}^{T-20}C_{\mathrm{P}}\end{aligned} \tag{A1.70}$$

where:

A_{NC} is the nitrogen to phytoplankton ratio;

A_{PC} is the phosphorus to phytoplankton ratio;

C_{P} is the phytoplankton population;

D is the total water depth;

D_{PI} is the phytoplankton death plus respiration rate constant;

$(G_{\mathrm{PI}})_{\mathrm{max}}$ is the maximum growth rate under optimum lighting and nutrient conditions;

G_{L} is the growth-limiting factor;

G_{N} is the nitrogen limitation factor;

G_{P} is the phosphorus limitation factor;

G_{PI} is the phytoplankton growth rate;

G_{MA} is the macroalgae growth rate;

G_{T} is the temperature adjustment factor;

I_H is the light level that causes growth rate of half of $(G_{PI})_{max}$;

I_O is the surface light intensity;

k_r is the reaeration rate;

K_A is the light attenuation coefficient;

K_N is the nitrogen half-saturation constant;

K_P is the phosphorus half-saturation constant;

C_{BOD} is the BOD concentration;

C_{DO} is the dissolved oxygen concentration;

C_S is the dissolved oxygen saturation concentration;

k_{BOD} is the half-saturation constant for BOD;

k_d is the deoxygenation rate;

k_{12} is the nitrification rate;

k_{71} is the dissolved organic nitrogen mineralisation rate;

k_{83} is the dissolved organic phosphorus mineralisation rate;

θ_{12} is the temperature coefficient for nitrification;

θ_{71} is the temperature coefficient for organic nitrogen mineralisation;

θ_{83} is the temperature coefficient for organic phosphorus mineralisation;

f_{D3} is the fraction of dissolved inorganic phosphorus;

f_{D7} is the fraction of dissolved organic nitrogen;

f_{D8} is the fraction of dissolved organic phosphorus;

SOD is the sediment oxygen demand;

V_{S3} is the organic matter settling velocity; and

V_{S4} is the inorganic sediment settling velocity

A1.9 Updated Biological Functions in the MSN_WQ model

Phytoplankton growth

$$\frac{\partial C_P}{\partial t} = \left(G_{PI} - D_{PI}\right) C_P \tag{A1.71}$$

Phytoplankton growth rate

$$G_{PI} = \left(G_{PI}\right)_{max} \left(G_T\right)_{PI} \left(G_N\right)_{PI} G_L \tag{A1.72}$$

Light-limited growth

$$G_L = \left[\log\left(\frac{I_H + I_O}{I_H + I_O^{-K_A H}}\right)\right] \frac{f}{K_A H} \tag{A1.73}$$

Light attenuation coefficient

$$K_A = 0.79012 + 0.004296(C_P) \tag{A1.74}$$

Phytoplankton temperature correction factor

$$G(T) = \exp\left(\ln(Q_{10})\frac{T - T_{ref}}{10}\right) \tag{A1.75}$$

Macroalgae growth

$$\frac{\partial C_{MA}}{\partial t} = (G_{MA} - D_{MA})C_{MA} \tag{A1.76}$$

Macroalgae growth rate

$$G_{MA} = \min\left\{G_{LMAX}, G_{DROOP(N,P)}\right\}G(T) \tag{A1.77}$$

Nitrogen-related phytoplankton growth

$$(G_N)_{PI} = (G_{PI})_{max}(G_T)\frac{(C_{NH3} + C_{NO3})}{K_{NITROGEN} + (C_{NH3} + C_{NO3})} \tag{A1.78}$$

Phosphorus-related phytoplankton growth

$$(G_P)_{PI} = (G_{PI})_{max}(G_T)\frac{C_{IP}}{K_{PHOSPHORUS} + C_{IP}} \tag{A1.79}$$

Phytoplankton death plus respiration constant

$$D_{PI} = D_{0,PI}G(T) \tag{A1.80}$$

Droop model macroalgae growth

$$G_{DROOP(N,P)} = \begin{cases} (G_{MA})_{max}\, G_L \dfrac{Q_N - Q_{Nmin}}{Q_{Nmax} - Q_{Nmin}} \left(Q_N / Q_P\right)_{MOL} < 16 \\ (G_{MA})_{max}\, G_L \dfrac{Q_N - Q_{Nmin}}{Q_{Nmax} - Q_{Nmin}} \left(Q_N / Q_P\right)_{MOL} > 24 \\ (G_{MA})_{max}\, G_L \;\; 24 > \left(Q_N / Q_P\right)_{MOL} > 16 \end{cases} \tag{A1.81}$$

$$G_{LMAX} = \propto \mathrm{I}_m(t) \tag{A1.82}$$

$$\mathrm{I}_m(t) = \max\left\{\frac{I_0(t)}{K_A}\left(1 - e^{-K_A D}\right) - r_0, I_{sat}\right\} \tag{A1.83}$$

Macroalgae death plus respiration constant

$$D_{MA} = k_d B^{\beta} + k_t \frac{\max\left[f_{resp}B - DO, 0\right]}{f_{resp}B} \tag{A1.84}$$

Temperature correction factor 1

$$g(T) = \left(1 + \exp\left[-\zeta_p\left(T - \theta_p\right)\right]\right)^{-1} \tag{A1.85}$$

Temperature correction factor 2

$$g(T) = K_a K_b g_x \tag{A1.86}$$

$$K_a = \frac{k_1 \exp\left(\gamma_1\left(T - T_{min}\right)\right)}{1 + k_1\left(\exp\left(\gamma_1\left(T - T_{min}\right)\right) - 1\right)} \tag{A1.87}$$

$$\gamma_1 = \frac{1}{T_{opt} - T_{min}} \ln\left(\frac{0.98\left(1 - k_1\right)}{0.02 k_1}\right) \tag{A1.88}$$

$$K_b = \frac{k_4 \exp\left(\gamma_2\left(T_{max} - T\right)\right)}{1 + k_4\left(\exp\left(\gamma_2\left(T_{max} - T\right)\right) - 1\right)} \tag{A1.89}$$

$$\gamma_2 = \frac{1}{T_{max} - T_{opt}} \ln\left(\frac{0.98\left(1 - k_4\right)}{0.02 k_4}\right) \tag{A1.90}$$

$$T_{opt} = T_{opt} + Ac\left(1 - \exp\left(-k_T\left(T_{avg} - T_{opt}\right)\right)\right) \tag{A1.91}$$

$$g_x = 1 - T_{rid} \frac{T_{opt} - Opt_{min}}{Opt_{max} - Opt_{min}} \tag{A1.92}$$

Salinity-related macroalgae growth function

$$\left(G_S\right)_{MA} = \begin{cases} 1 - \left(\dfrac{S - S_{opt}}{S_x - S_{opt}}\right) & S \geq 5\text{psu} \\ \dfrac{S - S_{opt}}{S_{opt} - S_{opt}} & S < 5\text{psu} \end{cases} \tag{A1.93}$$

Growth limitation by bed carrying capacity

$$\left(G_K\right)_{MA} = 1 - \frac{C_{MA}}{K} \tag{A1.94}$$

$$\left(G_\gamma\right)_{MA} = \frac{1}{1 + \exp\left[\dfrac{\tau - \tau_c}{\delta}\right]} \tag{A1.95}$$

$$NH_{pro} = \frac{NH}{NO + NH} \tag{A1.96}$$

$$N_{rep} = \frac{Q_{Nmax} - N}{Q_{Nmax} - Q_{Nmin}} \tag{A1.97}$$

$$NH_{upt} = \frac{V_{mNH} N_{rep} NH_{pro} NH}{NH + K_{mNH}} \tag{A1.98}$$

$$NO_{upt} = \frac{V_{mNO} N_{rep} \left(1 - NH_{pro}\right) NO}{NO + K_{mNO}} \tag{A1.99}$$

$$PO_{upt} = \frac{V_{mPO} P_{rep} PO}{NH + K_{mNH}} \tag{A1.100}$$

$$P_{rep} = \frac{Q_{Pmax} - P}{Q_{Pmax} - Q_{Pmin}} \tag{A1.101}$$

Dissolved available inorganic phosphorus

$$\frac{\delta}{\delta t}\left(C_{DAIP}\right) = -G_{PI} C_P A_{PC} - G_{MA} C_{MA} PO_{upt} \tag{A1.102}$$

Dissolved available inorganic nitrogen

$$\frac{\delta}{\delta t}\left(C_{DAIN}\right) = -G_{PI} C_P A_{PC} - G_{MA} C_{MA} NH_{upt} - G_{MA} C_{MA} NO_{upt} \tag{A1.103}$$

Dissolved oxygen

$$\frac{\delta}{\delta t}\left(C_{DO}\right) = \left[k_r \theta_A^{T-20}\left(C_S - C_{DO}\right)\right] - \left[k_D \theta_D^{T-20}\left(\frac{C_{DO}}{k_{BOD} + C_{DO}} C_{BOD}\right)\right] - \frac{SOD}{D} - \left[\frac{64}{14} k_{12} \theta_{12}^{T-20}\left(\frac{C_{DO}}{k_{NIT} + C_{DO}}\right) C_{NH4}\right]$$
$$+ G_{PI} C_P \left[A_{OC} + \frac{48}{14} A_{NC}\left(1 - P_{NH4}\right)\right] - \left[A_{OC} k_{IR\_P} \theta_{IR\_P}^{T-20} C_P\right] + \left[G_{MA} C_{MA}\left(A_{OC} + \frac{48}{14} A_{NC}\left(1 - P_{NH4}\right)\right)\right] - \left[A_{OC} k_{IR\_MA} \theta_{IR\_MA}^{T-20} C_{MA}\right] \tag{A1.104}$$

where:

A_{NC} is the nitrogen to chlorophyll ratio;

A_{OC} is the oxygen to chlorophyll ratio;

A_{PC} is the phosphorus to chlorophyll ratio;

C_{BOD} is the BOD concentration;

C_{DO} is the dissolved oxygen concentration;

C_{NH4} is the NH_4 concentration;

C_{MA} is the macroalgae dry weight;

C_P is the phytoplankton population;

C_S is the dissolved oxygen saturation concentration;

D is the total water depth;

D_{PI} is the phytoplankton death plus respiration rate constant;

D_{MA} is the macroalgae death plus respiration rate constant;

f is the fraction of day exposed to sunlight;

$(G_{PI})_{max}$ is the maximum growth rate under optimum lighting and nutrient conditions;

G_L is the growth-limiting factor;

G_N is the nutrient limitation factor;

G_{PI} is the phytoplankton growth rate;

G_{MA} is the macroalgae growth rate;

G_T is the temperature adjustment factor;

I_H is the light level that causes a growth rate of half of $(G_{PI})_{max}$;

I_O is the surface light intensity;

k_r is the reaeration rate:

k_{BOD} is the half-saturation constant for BOD;

k_d is the deoxygenation rate;

k_{IR_P} is the rate of dissolved oxygen uptake through phytoplankton respiration and excretion;

k_{IR_MA} is the rate of dissolved oxygen uptake through macroalgae respiration and excretion;

k_{NIT} is the half-saturation constant for nitrogen;

k_D is the deoxygenation rate;

k_{NO3} is the NO_3 half-saturation constant;

k_A is the light attenuation coefficient;

k_N is the nitrogen half-saturation constant;

k_P is the phosphorus half-saturation constant;

NO refers to nitrate

NH refers to ammonium

PO refers to orthophosphate;

P_{NH4} is the NH_4 preference factor;

θ_A is the temperature coefficient for aeration;

θ_D is the temperature coefficient for deoxygenation;

θ_{IR_P} is the temperature coefficient for DO uptake through phytoplankton respiration and excretion;

θ_{IR_MA} is the temperature coefficient for DO uptake through macroalgae respiration and excretion;

α is the photosynthetic efficiency;

I is the depth-averaged and 24-hour averaged photosynthetically active radiation (PAR) for phytoplankton in micro-einsteins per square metre per second ($\mu E\, m^{-2}\, s^{-1}$);

I_0 is the surface PAR;

r_0 is the basal respiration rate;

τ_{max} is the bed stress;

τ_c is the critical shear stress;

δ is the transition factor between no effect and growth inhibition;

ϑ_p is the optimum temperature; and

ζ_p is the temperature correction coefficient.

Appendix 2 DCPM

A2.1 DCPM

The DCPM model is a simple box model that simulates the growth of phytoplankton and macroalgae and their interactions with the nitrogen and phosphorus cycles in estuaries. It is a combination of two previous models: the "static" version of the combined phytoplankton and macroalgae (CPM) model (Aldridge and Trimmer, 2009), which simulates macroalgae and phytoplankton, and the dynamic CSTT (Comprehensive Studies Task Team) model (Painting *et al.*, 2007), which simulates phytoplankton in waters of restricted exchange.

The first version of the DCPM model was based on the LESV model (Portilla *et al.*, 2009), which uses the ACExR module to describe physical exchange of waters both horizontally and vertically, but in the DCPM model exchange is simplified to a single vertical layer. The DCPM model was later developed to incorporate the capability to increase spatial resolution by coupling adjacent water bodies. The limitations of the current model (Aldridge *et al.*, 2013) include the single-layer structure, which assumes vertically well-mixed conditions, and the exclusion of sediment processes from nutrient cycling in the system. Figure A2.1 presents an overview of the interactions described by the DCPM model.

The model describes the physical exchange of nutrients and phytoplankton along with the biological growth and decay of phytoplankton and macroalgae. For a parameter *Y*, the physical exchange between compartments i and j and the biological growth in compartment i is given by equation A2.1 (Aldridge *et al.*, 2010):

$$\frac{dY_i}{dt} = \frac{1}{V}\left(\Phi_{ij} + V\beta_Y + \Gamma_Y\right) \qquad \text{(A2.1)}$$

where Φ_{ij} is physical exchange with neighbouring water, V is volume, β_Y is the biochemical processes of growth, decay and conversion and the final term, Γ_Y, is nutrient addition. In the case of macroalgae assumed bound to

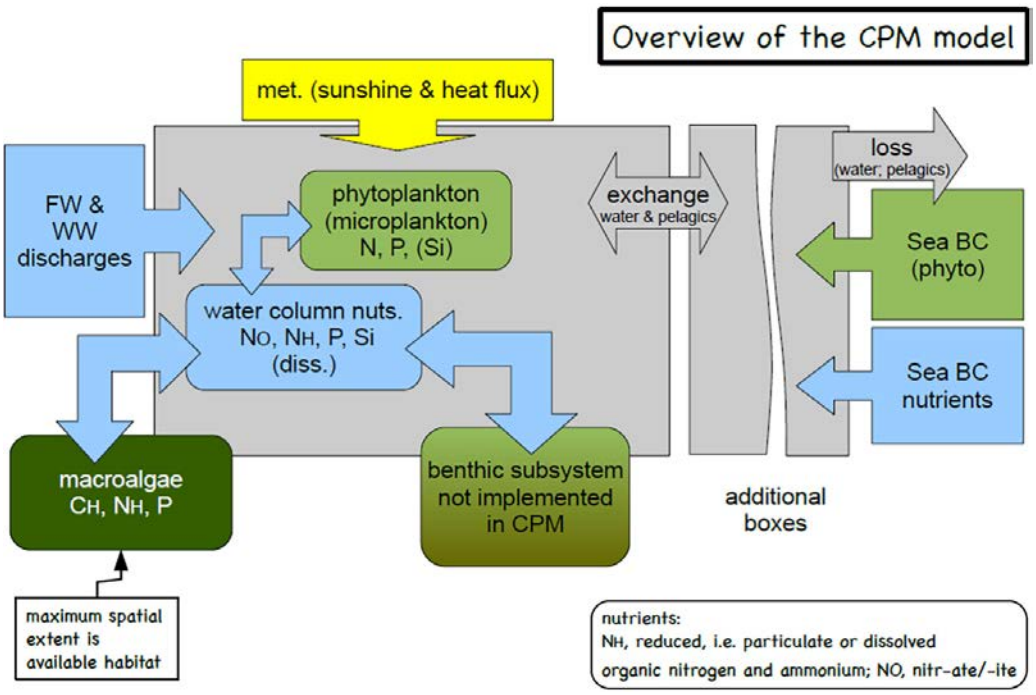

Figure A2.1. Schematic of CPM model components and processes (Aldridge *et al.*, 2013).BC, boundary conditions; CH, carbon; FW, freshwater; NH, ammonium; NO, nitrate; WW, wastewater.

the seabed, the first and last terms in equation A2.1 are nullified by the absence of advection or fresh inputs. Removal of macroalgae under shear stress is incorporated in the middle term, describing biological growth and decay.

The physical exchange of a parameter *Y* is described in general by equation A2.2:

$$\Phi_y = Q_T\left(Y_E - Y\right) + Q_F\left(Y_F - Y\right) \tag{A2.2}$$

where Q_T is the exchange rate with the downstream compartment or the open sea, Y_E is the coastal or downstream concentration, Q_F is the freshwater or upstream inflow, Y_F is the upstream concentration of parameter *Y* and *Y* is the concentration in the compartment of concern.

The central term in equation A2.1 annotates the growth of each species as a function of available incident light, nitrogen and phosphorus, the last two which are assimilated as a function of temperature. Biological growth within the model domain is considered as a community of autotrophs (macroalgae and phytoplankton) and heterotrophs, although the heterotrophic portion is ignored and the state variables remain macroalgae dry weight and phytoplankton concentrations. The term β in equation A2.1 can be expanded to the case of macroalgae or phytoplankton as presented in equation A2.3, or the case of nitrogen or phosphorus as presented in equation 2.4:

$$\beta_X\left[m\right] = \left(G_m - L_m\right)X_m \tag{A2.3}$$

$$\beta_S\left[nt\right] = \sum_m \left(G_m - e_m^{(nt)}L_m\right)X_m \frac{1}{q_m^{nt}} \tag{A2.4}$$

where G_m is the net growth rate, L_m is the net biological loss rate and X_m is the net biomass concentration, and the subscript *m* refers to macroalgae and the subscript *p* refers to phytoplankton. $e_m^{(nt)}$ is a grazing coefficient, which reflects the recycling of decayed autotrophs into nutrients. The term *q* is the yield of phytoplankton or macroalgae per unit of each nutrient; thus, the term q_m^{nt} joins equations A2.3 and A2.4 and relates the abundance of primary producers to nutrient concentrations.

Biological growth in the DCPM model is considered a threshold function of the limiting factors of temperature-dependent nutrient uptake or light availability, as in equation A2.5. The nutrient concentration function in equation A2.6 is a linear combination of the maximum growth under nutrient enrichment, an exponential light function in equation A2.8 and a Monod-type equation describing growth due to nutrient availability contained in equation A2.7, which assumes that nutrient uptake and growth occur simultaneously.

$$\mu\left(S^N, S^P, I\right) = \min\left\{f_m\left(I\right), f_m\left(\theta, S^N\right), f_m\left(\theta, S^P\right)\right\} \tag{A2.5}$$

$$f_m\left(\theta, S^{NT}\right) = \mu_{max,m} f\left(\theta\right) \min_{NT}\left\{g_m\left(S^{NT}\right)\right\} \tag{A2.6}$$

$$g_m\left(S^{NT}\right) = \frac{S^{NT}}{k_{S,m}^{NT} + S^{NT}} \tag{A2.7}$$

$$f\left(\theta\right) = \exp\left(\ln\left(Q_{10}\right)\frac{\theta - \theta_{ref}}{10}\right) \tag{A2.8}$$

$$L_m = L_{0,m} f\left(\theta\right) \tag{A2.9}$$

The basic term for growth as a function of incident light, assuming that growth is limited due to turbidity, is given by equations A2.10 and A2.11:

$$\mu\left(I\right) = \alpha\left(I - I_c\right) \tag{A2.10}$$

$$I = I_0 \frac{m_4\left(1-e^{\zeta}\right)}{\zeta} \tag{A2.11}$$

$$I_c = \frac{r_0}{\alpha\left(1+b\right)} \tag{A2.12}$$

$$r_0 = r_{0,a}\left(1-\eta\right) + r_{0,h}\eta\left(1+b_a\right) \tag{A2.13}$$

$$b = b_a\left(1+b_h\eta\right) + b_h\eta \tag{A2.14}$$

where α is the photosynthetic efficiency, I is the depth-averaged and 24-hour-averaged PAR for phytoplankton in $\mu E\, m^{-2}\, s^{-1}$, I_0 is the surface PAR and m_4 is a coefficient that accounts for the loss of PAR due to surface reflection and near surface loss of light. ζ is optical depth, which is the product of the light attenuation coefficient and the height of the water column, and I_c is the compensation PAR, which accounts for the PAR at which respiration consumes the product of photosynthesis within a 24-hour period. The basal respiration rate, r_0, consists of an autotrophic and heterotrophic component, $r_{0,a}$ and $r_{0,h}$, respectively; η is the heterotroph fraction that partitions between autotrophic and heterotrophic phytoplankton, b is the slope of the graph of the respiration of all autotrophic and heterotrophic plankton on growth rate, with b_a the slope of the graph of algal respiration versus growth rate and b_h the slope of the graph of heterotroph respiration versus growth rate.

The term for growth as a function of available PAR is modified in the DCPM model for shallow well-mixed, nutrient-rich waters, as presented in equation A2.15, which differs from equation A2.10 by introducing a Monod-type equation to describe PAR as it tends towards saturation:

$$\mu\left(I\right) = \frac{p_{max}\dfrac{I}{I+I_{sat}}q^B - r_0}{1+b} \tag{A2.15}$$

where p_{max} is the maximum photosynthesis rate, and q^B is the yield of biomass per unit carbon.

The explicit term for phytoplankton photosynthetic efficiency is given by the following expression:

$$\alpha_p = k\phi m_3 q_a^N Q_{max,a} a_{PH}\frac{1-\eta}{1+b} \tag{A2.16}$$

where Q_{max} is the maximum algal nitrogen content, q_a^N is the algal chlorophyll to nitrogen ratio, a_{PH} is the absorption cross-sectional area of phytoplankton within the water column for photosynthetically active radiation, m_3 increases the light availability to account for scattered light, k converts the units of photosynthetic efficiency calculations to the right units and ϕ is the photosynthetic quantum yield, or the amount of carbon fixed per photon of absorbed light.

No explicit representation of macroalgae photosynthetic efficiency is included in the DCPM model and, therefore, the parameters α_{ma} and $I_{c(ma)}$ are tuned during calibration.

The time evolution of incident PAR, I_0, at the surface as it varies with the tidal amplitude is given by equations A2.17 and A2.18:

$$I_0\left(t\right) = \overline{\overline{I_0}}\gamma\left(t\right) \tag{A2.17}$$

$$\gamma\left(t\right) = AE^{-\left[\frac{t-12}{r}\right]^2} \tag{A2.18}$$

where A is the tidal amplitude, t is the time elapsed since midnight and r is the width of the Gaussian curve, which is 0.29 × day length.

An exact value for the incident light for each species in the DCPM model is determined by taking into account the wetting and drying of each depth bin in equation A2.19; the value w_i is calculated for each bin based on knowledge of the water depth as it varies with time. The weighted average of incident light for each species across the area in which it is present is determined by equations A2.20 and A2.21 for macroalgae and phytoplankton, respectively:

$$I_m(t) = \begin{cases} w_i I + (1 - w_i) I_0; \textit{ macroalgae} \\ w_i I; \textit{ phytoplankton} \end{cases} \quad \text{(A2.19)}$$

$$\left\langle \hat{I}_{ma} \right\rangle_A = \frac{\sum_{i \in r} \left(p_i \times \hat{I}_{ma} \right)}{\sum_{i \in r} p_i} \quad \text{(A2.20)}$$

$$\left\langle \hat{I}_p \right\rangle_A = \frac{\sum_{d_i > 0} \left(p_i \times \hat{I}_{ma} \right)}{\sum_{d_i > 0} p_i} \quad \text{(A2.21)}$$

$$n(t) = A\cos\left(\omega_{M_2} t - \phi\right) + \frac{A}{3}\cos\left(\omega_{M_2} t - \phi - \frac{\pi}{6}\right) \quad \text{(A2.22)}$$

where w_i is a binary value indicating whether the area is wet or dry, the M_2 tidal constituent has the frequency ω_{M_2}, amplitude A and phase Φ and the S_2 tidal constituent has a third of the magnitude of M_2 and the phase is shifted by 30°.

A2.2 DCPM Model Set-up Preliminaries

The DCPM model is a 0-D box model that describes the growth and decay of chlorophyll and macroalgae as a function of nutrients and available light. As the nutrient concentrations are defined as mass per unit volume, the model's accuracy is predicated upon the declared volumes and nutrient mass loadings, and subsequently the renewal of water from upstream (Q_{AV} – average annual discharge) and downstream (E – tidal exchange rate). Water body volumes are described in terms of depth bins, which are graded in 1-m steps from 10 m below lowest astronomical tide (LAT) to 10 m above LAT.

Freshwater loading is defined as an annual average riverine discharge, with the associated ratio of summer to annual loading, R_{SA} (equation A2.23), enabling the fitting of an annual curve describing flow variation to the declared annual average riverine discharge (see DCPM user's manual – Aldridge *et al*., 2013).

$$R_{SA} = \frac{2R_{SW}}{1 + R_{SW}} \quad \text{(A2.23)}$$

where R_{SW} is the ratio of summer to winter average discharges, and summer is defined as April to September, inclusive, and winter as October to March, inclusive. Freshwater DAIN and DAIP loadings are also described in similar terms, with an annual nutrient load declared along with a value for R_{SA}.

The exchange rate, E, is related to residence time, τ_r, by equation A2.24, which is given by Aldridge *et al.* (2013):

$$E = -\log\left(1 - 1/\tau_r\right) \quad \text{(A2.24)}$$

Residence time is the time required to entirely flush an initial concentration of conservative tracer from a water body, or part thereof, subject to the influence of riverine discharge, and the tidal ebb and flood. Equation A2.25, as proposed by Hartnett *et al.* (2011b), provides an initial estimate of residence time τ_r' based on the length of a water body (L) in kilometres, the width of the mouth of the water body (B_0) in kilometres and the dimensionless tidal prism ratio (TPR).

$$\tau_r' = \frac{8.65}{\text{TPR}} - 2.45B_0 + 0.59L - 5.05 \quad \text{(A2.25)}$$

The first step in the model calibration process entails:

1. for each water body, tuning the initially estimated value of the exchange rate, E;
2. changing the R_{SA} if flow measurements are not available throughout the year and there is doubt about the annual variation in riverine discharges.

The aim of this preliminary step is to force the seasonal averaged model salinity values towards the seasonal average observations. The exchange rate determines the baseline salinity throughout the year in each water body, while the river ratio influences the dilution of salinity seasonally.

Accurate estimation of biological growth of chlorophyll and macroalgae relies on accurate specification of the light attenuation coefficient, k_d. For the purposes of this work, the expressions of Devlin *et al*. (2009) were applied to Secchi disc readings taken as part of routine monitoring by the EPA Transitional and Coastal team. Equations A2.26 and A2.27 apply to transitional and coastal waters, respectively:

$$k_d = 0.253 - 1.029 \log_e(\text{secchi depth}) \quad \text{(A2.26)}$$

$$k_d = -0.010 - 0.861 \log_e(\text{secchi depth}) \quad \text{(A2.27)}$$

Appendix 3 DCPM Model Parametrisation

Case study	Water body						
	Courtmacsherry Inner Bay	Lower Argideen Estuary	Argideen Macroalgae	Timoleague Receiving Waters	Upper Argideen Estuary	Courtmacsherry Bay North	Flaxfort Strand
Courtmacsherry 2010							
Latitude (°N)	51.6150	51.6330	51.6350	51.6400	51.6330	51.6470	51.6330
Longitude (°W)	–8.7020	–8.7330	–8.7590	–8.7640	–8.7330	–8.6790	–8.7330
Area average of MHWS and MLWS (km^2)	6.88	2.14	1.47	0.25	0.21	0.78	0.90
Available intertidal area (%)	0.00	0.00	68.90	0.00	0.00	42.50	90.30
Tidal phase (degrees)	30	30	30	30	30	30	30
Spring tidal range (m)	3.40	3.40	3.40	3.40	3.40	3.40	3.40
River flow ($m^3 s^{-1}$) (annual average)	0.00	0.00	0.00	0.35	3.12	0.54	0.13
River discharge ratio, summer/annual	0.00	0.00	0.00	0.61	0.61	0.61	0.61
Annual N load ($kg y^{-1}$)	0.00	0.00	0.00	62,215.55	550,092.25	94,646.54	22,029.80
N load ratio, summer/annual	1.000	1.000	1.000	0.558	0.548	0.548	0.548
Annual P load ($kg y^{-1}$)	0.00	0.00	0.00	842.89	5579.13	959.92	223.43
P load ratio, summer/annual	1.000	1.000	1.000	0.712	0.606	0.606	0.606
Annual chlorophyll load ($kg y^{-1}$)	0.00	0.00	0.00	33.29	353.02	60.74	0.00
Chlorophyll load ratio, summer/annual	1.000	1.000	1.000	1.100	1.050	1.050	1.000
Winter (Oct–Mar) N concentration in adjacent seawater (N_0) (µM)	32.14	0.00	0.00	0.00	0.00	0.00	0.00
Summer (Apr–Sep) N concentration in adjacent seawater (N_0) (µM)	2.85	0.00	0.00	0.00	0.00	0.00	0.00
Winter (Oct–Mar) P concentration in adjacent seawater (P_0) (µM)	0.63	0.00	0.00	0.00	0.00	0.00	0.00
Summer (Apr–Sep) P concentration in adjacent seawater (P_0) (µM)	0.25	0.00	0.00	0.00	0.00	0.00	0.00
Winter (Oct–Mar) chlorophyll concentration in adjacent seawater (X_0) ($mg l^{-1}$)	1.57	0.00	0.00	0.00	0.00	0.00	0.00
Summer (Apr–Sep) chlorophyll concentration in adjacent seawater (X_0) ($mg l^{-1}$)	0.85	0.00	0.00	0.00	0.00	0.00	0.00
Salinity in adjacent seawater (psu)	34.89	0	0	0	0	0	0
Exchange rate (E) (day^{-1})	0.50	0.75	0.44	0.44	0.22	0.30	0.35
Loss of microplankton (L) (day^{-1})	0.1	0.1	0.1	0.08	0.08	0.1	0.1
Proportion of nutrient recycled (%)	30	30	30	30	30	30	30
N loss term due to denitrification etc. (%)	0	0	0	0	0	0	0
Mean K_d (m^{-1})	0.29	0.44	0.70	0.95	0.95	0.10	0.37
Phytoplankton heterotroph proportion (%)	0.4	0.4	0.4	0.4	0.4	0.4	0.4
Phytoplankton yield per unit N (Q_N) (mg Chl $mmol^{-1}$ N)	2.2	2.2	2.2	2.2	2.2	2.2	2.2
Phytoplankton yield per unit P (Q_P) (mg Chl $mmol^{-1}$ P)	50	50	50	50	50	50	50

Case study	Water body						
	Courtmacsherry Inner Bay	Lower Argideen Estuary	Argideen Macroalgae	Timoleague Receiving Waters	Upper Argideen Estuary	Courtmacsherry Bay North	Flaxfort Strand
Phytoplankton C:Chl ratio	40	40	40	40	40	40	40
Phytoplankton half-saturation N (k_N) (µM l^{-1})	2	2	2	2	2	2	2
Phytoplankton half-saturation P (k_P) (µM l^{-1})	0.2	0.2	0.2	0.2	0.2	0.2	0.2
Phytoplankton half-saturation irradiance (k_I) (µE m^{-2} s^{-1})	100	100	100	100	100	100	100
Macroalgae growth rate (µMax) (day^{-1})	0.45	0.45	0.45	0.45	0.45	0.45	0.45
Macroalgae turnover time/loss rate (day^{-1})	0.033	0.033	0.033	0.033	0.033	0.033	0.033
Macroalgae C:N ratio (g g^{-1})	8.23	8.23	8.23	8.23	8.23	8.23	8.23
Macroalgae C:P ratio (g g^{-1})	134.4	134.4	134.4	134.4	134.4	134.4	134.4
Macroalgae carbon to macroalgae dry weight ratio (g g^{-1})	5	5	5	5	5	5	5
Macoalgae dry to wet weight ratio (g g^{-1})	5	5	5	5	5	5	5
Macroalgae half-saturation N (k_N) (µM l^{-1})	18	18	18	18	18	18	18
Macroalgae half-saturation P (k_P) (µM l^{-1})	0.3	0.3	0.3	0.3	0.3	0.3	0.3
Macroalgae maximum biomass density (g dw m^{-2})	600	600	600	600	600	600	600
Macroalgae overwinter biomass density (g dw m^{-2})	0.5	0.5	0.5	0.5	0.5	0.5	0.5
Macroalgae half-saturation irradiance (k_I) (µE m^{-2} s^{-1})	140	140	140	140	140	140	140
Correction mean spring to LAT (%) range (m)	3.40	3.40	3.40	3.40	3.40	3.40	3.40
General subtidal depth value (m)	–11.2	0.0	0.0	0.0	0.0	0.0	0.0
Area represented by general subtidal depth (%)	10.7	0.0	0.0	0.0	0.0	0.0	0.0
Area 9–10 m below LAT (%)	6.1	0.0	0.0	0.0	0.0	0.0	0.0
Area 8–9 m below LAT (%)	4.4	0.0	0.0	0.0	0.0	0.0	0.0
Area 7–8 m below LAT (%)	5.6	0.0	0.0	0.0	0.0	0.0	0.0
Area 6–7 m below LAT (%)	6.2	0.0	0.0	0.0	0.0	0.0	0.0
Area 5–6 m below LAT (%)	17.5	0.0	0.0	0.0	0.0	0.0	0.0
Area 4–5 m below LAT (%)	6.5	0.0	0.0	0.0	0.0	0.0	0.0
Area 3–4 m below LAT (%)	8.2	1.0	0.0	0.0	0.0	0.0	0.0
Area 2–3 m below LAT (%)	9.5	4.5	0.0	0.0	0.0	0.0	0.0
Area 1–2 m below LAT (%)	8.9	8.0	0.0	33.9	46.5	15.2	0.0
Area 0–1 m below LAT (%)	16.4	31.4	20.6	44.6	53.5	36.8	0.0
Area 0–1 m above LAT (%)	0.0	31.0	10.5	21.5	0.0	5.5	9.7
Area 1–2 m above LAT (%)	0.0	24.1	13.1	0.0	0.0	10.1	18.4
Area 2–3 m above LAT (%)	0.0	0.0	28.8	0.0	0.0	9.7	40.4
Area 3–4 m above LAT (%)	0.0	0.0	27.0	0.0	0.0	22.6	31.5
Area 4–5 m above LAT (%)	0.0	0.0	0.0	0.0	0.0	0.0	0.0
Area 5–6 m above LAT (%)	0.0	0.0	0.0	0.0	0.0	0.0	0.0
Area 6–7 m above LAT (%)	0.0	0.0	0.0	0.0	0.0	0.0	0.0
Area 7–8 m above LAT (%)	0.0	0.0	0.0	0.0	0.0	0.0	0.0
Area 8–9 m above LAT (%)	0.0	0.0	0.0	0.0	0.0	0.0	0.0
Area 9–10 m above LAT (%)	0.0	0.0	0.0	0.0	0.0	0.0	0.0
Area represented by general intertidal depth (%)	0.0	0.0	0.0	0.0	0.0	0.0	0.0

Case study	Water body						
	Courtmacsherry Inner Bay	Lower Argideen Estuary	Argideen Macroalgae	Timoleague Receiving Waters	Upper Argideen Estuary	Courtmacsherry Bay North	Flaxfort Strand
Courtmacsherry 2011							
Latitude (°N)	51.6150	51.6330	51.6350	51.6400	51.6330	51.6470	51.6330
Longitude (°W)	–8.7020	–8.7330	–8.7590	–8.7640	–8.7330	–8.6790	–8.7330
Area average MHWS and MLWS (km^2)	6.88	2.14	1.47	0.35	0.21	0.78	0.90
Available intertidal area (%)	0.00	0.00	68.90	0.00	0.00	42.50	90.30
Tidal phase (degrees)	30	30	30	30	30	30	30
Spring tidal range (m)	3.40	3.40	3.40	3.40	3.40	3.40	3.40
River flow ($m^3 s^{-1}$) (annual average)	0.00	0.00	0.00	0.34	3.03	0.52	0.12
River discharge ratio, summer/annual	0.00	0.00	0.00	0.34	0.34	0.34	0.34
Annual N load ($kg y^{-1}$)	0.00	0.00	0.00	64,900.99	574,394.59	98,827.90	23,003.05
N load ratio, summer/annual	1.000	1.000	1.000	0.282	0.265	0.265	0.265
Annual P load ($kg y^{-1}$)	0.00	0.00	0.00	838.79	5542.04	953.54	221.94
P load ratio, summer/annual	1.000	1.000	1.000	0.515	0.335	0.335	0.335
Annual chlorophyll load ($kg y^{-1}$)	0.00	0.00	0.00	33.29	353.02	60.74	0.00
Chlorophyll load ratio, summer/annual	1.000	1.000	1.000	1.100	1.050	1.050	1.000
Winter (Oct-Mar) N concentration in adjacent seawater (N_0) (μM)	32.00	0.00	0.00	0.00	0.00	0.00	0.00
Winter (Oct–Mar) N concentration in adjacent seawater (N_0) (μM)	4.50	0.00	0.00	0.00	0.00	0.00	0.00
Summer (Apr–Sep) N concentration in adjacent seawater (N_0) (μM)	0.63	0.00	0.00	0.00	0.00	0.00	0.00
Winter (Oct–Mar) P concentration in adjacent seawater (P_0) (μM)	0.30	0.00	0.00	0.00	0.00	0.00	0.00
Summer (Apr–Sep) P concentration in adjacent seawater (P_0) (μM)	1.57	0.00	0.00	0.00	0.00	0.00	0.00
Winter (Oct–Mar) chlorophyll concentration in adjacent seawater (X_0) ($mg l^{-1}$)	0.6	0.00	0.00	0.00	0.00	0.00	0.00
Summer (Apr–Sep) chlorophyll concentration in adjacent seawater (X_0) ($mg l^{-1}$)	34.66	0	0	0	0	0	0
Exchange rate (E) (day^{-1})	0.50	0.75	0.44	0.44	0.22	0.30	0.35
Loss of microplankton (L) (day^{-1})	0.1	0.1	0.1	0.08	0.08	0.1	0.1
Proportion of nutrient recycled (%)	30	30	30	30	30	30	30
N loss term due to denitrification etc. (%)	0	0	0	0	0	0	0
Mean K_d (m^{-1})	0.29	0.44	0.70	0.95	0.95	0.10	0.37
Phytoplankton heterotroph proportion (%)	0.4	0.4	0.4	0.4	0.4	0.4	0.4
Phytoplankton yield per unit N (Q_N) ($mg Chl mmol^{-1} N$)	2.2	2.2	2.2	2.2	2.2	2.2	2.2
Phytoplankton yield per unit P (Q_P) ($mg Chl mmol^{-1} P$)	50	50	50	50	50	50	50
Phytoplankton C:Chl ratio	40	40	40	40	40	40	40
Phytoplankton half-saturation N (k_N) ($μM l^{-1}$)	2	2	2	2	2	2	2
Phytoplankton half-saturation P (k_P) ($μM l^{-1}$)	0.2	0.2	0.2	0.2	0.2	0.2	0.2

Case study	Water body						
	Courtmacsherry Inner Bay	Lower Argideen Estuary	Argideen Macroalgae	Timoleague Receiving Waters	Upper Argideen Estuary	Courtmacsherry Bay North	Flaxfort Strand
Phytoplankton half-saturation irradiance (k_I) (μE m^{-2} s^{-1})	100	100	100	100	100	100	100
Macroalgae growth rate (μMax) (day^{-1})	0.45	0.45	0.45	0.45	0.45	0.45	0.45
Macroalgae turnover time/loss rate (day^{-1})	0.033	0.033	0.033	0.033	0.033	0.033	0.033
Macroalgae C:N ratio (g g^{-1})	8.23	8.23	8.23	8.23	8.23	8.23	8.23
Macroalgae C:P ratio (g g^{-1})	134.4	134.4	134.4	134.4	134.4	134.4	134.4
Macroalgae carbon to macroalgae dry weight ratio (g g^{-1})	5	5	5	5	5	5	5
Macoalgae dry to wet weight ratio (g g^{-1})	7	7	7	7	7	7	7
Macroalgae half-saturation N (k_N) (μM l^{-1})	18	18	18	18	18	18	18
Macroalgae half-saturation P (k_P) (μM l^{-1})	0.3	0.3	0.3	0.3	0.3	0.3	0.3
Macroalgae maximum biomass density (g dw m^{-2})	600	600	600	600	600	600	600
Macroalgae overwinter biomass density (g dw m^{-2})	0.5	0.5	0.5	0.5	0.5	0.5	0.5
Macroalgae half-saturation irradiance (k_I) (μE m^{-2} s^{-1})	140	140	140	140	140	140	140
Correction mean spring to LAT (%) range (m)	3.40	3.40	3.40	3.40	3.40	3.40	3.40
General subtidal depth value (m)	$^{-1}$1.2	0.0	0.0	0.0	0.0	0.0	0.0
Area represented by general subtidal depth (%)	10.7	0.0	0.0	0.0	0.0	0.0	0.0
Area 9–10 m below LAT (%)	6.1	0.0	0.0	0.0	0.0	0.0	0.0
Area 8–9 m below LAT (%)	4.4	0.0	0.0	0.0	0.0	0.0	0.0
Area 7–8 m below LAT (%)	5.6	0.0	0.0	0.0	0.0	0.0	0.0
Area 6–7 m below LAT (%)	6.2	0.0	0.0	0.0	0.0	0.0	0.0
Area 5–6 m below LAT (%)	17.5	0.0	0.0	0.0	0.0	0.0	0.0
Area 4–5 m below LAT (%)	6.5	0.0	0.0	0.0	0.0	0.0	0.0
Area 3–4 m below LAT (%)	8.2	1.0	0.0	0.0	0.0	0.0	0.0
Area 2–3 m below LAT (%)	9.5	4.5	0.0	0.0	0.0	0.0	0.0
Area 1–2 m below LAT (%)	8.9	8.0	0.0	33.9	46.5	15.2	0.0
Area 0–1 m below LAT (%)	16.4	31.4	20.6	44.6	53.5	36.8	0.0
Area 0–1 m above LAT (%)	0.0	31.0	10.5	21.5	0.0	5.5	9.7
Area 1–2 m above LAT (%)	0.0	24.1	13.1	0.0	0.0	10.1	18.4
Area 2–3 m above LAT (%)	0.0	0.0	28.8	0.0	0.0	9.7	40.4
Area 3–4 m above LAT (%)	0.0	0.0	27.0	0.0	0.0	22.6	31.5
Area 4–5 m above LAT (%)	0.0	0.0	0.0	0.0	0.0	0.0	0.0
Area 5–6 m above LAT (%)	0.0	0.0	0.0	0.0	0.0	0.0	0.0
Area 6–7 m above LAT (%)	0.0	0.0	0.0	0.0	0.0	0.0	0.0
Area 7–8 m above LAT (%)	0.0	0.0	0.0	0.0	0.0	0.0	0.0
Area 8–9 m above LAT (%)	0.0	0.0	0.0	0.0	0.0	0.0	0.0
Area 9–10 m above LAT (%)	0.0	0.0	0.0	0.0	0.0	0.0	0.0
Area represented by general intertidal depth (%)	0.0	0.0	0.0	0.0	0.0	0.0	0.0

Case study	Water body						
	Courtmacsherry Inner Bay	Lower Argideen Estuary	Argideen Macroalgae	Timoleague Receiving Waters	Upper Argideen Estuary	Courtmacsherry Bay North	Flaxfort Strand
Courtmacsherry 2015							
Latitude (°N)	51.6150	51.6330	51.6350	51.6400	51.6330	51.6470	51.6330
Longitude (°W)	–8.7020	–8.7330	–8.7590	–8.7640	–8.7330	–8.6790	–8.7330
Area average of MHWS and MLWS (km^2)	6.88	2.14	1.47	0.35	0.21	0.78	0.90
Available intertidal area (%)	0.00	0.00	68.90	0.00	0.00	42.50	90.30
Tidal phase (degrees)	30	30	30	30	30	30	30
Spring tidal range (m)	3.40	3.40	3.40	3.40	3.40	3.40	3.40
River flow ($m^3 s^{-1}$) (annual average)	0.00	0.00	0.00	0.66	6.01	1.03	0.24
River discharge ratio, summer/annual	0.00	0.00	0.00	0.56	0.56	0.56	0.56
Annual N load ($kg y^{-1}$)	0.00	0.00	0.00	136,416.64	1,221,587.23	181,167.23	42,168.23
N load ratio, summer/annual	1.000	1.000	1.000	0.587	0.582	0.503	0.503
Annual P load ($kg y^{-1}$)	0.00	0.00	0.00	2115.18	17,092.90	2940.93	684.53
P load ratio, summer/annual	1.000	1.000	1.000	0.642	0.598	0.598	0.598
Annual chlorophyll load ($kg y^{-1}$)	0.00	0.00	0.00	50.96	411.47	70.80	0.00
Chlorophyll load ratio, summer/annual	1.000	1.000	1.000	0.930	0.770	0.770	1.000
Winter (Oct–Mar) N concentration in adjacent seawater (N_0) (µM)	19.60	0.00	0.00	0.00	0.00	0.00	0.00
Summer (Apr–Sep) N concentration in adjacent seawater (N_0) (µM)	2.95	0.00	0.00	0.00	0.00	0.00	0.00
Winter (Oct–Mar) P concentration in adjacent seawater (P_0) (µM)	0.81	0.00	0.00	0.00	0.00	0.00	0.00
Summer (Apr–Sep) P concentration in adjacent seawater (P_0) (µM)	0.13	0.00	0.00	0.00	0.00	0.00	0.00
Winter (Oct–Mar) chlorophyll concentration in adjacent seawater (X_0) ($mg l^{-1}$)	1.225	0.00	0.00	0.00	0.00	0.00	0.00
Summer (Apr–Sep) chlorophyll concentration in adjacent seawater (X_0) ($mg l^{-1}$)	3.38	0.00	0.00	0.00	0.00	0.00	0.00
Salinity in adjacent seawater (psu)	34.51	0	0	0	0	0	0
Exchange rate (E) (day^{-1})	0.50	0.75	0.54	0.25	0.30	0.30	0.75
Loss of microplankton (L) (day^{-1})	0.1	0.1	0.1	0.08	0.08	0.1	0.1
Proportion of nutrient recycled (%)	30	30	30	30	30	30	30
N loss term due to denitrification etc. (%)	0	0	0	0	0	0	0
Mean K_d (m^{-1})	0.29	0.44	0.70	0.95	0.95	0.10	0.37
Phytoplankton heterotroph proportion (%)	0.4	0.4	0.4	0.4	0.4	0.4	0.4
Phytoplankton yield per unit N (Q_N) (mg Chl $mmol^{-1}$ N)	2.2	2.2	2.2	2.2	2.2	2.2	2.2
Phytoplankton yield per unit P (Q_P) (mg Chl $mmol^{-1}$ P)	50	50	50	50	50	50	50
Phytoplankton C:Chl ratio	40	40	40	40	40	40	40
Phytoplankton half-saturation N (k_N) ($µM l^{-1}$)	2	2	2	2	2	2	2

Case study	Water body						
	Courtmacsherry Inner Bay	Lower Argideen Estuary	Argideen Macroalgae	Timoleague Receiving Waters	Upper Argideen Estuary	Courtmacsherry Bay North	Flaxfort Strand
Phytoplankton half-saturation P (k_P) (µM l^{-1})	0.2	0.2	0.2	0.2	0.2	0.2	0.2
Phytoplankton half-saturation irradiance (k_I) (µE m^{-2} s^{-1})	100	100	100	100	100	100	100
Macroalgae growth rate (µMax) (day^{-1})	0.45	0.45	0.45	0.45	0.45	0.45	0.45
Macroalgae turnover time/loss rate (day^{-1})	0.05	0.05	0.05	0.05	0.05	0.05	0.05
Macroalgae C:N ratio (g g^{-1})	8.23	8.23	8.23	8.23	8.23	8.23	8.23
Macroalgae C:P ratio (g g^{-1})	134.4	134.4	134.4	134.4	134.4	134.4	134.4
Macroalgae carbon to macroalgae dry weight ratio (g g^{-1})	5	5	5	5	5	5	5
Macoalgae dry to wet weight ratio (g g^{-1})	4.9	4.9	4.9	4.9	4.9	4.9	4.9
Macroalgae half-saturation N (k_N) (µM l^{-1})	18	18	18	18	18	18	18
Macroalgae half-saturation P (k_P) (µM l^{-1})	0.3	0.3	0.3	0.3	0.3	0.3	0.3
Macroalgae maximum biomass density (g dw m^{-2})	600	600	600	600	600	600	600
Macroalgae overwinter biomass density (g dw m^{-2})	0.5	0.5	0.5	0.5	0.5	0.5	0.5
Macroalgae half-saturation irradiance (k_I) (µE m^{-2} s^{-1})	140	140	140	140	140	140	140
Correction mean spring to LAT (%) range (m)	3.40	3.40	3.40	3.40	3.40	3.40	3.40
General subtidal depth value (m)	–11.2	0.0	0.0	0.0	0.0	0.0	0.0
Area represented by general subtidal depth (%)	10.7	0.0	0.0	0.0	0.0	0.0	0.0
Area 9–10 m below LAT (%)	6.1	0.0	0.0	0.0	0.0	0.0	0.0
Area 8–9 m below LAT (%)	4.4	0.0	0.0	0.0	0.0	0.0	0.0
Area 7–8 m below LAT (%)	5.6	0.0	0.0	0.0	0.0	0.0	0.0
Area 6–7 m below LAT (%)	6.2	0.0	0.0	0.0	0.0	0.0	0.0
Area 5–6 m below LAT (%)	17.5	0.0	0.0	0.0	0.0	0.0	0.0
Area 4–5 m below LAT (%)	6.5	0.0	0.0	0.0	0.0	0.0	0.0
Area 3–4 m below LAT (%)	8.2	1.0	0.0	0.0	0.0	0.0	0.0
Area 2–3 m below LAT (%)	9.5	4.5	0.0	0.0	0.0	0.0	0.0
Area 1–2 m below LAT (%)	8.9	8.0	0.0	33.9	46.5	15.2	0.0
Area 0–1 m below LAT (%)	16.4	31.4	20.6	44.6	53.5	36.8	0.0
Area 0–1 m above LAT (%)	0.0	31.0	10.5	21.5	0.0	5.5	9.7
Area 1–2 m above LAT (%)	0.0	24.1	13.1	0.0	0.0	10.1	18.4
Area 2–3 m above LAT (%)	0.0	0.0	28.8	0.0	0.0	9.7	40.4
Area 3–4 m above LAT (%)	0.0	0.0	27.0	0.0	0.0	22.6	31.5
Area 4–5 m above LAT (%)	0.0	0.0	0.0	0.0	0.0	0.0	0.0
Area 5–6 m above LAT (%)	0.0	0.0	0.0	0.0	0.0	0.0	0.0
Area 6–7 m above LAT (%)	0.0	0.0	0.0	0.0	0.0	0.0	0.0
Area 7–8 m above LAT (%)	0.0	0.0	0.0	0.0	0.0	0.0	0.0
Area 8–9 m above LAT (%)	0.0	0.0	0.0	0.0	0.0	0.0	0.0
Area 9–10 m above LAT (%)	0.0	0.0	0.0	0.0	0.0	0.0	0.0
Area represented by general intertidal depth (%)	0.0	0.0	0.0	0.0	0.0	0.0	0.0

Case study	Water body						
	Courtmacsherry Inner Bay	Lower Argideen Estuary	Argideen Macroalgae	Timoleague Receiving Waters	Upper Argideen Estuary	Courtmacsherry Bay North	Flaxfort Strand
Courtmacsherry 2016							
Latitude (°N)	51.6150	51.6330	51.6350	51.6400	51.6330	51.6470	51.6330
Longitude (°W)	–8.7020	–8.7330	–8.7590	–8.7640	–8.7330	–8.6790	–8.7330
Area average of MHWS and MLWS (km^2)	6.88	2.14	1.47	0.20	0.21	0.78	0.90
Available intertidal area (%)	0.00	0.00	68.90	0.00	0.00	42.50	90.30
Tidal phase (degrees)	30	30	30	30	30	30	30
Spring tidal range (m)	3.40	3.40	3.40	3.40	3.40	3.40	3.40
River flow ($m^3 s^{-1}$) (annual average)	0.00	0.00	0.00	0.45	4.10	0.69	0.16
River discharge ratio, summer/annual	0.00	0.00	0.00	0.41	0.41	0.41	0.41
Annual N load ($kg y^{-1}$)	0.00	0.00	0.00	86,674.28	788,004.32	128,909.61	30,004.82
N load ratio, summer/annual	1.000	1.000	1.000	0.364	0.346	0.331	0.331
Annual P load ($kg y^{-1}$)	0.00	0.00	0.00	1332.48	10,316.74	1722.24	400.87
P load ratio, summer/annual	1.000	1.000	1.000	0.563	0.458	0.472	0.472
Annual chlorophyll load ($kg y^{-1}$)	0.00	0.00	0.00	50.96	411.47	70.80	0.00
Chlorophyll load ratio, summer/annual	1.000	1.000	1.000	0.930	0.770	0.770	1.000
Winter (Oct–Mar) N concentration in adjacent seawater (N_0) (µM)	19.60	0.00	0.00	0.00	0.00	0.00	0.00
Summer (Apr–Sep) N concentration in adjacent seawater (N_0) (µM)	1.98	0.00	0.00	0.00	0.00	0.00	0.00
Winter (Oct–Mar) P concentration in adjacent seawater (P_0) (µM)	0.79	0.00	0.00	0.00	0.00	0.00	0.00
Summer (Apr–Sep) P concentration in adjacent seawater (P_0) (µM)	0.08	0.00	0.00	0.00	0.00	0.00	0.00
Winter (Oct–Mar) chlorophyll concentration in adjacent seawater (X_0) ($mg l^{-1}$)	1.55	0.00	0.00	0.00	0.00	0.00	0.00
Summer (Apr–Sep) chlorophyll concentration in adjacent seawater (X_0) ($mg l^{-1}$)	2.6	0.00	0.00	0.00	0.00	0.00	0.00
Salinity in adjacent seawater (psu)	34.51	0	0	0	0	0	0
Exchange rate (E) (day^{-1})	0.50	0.60	0.29	0.20	0.11	0.30	0.30
Loss of microplankton (L) (day^{-1})	0.1	0.1	0.1	0.1	0.1	0.1	0.1
Proportion of nutrient recycled (%)	30	30	30	30	30	30	30
N loss term due to denitrification etc. (%)	0	0	0	0	0	0	0
Mean K_d (m^{-1})	0.29	0.44	0.70	0.95	0.95	0.10	0.37
Phytoplankton heterotroph proportion (%)	0.4	0.4	0.4	0.4	0.4	0.4	0.4
Phytoplankton yield per unit N (Q_N) ($mg Chl mmol^{-1} N$)	2.2	2.2	2.2	2.2	2.2	2.2	2.2
Phytoplankton yield per unit P (Q_P) ($mg Chl mmol^{-1} P$)	50	50	50	50	50	50	50
Phytoplankton C:Chl ratio	40	40	40	40	40	40	40
Phytoplankton half-saturation N (k_N) ($µM l^{-1}$)	2	2	2	2	2	2	2

Case study	Water body						
	Courtmacsherry Inner Bay	Lower Argideen Estuary	Argideen Macroalgae	Timoleague Receiving Waters	Upper Argideen Estuary	Courtmacsherry Bay North	Flaxfort Strand
Phytoplankton half-saturation P (k_P) (µM l^{-1})	0.2	0.2	0.2	0.2	0.2	0.2	0.2
Phytoplankton half-saturation irradiance (k_I) (µE m^{-2} s^{-1})	100	100	100	100	100	100	100
Macroalgae growth rate (µMax) (day^{-1})	0.45	0.45	0.45	0.45	0.45	0.45	0.45
Macroalgae turnover time/loss rate (day^{-1})	0.06	0.06	0.06	0.06	0.06	0.06	0.06
Macroalgae C:N ratio (g g^{-1})	8.23	8.23	8.23	8.23	8.23	8.23	8.23
Macroalgae C:P ratio (g g^{-1})	134.4	134.4	134.4	134.4	134.4	134.4	134.4
Macroalgae carbon to macroalgae dry weight ratio (g g^{-1})	5	5	5	5	5	5	5
Macoalgae dry to wet weight ratio (g g^{-1})	4.9	4.9	4.9	4.9	4.9	4.9	4.9
Macroalgae half-saturation N (k_N) (µM l^{-1})	18	18	18	18	18	18	18
Macroalgae half-saturation P (k_P) (µM l^{-1})	0.3	0.3	0.3	0.3	0.3	0.3	0.3
Macroalgae maximum biomass density (g dw m^{-2})	600	600	600	600	600	600	600
Macroalgae overwinter biomass density (g dw m^{-2})	0.5	0.5	0.5	0.5	0.5	0.5	0.5
Macroalgae half-saturation irradiance (k_I) (µE m^{-2} s^{-1})	140	140	140	140	140	140	140
Correction mean spring to LAT (%) range (m)	3.40	3.40	3.40	3.40	3.40	3.40	3.40
General subtidal depth value (m)	–11.2	0.0	0.0	0.0	0.0	0.0	0.0
Area represented by general subtidal depth (%)	10.7	0.0	0.0	0.0	0.0	0.0	0.0
Area 9–10 m below LAT (%)	6.1	0.0	0.0	0.0	0.0	0.0	0.0
Area 8–9 m below LAT (%)	4.4	0.0	0.0	0.0	0.0	0.0	0.0
Area 7–8 m below LAT (%)	5.6	0.0	0.0	0.0	0.0	0.0	0.0
Area 6–7 m below LAT (%)	6.2	0.0	0.0	0.0	0.0	0.0	0.0
Area 5–6 m below LAT (%)	17.5	0.0	0.0	0.0	0.0	0.0	0.0
Area 4–5 m below LAT (%)	6.5	0.0	0.0	0.0	0.0	0.0	0.0
Area 3–4 m below LAT (%)	8.2	1.0	0.0	0.0	0.0	0.0	0.0
Area 2–3 m below LAT (%)	9.5	4.5	0.0	0.0	0.0	0.0	0.0
Area 1–2 m below LAT (%)	8.9	8.0	0.0	33.9	46.5	15.2	0.0
Area 0–1 m below LAT (%)	16.4	31.4	20.6	44.6	53.5	36.8	0.0
Area 0–1 m above LAT (%)	0.0	31.0	10.5	21.5	0.0	5.5	9.7
Area 1–2 m above LAT (%)	0.0	24.1	13.1	0.0	0.0	10.1	18.4
Area 2–3 m above LAT (%)	0.0	0.0	28.8	0.0	0.0	9.7	40.4
Area 3–4 m above LAT (%)	0.0	0.0	27.0	0.0	0.0	22.6	31.5
Area 4–5 m above LAT (%)	0.0	0.0	0.0	0.0	0.0	0.0	0.0
Area 5–6 m above LAT (%)	0.0	0.0	0.0	0.0	0.0	0.0	0.0
Area 6–7 m above LAT (%)	0.0	0.0	0.0	0.0	0.0	0.0	0.0
Area 7–8 m above LAT (%)	0.0	0.0	0.0	0.0	0.0	0.0	0.0
Area 8–9 m above LAT (%)	0.0	0.0	0.0	0.0	0.0	0.0	0.0
Area 9–10 m above LAT (%)	0.0	0.0	0.0	0.0	0.0	0.0	0.0
Area represented by general intertidal depth (%)	0.0	0.0	0.0	0.0	0.0	0.0	0.0

	Water body						
	Dublin Bay	**Liffey Tolka Junction**	**Liffey Estuary Lower**	**Liffey Estuary Upper**	**Tolka Estuary**	**Tolka Sediment**	**North Bull Island**
Dublin Bay 2010–2012							
Latitude (°N)	53.3295	53.3459	53.3451	53.3450	53.3555	53.3658	53.3804
Longitude (°W)	–6.1339	–6.1638	–6.2098	–6.3180	–6.1938	–6.1703	–6.1376
Area average of MHWS and MLWS (km^2)	48.05	3.37	1.42	0.20	2.86	0.70	2.13
Available intertidal area (%)	0.00	0.00	0.00	0.00	0.00	83.60	95.20
Tidal phase (degrees)	30	30	30	30	30	30	30
Spring tidal range (m)	4.20	4.20	4.20	4.20	4.20	4.20	4.20
River flow ($m^3 s^{-1}$) (annual average)	0.00	4.86	2.58	10.73	1.90	0.00	0.00
River discharge ratio, summer/annual	0.00	1.08	0.34	0.80	0.75	0.00	0.00
Annual N load ($kg y^{-1}$)	0.00	2,680,900.00	118,720.00	825,947.00	87,993.53	0.00	0.00
N load ratio, summer/annual	0.000	1.000	0.400	0.817	0.472	0.000	0.000
Annual P load ($kg y^{-1}$)	0.00	437,256.00	1460.00	10,776.00	4352.84	0.00	0.00
P load ratio, summer/annual	0.000	1.000	0.980	0.971	0.930	0.000	0.000
Annual chlorophyll load ($kg y^{-1}$)	0.00	0.00	75.00	517.00	395.00	0.00	0.00
Chlorophyll load ratio, summer/annual	0.000	0.000	0.890	0.890	1.050	0.000	0.000
Winter (Oct–Mar) N concentration in adjacent seawater (N_0) (µM)	12.39	0.00	0.00	0.00	0.00	0.00	0.00
Summer (Apr–Sep) N concentration in adjacent seawater (N_0) (µM)	2.96	0.00	0.00	0.00	0.00	0.00	0.00
Winter (Oct–Mar) P concentration in adjacent seawater (P_0) (µM)	0.60	0.00	0.00	0.00	0.00	0.00	0.00
Summer (Apr–Sep) P concentration in adjacent seawater (P_0) (µM)	0.25	0.00	0.00	0.00	0.00	0.00	0.00
Winter (Oct–Mar) chlorophyll concentration in adjacent seawater (X_0) ($mg l^{-1}$)	1.75	0.00	0.00	0.00	0.00	0.00	0.00
Summer (Apr–Sep) chlorophyll concentration in adjacent seawater (X_0) ($mg l^{-1}$)	3.81	0.00	0.00	0.00	0.00	0.00	0.00
Salinity in adjacent seawater (psu)	34	0	0	0	0	0	0
Exchange rate (E) (day^{-1})	0.95	0.95	0.40	0.30	0.30	0.20	0.30
Loss of microplankton (L) (day^{-1})	0.15	0.15	0.15	0.15	0.15	0.15	0.15
Proportion of nutrient recycled (%)	30	30	30	30	30	30	30
N loss term due to denitrification etc. (%)	0	0	0	0	0	0	0
Mean K_d (m^{-1})	0.500	0.667	0.970	0.000	1.070	0.570	0.970
Phytoplankton heterotroph proportion (%)	0.4	0.4	0.4	0.4	0.4	0.4	0.4
Phytoplankton yield per unit N (Q_N) ($mg Chl mmol^{-1} N$)	2.2	2.2	2.2	2.2	2.2	2.2	2.2
Phytoplankton yield per unit P (Q_P) ($mg Chl mmol^{-1} P$)	50	50	50	50	50	50	50
Phytoplankton C:Chl ratio	40	40	40	40	40	40	40
Phytoplankton half-saturation N (k_N) ($µM l^{-1}$)	2	2	2	2	2	2	2
Phytoplankton half-saturation P (k_P) ($µM l^{-1}$)	0.2	0.2	0.2	0.2	0.2	0.2	0.2
Phytoplankton half-saturation irradiance (k_I) ($µE m^{-2} s^{-1}$)	100	100	100	100	100	100	100
Macroalgae growth rate (µMax) (day^{-1})	0.45	0.45	0.45	0.45	0.45	0.45	0.45
Macroalgae turnover time/loss rate (day^{-1})	0.033	0.033	0.033	0.033	0.033	0.033	0.033
Macroalgae C:N ratio ($g g^{-1}$)	8.23	8.23	8.23	8.23	8.23	8.23	8.23
Macroalgae C:P ratio ($g g^{-1}$)	134.4	134.4	134.4	134.4	134.4	134.4	134.4
Macroalgae carbon to macroalgae dry weight ratio ($g g^{-1}$)	5	5	5	5	5	5	5
Macoalgae dry to wet weight ratio ($g g^{-1}$)	7	7	7	7	7	7	7
Macroalgae half-saturation N (k_N) ($µM l^{-1}$)	18	18	18	18	18	18	18
Macroalgae half-saturation P (k_P) ($µM l^{-1}$)	0.3	0.3	0.3	0.3	0.3	0.3	0.3
Macroalgae maximum biomass density ($g dw m^{-2}$)	600	600	600	600	600	600	600

	Water body						
	Dublin Bay	Liffey Tolka Junction	Liffey Estuary Lower	Liffey Estuary Upper	Tolka Estuary	Tolka Sediment	North Bull Island
Macroalgae overwinter biomass density (g dw m^{-2})	0.5	0.5	0.5	0.5	0.5	0.5	0.5
Macroalgae half-saturation irradiance (k_I) (µE m^{-2} s^{-1})	140	140	140	140	140	140	140
Correction mean spring to LAT (%) range (m)	2.16	2.16	2.16	2.16	2.16	2.16	2.16
General subtidal depth value (m)	13.3	0.0	0.0	0.0	0.0	0.0	0.0
Area represented by general subtidal depth (%)	7.1	0.0	0.0	0.0	0.0	0.0	0.0
Area 9–10 m below LAT (%)	1.6	0.0	0.0	0.0	0.0	0.0	0.0
Area 8–9 m below LAT (%)	3.1	0.0	0.0	0.0	0.0	0.0	0.0
Area 7–8 m below LAT (%)	5.4	0.0	0.0	0.0	0.0	0.0	0.0
Area 6–7 m below LAT (%)	2.5	0.2	0.0	0.0	0.0	0.0	0.0
Area 5–6 m below LAT (%)	6.3	13.3	75.0	0.0	0.0	0.0	0.0
Area 4–5 m below LAT (%)	6.9	6.7	25.0	87.5	0.0	0.0	0.0
Area 3–4 m below LAT (%)	5.6	11.3	0.0	6.3	0.0	0.0	0.0
Area 2–3 m below LAT (%)	7.6	13.7	0.0	3.1	0.0	0.0	0.0
Area 1–2 m below LAT (%)	7.7	24.6	0.0	3.1	1.9	0.0	0.0
Area 0–1 m below LAT (%)	9.1	30.2	0.0	0.0	4.9	0.0	1.0
Area 0–1 m above LAT (%)	7.1	0.0	0.0	0.0	31.5	10.1	1.7
Area 1–2 m above LAT (%)	8.0	0.0	0.0	0.0	58.9	21.4	2.1
Area 2–3 m above LAT (%)	16.4	0.0	0.0	0.0	1.6	42.7	55.6
Area 3–4 m above LAT (%)	5.0	0.0	0.0	0.0	1.0	25.8	39.6
Area 4–5 m above LAT (%)	0.6	0.0	0.0	0.0	0.2	0.0	0.0
Area 5–6 m above LAT (%)	0.0	0.0	0.0	0.0	0.0	0.0	0.0
Area 6–7 m above LAT (%)	0.0	0.0	0.0	0.0	0.0	0.0	0.0
Area 7–8 m above LAT (%)	0.0	0.0	0.0	0.0	0.0	0.0	0.0
Area 8–9 m above LAT (%)	0.0	0.0	0.0	0.0	0.0	0.0	0.0
Area 9–10 m above LAT (%)	0.0	0.0	0.0	0.0	0.0	0.0	0.0
Area represented by general intertidal depth (%)	0.0	0.0	0.0	0.0	0.0	0.0	0.0

	Water body			
	Clonakilty Inner Bay	**Ashgrove Receiving Waters**	**Clonakilty Inner Harbour**	**Clonakilty Intertidal Macroalgae**
Clonakilty Bay 2010–2011				
Latitude (°N)	51.5893	51.6085	51.6140	51.6107
Longitude (°W)	–8.8527	–8.8519	8.8680	–8.8725
Area average of MHWS and MLWS (km^2)	4.20	0.26	0.73	0.80
Available intertidal area (%)	0.00	0.00	0.00	95.30
Tidal phase (degrees)	30	30	30	30
Spring tidal range (m)	3.40	3.40	3.40	3.40
River flow ($m^3 s^{-1}$) (annual average)	0.00	0.16	0.40	0.00
River discharge ratio, summer/annual	0.00	0.75	0.75	0.00
Annual N load ($kg y^{-1}$)	0.00	26,759.70	30,629.75	0.00
N load ratio, summer/annual	1.000	0.850	0.750	1.000
Annual P load ($kg y^{-1}$)	0.00	221.58	402.38	0.00
P load ratio, summer/annual	1.000	0.850	1.030	1.000
Annual chlorophyll load ($kg y^{-1}$)	0.00	0.00	0.00	0.00
Chlorophyll load ratio, summer/annual	0.000	0.000	0.000	0.000
Winter (Oct–Mar) N concentration in adjacent seawater (N_0) (µM)	20.61	0.00	0.00	0.00
Summer (Apr–Sep) N concentration in adjacent seawater (N_0) (µM)	2.43	0.00	0.00	0.00
Winter (Oct–Mar) P concentration in adjacent seawater (P_0) (µM)	0.58	0.00	0.00	0.00
Summer (Apr–Sep) P concentration in adjacent seawater (P_0) (µM)	0.17	0.00	0.00	0.00
Winter (Oct–Mar) chlorophyll concentration in adjacent seawater (X_0) ($mg l^{-1}$)	1.02	0.00	0.00	0.00
Summer (Apr–Sep) chlorophyll concentration in adjacent seawater (X_0) ($mg l^{-1}$)	1.49	0.00	0.00	0.00
Salinity in adjacent seawater (psu)	34.8	0	0	0
Exchange rate (E) (day^{-1})	1.00	0.60	0.25	1.00
Loss of microplankton (L) (day^{-1})	0	0.13	0.1	0.1
Proportion of nutrient recycled (%)	30	30	30	30
N loss term due to denitrification etc. (%)	0	0	0	0
Mean K_d (m^{-1})	0.29	1.08	3.83	1.03
Phytoplankton heterotroph proportion (%)	0.4	0.4	0.4	0.4
Phytoplankton yield per unit N (Q_N) ($mg Chl mmol^{-1} N$)	2.2	2.2	2.2	2.2
Phytoplankton yield per unit P (Q_P) ($mg Chl mmol^{-1} P$)	50	50	50	50
Phytoplankton C:Chl ratio	40	40	40	40
Phytoplankton half-saturation N (k_N) ($µM l^{-1}$)	2	2	2	2
Phytoplankton half-saturation P (k_P) ($µM l^{-1}$)	0.2	0.2	0.2	0.2
Phytoplankton half-saturation irradiance (k_I) ($µE m^{-2} s^{-1}$)	100	100	100	100
Macroalgae growth rate (µMax) (day^{-1})	0.45	0.45	0.45	0.45
Macroalgae turnover time/loss rate (day^{-1})	0.033	0.033	0.033	0.033
Macroalgae C:N ratio ($g g^{-1}$)	8.23	8.23	8.23	8.23
Macroalgae C:P ratio ($g g^{-1}$)	134.4	134.4	134.4	134.4
Macroalgae carbon to macroalgae dry weight ratio ($g g^{-1}$)	5	5	5	5
Macoalgae dry to wet weight ratio ($g g^{-1}$)	7	7	7	7
Macroalgae half-saturation N (k_N) ($µM l^{-1}$)	18	18	18	18
Macroalgae half-saturation P (k_P) ($µM l^{-1}$)	0.3	0.3	0.3	0.3
Macroalgae maximum biomass density ($g dw m^{-2}$)	600	600	600	600
Macroalgae overwinter biomass density ($g dw m^{-2}$)	0.5	0.5	0.5	0.5
Macroalgae half-saturation irradiance (k_I) ($µE m^{-2} s^{-1}$)	140	140	140	140
Correction mean spring to LAT (%) range (m)	1.10	0.60	0.25	0.25
General subtidal depth value (m)	–11.8	0.0	0.0	0.0

	Water body			
	Clonakilty Inner Bay	Ashgrove Receiving Waters	Clonakilty Inner Harbour	Clonakilty Intertidal Macroalgae
Area represented by general subtidal depth (%)	15.7	0.0	0.0	0.0
Area 9–10 m below LAT (%)	4.8	0.0	0.0	0.0
Area 8–9 m below LAT (%)	4.5	0.0	0.0	0.0
Area 7–8 m below LAT (%)	5.1	0.0	0.0	0.0
Area 6–7 m below LAT (%)	7.7	0.0	0.0	0.0
Area 5–6 m below LAT (%)	9.2	0.0	0.0	0.0
Area 4–5 m below LAT (%)	7.7	0.0	0.0	0.0
Area 3–4 m below LAT (%)	6.2	0.0	0.0	0.0
Area 2–3 m below LAT (%)	8.3	0.0	0.0	0.0
Area 1–2 m below LAT (%)	5.5	7.6	0.0	0.9
Area 0–1 m below LAT (%)	6.9	17.9	27.6	6.2
Area 0–1 m above LAT (%)	8.6	12.4	24.4	19.5
Area 1–2 m above LAT (%)	5.2	17.4	15.0	37.2
Area 2–3 m above LAT (%)	2.4	26.3	12.4	36.3
Area 3–4 m above LAT (%)	1.1	17.6	20.6	0.0
Area 4–5 m above LAT (%)	1.1	0.8	0.0	0.0
Area 5–6 m above LAT (%)	0.0	0.0	0.0	0.0
Area 6–7 m above LAT (%)	0.0	0.0	0.0	0.0
Area 7–8 m above LAT (%)	0.0	0.0	0.0	0.0
Area 8–9 m above LAT (%)	0.0	0.0	0.0	0.0
Area 9–10 m above LAT (%)	0.0	0.0	0.0	0.0
Area represented by general intertidal depth (%)	0.0	0.0	0.0	0.0

Chl, chlorophyll; MHWS, mean high water at spring tide; MLWS, mean low water at spring tide; summer, April to September, inclusive; winter, October to March, inclusive.

AN GHNÍOMHAIREACHT UM CHAOMHNÚ COMHSHAOIL
Tá an Ghníomhaireacht um Chaomhnú Comhshaoil (GCC) freagrach as an gcomhshaol a chaomhnú agus a fheabhsú mar shócmhainn luachmhar do mhuintir na hÉireann. Táimid tiomanta do dhaoine agus don chomhshaol a chosaint ó éifeachtaí díobhálacha na radaíochta agus an truaillithe.

Is féidir obair na Gníomhaireachta a roinnt ina trí phríomhréimse:

Rialú: *Déanaimid córais éifeachtacha rialaithe agus comhlíonta comhshaoil a chur i bhfeidhm chun torthaí maithe comhshaoil a sholáthar agus chun díriú orthu siúd nach gcloíonn leis na córais sin.*

Eolas: *Soláthraímid sonraí, faisnéis agus measúnú comhshaoil atá ar ardchaighdeán, spriocdhírithe agus tráthúil chun bonn eolais a chur faoin gcinnteoireacht ar gach leibhéal.*

Tacaíocht: *Bímid ag saothrú i gcomhar le grúpaí eile chun tacú le comhshaol atá glan, táirgiúil agus cosanta go maith, agus le hiompar a chuirfidh le comhshaol inbhuanaithe.*

Ár bhFreagrachtaí

Ceadúnú
Déanaimid na gníomhaíochtaí seo a leanas a rialú ionas nach ndéanann siad dochar do shláinte an phobail ná don chomhshaol:
- saoráidí dramhaíola *(m.sh. láithreáin líonta talún, loisceoirí, stáisiúin aistrithe dramhaíola)*;
- gníomhaíochtaí tionsclaíocha ar scála mór *(m.sh. déantúsaíocht cógaisíochta, déantúsaíocht stroighne, stáisiúin chumhachta)*;
- an diantalmhaíocht *(m.sh. muca, éanlaith)*;
- úsáid shrianta agus scaoileadh rialaithe Orgánach Géinmhodhnaithe *(OGM)*;
- foinsí radaíochta ianúcháin *(m.sh. trealamh x-gha agus radaiteiripe, foinsí tionsclaíocha)*;
- áiseanna móra stórála peitril;
- scardadh dramhuisce;
- gníomhaíochtaí dumpála ar farraige.

Forfheidhmiú Náisiúnta i leith Cúrsaí Comhshaoil
- Clár náisiúnta iniúchtaí agus cigireachtaí a dhéanamh gach bliain ar shaoráidí a bhfuil ceadúnas ón nGníomhaireacht acu.
- Maoirseacht a dhéanamh ar fhreagrachtaí cosanta comhshaoil na n-údarás áitiúil.
- Caighdeán an uisce óil, arna sholáthar ag soláthraithe uisce phoiblí, a mhaoirsiú.
- Obair le húdaráis áitiúla agus le gníomhaireachtaí eile chun dul i ngleic le coireanna comhshaoil trí chomhordú a dhéanamh ar líonra forfheidhmiúcháin náisiúnta, trí dhíriú ar chiontóirí, agus trí mhaoirsiú a dhéanamh ar leasúchán.
- Cur i bhfeidhm rialachán ar nós na Rialachán um Dhramhthrealamh Leictreach agus Leictreonach (DTLL), um Shrian ar Shubstaintí Guaiseacha agus na Rialachán um rialú ar shubstaintí a ídíonn an ciseal ózóin.
- An dlí a chur orthu siúd a bhriseann dlí an chomhshaoil agus a dhéanann dochar don chomhshaol.

Bainistíocht Uisce
- Monatóireacht agus tuairisciú a dhéanamh ar cháilíocht aibhneacha, lochanna, uiscí idirchriosacha agus cósta na hÉireann, agus screamhuiscí; leibhéil uisce agus sruthanna aibhneacha a thomhas.
- Comhordú náisiúnta agus maoirsiú a dhéanamh ar an gCreat-Treoir Uisce.
- Monatóireacht agus tuairisciú a dhéanamh ar Cháilíocht an Uisce Snámha.

Monatóireacht, Anailís agus Tuairisciú ar an gComhshaol
- Monatóireacht a dhéanamh ar cháilíocht an aeir agus Treoir an AE maidir le hAer Glan don Eoraip (CAFÉ) a chur chun feidhme.
- Tuairisciú neamhspleách le cabhrú le cinnteoireacht an rialtais náisiúnta agus na n-údarás áitiúil *(m.sh. tuairisciú tréimhsiúil ar staid Chomhshaol na hÉireann agus Tuarascálacha ar Tháscairí)*.

Rialú Astaíochtaí na nGás Ceaptha Teasa in Éirinn
- Fardail agus réamh-mheastacháin na hÉireann maidir le gáis cheaptha teasa a ullmhú.
- An Treoir maidir le Trádáil Astaíochtaí a chur chun feidhme i gcomhair breis agus 100 de na táirgeoirí dé-ocsaíde carbóin is mó in Éirinn.

Taighde agus Forbairt Comhshaoil
- Taighde comhshaoil a chistiú chun brúnna a shainaithint, bonn eolais a chur faoi bheartais, agus réitigh a sholáthar i réimsí na haeráide, an uisce agus na hinbhuanaitheachta.

Measúnacht Straitéiseach Timpeallachta
- Measúnacht a dhéanamh ar thionchar pleananna agus clár beartaithe ar an gcomhshaol in Éirinn *(m.sh. mórphleananna forbartha)*.

Cosaint Raideolaíoch
- Monatóireacht a dhéanamh ar leibhéil radaíochta, measúnacht a dhéanamh ar nochtadh mhuintir na hÉireann don radaíocht ianúcháin.
- Cabhrú le pleananna náisiúnta a fhorbairt le haghaidh éigeandálaí ag eascairt as taismí núicléacha.
- Monatóireacht a dhéanamh ar fhorbairtí thar lear a bhaineann le saoráidí núicléacha agus leis an tsábháilteacht raideolaíochta.
- Sainseirbhísí cosanta ar an radaíocht a sholáthar, nó maoirsiú a dhéanamh ar sholáthar na seirbhísí sin.

Treoir, Faisnéis Inrochtana agus Oideachas
- Comhairle agus treoir a chur ar fáil d'earnáil na tionsclaíochta agus don phobal maidir le hábhair a bhaineann le caomhnú an chomhshaoil agus leis an gcosaint raideolaíoch.
- Faisnéis thráthúil ar an gcomhshaol ar a bhfuil fáil éasca a chur ar fáil chun rannpháirtíocht an phobail a spreagadh sa chinnteoireacht i ndáil leis an gcomhshaol *(m.sh. Timpeall an Tí, léarscáileanna radóin)*.
- Comhairle a chur ar fáil don Rialtas maidir le hábhair a bhaineann leis an tsábháilteacht raideolaíoch agus le cúrsaí práinnfhreagartha.
- Plean Náisiúnta Bainistíochta Dramhaíola Guaisí a fhorbairt chun dramhaíl ghuaiseach a chosc agus a bhainistiú.

Múscailt Feasachta agus Athrú Iompraíochta
- Feasacht chomhshaoil níos fearr a ghiniúint agus dul i bhfeidhm ar athrú iompraíochta dearfach trí thacú le gnóthais, le pobail agus le teaghlaigh a bheith níos éifeachtúla ar acmhainní.
- Tástáil le haghaidh radóin a chur chun cinn i dtithe agus in ionaid oibre, agus gníomhartha leasúcháin a spreagadh nuair is gá.

Bainistíocht agus struchtúr na Gníomhaireachta um Chaomhnú Comhshaoil
Tá an ghníomhaíocht á bainistiú ag Bord lánaimseartha, ar a bhfuil Ard-Stiúrthóir agus cúigear Stiúrthóirí. Déantar an obair ar fud cúig cinn d'Oifigí:
- An Oifig um Inmharthanacht Comhshaoil
- An Oifig Forfheidhmithe i leith cúrsaí Comhshaoil
- An Oifig um Fianaise is Measúnú
- Oifig um Chosaint Radaíochta agus Monatóireachta Comhshaoil
- An Oifig Cumarsáide agus Seirbhísí Corparáideacha

Tá Coiste Comhairleach ag an nGníomhaireacht le cabhrú léi. Tá dáréag comhaltaí air agus tagann siad le chéile go rialta le plé a dhéanamh ar ábhair imní agus le comhairle a chur ar an mBord.

EPA Research Report 359

Modelling Irish Transitional and Coastal Systems to Determine Nutrient Reduction Measures to Achieve Good Status

Authors: Joseph V. McGovern, Stephen Nash and Michael Hartnett

Identifying Pressures

Three Irish estuaries were modelled with the aim of quantifying the impact on water quality of existing nutrient loading from direct and diffuse inputs. One commonality between the three chosen estuaries was the prevalence of opportunistic macroalgae blooms, although the upstream catchments and thus the causative factors differed.

In the Liffey–Tolka–Dublin Bay system, wastewater was found to be the greatest pressure on water quality. The two other estuarine systems, namely the Argideen Estuary and Clonakilty Harbour, were both found to be under considerable pressure from diffuse nutrient inputs from agriculture.

Informing Policy

A range of scenarios was explored using calibrated models of the three estuarine systems to establish what conditions, if any, could meet ambient water quality standards and reduce macroalgae bloom magnitudes to the compliance limits:

- In the Liffey–Tolka–Dublin Bay system, either reducing river nitrogen and phosphorus inputs by 50% or upgrading wastewater treatment at the main facility to include aerobic granular sludge technologies would reduce macroalgae bloom magnitudes to the compliance limits.
- In Clonakilty Harbour, a 25% reduction in river phosphorus inputs would similarly restore macroalgae compliance.
- In the system including the Argideen Estuary, reducing river nitrogen and phosphorus inputs by 66% would restore compliance with trophic status parameters. However, none of the scenarios considered could reduce macroalgae bloom magnitudes in the Argideen Estuary to within compliance limits.

The Argideen Estuary was modelled using sub-hourly riverine nutrient measurements provided by the Teagasc Agricultural Catchments Programme. Advances in catchment management practices in the Argideen catchment have yielded reductions in flow-normalised phosphorus transfer. In spite of these improvements, macroalgae bloom magnitudes downstream increased because of higher river flows and higher tidally exchanged nutrient concentrations.

Developing Solutions

This project entailed a detailed assessment of a simple box model, with a view to increasing use of the box model in future. High-, medium- and low-resolution nutrient loading information was applied to the Courtmacsherry, Dublin and Clonakilty models, respectively, facilitating a critical analysis of the consequences of adopting different nutrient loading estimates or measurements in box model calibration and scenario modelling.

Although the simple box model performed well with regard to the simulated water column nutrient and chlorophyll a concentrations and macroalgae wet weights, a number of recommendations are made to increase the confidence in the model results; these actions encompass refinements to upstream riverine and downstream tidal nutrient loadings and concentrations, respectively.

Recommendations on the necessary nutrient load reductions to improve estuarine water quality and the appropriate pressure to target in nutrient load reductions for the three systems studied are provided.

EPA Research: McCumiskey House,
Richiew, Clonskeagh, Dublin 14.

Phone: 01 268 0100
Twitter: @EPAResearchNews
Email: research@epa.ie

www.epa.ie

EPA Research Webpages
www.epa.ie/researchandeducation/research/